



DOCUMENT 265-06

ELECTRONIC TRAJECTORY MEASUREMENTS GROUP

RADAR TRANSPONDER ANTENNA SYSTEMS EVALUATION HANDBOOK

WHITE SANDS MISSILE RANGE
REAGAN TEST SITE
YUMA PROVING GROUND
DUGWAY PROVING GROUND
ABERDEEN TEST CENTER
NATIONAL TRAINING CENTER
ELECTRONIC PROVING GROUND

NAVAL AIR WARFARE CENTER WEAPONS DIVISION, PT. MUGU
NAVAL AIR WARFARE CENTER WEAPONS DIVISION, CHINA LAKE
NAVAL AIR WARFARE CENTER AIRCRAFT DIVISION, PATUXENT RIVER
NAVAL UNDERSEA WARFARE CENTER DIVISION, NEWPORT
PACIFIC MISSILE RANGE FACILITY
NAVAL UNDERSEA WARFARE CENTER DIVISION, KEYPORT

30TH SPACE WING
45TH SPACE WING
AIR FORCE FLIGHT TEST CENTER
AIR ARMAMENT CENTER
ARNOLD ENGINEERING DEVELOPMENT CENTER
BARRY M. GOLDWATER RANGE

NATIONAL NUCLEAR SECURITY ADMINISTRATION (NEVADA)

DISTRIBUTION A: APPROVED FOR PUBLIC RELEASE
DISTRIBUTION IS UNLIMITED

Report Documentation Page			Form Approved OMB No. 0704-0188	
<p>Public reporting burden for the collection of information is estimated to average 1 hour per response, including the time for reviewing instructions, searching existing data sources, gathering and maintaining the data needed, and completing and reviewing the collection of information. Send comments regarding this burden estimate or any other aspect of this collection of information, including suggestions for reducing this burden, to Washington Headquarters Services, Directorate for Information Operations and Reports, 1215 Jefferson Davis Highway, Suite 1204, Arlington VA 22202-4302. Respondents should be aware that notwithstanding any other provision of law, no person shall be subject to a penalty for failing to comply with a collection of information if it does not display a currently valid OMB control number.</p>				
1. REPORT DATE JUL 2006	2. REPORT TYPE	3. DATES COVERED 00-12-2003 to 00-12-2005		
Radar Transponder Antenna Systems Evaluation Handbook			5a. CONTRACT NUMBER	
			5b. GRANT NUMBER	
			5c. PROGRAM ELEMENT NUMBER	
6. AUTHOR(S)			5d. PROJECT NUMBER	
			5e. TASK NUMBER ET-034	
			5f. WORK UNIT NUMBER	
7. PERFORMING ORGANIZATION NAME(S) AND ADDRESS(ES) Range Commanders Council, 1510 Headquarters Avenue, White Sands Missile Range, NM, 88002			8. PERFORMING ORGANIZATION REPORT NUMBER 265-06	
			10. SPONSOR/MONITOR'S ACRONYM(S)	
			11. SPONSOR/MONITOR'S REPORT NUMBER(S)	
			12. DISTRIBUTION/AVAILABILITY STATEMENT Approved for public release; distribution unlimited	
13. SUPPLEMENTARY NOTES				
14. ABSTRACT Gives the necessary background to understand the operation of the radar transponder antenna system of a target vehicle. The antenna systems evaluator will be able to use this handbook as a reference for the principles of design, measurement, and analysis of antenna systems in a variety of environments. Many antenna scenarios are outlined and explained in detail as to its function and utility.				
15. SUBJECT TERMS Electronic Trajectory Measurements Group; antenna principles; antenna patterns; EWR 127-1				
16. SECURITY CLASSIFICATION OF:			17. LIMITATION OF ABSTRACT Same as Report (SAR)	18. NUMBER OF PAGES 175
a. REPORT unclassified	b. ABSTRACT unclassified	c. THIS PAGE unclassified	19a. NAME OF RESPONSIBLE PERSON	

Report Documentation Page			Form Approved OMB No. 0704-0188	
<p>Public reporting burden for the collection of information is estimated to average 1 hour per response, including the time for reviewing instructions, searching existing data sources, gathering and maintaining the data needed, and completing and reviewing the collection of information. Send comments regarding this burden estimate or any other aspect of this collection of information, including suggestions for reducing this burden, to Washington Headquarters Services, Directorate for Information Operations and Reports, 1215 Jefferson Davis Highway, Suite 1204, Arlington VA 22202-4302. Respondents should be aware that notwithstanding any other provision of law, no person shall be subject to a penalty for failing to comply with a collection of information if it does not display a currently valid OMB control number.</p>				
1. REPORT DATE JUL 2006	2. REPORT TYPE	3. DATES COVERED 00-12-2003 to 00-12-2005		
Radar Transponder Antenna Systems Evaluation Handbook			5a. CONTRACT NUMBER	
			5b. GRANT NUMBER	
			5c. PROGRAM ELEMENT NUMBER	
6. AUTHOR(S)			5d. PROJECT NUMBER	
			5e. TASK NUMBER ET-034	
			5f. WORK UNIT NUMBER	
7. PERFORMING ORGANIZATION NAME(S) AND ADDRESS(ES) Range Commanders Council, 1510 Headquarters Avenue, White Sands Missile Range, NM, 88002			8. PERFORMING ORGANIZATION REPORT NUMBER 265-06	
			10. SPONSOR/MONITOR'S ACRONYM(S)	
			11. SPONSOR/MONITOR'S REPORT NUMBER(S)	
			12. DISTRIBUTION/AVAILABILITY STATEMENT Approved for public release; distribution unlimited	
13. SUPPLEMENTARY NOTES				
14. ABSTRACT Gives the necessary background to understand the operation of the radar transponder antenna system of a target vehicle. The antenna systems evaluator will be able to use this handbook as a reference for the principles of design, measurement, and analysis of antenna systems in a variety of environments. Many antenna scenarios are outlined and explained in detail as to its function and utility.				
15. SUBJECT TERMS Electronic Trajectory Measurements Group; antenna principles; antenna patterns; EWR 127-1				
16. SECURITY CLASSIFICATION OF:			17. LIMITATION OF ABSTRACT Same as Report (SAR)	18. NUMBER OF PAGES 175
a. REPORT unclassified	b. ABSTRACT unclassified	c. THIS PAGE unclassified	19a. NAME OF RESPONSIBLE PERSON	

This page intentionally left blank.

**RADAR TRANSPONDER ANTENNA SYSTEMS EVALUATION
HANDBOOK**

JULY 2006

Prepared by

**TRANSPONDER AD-HOC COMMITTEE
ELECTRONIC TRAJECTORY MEASUREMENTS GROUP
(ETMG)**

RANGE COMMANDERS COUNCIL

Published by

**Secretariat
Range Commanders Council
U.S. Army White Sands Missile Range,
New Mexico 88002-5110**

This page intentionally left blank.

TABLE OF CONTENTS

LIST OF FIGURES	v
PREFACE	ix
ACRONYMS AND ABBREVIATIONS	xi
CHAPTER 1: HANDBOOK PURPOSE AND SCOPE	1-1
1.1 Introduction	1-1
1.2 Evaluator's Handbook.....	1-1
1.3 Some General Questions	1-4
1.4 List of Topics Dealing With Radar Transponder Antenna Study	1-8
CHAPTER 2: RANGE USERS INTERFACE.....	2-1
2.1 Contacting Lead Ranges	2-1
2.2 Range Requirements and Restrictions	2-1
2.3 Range User Responsibilities	2-1
CHAPTER 3: ANTENNA SYSTEM DOCUMENTATION.....	3-1
3.1 System Performance Requirements Review	3-1
3.2 System Documentation Requirements Review	3-1
3.3 Design Summary.....	3-1
3.4 Component Configuration.....	3-1
CHAPTER 4: RADAR TRANSPONDER ANTENNA SYSTEMS	4-1
4.1 Introduction	4-1
4.2 Antenna System Components	4-2
4.3 Sample Antennas.....	4-2
4.4 Antenna System Design Considerations	4-8
4.5 Placement of Unit Radiators on Target Vehicle	4-9
CHAPTER 5: SOME BASIC ANTENNA PRINCIPLES.....	5-1
5.1 General Overview	5-1
5.2 Spherical Coverage Basics.....	5-1
5.3 Antenna Pattern Spherical Coverage	5-8
5.4 Examples of Spherical Coverage from Pattern Measurement	5-9
5.5 Two Coherent Radiating Elements	5-12
5.6 Phasor Addition and Null Formation	5-14
5.7 Phasor Sum Phase Rate of Change	5-16
5.8 Phase Gradient at Pattern Minimum	5-18
5.9 Data and Graphs of Subtended Angles	5-20
5.10 Tracker Error Angle From Phase Front Distortion	5-21
5.11 Transponder Antenna System Phase Patterns	5-34
5.12 A Problem with Phase Patterns	5-36
5.13 Polarization Basic Concepts.....	5-37
5.14 The Poincare Sphere in Polarization Analysis	5-40
5.15 Polarization Considerations in Radar Returns	5-64

5.16	Notes on Link Analysis	5-65
5.17	Polarization Applied to Receiving Antennas	5-66
CHAPTER 6: ANTENNA SYSTEM MEASUREMENT AND ANALYSIS.....		6-1
6.1	Generalizations.....	6-1
6.2	Radar Transponder Antenna Measurements	6-2
6.3	Computer Simulations in Radar Target Tracking	6-5
6.4	Antenna System Performance	6-6
6.5	Measurement of the Time Delay in Transponder Antenna Systems.....	6-6
6.6	Antenna "Hat" Couplers	6-7
6.7	Choosing a Test Vehicle for Antenna Measurements.....	6-8
6.8	Analog Roll Plane Pattern Vs. Sampled Pattern	6-16
6.9	Analysis of the Interference Lobe Structure and Sampling	6-17
6.10	Strobing or Vernier Effect in Digitized Patterns.....	6-18
6.11	Three Antennas on a Cylinder.....	6-19
6.12	Harness Testing and Documentation	6-20
6.13	Antenna Test Range Sketch	6-23
6.14	Pattern Comparisons	6-28
6.15	Antenna Pattern Gain Practical Determination	6-34
6.16	Antenna Pattern Test Range Siting	6-36
6.17	Standing Wave Fields and Probing	6-38
6.18	Probing by Sweeping Frequency	6-52
6.19	Antenna Analysis Quick References.....	6-55
CHAPTER 7: EXISTING STANDARDS AND GUIDELINES.....		7-1
7.1	Introduction	7-1
7.2	Considerations of Existing Guideline Documents	7-2
7.3	Suggested References To EWR 127-1 Document	7-3
CHAPTER 8: FREQUENTLY ASKED QUESTIONS (FAQ).....		8-1

LIST OF FIGURES

Figure 4-1.	Tecom cavity backed helix.....	4-3
Figure 4-2.	Vega cavity backed helix.	4-3
Figure 4-3.	Vega tilted slotted blade.....	4-4
Figure 4-4.	U B Corp examples.	4-4
Figure 4-5.	PSL Scimitar wide band.....	4-5
Figure 4-6.	PSL folded valentine (ram's horn).	4-5
Figure 4-7.	PSL Quadraloop (blade).....	4-6
Figure 4-8.	Early style PSL low profile C-band blade.....	4-6
Figure 4-9.	PSL Combination S/C band wraparound.	4-6
Figure 4-9.	PSL Combination S/C band wraparound.	4-7
Figure 4-10.	Haigh-Farr wraparound.	4-7
Figure 5-1.	Area centered on pole.....	5-2
Figure 5-2.	Single surface patch.	5-3
Figure 5-3.	Single 2 x 2 degree patch.	5-4
Figure 5-4.	Areas near pole.....	5-4
Figure 5-5.	Dipole on Z-axis.....	5-7
Figure 5-6.	Comparison of analog and digital patterns for same measurement.	5-9
Figure 5-7.	Contour plot of right hand circular gain for three vega antennas.	5-10
Figure 5-8.	Typical graph of spherical coverage obtained from RDP data.	5-11
Figure 5-9.	Diagram of two radiating elements.	5-12
Figure 5-10.	Phasor addition diagram.....	5-14
Figure 5-11.	Graph of angle subtended by tracker dish at various distances.	5-20
Figure 5-12.	Geometry of tracker subtended from target vehicle.....	5-21
Figure 5-13.	Phase front slope.	5-22
Figure 5-14.	Angle error versus range for various null depths.	5-30
Figure 5-15.	Angle error versus range for 40 dB null depth.	5-30
Figure 5-16.	Error angle versus ripple rate at 10K yards, various null depths.	5-31
Figure 5-17.	Angle error as a function of null angular spacing.	5-31
Figure 5-18.	Angle error versus null depth for various ripple rates.....	5-32
Figure 5-19.	Angle error versus null depth.	5-32
Figure 5-20.	Pattern magnitude versus phasor rotation angle.....	5-33
Figure 5-21.	Pattern resultant phase versus phasor rotation angle.....	5-33
Figure 5-22.	Phase slope near a null.	5-34
Figure 5-23.	Radiation sphere definitions.....	5-37
Figure 5-24.	Poincare sphere definitions.	5-38
Figure 5-25.	State located by polarization ratio and phase.	5-38
Figure 5-26.	State located by axial ratio and tilt angle.	5-38
Figure 5-27.	Contours of constant axial ratio, tilt angle, component ratio and phase.	5-39
Figure 5-28.	Coupling between two states.	5-39
Figure 5-29.	Radiation sphere definitions.....	5-40
Figure 5-30.	Definitions of directions.....	5-41
Figure 5-31.	Tilt angle and axial ratio definitions.	5-42
Figure 5-32.	Definitions of E ₄₅ and E ₁₃₅ components.....	5-43
Figure 5-33.	Axial ratio definition.	5-44
Figure 5-34.	Poincare sphere definitions.	5-45

Figure 5-35.	Polarization state located by polarization ratio and phase angle.....	5-47
Figure 5-36.	Polarization state located by axial ratio and tilt angle.....	5-47
Figure 5-37.	Contours of constant axial ratio.	5-48
Figure 5-38.	Contours of constant tilt angle.	5-48
Figure 5-39.	Contours of constant polarization ratio.	5-49
Figure 5-40.	Contours of constant phase angle.....	5-49
Figure 5-41.	Polarization coupling between two states.	5-52
Figure 5-42.	Construction of 2-gamma (2γ) circle.	5-54
Figure 5-43.	Construction of the 2-gamma double-prime ($2\gamma''$) circle.	5-54
Figure 5-44.	Axial Ratio as a function of the ratios Ephi-to-Etheta and E45-to-Etheta (in dB).	5-56
Figure 5-45.	Tilt Angle as a function of the ratios Ephi-to-Etheta and E45-to-Etheta.	5-57
Figure 5-46.	Antenna image in plane mirror.	5-68
Figure 5-47.	An identical antenna receiving.....	5-69
Figure 5-48.	Matching polarizations in transmit-receive configuration.	5-70
Figure 5-49.	Poincare sphere for transmit-receive configuration.	5-71
Figure 5-50.	Poincare sphere for mirror image transmit-receive configuration.	5-72
Figure 6-1.	Firebee drone on positioner during pattern measurements.	6-8
Figure 6-2.	Pegasus bulbous fairing mockup prior to antenna testing (PSL).	6-9
Figure 6-3.	Photo gallery: Firebee Drones and mockups.	6-11
Figure 6-4.	Example: Sampling error for two antennas on a 64-inch diameter vehicle.	6-16
Figure 6-5.	Example: Sampling error for three antennas on a 38-inch diameter vehicle.	6-16
Figure 6-6.	Analog measured pattern.....	6-17
Figure 6-7.	Digital measured pattern.	6-17
Figure 6-8.	Analog pattern.....	6-18
Figure 6-9.	Digital pattern.....	6-18
Figure 6-10.	Diagram of three elements.	6-19
Figure 6-11.	Analog pattern of three elements.	6-19
Figure 6-12.	Example of harness sketch.	6-20
Figure 6-13.	Example of harness measurement results sketch.	6-21
Figure 6-14.	Example of sketch combining harness and pattern testing results.	6-22
Figure 6-15.	Example of measurement configuration sketch.	6-23
Figure 6-16.	Mockup critical dimensions sketch example.	6-24
Figure 6-17.	Coordinate system attachment to mockup sketch.	6-25
Figure 6-18.	Sketch of pattern measurement range equipment configuration.	6-26
Figure 6-19.	Sketch of signal flow configuration.	6-27
Figure 6-20.	Sketch of antenna configuration on mockup.....	6-29
Figure 6-21.	Sketch of theta constant / phi variable pattern cuts.....	6-30
Figure 6-22.	Sketch of phi constant / theta variable pattern cuts.....	6-31
Figure 6-22.	Sketch of phi constant / theta variable pattern cuts.....	6-31
Figure 6-23.	Analog phi constant patterns.....	6-33
Figure 6-24.	Analog phi constant patterns.....	6-33
Figure 6-25.	Example of gain determination worksheet.....	6-35

Figure 6-26.	Sketch showing section meeting far field criterion.....	6-38
Figure 6-27.	Sketch of two interfering wavefronts.....	6-39
Figure 6-28.	Standing wavelength for both horizontal and vertical probing.....	6-42
Figure 6-29.	Standing wavelength for vertical probing.....	6-42
Figure 6-30.	Standing wavelength for horizontal probing.....	6-43
Figure 6-31.	Mockup sketch used in arc probing (side view).....	6-44
Figure 6-32.	Sketch of motion for arc probing.	6-45
Figure 6-33.	Phasor separation graph.	6-49
Figure 6-34.	Graph for smaller phasor for ripple zero dB to 7 Db.	6-50
Figure 6-35.	Graph for smaller phasor for ripple 7 dB to 14 dB.	6-51
Figure 6-36.	Sketch of ellipse associated with path length difference.	6-53

This page intentionally left blank.

PREFACE

This handbook is intended to give the necessary background to understand the operation of the radar transponder antenna system of a target vehicle. The antenna systems evaluator will be able to use this handbook as a reference for the principles of design, measurement, and analysis of antenna systems in a variety of environments. Many antenna scenarios are outlined and explained in detail as to its function and utility.

The Electronic Trajectory Measurements Group (ETMG) would like to acknowledge production of this document for the RCC by the Transponder Ad-Hoc Committee. Specific credit is issued to the author:

Author: Morris Drexler
NewTec Corp
White Sands Missile Range, NM 88002
Phone: COM (575) 523-4000
E-Mail: morris.drexler@us.army.mil

Statement of legal rights of Mr. Drexler

Much of the material contained in this document is original material written by Mr. Drexler and extracted from his personal notes and unpublished papers. Some of the materials have been presented in various seminars, classes, reports, conferences and meetings. Mr. Drexler has the right to use and publish this material in other venues in the future; when doing so he must state that the document is owned by DoD, but he can also state that he authored the entire document.

Please direct any questions to:

Secretariat, Range Commanders Council
ATTN: TEDT-WS-RCC
1510 Headquarters Avenue
White Sands Missile Range, New Mexico 88002-5110
Telephone: (575) 678-1107, DSN 258-1107
E-mail usarmy.wsmr.atec.list.rcc@mail.mil

This page intentionally left blank.

ACRONYMS AND ABBREVIATIONS

AUT	antenna under test
CDR	critical design review
CW	continuous wave
ECM	electronic countermeasures (now known as electronic attack)
FCC	Federal Communications Commission
FTS	Flight Termination System
HPBW	half-power beamwidth
LHCP	left hand circular polarization
LHEP	left hand elliptical polarization
NBS	National Bureau of Standards
NIST	The National Institute of Standards and Technology
PDR	preliminary design review
PSL	Physical Science Laboratory (New Mexico State University)
QPSK	quadrature phase shift keying
RF	radio frequency
RAM	radar absorbing material
RDP	radiation distribution plot or radiation distribution pattern
RHCP	right hand circular polarization
RHEP	right hand elliptical polarization
SWR	standing wave ratio
VSWR	voltage standing wave ratio

This page intentionally left blank.

CHAPTER 1

HANDBOOK PURPOSE AND SCOPE

1.1 Introduction

This document is a handbook for the person who has responsibility to assess the radar transponder antenna system of a target vehicle. The target vehicle is any object fitted with a radar transponder and which must be radar-tracked on a specific test or training range.

1.1.1 Purpose and scope. The purpose of this handbook is to provide the antenna system evaluator with a reference document for answering certain questions that arise when considering specific antenna configurations on target vehicles. The handbook concentrates on the principles of antenna system design, measurement, and analysis. The sections on acceptable practices in design and measurement are based on the practical aspects of these activities. The ultimate goal of the handbook is to help improve tracking accuracy and provide the most meaningful and useful documentation possible.

1.1.2 Document organization and usage. This handbook is organized in chapters based upon general aspects of transponder antenna systems considerations. The chapters are populated with individual papers that treat specific topics that should be of concern to the antenna system designer, measurer, analyst or evaluator. Included are topics written especially for this handbook, papers previously published, sections of data reports, and references to RCC and other standards. An alphabetic list of topics with hyperlinks to associated paragraphs in this document is provided at Paragraph [1.4](#). The supplement to this document also has many excellent references and documents (See note at Paragraph [1.2.6](#)). The entire handbook is to be used primarily as a computer-based tool and has hyperlinks to specific references. It should be possible to use a hardcopy in much the same way.

1.2 Evaluator's Handbook

1.2.1 Background. Some basic assertions and assumptions should be stated if this document is to be used as a handbook for the person (government engineer) who is charged with the responsibility of evaluating an antenna system. These assertions and assumptions are discussed in the following subparagraphs.

1.2.2 Evaluator's Involvement. It is likely that the evaluator will become involved in system evaluation early in that system's development. The evaluator is assumed to be a competent engineer who is not an antenna systems expert. The government technical representative will probably be present and involved in the discussions as early as the preliminary design review. He will need to know some basic parameters of the radars that will be used in tracking the system. Some important facts will revolve around the number of launch vehicle stages and how the staging will be accomplished in terms of the antenna system. He will need to be interested in the locations of the radars with respect to the planned trajectory of the target. The radar link parameters (which include the polarizations required) depend strongly on the target's radiation pattern. The evaluator will need to have some background information as to how certain unit radiators are affected by the target's skin geometry. Understanding the polarization

characteristics of some of the more common antennas and how these antennas act when formed into a small array will be important for evaluating a potential design.

1.2.3 Qualification Testing. Qualification testing for an antenna system to be flown on a national range should be taken very seriously because the quality of radar tracking depends so strongly on the antenna system on the target. For years there have been attempts to qualify many antenna systems by “similarity” to previously tested systems. While this approach is undoubtedly less expensive for the supplier and is sometimes justified, it should be approached cautiously when target diameters, fin geometry, staging, and trajectory changes render the “similarity” marginal. The final antenna system should be subjected to critical testing which includes all the harness in its final configuration and the radiation characteristics of the final configuration. For very large vehicles (some launch vehicles) it is necessary to compromise by measuring limited sections of the vehicle. In many cases, lightweight mockups (paragraph [6.7](#)) of the important sections can quite satisfactorily represent the flight section. In some cases it is acceptable to make scale models of the target vehicle for radiation pattern measurements. Another technique which (when carefully done) can be acceptable is to make measurements on several sections and then compute the interactions of the sections to produce an overall result. There has been progress in the ability to simulate radiation patterns by computer calculations. For relatively simple structures and simple unit radiators, these simulations can yield useful results. However, the engineer should at least make some limited measurements to verify that the simulations produce acceptably accurate patterns for non-simple configurations.

1.2.4 Bench Testing. Bench testing is an area which is sometimes given too little attention. In the case of multi-element arrays on the larger vehicles, the harness parameters can become especially important. In some cases the transmission lines to the various elements in the array are of vastly different lengths. These differences in lengths result in different losses from the different elements; even more importantly, time delay differences can become very large and affect the quality of the radar track. When designing the bench testing of the harness one should be careful to include both the phase and time delay as well as loss measurements for each leg. When the harness is to be used in a multi-stage vehicle, it is important to make measurements of the entire system including the “disconnect device” terminated as in flight for each staging configuration. Some of the harness tests require terminations with antenna impedances other than the normal 50 ohms; although this is unusual, the test plan designer should be aware of such conditions and be prepared to have “antenna impedance simulators” available to terminate the appropriate lines. It is sometimes required to connect the actual antennas for some testing. Care should be taken to have the antennas mounted on the actual section (or a good mockup) so that the interaction of antennas is the same as in flight. For high power testing such as transponder testing through the entire harness, it is sometimes necessary to use coupling “hoods” or “hats” (paragraph [6.6](#)) over the radiating elements. Care should be taken to ensure that the “hoods” do not unduly disturb the normal functioning of the radiating element which is being covered. Special tests should be performed on the “antenna/hood” combination prior to committing to final testing. At least impedance disturbance tests should be performed with the antenna alone and then with the hood over the antenna. Leakage tests should be performed at the same time when practicable. Whenever tests are being made on the system impedance with the antennas attached, it should be confirmed that the antennas are essentially in a free space environment.

Special anechoic chambers are normally used for this confirmation to eliminate (or minimize) reflections from entering the antennas under test.

1.2.5 Radiation Testing. Measurement of the radiation characteristics of any antenna system can be very important and sometimes become quite complex. In the case of flight vehicles it is important to place the antenna to be measured in an environment which simulates free-space as closely as possible. Basically, this means that unintended reflections must be kept to a minimum. Actually, radiation patterns are sometimes measured on ranges that make use of carefully controlled reflections. These ranges are usually known as “groundplane ranges”. Sometimes it is possible to utilize “compact ranges” or even “near-field” measurement ranges. Each type of range presents its own set of problems and limitations, although when properly applied, most of these ranges are capable of producing acceptable pattern measurements. The elevated far-field range is probably the most common and possibly the simplest type of range to use for fairly large target vehicle antenna pattern measurements.

For antenna radiation pattern testing to be meaningful several considerations are important. These considerations are as follows:

- a. The antenna system must be configured to represent the flight condition.
- b. The antenna measurement range must be ready in terms of mechanical alignment, motion, and stability.
- c. Signal reflections must be reduced to an acceptable level and their magnitude demonstrated and documented.
- d. The equipment used to generate signals and record angular position and signal levels must be accurate and stable.
- e. Proper test procedures must be followed and a system of documentation must be utilized in order to ensure that no significant oversights occur which would compromise the validity of recorded data.
- f. A well-kept operator’s log should be maintained because it is an essential element in the documentation effort.

To properly determine the radiation characteristics of the system under test, measurements must be carefully planned and executed. The characteristics that must be accurately determined include the gains and polarization states of the measured patterns. Accurate angular alignment of the positioning system is sometimes given less attention than it deserves. An acceptable test plan should include detailed explanations on the alignment of the positioner angular indications and should describe the possible angular errors for both static and dynamic conditions.

Of primary concern is the treatment of the measured pattern data in order to yield the desired gains and polarization states. Display of the results in terms of the IRIG standard coordinate system should be considered a very important deliverable. Unusual or unauthorized terminology should be avoided in the analysis and reporting of the qualification testing.

1.2.6 Document Review. The person responsible for reviewing the documentation for the qualification of a new antenna system needs to have a minimum amount of key data available in

a form that allows for a rapid analysis. This documentation should include the basic performance objectives of the antenna system, the design philosophy, specifics of the antenna system configuration, the test plan and the test report. The evaluator will have to obtain specific operational data and trajectory information (with simulator results when available) from the radar group. The link analysis (which incorporates the pertinent data from both the radar and the target) must be used to determine the acceptability of the target antenna design (see Eastern and Western Range (EWR) 127-1 Range Safety Requirements section 4.11.1.1.3 (Range User Responsibilities)). References to EWR 127-1 are made throughout this document and readers may access the document using the following link to the EWR 127-1 web site. Also, the reader is advised that there is a list of document references in Chapter 7 of this document.

<http://snebulos.mit.edu/projects/reference/NASA-Generic/EWR/EWR-127-1.html>



NOTE
The EWR 127-1 document was published jointly by the 45th Space Wing (Cape Canaveral Air Station, FL) and the 30th Space Wing (Vandenberg Air Force Base, CA). The document presents the users of the Eastern and Western Ranges with a common set of requirements that will help minimize safety risks and maximize range user objectives.



NOTE
Standards and guidelines referred to herein are also shown in the on-line companion document: RCC Document 265-06, Radar Transponder Antenna Systems Evaluation Handbook (Supplement). The [RCC web site](#) provides linkage access to the supplement.

1.3 Some General Questions

There are many questions that the engineer assessing the proposed transponder antenna system is likely to ask. Some of these questions, discussed below, are as follows:

- a. What constitutes a good design?
- b. How should the antenna system be tested?
- c. What kind of documents should result from the testing?
- d. How should the documents be evaluated?

1.3.1 What Constitutes A Good Design? A good design is one which meets the technical requirements of the overall system. The design should be as simple as practicable while maintaining reliability. It should address failure modes so that single-point failures are avoided. In the case of radar transponder antenna systems the reliability and accuracy of the radar track are of paramount importance. Adequate coverage of the radiation sphere for the expected trajectory scenario and for some anomalies must be provided. Gain patterns with areas of many deep, sharp nulls should be avoided. When arrays of unit radiators must be employed the generalization that says “the fewer, the better” is appropriate. However, large spacing between unit radiators with broad patterns, usually results in large angular regions with many sharp nulls (See Paragraph [6.11](#)). These nulls can cause tracking errors in both angle and range. If the

pattern is used for data links, the nulls can cause data errors as well. Generally, if many “elements” are used in the antenna array, the spacing should not exceed half wavelength. These issues are discussed later in Paragraph [5.5](#). If the radar target is to have antennas on several stages yet use the same transponder for all stages, proper harness provisions must be made at the separation points (disconnect units). A good design will avoid large differences in cable harness lengths to the various elements.

Good designs result from adequate preparation, including review of fundamental antenna theory, design experience, computer simulations, and prototype testing. In many cases a good design is difficult to achieve due to lack of availability of the desired components or space on the vehicle. During a design review, it is not uncommon to hear a recommendation to place the antennas in a specific location only to be told that the location is not available due to range operations or other restrictions. The evaluators of a design should keep in mind that in many cases (if not most cases) the antenna designer is relegated vehicle territory only after the other systems engineers (propulsion, payload, aerodynamicists, etc.) have had their pick. Then the antenna engineer is told to “do the best you can with what is left ...”

A good design should have good documentation. From initial concept through to final testing of the system, documentation is sometimes the key to ultimate success. Good documentation need not be highly formalized, but it must be clear and useful. There are certain standards and requirements which should be honored, but a highly rigid system of documentation can become (or appear) restrictive and sometimes results in the loss of important information. The design and test engineers should keep detailed logbooks of a design project. These are sometimes proprietary to a company but should be available for review (by the company or designer) during government design or project reviews.

1.3.2 How should the antenna system be tested? The transponder antenna system should be tested in a manner that will expose any existing major flaws as well as substantiate the strong points of the antenna design. Tests should include bench testing of the antenna subsystems and system components which may be adequately tested without substantial radiation. The phasing harness used in multi-element arrays is a good example. Some simple bench tests may be carried out on certain types of radiating elements, but the final radiation characteristics must be measured on an appropriate antenna pattern range.

It is assumed that the transponder itself has undergone extensive testing in the “beacon lab” and is certified to be used on the particular RCC range in question. Testing of the transponder itself will not be covered in detail in this handbook, although the paper NR-DR 76-1 (Analysis Of Transponder Induced Bias Errors) deals with transponder induced tracking errors which can be associated with the functioning of the antenna system. The NR-DR 76-1 is located at the online supplement to this document at the RCC web site. The document name is RCC Document 265-06, Radar Transponder Antenna Systems Evaluation Handbook (Supplement).

Bench testing should involve the use of certain basic microwave test equipment, such as a vector network analyzer, synthesized signal source, frequency counter, and spectrum analyzer. The combination of synthesized signal source and vector network analyzer is at the heart of many tests. The most important of these tests may be the insertion loss measurements and the

impedance measurements. The antenna system (usually) includes coaxial cables, power divider/combiners and unit radiating elements. Each component should be tested separately and in combination with the other components to demonstrate that all parts and interconnections perform acceptably. Each cable should be measured for insertion (loss, phase and time or RF. length) as well as for impedance. Each power divider/combiner should be tested for both of the following:

- a. Impedance at each port
- b. The power splitting characteristics in amplitude and phase.

Since the nominal characteristic impedance of the components in these antenna systems is 50 ohms, measurements should be made with 50 ohms terminating all (otherwise open) ports. As the harness is pieced together on the bench the measurements should be made to demonstrate that no combination of components yields an unacceptable overall result in impedance or insertion (loss or phase). Each measurement should be recorded as to procedure and result. (For more details see Chapter [6](#).

Radiation testing often begins with the measurement of the patterns of the individual (unit) radiating elements. The designer needs to know what the element pattern is in order to design an adequate array. The final radiation pattern measurements must involve the actual radiating elements mounted on a vehicle (flight hardware or appropriate mockup) of the correct size, shape and skin characteristics to simulate the flight vehicle. This antenna system must then be placed in an essentially “free space” environment for the pattern measurements. The final impedance measurement of the antenna system (and unit radiators) may best be done when the “mockup” is mounted for radiation pattern measurements. A few basic things that the “assessor” should be looking for include pattern range preparation, calibration and operation. Part of the preparation of a pattern measurement range is establishing how “clean” the range is. This means that some demonstration should be required to assess the amount of range reflections that are present in the measurement aperture. Field probing (paragraph [6.17](#)) is generally used to determine the magnitude of the range reflections and to demonstrate that the reflections are small enough (far field elevated ranges). On ground plane (or “ground reflection”) ranges the heights of the test article and the range antenna must be properly set and demonstrated.

Other issues for preparation and calibration of the pattern measurement range surround the accuracy of the angle measurement used in reporting patterns. Usually, the patterns are measured by reference to positioner angles reported by synchros or encoders on the positioner axes. Normally, optical methods (lasers or theodolites and mirrors) are employed to align the various axes to the desired RF. axes. In multi-axis positioners it is important to set and demonstrate the orthogonality of the system. The angle zeros and axis orthogonality are very important to the accuracy of the ultimately reported patterns, especially near theta equal zero and 180 degrees.

Operation of the range is something that the “assessor” typically observes. He should be aware that the overall accuracy of the gain measurements will depend on the deployment of the gain standard as well as its degree of calibration. Simply knowing that the “gain horn” was calibrated by The National Institute of Standards and Technology (NIST)/National Bureau of

Standards (NBS) to a certain value is not an assurance that it will display this gain when employed in the “transfer” or “substitution” gain measurement. All cables, adapters, and connectors involved are important. Also important is the ability of the gain horn to “see” the same wave or waves that the test article sees. A narrow beam gain horn and an omni-directional test antenna will generally see different waves on the test range (that has reflections), and consequently show an inaccurate comparison.

The gain and efficiency of the antenna system are quantities of great interest to the antenna engineer. The gain is usually determined by a substitution method in which the antenna under test (AUT) is substituted for a known gain standard (see section [6.15.2](#) for an example Gain Worksheet). The efficiency is determined by comparison of the gain with the integration of the power pattern over the entire radiation sphere. In order to obtain an accurate value of efficiency, both the gain and the integration must be accurate. In Paragraph [6.9](#) (LobeDetails) and Paragraph [6.10](#) (Strobing), it is shown that the integration accuracy can be compromised by an improper selection of sample spacing during the measurement of the spherical pattern, radiation distribution pattern (RDP).

1.3.3 What kind of documents should result from the testing? The design approach should be described in some form of report. The report should identify the assumptions on what the antenna system is required to do and how the proposed design will accomplish the goals. Simulations of the unit radiators and the array should be explained and the results shown.

Choice of the components and the configuration should be explained in adequate detail to allow the evaluator to understand why the particular selections were made. The bench testing approach should also be discussed in detail. The equipment used and the methods employed in making each type bench test should be described and including sketches of the test equipment configurations. The measured results for all the components and combinations should be shown; examples of some of these items are shown in Paragraph [6.12](#) and Paragraph [6.13](#).

Since the radiation pattern is of such great importance to the overall radar/transponder link, its measurement should be documented in exceptionally thorough and lucid form. The choice of the pattern measurement range should include the essential parameters of range length, range axis height, positioner types, range antenna types, and gain standards. The equipment used for pattern measurements and the method of generating desired polarization components should be explained. Sketches of the range geometry and measurement equipment should be included. Range reflection probing methods should be discussed and incorporate examples demonstrating the estimated reflection level. Methods and results of positioner alignments should be presented.

Data analysis programs and approaches should be included and demonstrated. All measured patterns should be available in formats suitable for ease of review and analysis. Results such as spherical coverage, gain, directivity, and efficiency, should be plotted and proper explanations given for each. In this regard, the accuracy of the digitized patterns and thus the accuracy of coverage and efficiency should be substantiated by displaying some analog patterns of the roll planes to show the extent to which interference nulls are misrepresented in the digital form. If analog patterns are not possible, then digitized patterns taken with much reduced sample spacing should be presented. The analog pattern surrogate should show the roll plane (at

least) with ten or more samples per cycle of interference lobes (examples, showing the sample spacing effects are presented in (Paragraph 6.8)).

1.3.4 How should the documents be evaluated? The “assessor” should have at his disposal all pertinent documentation with which to analyze the design and performance of the antenna system presented. A checklist should be used to ensure that no major area of concern is overlooked in the assessment of the antenna system. Everything from the configuration design to the radiation pattern testing should be considered as to whether it is appropriate and adequate. The testing should be thorough enough and include enough documentation to ensure the effectiveness and reliability of the overall system in the expected flight scenario. Testing is to be made under proper circumstances and on appropriate mockups for meaningful results.

1.4 List of Topics Dealing With Radar Transponder Antenna Study

<u>Short Title</u>	<u>Description</u>	<u>Cross Reference</u>
<u>A/D Roll Plane Patterns</u>	Comparison of Measured Digital and Analog Roll Plane Patterns	Para 6.8
<u>Angle Error</u>	Tracking angle Error Graphs	Para 5.10.3
<u>Antenna Sys Components</u>	Antenna System Components	Para 4.2
<u>Antenna Sys Design</u>	Antenna Systems Design Considerations	Para 4.4
<u>Antenna Measurements</u>	Basic Areas of Consideration for Antenna Systems Measurement	Para 6.2
<u>Antenna Range Setup</u>	Antenna Test Range Sketch	Para 6.13
<u>Antenna Hoods & Hats</u>	Thoughts on use of antenna “Hoods” (or “Hats”)	Para 6.6
<u>Antenna System Perf</u>	Antenna System Performance	Para 6.4
<u>Coverage</u>	Antenna Pattern Spherical Coverage	Para 5.3
<u>Coverage Examples</u>	Examples of Spherical Coverage from Pattern Measurement	Para 5.4
<u>Choose Test Vehicle</u>	Choosing a Test Vehicle for Antenna Measurements	Para 6.7
<u>Cross-Eye</u>	Phase patterns and phase-front distortion	Para 5.11
<u>Delay Measurement</u>	Drawing attention to NR-DR 76-1 report	Para 6.5
<u>Ellipse/Range Reflections</u>	Probing by Sweeping Frequency	Para 6.18
<u>Evaluator Considerations</u>	What an evaluator should consider (Handbook)	Para 1.2
<u>Firebee Drone</u>	Picture Gallery of Firebee Drone	Fig 6-3
<u>Good Design Questions</u>	Some General Questions	Para 1.3
<u>Guidelines</u>	Considers Specific Existing Standards Documents	Para 7.2
<u>Harness Measurements</u>	Harness Testing and Documentation	Para 6.12

<u>Short Title</u>	<u>Description</u>	<u>Cross Reference</u>
<u>Lobe Details</u>	Analysis of Interference Lobe Structure and Sampling	Para 6.9
<u>Mockups (Drones)</u>	Drone Mockups (In Picture Gallery of Drones)	Fig 6-3
<u>PatternNull</u>	Computing a Cycle of Ripple Pattern	Para 5.10.7
<u>Phase Pattern Problem</u>	A Problem with Phase Patterns	Para 5.12
<u>Phasors</u>	Phasor Addition and Null Formation	Para 5.6
<u>Phasor Rate of Change</u>	Derivation of Phase Rate-of-Change for Two Phasors	Para 5.7
<u>Placement/Unit Radiators</u>	Placement of Unit Radiators on Target Vehicle	Para 4.5
<u>Polarization Basics</u>	Introduction to Poincare Sphere	Para 5.13
<u>Poincare Sphere</u>	The Poincare Sphere in Polarization Analysis	Para 5.14
<u>Quick References</u>	Antenna Analysis Quick References	Para 6.19
<u>Range Siting</u>	Antenna Pattern Test Range Siting	Para 6.16
<u>Rate of Change</u>	Phase Gradient at Pattern Minimum	Para 5.8
<u>RCS & Polarization</u>	Some Polarization Considerations for Radar Returns	Para 5.15
<u>References to EWR 127-1</u>	Suggested References to EWR 127-1 Document	Para 7.3
<u>Sample Antennas</u>	Illustrations of Some Radar Transponder Antennas	Para 4.3
<u>Sample Patterns</u>	Examples of Measured Patterns	Para 6.14
<u>Simulations</u>	Thoughts on the use of Simulations	Para 6.3
<u>Sphere Cover</u>	Spherical Coverage Basics	Para 5.2
<u>Standing Wave</u>	Standing Wave Fields and Probing	Para 6.17
<u>Three Antennas (Pattern)</u>	Pattern Example for Three Antennas on a Cylinder	Para 6.11
<u>Tracker Error</u>	Tracker Error Angle from Phase Front Distortion	Para 5.10
<u>Two Elements</u>	Pattern Nulls versus Antenna Separation	Para 5.5

This page intentionally left blank.

CHAPTER 2

RANGE USERS INTERFACE

2.1 Contacting Lead Ranges

Any prospective user of a test range should contact that range well in advance of any desired testing. A new target vehicle or configuration must be assessed by the range safety and radar personnel of the test range. A good starting point for finding the proper contacts would be the RCC secretary at:

**Secretariat
Range Commanders Council
U.S. Army
White Sands Missile Range
New Mexico 88002-5110**

or visit

<http://www.jcte.jcs.mil/rcc/ORGAN/sec.htm>

or

http://www.jcte.jcs.mil/rcc/site_map.html

2.2 Range Requirements and Restrictions

Each test range has some form of range users reference manual or range users guide that set forth the basic requirements of that range with respect to the acceptable target vehicles. Many details to be agreed on include the certification of components, required trajectories, and scheduling. The lead range requires specific documentation that applies to the proposed target vehicle. Transponder and antenna system designs are of special interest and will be considered in detail. Range safety considerations are of utmost importance and usually involve telemetry systems and radar systems as well as flight termination systems.

2.3 Range User Responsibilities

In several of the RCC documents, the responsibilities of the range user are discussed. A starting point for the prospective user concerned with the radar transponder antenna system on a target might be EWR 127-1 (1997). Selected portions of EWR 127-1 can be viewed at the Supplement to RCC Document 265-06. Section 4.11 of EWR 127-1 deals specifically with the antenna system. Transponder Antenna System General Design Requirements is covered in section 4.11.1.1 which provides the basic overview. Antenna System Electrical Performance requirements are discussed in section 4.11.1.2 and should be understood by any interested potential range user. Of specific interest is the required link analysis section, (mentioned in section 4.11.1.3) containing the implications that characteristics of the ground based radars' radiation as well as those of the target must be considered in detail. The antenna analysis

required is mentioned in section 4.11.1.1.4. Prelaunch tests for the Transponder Antenna system should be understood and a description may be found in section 4.15.3.5.2 which mentions the use of antenna “hats” or couplers. Included in EWR 127-1 is an appendix that lists the requirements for the documentation in terms of the diagrams, analyses and descriptions for the Transponder Antenna System (section 4A.2.2.2). A more complete version of the EWR 127-1 document is at

<http://snebulos.mit.edu/projects/reference/NASA-Generic/EWR/EWR-127-1.html>

A list of other key documents of earlier dates is included in Chapter 7, with information on how to obtain them. These references provide good information and provide other perspectives on some of the same issues discussed here.

CHAPTER 3

ANTENNA SYSTEM DOCUMENTATION

3.1 System Performance Requirements Review

The radar transponder antenna system on a flight vehicle is required to meet performance requirements. Some of these requirements may be specific to a particular test range, but most of them are common to nearly all the RCC ranges. At the outset of a project, the antenna system designer must be provided a list of specific requirements that the new design must meet. This same list should be given to the evaluator in order to evaluate the design and implementation of the antenna system. Parameters such as the proposed trajectory, frequency of the radar signal, roll stability of the target vehicle, and required tracking accuracy are essential inputs to the antenna designer and antenna system evaluator.

3.2 System Documentation Requirements Review

The antenna system design evaluator, like the designer, needs to have a specific list of the required documents for the antenna system on a target vehicle. Many of the required documents are specified in the RCC documents, including the RCC-253-93 and EWR 127-1. The lead range upon which the vehicle is to be flown should provide a complete list of requirements to the designer very early in discussions about the proposed program.

3.3 Design Summary

A preliminary design review should yield a detailed (proposed) design document for the antenna system. This document should be available to the evaluator at the earliest possible time. In some cases the person who is assigned to be the final evaluator may not have been present at the preliminary design review (PDR) nor even at the critical design review (CDR) but yet must become fully informed as to the project's design and testing. He should insist upon having enough documentation time to study and analyze the project's documentation.

3.4 Component Configuration

Diagrams of the antenna system configuration should contain adequate detail to allow the evaluator to make critical calculations and estimates of the overall system performance. The diagrams should show the component descriptions, designations, and placement(s) on the vehicle. Line lengths and insertion-loss values should be clearly marked on the diagrams. Although measured values are preferred, they may not be available in the early design phase and therefore estimates may be the only values available. These diagrams give the evaluator an overview of the antenna system.

This page intentionally left blank

CHAPTER 4

RADAR TRANSPONDER ANTENNA SYSTEMS

4.1 Introduction

This chapter presents an overview of the general aspects of radar transponder antenna systems.

4.1.1 Usage and Frequency Bands. The frequency allocations for radar transponder use are discussed in the RCC document 250-91. A brief paraphrase of those frequencies is given below. Note that some of the frequency bands listed below are being modified by government agencies such as the FCC, so it is recommended that a careful search be made for the latest band limits.

<u>L-Band</u>	<u>1215 to 1400 MHz</u> (1215 to 1300 and 1350 to 1400) Primary (1300 to 1350) Secondary
<u>S-Band</u>	<u>2300 to 3700 MHz</u> (2300 to 2450 and 3100 to 3700) Primary (2450 to 2500 and 2900 to 3100) Secondary
<u>C-Band</u>	<u>5250 to 5925 MHz</u> (5250 to 5460 and 5650 to 5925) Primary (5470 to 5600 and 5600 to 5650) Secondary
<u>X-Band</u>	<u>8500 to 10000 MHz</u> (8500 to 9000 and 9200 to 9300 and 9500 to 10000) Primary (9000 to 9200 and 9300 to 9500) Secondary

4.1.2 Configurations. Radar tracking transponders and antennas are usually installed in all vehicles or sections that must be tracked during flight. Configurations vary from a simple single stub antenna and one transponder on an aircraft to multiple transponders and antennas on multiple sections of launch vehicles. There are cases in which each section has its own transponder and antenna system. Other configurations utilize one transponder and multiple antenna systems for multi-stage targets. Special considerations must be given to the jettisoning of spent stages that have active antennas. The switching to succeeding stages has implications as to antenna impedance and antenna patterns that affect the radar tracking quality.

4.2 Antenna System Components

Although target vehicle antenna systems may appear quite simple, the design and performance of those systems depend upon many inter-related factors. The individual component groups of an antenna system include the unit radiating elements, the interconnecting cabling, the power dividers/combiners and any special devices required to ensure proper functioning for the planned flights.

4.2.1 Unit Radiators. The unit radiators are the individual antennas that receive the radar interrogation signal and transmit the transponder's response. The design and configuration of these on a given target can become quite complex depending upon the radar parameters and the test scenario. Consideration to the number and placement of the unit radiators must be given to ensure adequate coverage of the required polarization components for the duration of the flights.

4.2.2 RF Cables. The transponder signal must be connected to the antenna system. The interconnecting RF harness is critical to proper operation and affects the tracking accuracy. The signal loss and the phase from each unit radiator must be carefully controlled. It is important to realize that specific definitions apply to the cable system which differentiates those which are considered to be part of the "antenna" from those which are "interconnecting" cables. In general, any cable which determines the "aperture distribution" is part of the antenna whereas the cables which are common to the entire antenna array are not part of the antenna itself; however, they are part of the overall "antenna system" and must be accounted in the overall loss budget.

4.2.3 Power Dividers and Switches. Power dividers, which function as power combiners on receive, are definitely part of the antenna when they are used to sum the signals from the individual unit radiators. The loss, power handling capabilities, frequency range, and phase length are important considerations for power dividers and switches use in antenna systems.

4.2.4 Stage Separation Connections. There are some special considerations which apply to certain "breakaway" connectors used in antenna systems on multi-stage targets. The effects on the antenna systems prior to separation and post separation must be carefully considered. If these devices are not correctly incorporated into the antenna harness, difficulties with reflected impedance might become detrimental to the antenna performance post separation.

4.3 Sample Antennas.

Photos of some sample antennas are shown on the following pages as:

- Figure 4-1. Tecom cavity backed helix.
- Figure 4-2. Vega cavity backed helix.
- Figure 4-3. Vega Tilted Slotted Blade.
- Figure 4-4. U B Corp examples.
- Figure 4-5. Physical Science Laboratory (PSL) Scimitar wide band.
- Figure 4-6. PSL Folded valentine (ram's horn).
- Figure 4-7. PSL Quadraloop (blade).
- Figure 4-8. Early style PSL low profile C-band blade.
- Figure 4-9. PSL Combination S/C band wraparound.
- Figure 4-10. Haigh-Farr wraparound.



Figure 4-1. Tecom cavity backed helix.

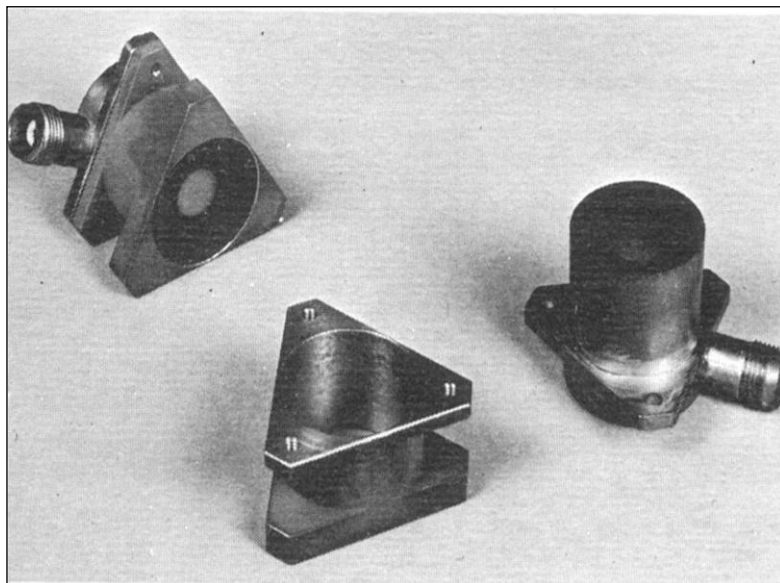


Figure 4-2. Vega cavity backed helix.

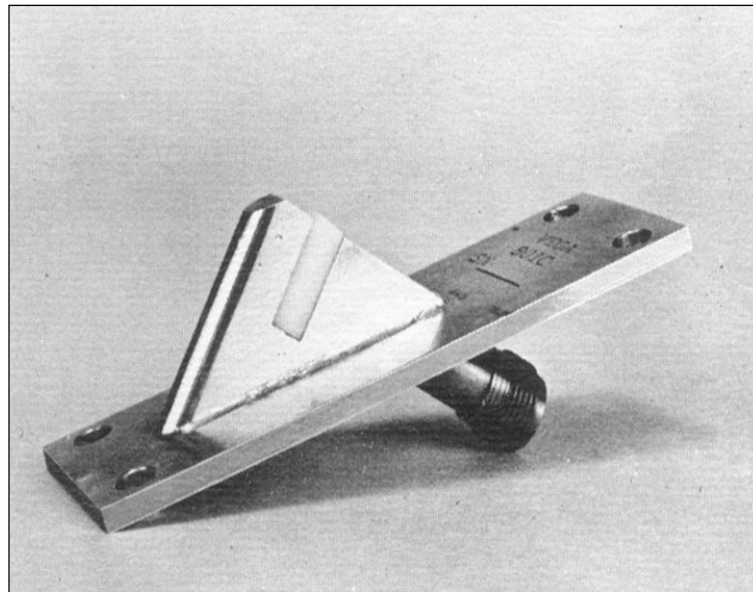


Figure 4-3. Vega tilted slotted blade.

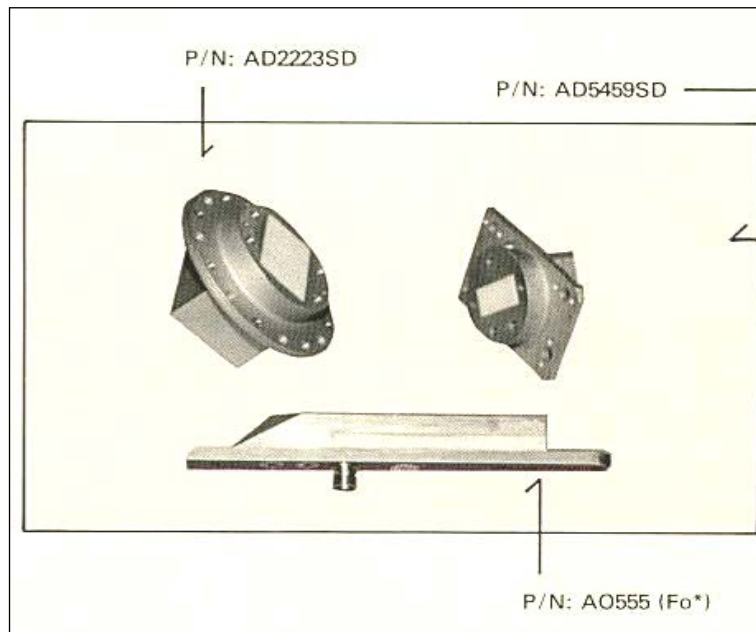


Figure 4-4. U B Corp examples.



Figure 4-5. PSL Scimitar wide band.

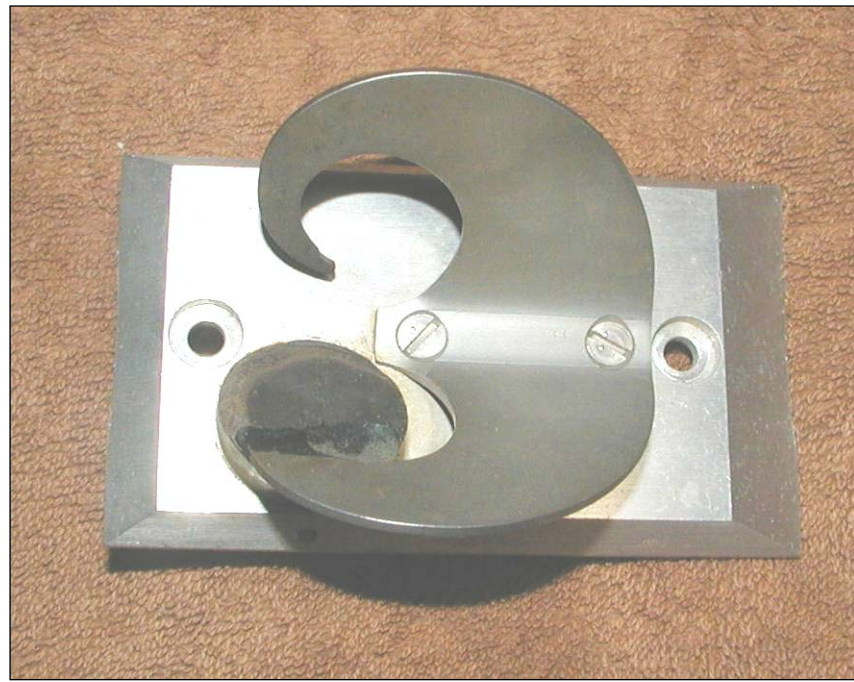


Figure 4-6. PSL folded valentine (ram's horn).

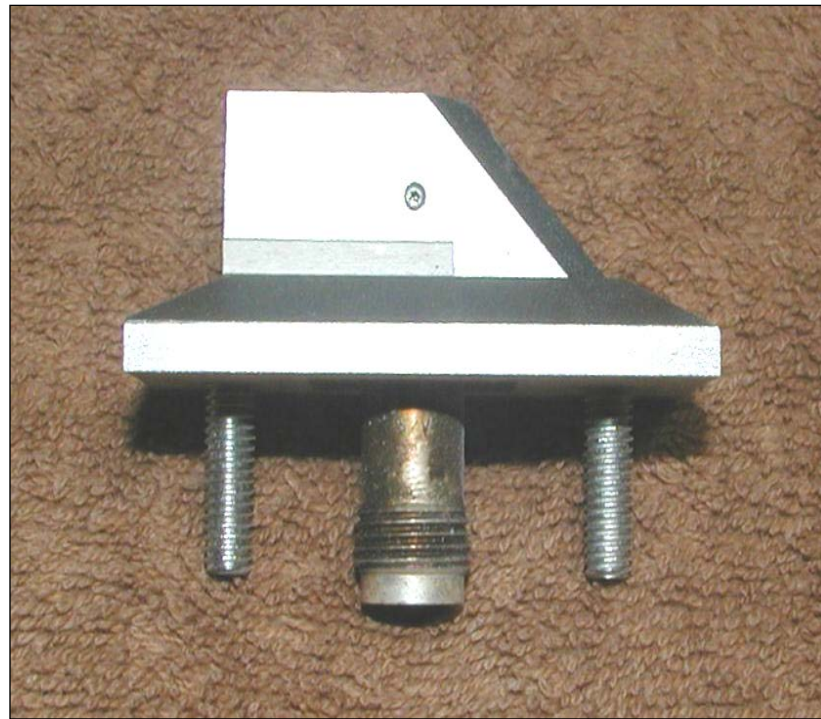


Figure 4-7. PSL Quadraloop (blade).



Figure 4-8. Early style PSL low profile C-band blade.

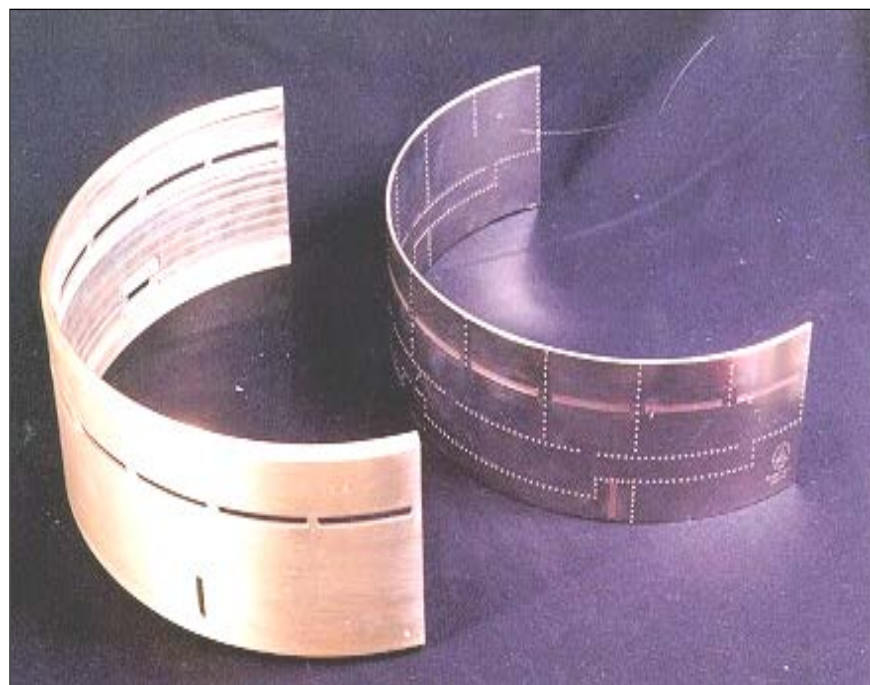


Figure 4-9. PSL Combination S/C band wraparound.



Figure 4-10. Haigh-Farr wraparound.

4.4 Antenna System Design Considerations

The following paragraphs describe some of the considerations during antenna design.

4.4.1 Vehicle Skin - Area and Type. The target vehicle skin parameters can have a profound impact on the performance of the individual radiators and thus on the overall antenna system performance. Aluminum skin, which is a reasonably good conductor, was for many years the only skin surface upon which antennas were mounted. Predictions of the antenna performance were made with great accuracy by assuming that the surface surrounding the individual antennas was a perfect conductor. With the advent of composite materials used in target vehicles, the designer must be aware of the skin conductivity and the possible losses associated with surface currents.

4.4.2 Unit Radiator - Type and Polarization. The most common types of antenna used as elements in arrays on target vehicles are generally categorized as “circularly polarized” and “linearly polarized”. However, the “flush-mounted” and the “blade” types are also categories of antenna types. There are “individual elements” and there are “wrap around” or “belly band” arrays (these are usually flush or nearly flush mounted types). Probably a more important antenna feature is the amount of local skin area it requires to function properly. Microstrip patch-type antennas depend very little on the nearby skin for determining the impedance loss or pattern shape. The flush mounted cavity backed quartz loaded helix types (made by several manufacturers) tend to depend only slightly on the local skin parameters. The “stub” and “blade” types are the ones which really need a lot of territory to function properly. The electrical parameters of the skin on which an antenna is mounted may well determine the type of antenna which should be used on a particular vehicle.

4.4.3 Tracking Radar - Characteristics. The interaction of radar and transponder antenna is at the heart of the transponder antenna system design. The polarization characteristics of the radar must be considered when designing or evaluating the target antenna design.

4.4.4 Local Obstructions - Fins, Antennas, Cavities. Many target vehicles must support three or four different antenna systems in a very limited area of skin. Best results are obtained if the radar transponder antennas are placed well away from the other antennas and reflecting obstructions. Sometimes the FTS antennas are of the “blade” or “quadraloop” type and could cause substantial “shadow” areas in the pattern of a nearby radar antenna. The S-band telemetry antennas are sometimes “blade” types and possibly “slots”. The radar antennas should be spaced many wavelengths from the other antennas whenever possible.

4.4.5 Reflections. Fins and other aerodynamic devices are generally large in terms of wavelengths and can cause major reflections and thus redirect waves from the transponder antennas. This redirection of waves causes shadow areas behind the fin and interference zones in other directions where direct and reflected waves can interact. It is possible to analyze these areas to a reasonable degree with simple ray tracing techniques to determine if the reflecting objects will cause difficulties in the patterns.

4.5 Placement of Unit Radiators on Target Vehicle

For many (if not most) target vehicles, the locations and space available for mounting the antennas are very limited. The mission specific essentials must be considered first in terms of weight, strength, and aerodynamics. After the mechanical engineers are reasonably satisfied with the vehicle design, then the antenna engineers are presented with a few (sometimes undesirable) possible antenna locations. Then the available territory must be shared with the requirements of the flight termination system (FTS), telemetry and Global Positioning System (GPS), and the radar antenna engineer. This situation is not an easy problem to solve in most cases.

For each band or service, the antenna system configuration must be able to negate all potential frequency interferences. The FTS antennas may be of the non-flush blade type that could cause both reflections and shadowing in the farfield patterns. The telemetry antennas are sometimes non-flush as well while the radar transponder antenna types are most often flush-mounted (on missiles, at least). The antenna systems of each type must not cause problems with other antenna types and simultaneously avoid trouble from the same antennas.

Different types of antennas rely differently on the surrounding skin area and surface type. Generally, the blade type antennas, including simple stubs, require substantial conductive skin area around the mounting position. The skin currents that are set up on the skin determine the radiation pattern and antenna impedance. It is important to avoid putting other antennas too close to these types of unit radiators. Normally, the flush mounted cavity backed spiral types used for radar transponder systems rely less on the surrounding skin than do the stub types. The flush (or nearly flush) mounting microstrip-type antennas are the least dependent on the surrounding skin for generating their impedance and pattern.

The location of large reflecting objects (such as fins) is to be considered even when they are a considerable distance from the unit radiator. If these large reflecting objects subtend a substantial angle from the unit radiator, they could cause undesirable pattern features from both shadowing and reflections. Sometimes only the shadowing is considered because it produces a reduced gain in that direction. Sometimes overlooked is the fact that that signal which is missing in the shadow region is adding vectorially in the direction away from the shadow. The area of summation for this reflected signal and the direct signal must be well thought-out in terms of signal strength and polarization.

The proper placement of radar transponder antennas is not always obvious. On generally cylindrical missiles the type, number, and placement of the radiators should be chosen to yield adequate coverage of the desired polarization component and to (above all) avoid the generation of many areas of deep, sharp nulls. On some targets that will not be rolling, it is possible to use a single well-placed antenna. For rolling targets the most desirable type antenna probably is the “wraparound” or “bellyband” antenna. This type antenna has individual radiators spaced approximately a half wavelength apart completely around the vehicle. The result is that no interference nulls will be generated and the coverage (in roll) is reasonably uniform. The general rule is that when it comes to the number of radiators, fewer is better unless they can be placed within a half wavelength of each other; on diameter vehicles and the higher frequencies, radiator placement becomes more and more difficult. Some ranges deal with aircraft more than with

missiles. Aircraft present some special antenna placement problems because of the missions being flown. Sometimes a single non-flush “stub” type antenna is used and placement is selected for convenience of access rather than for best radiation characteristics. The loss in a long cable from the transponder to an antenna must be considered, but retrofitting a transponder to a place close to the antenna can cause difficulties. If possible, the antenna should be mounted such that it is “visible” to all azimuth angles in level flight. When the missions call for the aircraft to be flying away from the radar, a nose mounted antenna probably will not perform well for tracking. On the other hand, an antenna (stub type) mounted on top of the vertical stabilizer probably will provide good coverage. If the aircraft will present its bottom side to the radar much of the time it would make sense to mount a stub type antenna on the bottom. Wing pods, external fuel tanks, and external weapons can make the choice of antenna placement on an aircraft more difficult. The mission flight profile is a factor for every transponder antenna placement. The possibility of using more than one unit radiator with switching has been explored and used in some installations; however, this can cause issues with precision tracking when widely spaced antennas are switched. On the other hand, if the multiple antenna system is not switched, that is all driven, then they form an array which will produce a pattern with many lobes and become virtually useless for tracking.

In many cases, the number and types of antennas used on a target vehicle are driven by economics. The limited bandwidth of most microstrip patch-type antennas may dictate the need for expensive duplication of similar designs, where use of individual wider bandwidth units would be far less costly. If the antennas must be mounted on a non-metallic skin with high signal losses, the type of unit radiator may well depend on the expected overall antenna system efficiency due to the skin material.

CHAPTER 5

SOME BASIC ANTENNA PRINCIPLES

5.1 General Overview

5.1.1 Amplitude - Gain Variations and Spherical Coverage. Gain variations in the radiation pattern of the transponder antenna system can be responsible for range tracking errors. As the target antenna pattern gain changes, the interrogate signal presented to the transponder varies. This variation in signal strength can cause changes in the trigger time of the transponder (and ultimately range errors) as seen by the radar. The reader is directed to the report NR-DR 76-1 which discusses this type of error in detail (See Paragraph [7.1.3](#)).

Spherical coverage values are of less concern to the radar transponder antenna design than they are to the flight termination system (FTS) antenna design because the radar usually has enough power density to “see through” relatively deep nulls in the target antenna pattern. The avoidance of many sharp, deep nulls is the primary concern about the transponder antenna pattern. See Paragraph [5.10](#) for a detailed discussion of this topic.

5.1.2 Phase - Harness Delays and Pattern Nulls. In multi-element arrays of unit radiators, the signal path lengths to the summing point sometime vary considerably. These variations can become tens of wavelengths in some installations. When a radar interrogate pulse stream enters through two or more of these paths, the pulse presented to the transponder can become distorted and cause triggering time variations or even mis-triggering (See Paragraph [6.5](#)).

5.1.3 Polarization - Mismatch Loss. The interrogating radar and the target vehicle antenna pattern should have matched polarizations in order to transfer the maximum signal. Understanding how the polarization states are specified and measured is essential to determining how the radar will interact with the target. A brief discussion of the principles of polarization analysis is given in Paragraph [5.13](#).

5.2 Spherical Coverage Basics

The following introduces computation of the spherical coverage by an antenna pattern.

5.2.1 Spherical Coverage Requirements.

- a. Analysis of full sphere pattern measurement (radiation distribution pattern (RDP)) data is required. A computer program usually performs level testing and summations. Tabular and graphical plots are the preferred display methods (see Paragraph [5.3](#))
- b. Usually specified as fraction of total radiation sphere which is at or above some specified gain level. Also, specific polarization components are considered as well as total gain (See Paragraph [5.4](#)).
- c. Result from trajectory and RF link calculations.
- d. Roll stable vehicle may ease some coverage requirements.
- e. Receiver sensitivities and ground station effective isotropic radiated power (EIRP) ultimately determine coverage level.

5.2.2 Spherical Coverage Computation.

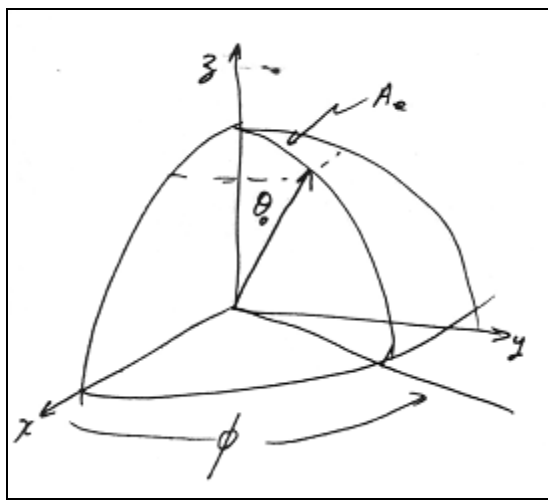


Figure 5-1. Area centered on pole.

Total Spherical Area

$$A_t = 4\pi$$

Single Area Centered On Pole (See Figure 5-1)

$$A_e = \int_0^{2\pi} \int_0^{\theta_0} \sin\theta \, d\theta \, d\phi$$

$$A_e = 2\pi \int_0^{\theta_0} \sin\theta \, d\theta$$

$$A_e = 2\pi | -\cos\theta |$$

Evaluated from 0 to θ_0

Which is $A_e = 2\pi (1 - \cos\theta_0)$

To find the fraction of spherical area from the pole ($\theta = 0$) to $\theta = \theta_0$,

$$A_p = \frac{A_e}{A_t} = \frac{2\pi (1 - \cos\theta_0)}{4\pi} = \frac{(1 - \cos\theta_0)}{2}$$

5.2.3 Examples of Coverage Calculations.

- a. What fraction of the spherical surface is included from $\theta = 0$ to $\theta_0 = 10^\circ$?

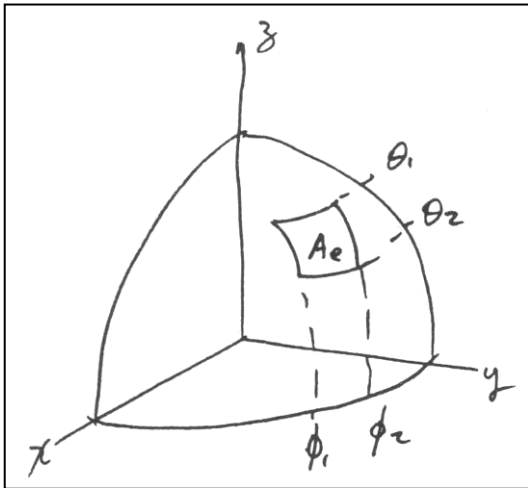
$$A_p = \frac{(1 - \cos\theta_0)}{2} = \frac{(1 - \cos(10^\circ))}{2} = 7.596 \times 10^{-3},$$

Which is $A_p = 0.76\%$

- b. How about from $\theta = 0$ to $\theta_0 = 26^\circ$

$$A_p = \frac{(1 - \cos\theta_0)}{2} = \frac{(1 - \cos(26^\circ))}{2} = 0.051,$$

Which is $A_p = 5.1\%$



Surface Patch

In the case of a general patch of surface (Figure 5-2) bounded by $\theta_1, \theta_2, \phi_1, \phi_2$

$$A_e = \int_{\phi_1}^{\phi_2} \int_{\theta_1}^{\theta_2} \sin \theta \, d\theta \, d\phi$$

$$A_e = (\phi_2 - \phi_1)(\cos \theta_1 - \cos \theta_2), \text{ (angles in radians)}$$

Figure 5-2. Single surface patch.

If both angles are expressed in degrees, we get

$$A_e = \left(\frac{\pi}{180} \right) (\phi_2 - \phi_1) (\cos \theta_1 - \cos \theta_2)$$

Then by normalizing to the total spherical surface

$$A_e = \left(\frac{1}{4\pi} \right) \left(\frac{\pi}{180} \right) (\phi_2 - \phi_1) (\cos \theta_1 - \cos \theta_2)$$

Which simplifies to:

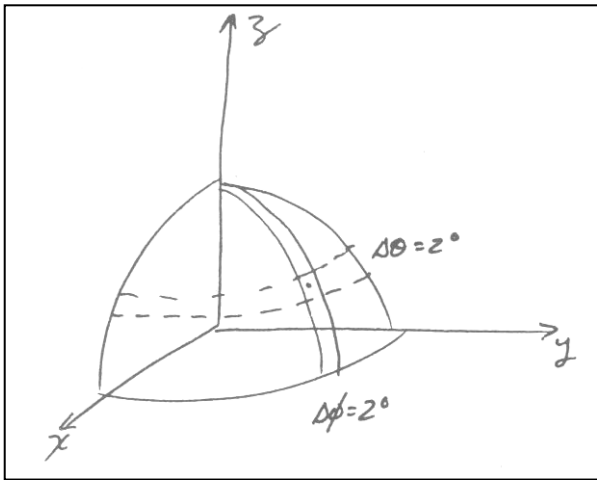
$$A_e = \left(\frac{\phi_2 - \phi_1}{720} \right) (\cos \theta_1 - \cos \theta_2)$$

What portion of the spherical surface is included within the bounds?

$$\phi_1 = 0^\circ; \quad \phi_2 = 45^\circ; \quad \theta_1 = 45^\circ; \quad \theta_2 = 90^\circ$$

$$A_e = \left(\frac{45^\circ - 0^\circ}{720^\circ} \right) (\cos(45^\circ) - \cos(90^\circ)) = \left(\frac{1}{16} \right) \left(\frac{\sqrt{2}}{2} - 0 \right) = 0.04419,$$

Which is 4.42 %

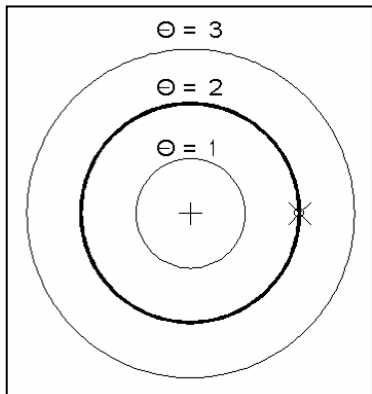


In the specific case of RDP's taken at $\Delta\phi = \Delta\theta = 2$ degrees, we need to know what area to assign to each sample. (See Figure 5-3)

Clearly, samples near $\theta = 0$ or $\theta = 180$ have less area for their 2° by 2° spacing than those samples near $\theta = 90$ degrees. Still the general case (normalized to unit sphere) is given by

$$A = \left(\frac{\phi_2 - \phi_1}{720} \right) (\cos \theta_1 - \cos \theta_2) \quad (\text{angles in degrees})$$

Figure 5-3. Single 2×2 degree patch.



The first non-zero theta value is $\theta = 2^\circ$. From construction, the area involved for a sample at $\theta = 2^\circ; \phi = N$ extends from $\theta_1 = 1^\circ$ to $\theta_2 = 3^\circ$ and from $\phi_1 = N-1$ to $\phi_2 = N+1$. (See Figure 5-4) The difference between any two adjacent phi sample points is 2 degrees. The numerator will be 2 degrees.

Thus, for any given sample point θ, ϕ (angles in degrees) the fraction of area is:

$$A = \left(\frac{1}{360} \right) [\cos(\theta-1) - \cos(\theta+1)]$$

Figure 5-4. Areas near pole.

But $\cos(x-y) = (\cos x)(\cos y) + (\sin x)(\sin y)$
and $\cos(x+y) = (\cos x)(\cos y) - (\sin x)(\sin y)$

so that $\cos(x-y) - \cos(x+y) = 2(\sin x)(\sin y)$.

Now identify $x = \theta$ and $y = 1^\circ$

So that $A = \left(\frac{1}{360} \right) [2 \sin \theta \sin 1^\circ]$

Or $A = \left(\frac{1}{180} \right) [\sin \theta \sin 1^\circ] = \left(\frac{\sin \theta}{10313.75} \right) = 9.6958 \times 10^{-5} \sin \theta$

As an example,

$$\text{At } \theta = 90^\circ, \sin \theta = 1 \text{ and therefore } A = 9.7 \times 10^{-5}$$

We will check this result against a direct substitution into the equation

$$A = \left(\frac{\phi_2 - \phi_1}{720} \right) (\cos \theta_1 - \cos \theta_2),$$

Which yields

$$A = \left(\frac{2}{720} \right) (\cos 89^\circ - \cos 91^\circ).$$

Evaluating

$$A = \left(\frac{1}{360} \right) (0.01745 + 0.01745),$$

we get

$$A = 9.6957 \times 10^{-5}$$

Which therefore indicates a successful check!

So now we can confidently use (for a 2° by 2° sample):

$$A = 9.7 \times 10^{-5} \sin \theta \quad \text{per sample fraction part of spherical area}$$

The **exceptions** are the $\theta = 0$ and $\theta = 180$ points. These have bounds of $\theta_1 = 0$; $\theta_2 = 1^\circ$ so that:

$$A_p = \left(\frac{1}{360} \right) (1 - \cos 1) = \frac{1.523 \times 10^{-4}}{360}$$

Which simplifies to:

$$A_p = 4.2307 \times 10^{-7} \quad \text{per sample for } \theta = 0^\circ \text{ and } 180^\circ$$

An interesting exercise:

From the $\theta = 0$ pole to what value of θ is 1 percent of the spherical surface contained?

$$A = \frac{1 - \cos \theta_0}{2} = 0.01$$

$$1 - \cos \theta_0 = 0.02$$

$$\cos \theta_0 = 1 - 0.02 = 0.98$$

$$\theta_0 = 11.47 \text{ degrees}$$

How many samples in a $2^\circ \times 2^\circ$ RDP does this represent?

The θ scans involved are 0, 2, 4, 6, 8 and 10. Therefore 6 lines for the RDP are used. Since we have 180 samples (in ϕ) in each line, the total number of samples is 6×180 or 1080. The entire RDP would have 91 lines (including both 0° and 180° in theta) times 180 (0° through 358° in phi) samples per line which computes to 16,380 total samples. As a matter of interest, a $1^\circ \times 1^\circ$ RDP would have 181 (0 through 180° in theta) \times 360 (0 through 359° in phi) or 65160 samples.

According to the derivation above the individual contributions should be:

$$\begin{aligned}\theta = 0 \quad (180)(4.2307 \times 10^{-7}) &= 7.615 \times 10^{-5} \\ \theta = 2 \quad (180)(9.7 \times 10^{-5})(\sin 2^\circ) &= 6.093 \times 10^{-4} \\ \theta = 4 \quad (180)(9.7 \times 10^{-5})(\sin 4^\circ) &= 1.218 \times 10^{-3} \\ \theta = 6 \quad (180)(9.7 \times 10^{-5})(\sin 6^\circ) &= 1.825 \times 10^{-3} \\ \theta = 8 \quad (180)(9.7 \times 10^{-5})(\sin 8^\circ) &= 2.430 \times 10^{-3} \\ \theta = 10 \quad (180)(9.7 \times 10^{-5})(\sin 10^\circ) &= 3.032 \times 10^{-3}\end{aligned}$$

The sum of these lines in the RDP is

$$\sum = 9.2 \times 10^{-3} = 0.92 \times 10^{-2} = 0.92\%$$

The remaining fraction comes between 11.00° and 11.47° which may be calculated by

$$A = \frac{\cos(11.00^\circ) - \cos(11.47^\circ)}{2} = 0.08 \times 10^{-2}$$

Which makes the grand total exactly 1 percent as would be expected!

Question: Assuming that a pair of nulls are running from pole-to-pole, how wide must they be to include 2.5 percent (each) of the spherical surface?

Answer: The general “patch” area (fraction of surface total) is

$$A = \left(\frac{\phi_2 - \phi_1}{720} \right) (\cos \theta_1 - \cos \theta_2)$$

In this case we have $\theta_1 = 0$ and $\theta_2 = 180$ degrees.

$$\cos(0^\circ) - \cos(180^\circ) = 2$$

Then

$$A = \frac{\phi_2 - \phi_1}{360}$$

But we desire this to equal 2.5 percent or 0.025 numerically, so

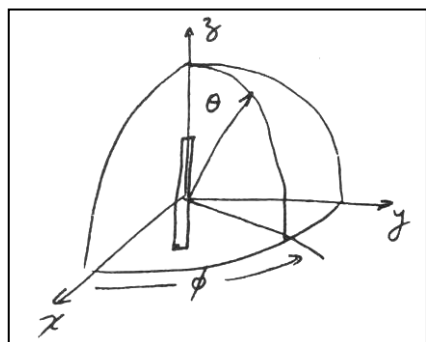
$$0.025 = \frac{\phi_2 - \phi_1}{360}$$

And therefore we have the phi angle difference of

$$\phi_2 - \phi_1 = (0.025)(360) = 9^\circ$$

Thus, a coverage failure of the “roll plane” in the order of 9 degrees in two places is enough to lower the coverage to 95 percent. Nulls near the poles will almost certainly exist, forcing the maximum roll plane nulls to a value less than 9 degrees each.

The dipole: Consider a “real antenna” as an example. A dipole coincident with the z-axis (See Figure 5-5) has a power pattern of



$$U(\theta) = \sin^2(\theta)$$

Compute the “percent coverage” at various levels down from the peak of the pattern and from isotropic. First, specify the pattern (relative) level in dB. This will determine the theta angle for that level which in turn will determine the fractional surface area from the pole to that theta angle.

Figure 5-5. Dipole on Z-axis.

Next calculate θ from the known power pattern.

$$\sin^2 \theta = 10^{\frac{dB}{10}} \quad \text{or} \quad \theta = \sin^{-1} \left(10^{\frac{dB}{20}} \right)$$

Remember that the equation for surface area from the pole to a given theta angle is

$$A_p = \left(\frac{1 - \cos(\theta)}{2} \right)$$

The coverage is the portion of the sphere above a given level (not below as we have from the null near the pole). Also, there will be two nulls (one for each pole). Then the percent coverage above a given specified level (for the dipole) is

$$\eta = 100 \left[1 - \left(2 \left(\frac{1 - \cos(\theta)}{2} \right) \right) \right] = 100(\cos(\theta)) \quad \text{percent coverage}$$

Results calculated at several interesting dB levels yield the following chart. The chart shows that the dipole has 95 percent coverage to the -10 dB (relative) level in copolarization. If its gain is taken to be $+2$ dBi, then the -8 dBi level is the 95 percent coverage level.

However, if a circular polarization reference is specified, then a mismatch loss of an additional 3 dB is involved. Thus, with respect to the left hand circular polarization (LHCP) the dipole has 95 percent coverage at or above the -11 dBic level.

Level (dB)	θ (deg)	η (%)
-3	45.1	70.63
-6	30.1	86.53
-10	18.4	94.87
-15	10.2	98.41
-20	5.7	99.50

5.3 Antenna Pattern Spherical Coverage

The term “coverage” may have different implications to those who deal with FTS than those who are concerned with radar tracking quality. Generally, 95 percent of the radiation sphere is required to exhibit gain levels above some specified value, usually -20 dBi to about -15 dBi. For the FTS the need to avoid broad areas of low signal level is the object, but for the Radar the avoidance of areas of many, deep, sharp, nulls is more important.

Spherical coverage, as an absolute number, should not be as strongly insisted upon as the absence of many deep nulls. The radars usually have adequate dynamic range to “see into nulls”, but it can be shown that many interference lobes (peaks and nulls) in a small angular region can

cause significant angular and range tracking errors. This same “lobe infested” pattern area may well provide what would be computed as adequate coverage.

In computing the coverage percentage for any specified polarization component, the antenna pattern is integrated to yield a final number. In the normal 2 by 2 degree digitized antenna pattern, each sample is measured for level and for the fraction of a sphere it represents. All samples are summed up and the level corresponding to gain above which 95 percent of the surface is covered is deemed to be the 95 percent coverage level. One broad null area is bad for the FTS but not as bad for radar. On the other hand, that same broad area if “filled in” with a system of interference lobes would improve the coverage percentage but would be very bad for radar tracking.

5.4 Examples of Spherical Coverage from Pattern Measurement

5.4.1 Polar Patterns (Analog and Digital). A three-element array which produces a roll plane pattern such as is seen in Figure 5-6 and Figure 5-7 can yield coverage values as those shown in Figure 5-8.

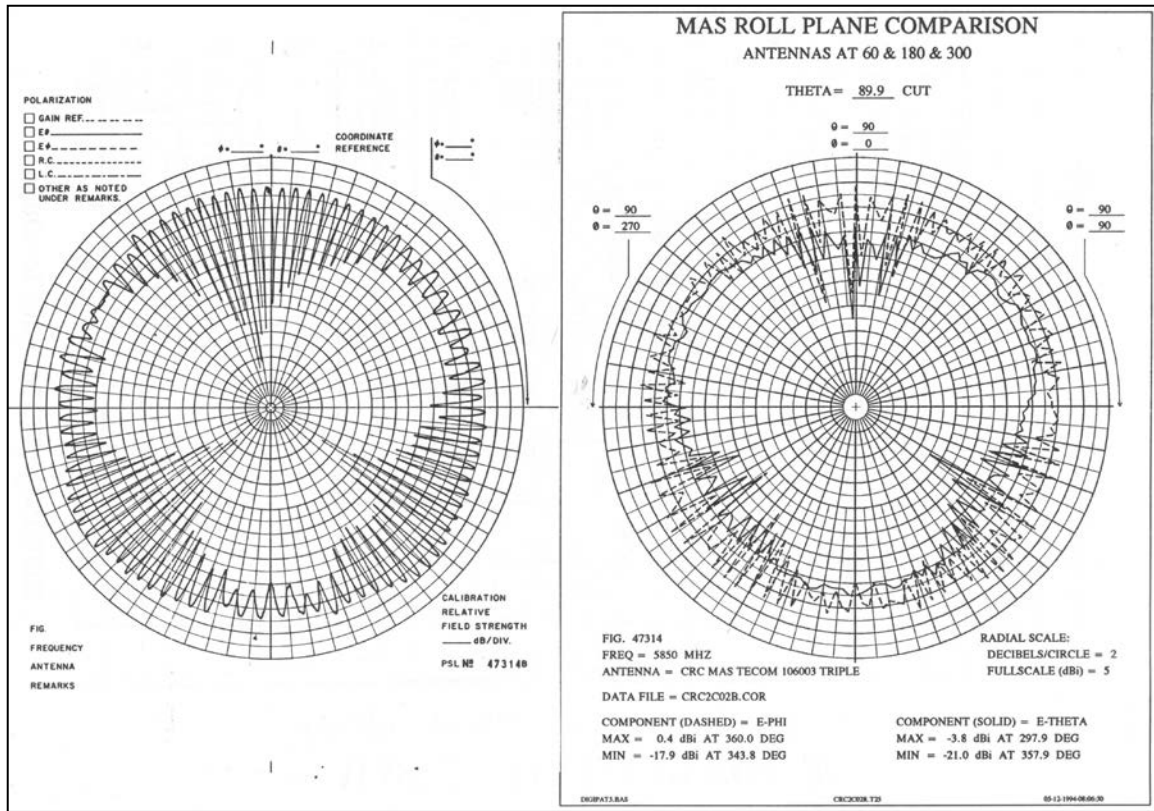


Figure 5-6. Comparison of analog and digital patterns for same measurement.

5.4.2 Rectangular Full Sphere Plot. A typical contour plot of the full spherical pattern (RDP) is shown in Figure 5-7.

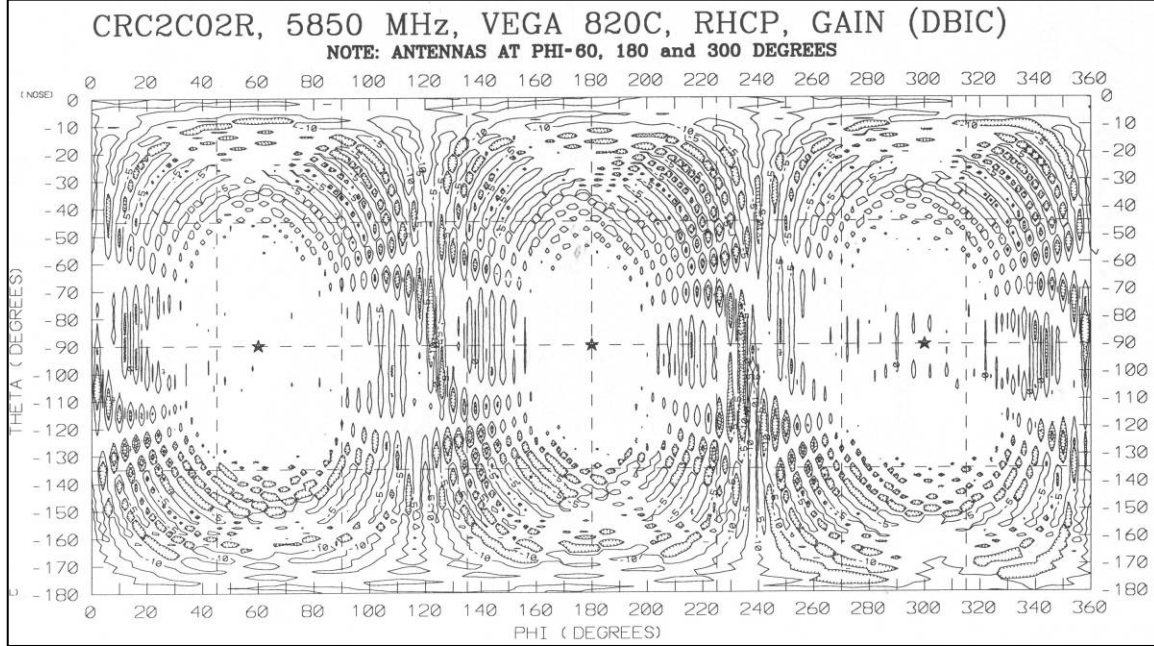


Figure 5-7. Contour plot of right hand circular gain for three vega antennas.

5.4.3 Coverage Level Graph. The resulting computed percent spherical coverage is shown in the graph in Figure 5-8. This particular coverage plot shows that the three-element array of cavity-backed helix type antennas yield a coverage of 95 percent at the -13 dBi level for the right hand circular polarization (RHCP) component. By reference to the roll plane comparison plots above, it is easy to imagine that with the sample spacing of 2 degrees (theta) by 2 degrees (phi), considerable error is possible in the integration of the samples near the three interference lobe regions.

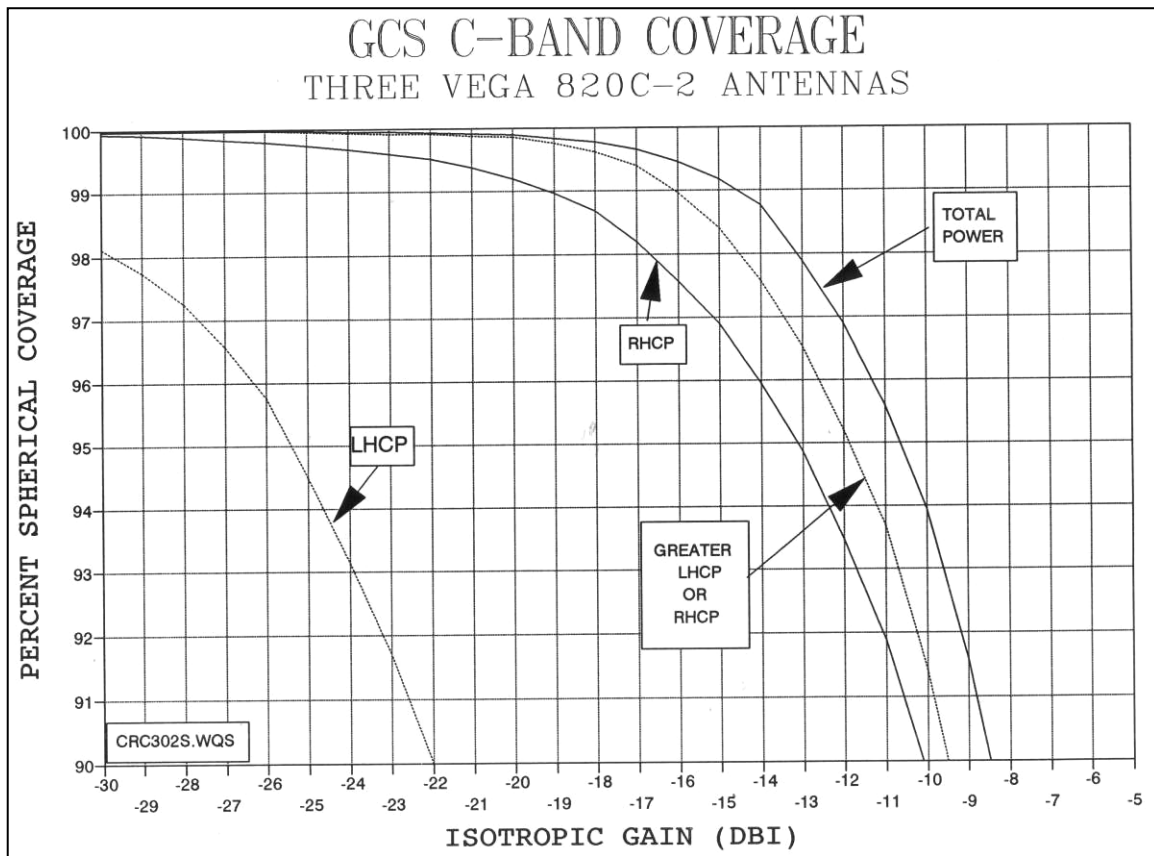


Figure 5-8. Typical graph of spherical coverage obtained from RDP data.

5.5 Two Coherent Radiating Elements

5.5.1 Definition of Phasing in Farfield. Using Figure 5-9 as a guide, the following define phasing in the farfield.

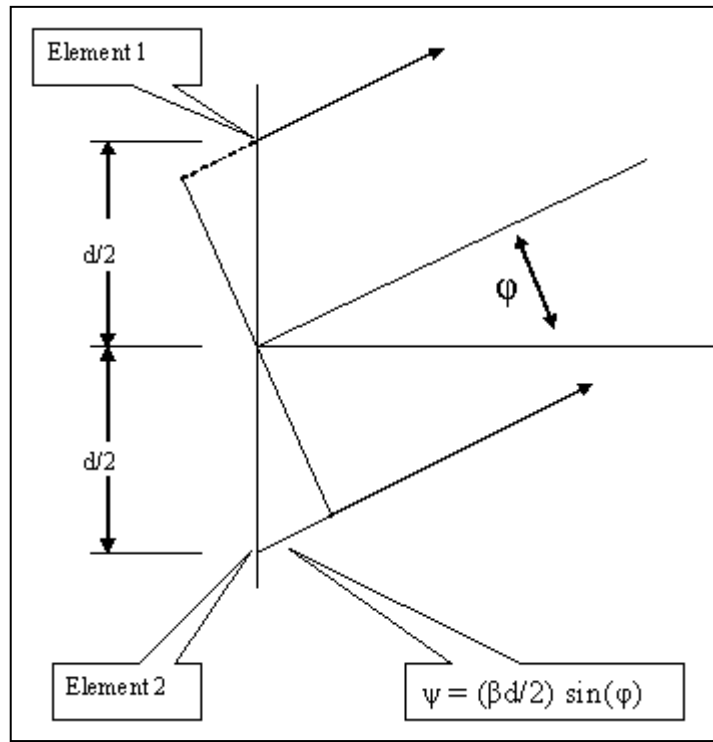


Figure 5-9. Diagram of two radiating elements.

- Define:
- d = the separation between elements
 - β = propagation constant = $2\pi/\lambda$
 - βd = electrical distance between elements
 - ϕ = the angle from the bisector plane
 - ψ = the farfield phase lead or lag due to the angle ϕ

$$\text{From each element, } \Psi = \frac{\beta d}{2} \sin(\phi)$$

On a plane bisecting the line joining the two elements (broadside), there will be a signal maximum due to constructive interference. This plane will be considered the reference of the angle ϕ . As ϕ increases from zero, the phase as seen at the farfield point in the ϕ direction will lead for element number 1 and lag for element number 2. The amount of the phase shift depends on the separation “ d ” and the wavelength of operation that determines the value of β .

The total phase difference is $\Delta\Psi = \beta d \sin(\phi)$

When the angle ϕ has increased to the point where the total phase difference between the rays from the two elements is half wavelength (or 180 degrees or π radians) a minimum will form. This will be a complete null if the elements have equal magnitudes.

At a null this becomes

$$\Delta\Psi = \frac{\lambda}{2} \quad \text{and thus} \quad \beta d \sin(\phi) = \frac{\lambda}{2}$$

5.5.2 Finding the null angle given the separation. The following is an example of finding the null angle given the separation in terms of lambda.

For 1λ separation, $\beta d = 1\lambda$ for a null $\beta d \sin(\phi) = \lambda/2$

$$\text{and } \phi = \sin^{-1}\left(\frac{1}{2\beta d}\right) \quad \phi = \sin^{-1}\left(\frac{1}{2}\right), \quad \text{thus } \phi = 30^\circ$$

A full cycle of interference, (i.e., null-to-null) will occupy the angular region

$$\phi = \pm \sin^{-1}\left(\frac{\lambda}{2\beta d}\right) \quad \text{for a total of} \quad \Delta\phi = 2 \sin^{-1}\left(\frac{\lambda}{2\beta d}\right)$$

The analysis of antenna patterns will yield this angle. It is usually easier to determine the null-to-null angle than to determine the peak-to-null from measured patterns; simply half the null-to-null angle range is taken to be the peak-to-null angle.

5.5.3 Finding Separation Given the Null Angle. The following provides an example of finding the separation between elements given the null-to-null angle

If $\Delta\phi$ is the null-to-null angular range then $\Delta\phi/2$ is the peak-to-null angle.

Since we have

$$\beta d = \frac{\lambda}{2 \sin\left(\frac{\Delta\phi}{2}\right)} \quad \text{so} \quad \beta d = K\lambda \quad \text{where } K = \frac{1}{2 \sin\left(\frac{\Delta\phi}{2}\right)}$$

Here K is the number of wavelengths of separation.

For a null-to-null angle of 60° , we would expect to have a separation of one wavelength.

$$\Delta\phi = 60^\circ \quad K = \frac{1}{2 \sin\left(\frac{\Delta\phi}{2}\right)} \quad K = \frac{1}{2 \sin(30^\circ)} \quad K = 1 \text{ wavelength}$$

Example 3: Find separation for null-to-null of 180 degrees.

$$\Delta\phi = 180^\circ, \quad K = \frac{1}{2 \sin\left(\frac{\Delta\phi}{2}\right)}, \quad K = \frac{1}{2 \sin(90^\circ)}, \quad \text{and } K = 0.5 \text{ wavelength}$$

From the expression for the angle of the null for two co-phase radiators,

$$\phi = \pm \sin^{-1}\left(\frac{\lambda}{2\beta d}\right)$$

It is clear that when βd is less than half wavelength, the denominator takes on a value less than unity and that no real angle will satisfy the arcsine function. Then for the formation of a null with two co-phase elements, the limiting value of separation is half wavelength; anything less will not produce a null in real angle space.

5.6 Phasor Addition and Null Formation

5.6.1 Phasor Diagram. Figure 5-10 is used to calculate the phasor sum magnitude and the phasor sum phase (see paragraph 5.6.2 and paragraph 5.6.3).

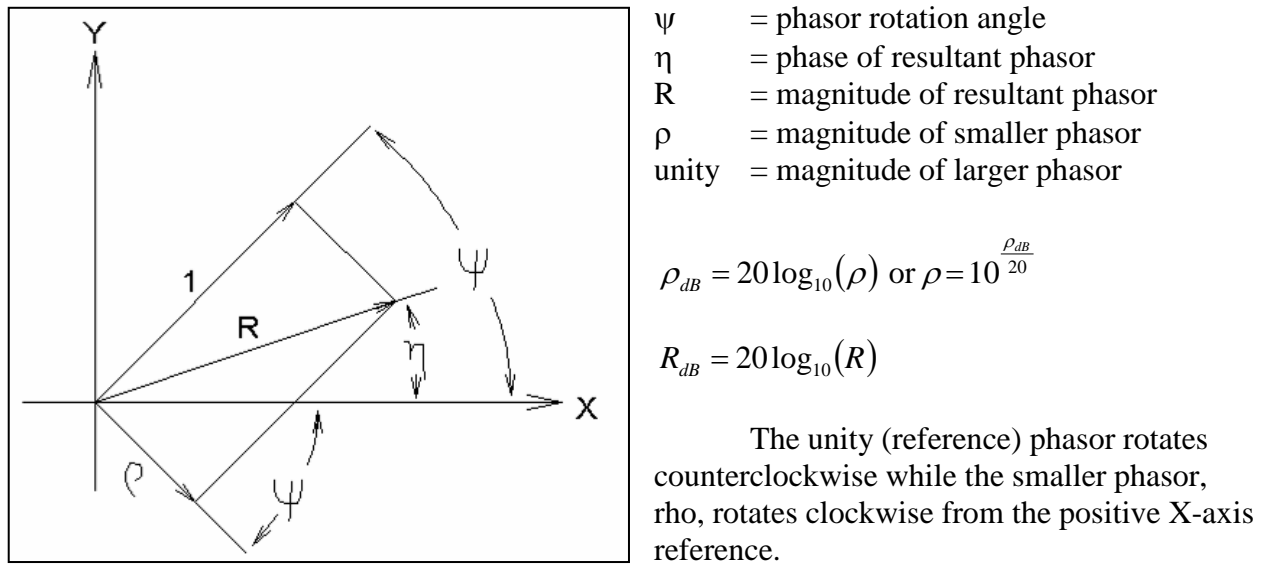


Figure 5-10. Phasor addition diagram.

The summation of the X- components is

$$SumX = \cos(\Psi) + \rho \cos(-\Psi) = \cos(\Psi) + \rho \cos(\Psi) = (1 + \rho) \cos(\Psi)$$

and the summation of the Y- components is

$$SumY = \sin(\Psi) + \rho \sin(-\Psi) = \sin(\Psi) - \rho \sin(\Psi) = (1 - \rho) \sin(\Psi)$$

5.6.2 Computing Phasor Sum Magnitude. The magnitude of the resultant phasor is

$$R = \sqrt{[(1 + \rho) \cos(\Psi)]^2 + [(1 - \rho) \sin(\Psi)]^2}$$

Note: This is referenced to the larger phasor magnitude, not the sum maximum.

The phase of the resultant phasor

$$\eta = \tan^{-1} \left[\frac{(1 - \rho) \sin(\Psi)}{(1 + \rho) \cos(\Psi)} \right] = \tan^{-1} \left[\frac{(1 - \rho)}{(1 + \rho)} \tan(\Psi) \right]$$

Care must be exercised here to maintain the proper quadrant information when taking the arc tangent.

The magnitude of resultant normalized to maximum is

$$R_{Norm} = \frac{R}{(1 + \rho)} = \frac{\sqrt{[(1 + \rho) \cos(\Psi)]^2 + [(1 - \rho) \sin(\Psi)]^2}}{(1 + \rho)}$$

5.6.3 Example: Computing Phasor Sum Phase. In this example the smaller phasor is 1 dB smaller than the larger phasor. Each phasor has rotated 90 degrees from the X-axis so that the larger phasor is at $+90^\circ$ while the smaller phasor is at -90° . This puts them in opposition, which should yield the minimum resultant magnitude. We would expect the resultant to lie along the $+Y$ axis (i.e. at $+90$ degrees).

Input conditions are

$$\rho_{dB} = -1 \text{ and } \psi = 90^\circ$$

By applying the equations derived above we obtain

$$\rho = 0.891 \text{ and } R = 0.109$$

The maximum resultant (at $\psi = 0$ and 180°) should be

$$(1+\rho) = (1+ 0.891) = 1.891 \text{ so that } R_{\max} = 20 \log_{10}(1.891) = 5.53 \text{ dB}$$

and the minimum should be

$$(1-\rho) = (1- 0.891) = 0.109 \text{ so that } R_{\min} = 20 \log_{10}(0.109) = -19.25 \text{ dB}$$

Then the minimum normalized to the maximum (peak-to-peak) variation is

$$R_{\min\text{Norm}} = -19.25 \text{ dB} - 5.53 \text{ dB} = -24.78 \text{ dB} \text{ (with roundoff)}$$

When applying the equation for the resultant phase it is noticed that the cosine of psi in the denominator becomes zero, forcing the arc tangent of infinity, which is 90° .

Then we have

$$\eta = 90$$

5.7 Phasor Sum Phase Rate of Change

This section includes the derivation of the rate of change of the phase of the sum of two phasors as a function of the “depth of null” (see Figure 5-10 above).

Define ρ (rho) as the relative magnitude of the smaller of two phasors

ψ (psi) as the phase angle of each of the two phasors

η (eta) as the phase of the resultant phasor

The resultant phase is η and is given by the equation

$$\eta = \tan^{-1} \left[\frac{(1-\rho)}{(1+\rho)} \tan(\psi) \right]$$

The derivative of this phase angle with respect to the angle ψ is needed as the rate of change of the resultant phase.

Define the max-to-min as a single symbol A_r (as in Axial Ratio of an ellipse).

$$A_r = \frac{(1+\rho)}{(1-\rho)}$$

So the phase of the resultant can be expressed as

$$\eta = \tan^{-1} \left[\frac{1}{A_r} \tan(\Psi) \right]$$

Taking the derivative of this is a bit messy but necessary.

$$\frac{d}{d\Psi} \left\{ \tan^{-1} \left[\frac{1}{A_r} \tan(\Psi) \right] \right\} = \frac{1}{A_r} \frac{\left(1 + \tan^2(\Psi) \right)}{\left(1 + \frac{1}{A_r^2} \tan^2(\Psi) \right)}$$

The identity for the numerator is

$$1 + \tan^2(x) = \sec^2(x) = \frac{1}{\cos^2(x)}$$

and then the derivative becomes

$$\frac{d\eta}{d\Psi} = \frac{\left(\frac{1}{\cos^2(\Psi)} \right)}{\left(A_r + \frac{1}{A_r} \left(\frac{\sin^2(\Psi)}{\cos^2(\Psi)} \right) \right)}$$

Multiplying both numerator and denominator by $\cos^2(\psi)$ yields

$$\frac{d\eta}{d\Psi} = \frac{1}{A_r \cos^2(\Psi) + \frac{\sin^2(\Psi)}{A_r}}$$

When ψ equals zero this becomes $1/A_r$ and when ψ equals 90° this becomes A_r .

It is interesting to apply this to the rotation of the polarization phasor (electric field vector) of a propagating wave. It shows that the maximum rate of rotation is numerically equal to the axial ratio of the polarization ellipse. This will be extended to the maximum rate of phase change associated with the depth of null in the antenna pattern.

It should be obvious that the same phasor diagram which was used to describe the two contra-rotating phasors here would apply to the phasors describing interfering sources which phase to form maxima and minima. Thus the “depth-of-null” is analogous to the “axial ratio”. By this reasoning the phase rate of change in the area of a null (in an antenna pattern, for example) is numerically equal to the depth of null.

5.8 Phase Gradient at Pattern Minimum

5.8.1 Angle Subtended by tracker from target. From the analysis shown in paragraph 5.7, we know that the rate of change (of phase) near “nulls” is equal to the “axial ratio” in the case of the polarization ellipse. The equality is based on the “full cycle” or peak-to-peak time which is just half the period of the microwave signal. The similarity with pattern null depth is shown to correspond so that if one knows the peak-to-peak (or null-to-null) angle in the antenna power pattern as well as the “depth of null”, then the rate of phase change per angle in space can be determined.

Near the maxima, the phase rate is low because it is the reciprocal of the axial ratio. At the minima, the phase rate is high, equal to the axial ratio. These rates are in comparison to the average rate for one cycle. We can think of these as “normalized” rates of change.

If a power pattern shows peak-to-null angle of $\Delta\Phi/2$ or null-to-null angle of $\Delta\Phi$ and a peak-to-null depth of ε_{dB} then the rate of phase change with space angle can be computed. The axial ratio ε_{dB} needs to be expressed in terms of the linear voltage

$$\varepsilon_{dB} = \text{peak-to-null ratio in decibels}$$

then

$$\varepsilon = 10^{\frac{\varepsilon_{dB}}{20}}$$

The maximum rate of change in the resultant phasor phase is equal to ε based on a 180 degree cycle (of each contra rotating phasor), but $\Delta\Phi$ is generally much less (in space angle) so that the resulting phase rate should be much greater.

$$\frac{d\Psi}{d\phi} = \varepsilon \frac{(180^\circ)}{\Delta\phi} \quad \text{or} \quad \eta = \varepsilon \frac{(180^\circ)}{\Delta\phi} \quad \text{degree phase / degree space}$$

5.8.2 Derivation Of Phase Difference Across Tracker Aperture.

a. Example 1. A power pattern on a launch vehicle antenna has ripples with 20 dB variation on a 3.6-degree null-to-null spacing. What is the phase rate of change near the null?

$$\varepsilon_{dB} = 20 \quad \varepsilon = 10^{\frac{\varepsilon_{dB}}{20}} \quad , \text{then} \quad \varepsilon_{dB} = 10$$

and

$$\Delta\phi = 3.6^\circ \quad \text{so} \quad \eta = (10) \frac{(180)}{\Delta\phi} = 500 \quad \text{deg phase / deg space}$$

b. Example 2. A radar target vehicle has an amplitude pattern that presents 30 dB nulls every 3.6 degrees of roll to a radar that is 30 miles away. The radar has a 12-foot diameter dish. Approximately how much phase difference is presented across the dish aperture when the target presents a null? What angular pointing error would result?

$$\varepsilon_{\text{dB}} = 30 \quad \varepsilon = 10^{\frac{\varepsilon_{\text{dB}}}{20}} = 31.623$$

$$\Delta\phi = 3.6^\circ \quad \eta = \varepsilon \frac{(180)}{\Delta\phi} = 1584.14 \quad \text{degrees phase/degree space}$$

The angle subtended by the 12-foot dish at 30 miles is given by:

$$\delta_d = \tan^{-1}\left(\frac{12}{(5280)(30)}\right) \quad \delta_d = 0.00434^\circ$$

The total phase across the aperture is equal to the rate-of-change of phase with roll angle (η), times the angle subtended.

$$\Psi_{\text{total}} = \eta(\delta_d) \quad \text{so that} \quad \Psi_{\text{total}} = 6.863^\circ$$

If the frequency is 5860 MHz the wavelength is:

$$\lambda = \frac{11803}{5860} \quad \lambda = 2.014 \quad \text{inches}$$

The phase across the aperture represents the distance:

$$\Psi_{\text{dish}} = \frac{\Psi_{\text{total}}}{360^\circ} \quad \Psi_{\text{dish}} = 0.019 \quad \text{wavelength}$$

$$\Psi_{\text{dishinch}} = \Psi_{\text{dish}} \lambda = 0.038 \text{ inch}$$

The equivalent angle that the “phase front” makes with the dish aperture is then

$$\alpha = \tan^{-1}\left(\frac{\Psi_{\text{dishinch}}}{144}\right) = 0.015^\circ$$

5.9 Data and Graphs of Subtended Angles

Figure 5-11 presents the data and graph of angles subtended by tracker dishes at various distances.

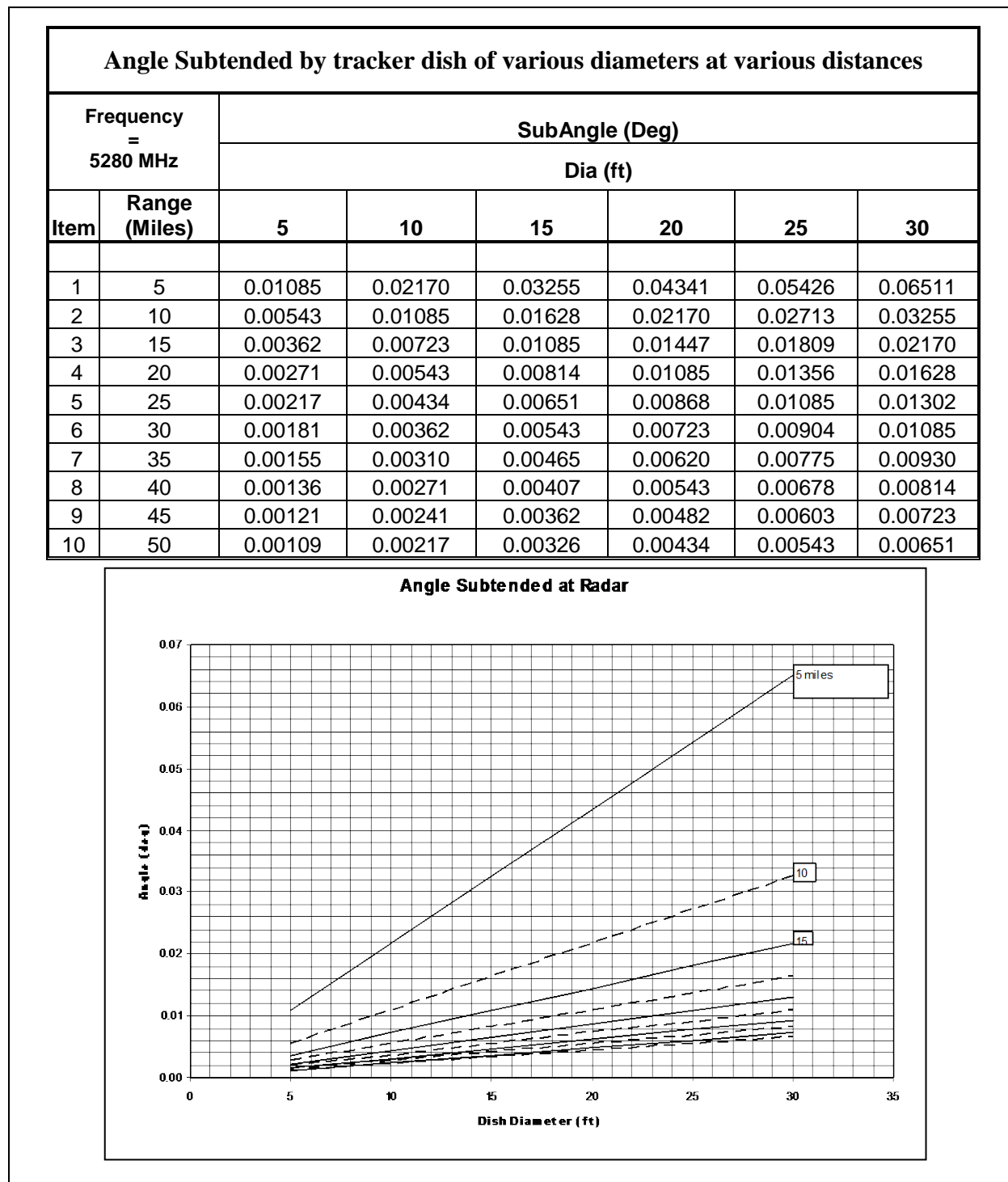


Figure 5-11. Graph of angle subtended by tracker dish at various distances.

5.10 Tracker Error Angle From Phase Front Distortion

5.10.1 Derivation of Angle Error. This analysis is based upon the transponder antenna pattern ripple parameters. The ripple is considered to be the amplitude variations as a function of angle around the antenna-equipped target vehicle. The peaks and nulls are modeled by the interference between two phasors. The amplitude and phase of the resultant interference is used to model the antenna pattern in the vicinity of a null. The resulting phase shift in the radiation near the null is referred to as phase front distortion.

When the radar target presents a pattern minimum to the tracker, it also presents a phase front, which is distorted from the expected constant phase. The tracker tends to point in the direction normal to the phase front instead of directly at the target. The tracker will try to minimize the phase gradient across the aperture by pointing off the target direction. The amount of this pointing error can be estimated by knowing certain values including the pattern ripple (peak-to-null ratio and angle spacing, operating frequency (wavelength) and target range.

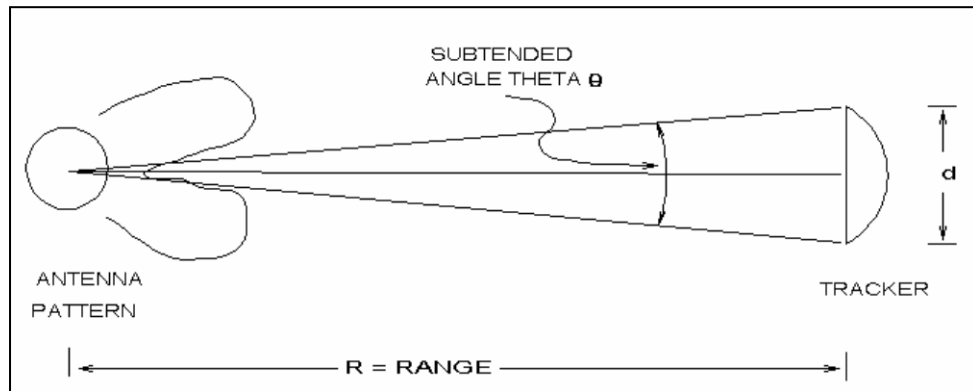


Figure 5-12. Geometry of tracker subtended from target vehicle.

From the geometry (See Figure 5-12 above) the angle subtended by the tracker aperture from the target is approximately

$$\theta = \tan^{-1} \left(\frac{d}{R} \right)$$

where d is the tracker aperture dimension, and
 R is the target range

Since the range is always much greater than the tracker aperture the angle is essentially equal to the tangent or the sine. Thus

$$\theta = \frac{d}{R} \text{ (in radians)}$$

From the pattern ripple parameters (peak-to-null ratio and peak-to-peak angle) it is possible to compute the phase gradient in the direction of a pattern minimum. The deeper the null and the smaller the peak-to-peak angle, the greater is the phase gradient or slope, η . Eta (η) is the rate of change of phase (in the far field) with respect to the space angle in the direction of the null. Eta may be expressed in terms of degrees phase per degree space angle or in terms of radians or a mixture of these. However it is expressed, the total phase in an aperture (d) at a distance (R) is equal to the subtended angle (θ) times the rate of phase per unit angle. Thus total phase across the aperture is

$$\Psi_{\text{total}} = \theta(\eta) \quad \text{which is also} \quad \Psi_{\text{total}} = \left(\frac{d}{R} \right) \eta$$

The phase per unit distance in the aperture is then the total phase divided by the aperture distance, or

$$\frac{\Psi_{\text{total}}}{d} = \frac{\eta}{R}$$

This result would yield the apparent slope across the aperture (See Figure 5-13) and, when scaled to the wavelength, would yield the actual apparent “angle of arrival” which is the “pointing angle error” (δ) which is sought.

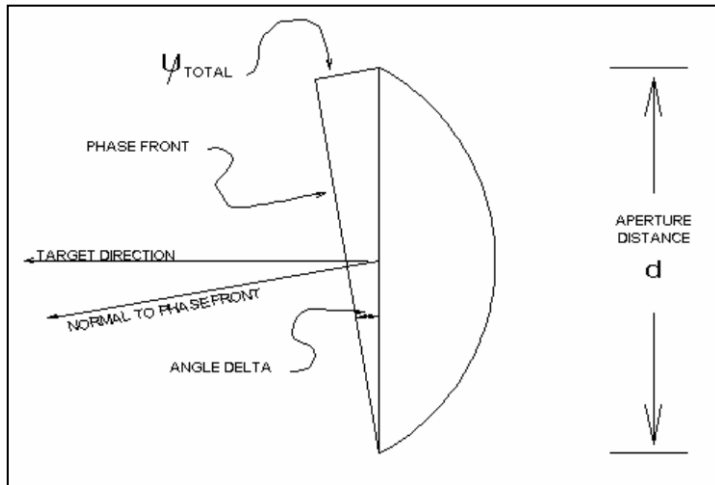


Figure 5-13. Phase front slope.

It appears that at a given range the slope of the phase distortion is not dependent upon the actual aperture size. In practice, the larger apertures would be associated with narrower beams and thus would have higher gains but more difficulty in reacquiring a target that is lost due to rapid and large errors caused by phase front distortion.

Finding the angle of the “normal to the phase front” is essentially that of solving for the angle (δ) which is the angle formed by the total phase in the aperture dimension.

Therefore:

$$\delta = \sin^{-1}\left(\frac{\Psi_{total}}{d}\right) \quad \text{or} \quad \delta = \sin^{-1}\left(\frac{\eta}{R}\right)$$

Of course, the dimensions will have to be converted to common units for both numerator and denominator.

It could be noted that the length represented by the total phase across the aperture is much smaller than the aperture size. Errors of one degree are exceptionally large and rare. Then we can approximate the arc sine by the angle in radians.

$$\delta = \frac{\eta}{R} \quad \text{when proper units are applied.}$$

The length associated with total phase across the aperture is obtained by scaling to a known wavelength

$$L_{\Psi t} = \text{Length associated with total phase across aperture}$$

The conversion is one wavelength per 2π radians. This yields the result

$$L_{\Psi t} = \left(\frac{\Psi_{total}}{2\pi}\right) \text{wavelengths}$$

The error angle is this length divided by the aperture distance (d), and so

$$\delta = \frac{L_{\Psi t}}{d} \quad \text{which is} \quad \delta = \left(\frac{\Psi_{total}}{2\pi d}\right)$$

If the aperture diameter (d) is given in wavelengths designated by d_λ then the angle formed by the phase length, ψ_{total} , across the aperture (d) is given by

$$\delta = \frac{\Psi_{total}}{2\pi d_\lambda} \quad \text{where } \psi \text{ is in radians and } d_\lambda \text{ is in wavelengths.}$$

From the geometry we have

$$\Psi_{total} = \left(\frac{d}{R}\right) \eta$$

Where d/R represents the subtended angle in radians.

For clarity let d and R be expressed in wavelengths with appropriate subscripts. Then

$$\delta = \left(\frac{d_\lambda}{R_\lambda} \right) \left(\frac{\eta}{2\pi d_\lambda} \right),$$

Cancelling, collecting terms, and being specific yields

$$\delta_{\text{rad}} = \frac{\eta}{2\pi R_\lambda} \text{ in radians.}$$

The value of Eta must be computed from parameters of the pattern ripple:

$$\begin{aligned}\varepsilon &= \text{peak-to-null voltage ratio} \\ \varepsilon_{\text{dB}} &= \text{peak-to-null ratio in decibels}\end{aligned}$$

$$\varepsilon = 10^{\frac{\varepsilon_{\text{dB}}}{20}}$$

The rate-of-change of phase at the null is numerically equal to ε based on a peak-to-peak angular range of half circle (π radians or 180 degrees) as shown in Paragraph [5.7](#). For a peak-to-peak cycle of $\Delta\phi$ the rate of phase change is

$$\frac{d\Psi}{d\phi} = \varepsilon \left(\frac{\pi}{\Delta\phi} \right)$$

This rate-of-change of phase with respect to the space angle is Eta (η). Thus,

$$\eta = \varepsilon \left(\frac{\pi}{\Delta\phi} \right) \quad \text{where } \Delta\phi \text{ is the peak-to-peak angle in the antenna pattern.}$$

Substituting for η in the equation for δ_{rad} yields

$$\delta_{\text{rad}} = \varepsilon \frac{\left(\frac{\pi}{\Delta\phi_{\text{rad}}} \right)}{2\pi R_\lambda}$$

Collecting terms yields

$$\delta_{\text{rad}} = \frac{\varepsilon}{2 R_\lambda \Delta\phi_{\text{rad}}}$$

This is the simplified expression for the angular error in the tracker angle associated with a pattern null. It shows that the angle error is directly proportional to the depth of null, inversely proportional to the range and inversely proportional to the null spacing angle on the target antenna pattern.

5.10.2 Examples in several common range measurement systems/common units of measure.

At this point, it may be useful to convert the basic equation to accept values more directly obtainable from antenna patterns and radar plots. Null depths are more commonly expressed in decibels, while null spacing angles are usually determined in degrees. Then

$$\delta_{\text{rad}} = \frac{10 \left(\frac{\varepsilon_{\text{dB}}}{20} \right)}{2R\lambda (\Delta\phi_{\text{deg}}) \left(\frac{\pi}{180} \right)}$$

Which reduces to

$$\delta_{\text{rad}} = \frac{90 \left(10 \frac{\varepsilon_{\text{dB}}}{20} \right)}{R\lambda (\Delta\phi_{\text{deg}})\pi}$$

The range in wavelengths must be converted by means of frequency and range. The frequency is usually known in gigahertz and the range in yards (or meters or kilometers). In general the conversion to wavelength (λ) is:

$$\lambda = \frac{c}{f} \quad \text{where } c \text{ is the speed of light and } f \text{ is the frequency of operation}$$

Specifically: $c = 2.997925 \times 10^8$ meters/second

$c = 2.997925 \times 10^5$ kilometers/sec

$c = 3.2785 \times 10^8$ yards/second

$$\text{and} \quad f_{\text{Hz}} = f_{\text{GHz}} \times 10^9 \quad \text{Hertz}$$

The conversions for range in yards, meters and kilometers with frequency in gigahertz are

Range In Yards

$$K_y = \frac{10^9}{3.2785 \times 10^8} \quad K_y = 3.050175 \quad R_\lambda = (K_y)(R_{\text{yards}})(f_{\text{GHz}})$$

Range in Meters

$$K_m = \frac{10^9}{2.997825 \times 10^8} \quad K_m = 3.33564 \quad R_\lambda = (K_m)(R_{\text{meter}})(f_{\text{GHz}})$$

Range in Kilometers

$$K_{km} = \frac{10^9}{2.997925 \times 10^5} \quad K_{km} = 3335.64 \quad R_\lambda = (K_{km})(R_{\text{km}})(f_{\text{GHz}})$$

These values would be substituted into the equation for the error angle, δ ,

$$\delta_{\text{rad}} = \frac{90 \left(10^{\frac{\varepsilon_{\text{dB}}}{20}} \right)}{R_\lambda (\Delta\phi_{\text{deg}}) \pi}$$

The error angle here is computed in radians, but it may be more convenient to have it directly in mils for better comparison with the angular sensitivity of the radar. By the definition of the U.S. version of the mil, there are 6400 mils in a circle (i.e., in 2π radians).

Therefore,

$$\delta_{\text{mils}} = \delta_{\text{rad}} \left(\frac{6400}{2\pi} \right)$$

And we have

$$\delta_{\text{mils}} = \left[\frac{90 \left(10^{\frac{\varepsilon_{\text{dB}}}{20}} \right)}{(R_\lambda)(\Delta\phi_{\text{deg}})(\pi)} \right] \left(\frac{6400}{2\pi} \right)$$

We could evaluate the constants here to be

$$K_1 = \frac{(90)(6400)}{(\pi)(\pi)(2)} \quad K_1 = 2.91805 \times 10^4$$

Then the resulting angle error, δ , in mils is given by

$$\delta_{\text{mils}} = K_1 \frac{\left(10^{\frac{\varepsilon_{\text{dB}}}{20}}\right)}{(R_\lambda)(\Delta\phi_{\text{deg}})}$$

When the range in wavelengths is replaced by the individual conversions (for yards, meters, or kilometers) above the final constants may be computed.

Note: Below are shown the final forms with constants and numerical examples for 30 dB null depth, 5 degrees ripple cycle, 5.9015 GHz and an equivalent range of about 20 nautical miles.

For Range in Yards

$$R_\lambda = (K_y)(R_{\text{yards}})(f_{\text{GHz}}) \quad \delta_{\text{mils}} = K_1 \frac{\left(10^{\frac{\varepsilon_{\text{dB}}}{20}}\right)}{(R_\lambda)(\Delta\phi_{\text{deg}})}$$

Substituting for R_λ we get

$$\delta_{\text{mils}} = \frac{K_1}{K_y} \left[\frac{10^{\frac{\varepsilon_{\text{dB}}}{20}}}{(R_{\text{yards}})(\Delta\phi_{\text{deg}})(f_{\text{GHz}})} \right]$$

Evaluating K_1/K_y yields

$$K_{\text{yards}} = \frac{K_1}{K_y} \quad K_{\text{yards}} = 9566.827$$

and finally we get (with example)

$$\varepsilon_{\text{dB}} = 30 \quad f_{\text{GHz}} = 5.9015 \quad \Delta\phi_{\text{deg}} = 5 \quad R_{\text{yards}} = 40507.44$$

$$\delta_{\text{mils}} = K_{\text{yards}} \frac{\left(10^{\frac{\epsilon_{\text{dB}}}{20}}\right)}{(f_{\text{GHz}})(R_{\text{yards}})(\Delta\phi_{\text{deg}})}$$

$$\delta_{\text{mils}} = 0.2531$$

For Range in Meters

$$R_{\lambda} = (K_m)(R_{\text{meters}})(f_{\text{GHz}})$$

$$\delta_{\text{mils}} = K_1 \frac{\left(10^{\frac{\epsilon_{\text{dB}}}{20}}\right)}{(R_{\lambda})(\Delta\phi_{\text{deg}})}$$

Substituting for R_{λ} we get

$$\delta_{\text{mils}} = \frac{\left(10^{\frac{\epsilon_{\text{dB}}}{20}}\right)}{(R_{\text{meters}})(\Delta\phi_{\text{deg}})(f_{\text{GHz}})} \left(\frac{K_1}{K_m}\right)$$

Evaluating K_1/K_m yields

$$K_{\text{meter}} = \frac{K_1}{K_m}$$

$$K_{\text{meter}} = 8748.095$$

And finally we get (with example)

$$\epsilon_{\text{dB}} = 30 \quad f_{\text{GHz}} = 5.9015 \quad \Delta\phi_{\text{deg}} = 5 \quad R_{\text{meters}} = 37040$$

$$\delta_{\text{mils}} = K_{\text{meter}} \frac{\left(10^{\frac{\epsilon_{\text{dB}}}{20}}\right)}{(R_{\text{meters}})(\Delta\phi_{\text{deg}})(f_{\text{GHz}})}$$

$$\delta_{\text{mils}} = 0.2531$$

For Range in Kilometers

$$R_\lambda = (K_{km})(R_{km})(f_{GHz}) \quad \delta_{mils} = K_1 \frac{\left(10^{\frac{\varepsilon_{dB}}{20}}\right)}{(R_\lambda)(\Delta\phi_{deg})}$$

Substituting for R_λ we get

$$\delta_{mils} = \frac{K_1}{K_{km}} \left(\frac{10^{\frac{\varepsilon_{dB}}{20}}}{(R_{km})(\Delta\phi_{deg})(f_{GHz})} \right)$$

Evaluating K_1/K_{km} yields

$$K_{kilometer} = \frac{K_1}{K_{km}} \quad K_{kilometer} = 8.748$$

And finally we get (with example)

$$\varepsilon_{dB} = 30 \quad f_{GHz} = 5.9015 \quad \Delta\phi_{deg} = 5 \quad R_{km} = 37.04$$

$$\delta_{mils} = K_{kilometer} \frac{\left(10^{\frac{\varepsilon_{dB}}{20}}\right)}{(R_{km})(\Delta\phi_{deg})(f_{GHz})} \quad \delta_{mils} = 0.2531$$

5.10.3 Graphical displays of angle errors.

An Excel spreadsheet was used to calculate some curves of angle error as a function of range, null angular spacing and null depth .

- a. Figure 5-14 and Figure 5-15 show the angle error as a function of range for various null depths.
- b. Figure 5-16 and Figure 5-17 show the angle error as a function of null angle spacing for various values of null depth.
- c. Figure 5-18 and Figure 5-19 show the angle error as a function of null depth for various ripple rates.

An Excel spreadsheet was also used to produce the following graphical displays:

- d. Figure 5-20. Pattern magnitude versus phasor rotation angle
- e. Figure 5-21. Pattern resultant phase versus phasor rotation angle
- f. Figure 5-22. Phase slope near a null

5.10.4 Angle Error as a Function of Range.

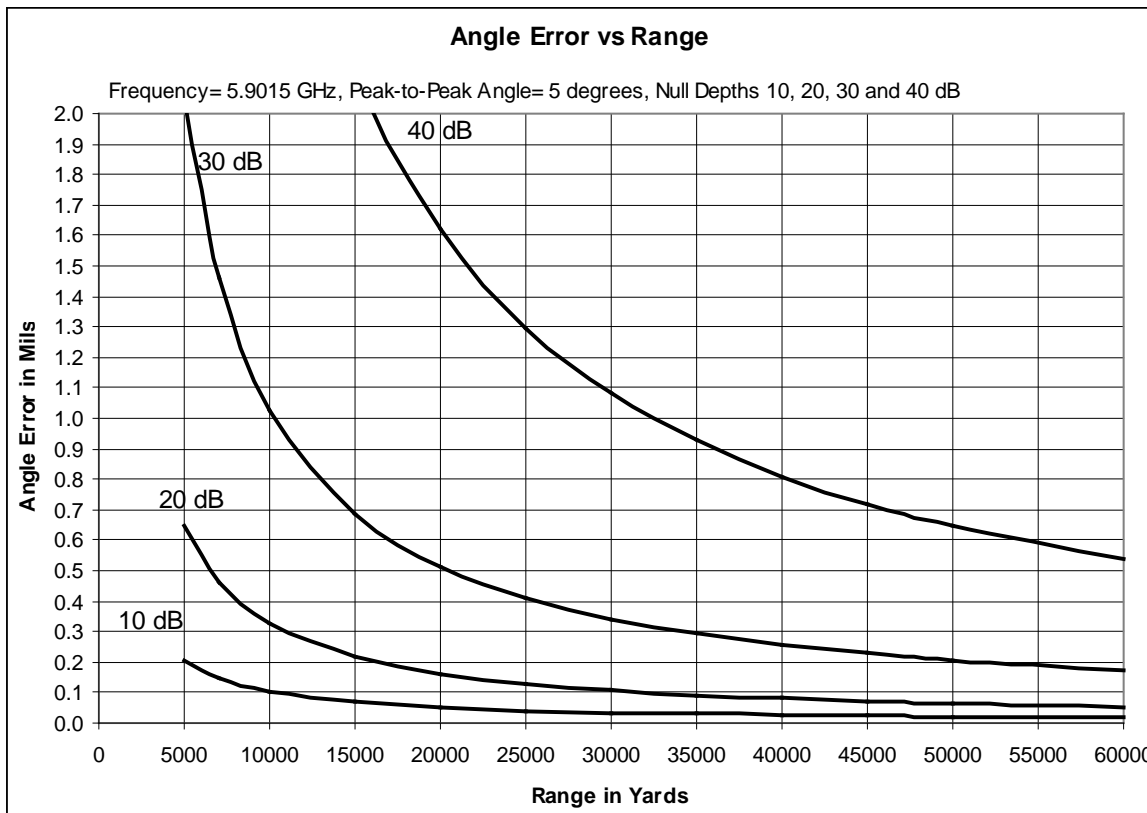


Figure 5-14. Angle error versus range for various null depths.



Figure 5-15. Angle error versus range for 40 dB null depth.

5.10.5 Angle Error as a Function of Null Depth.

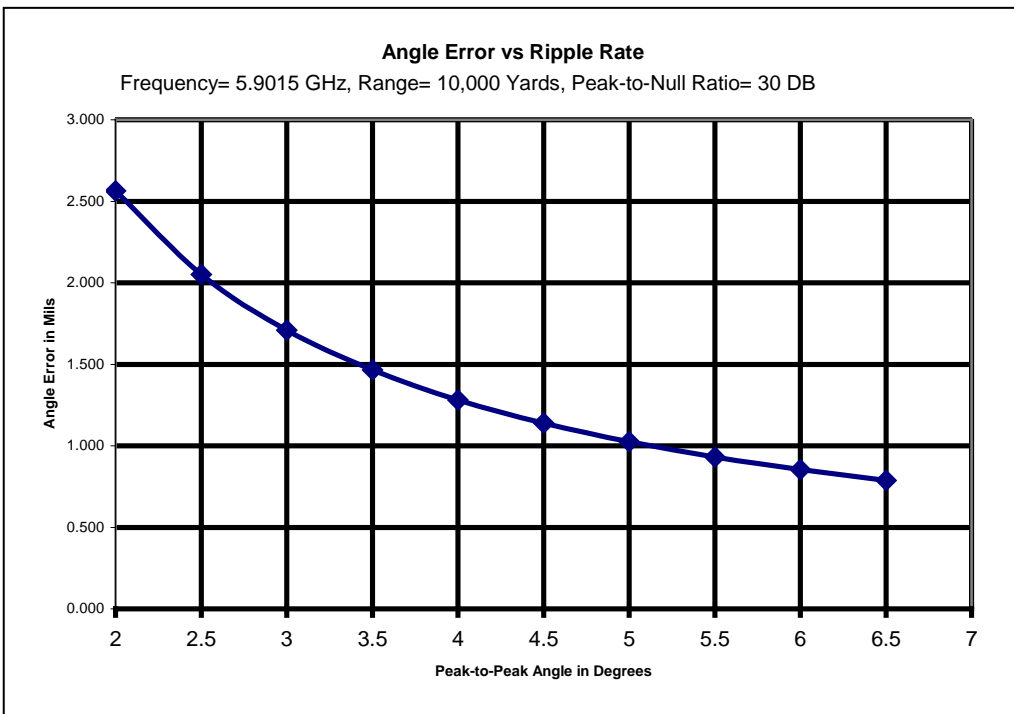


Figure 5-16. Error angle versus ripple rate at 10K yards, various null depths.

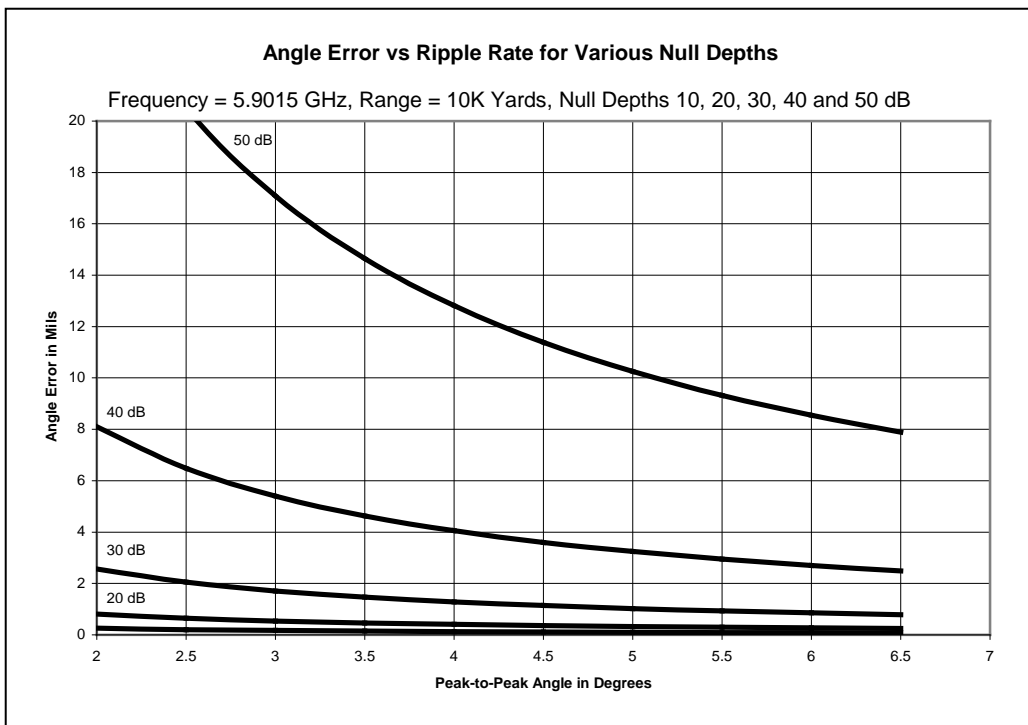


Figure 5-17. Angle error as a function of null angular spacing.

5.10.6 Graphical Displays of Peak-to-Peak Errors.

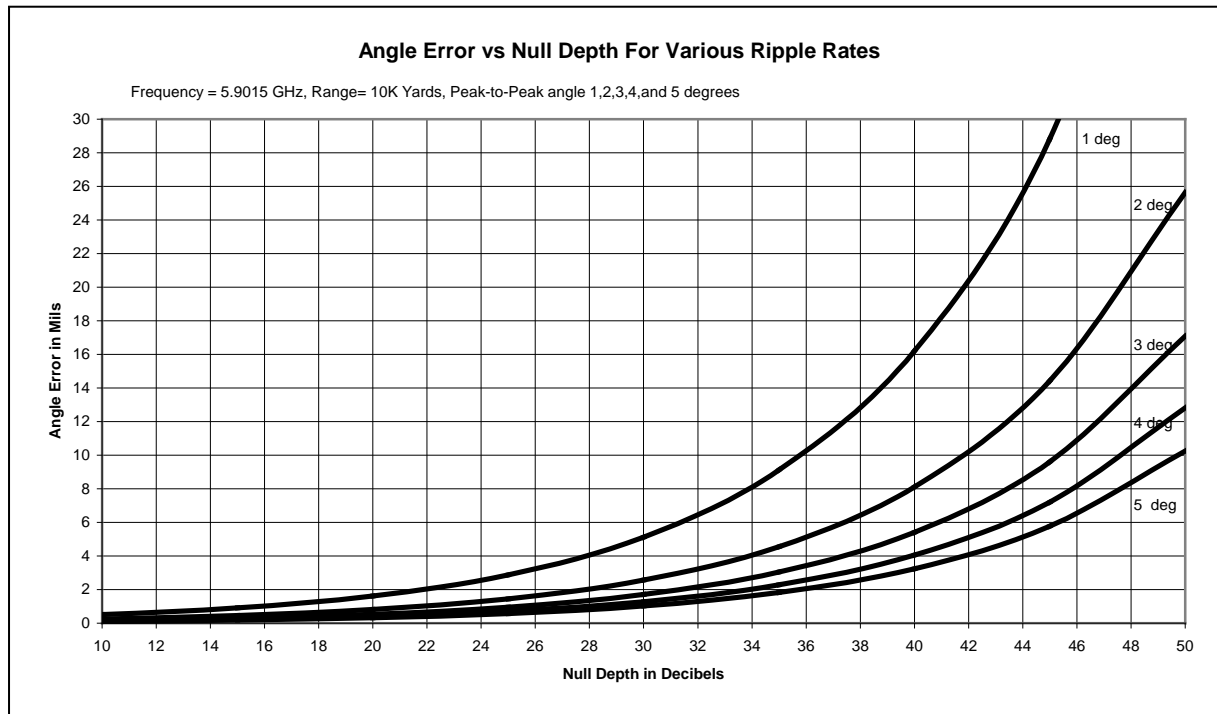


Figure 5-18. Angle error versus null depth for various ripple rates.

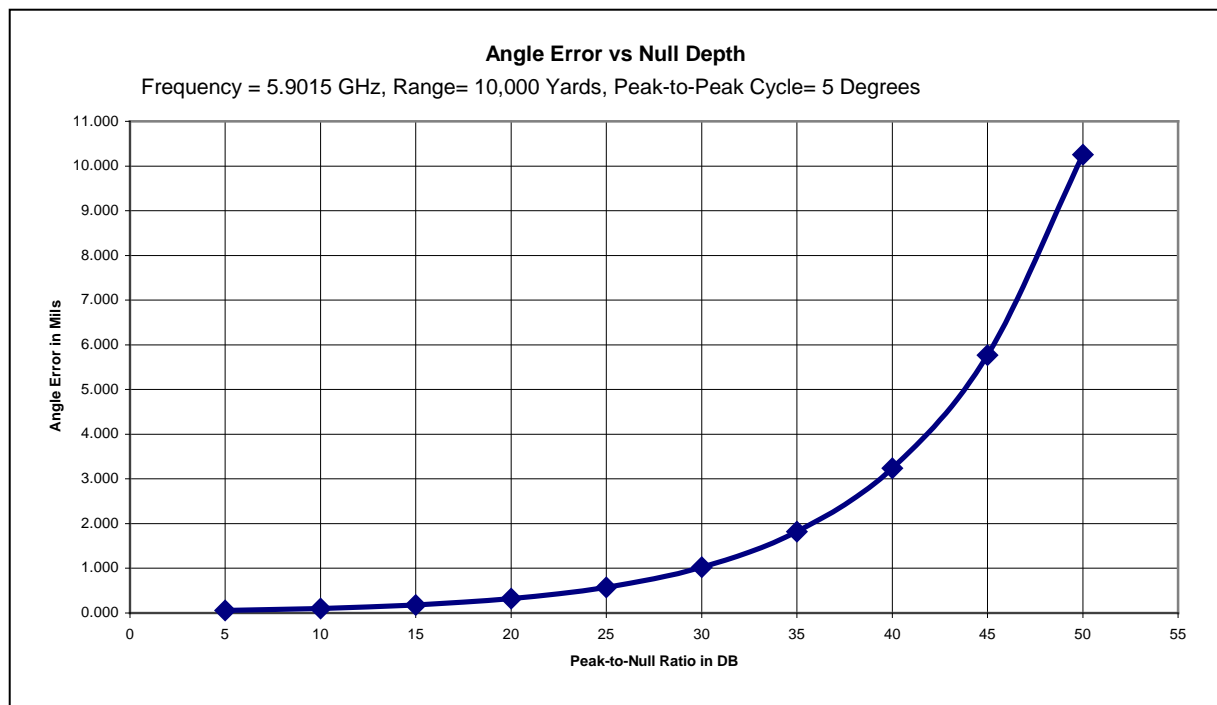


Figure 5-19. Angle error versus null depth.

5.10.7 Computes a cycle of pattern null and phase slope. A spreadsheet was used to calculate one cycle of the pattern formed by the phasor addition. Figure 5-20 shows the null formation (amplitude). Figure 5-21 shows the phase shift near the null. Figure 5-22 adds the tangent line showing the maximum slope of phase.

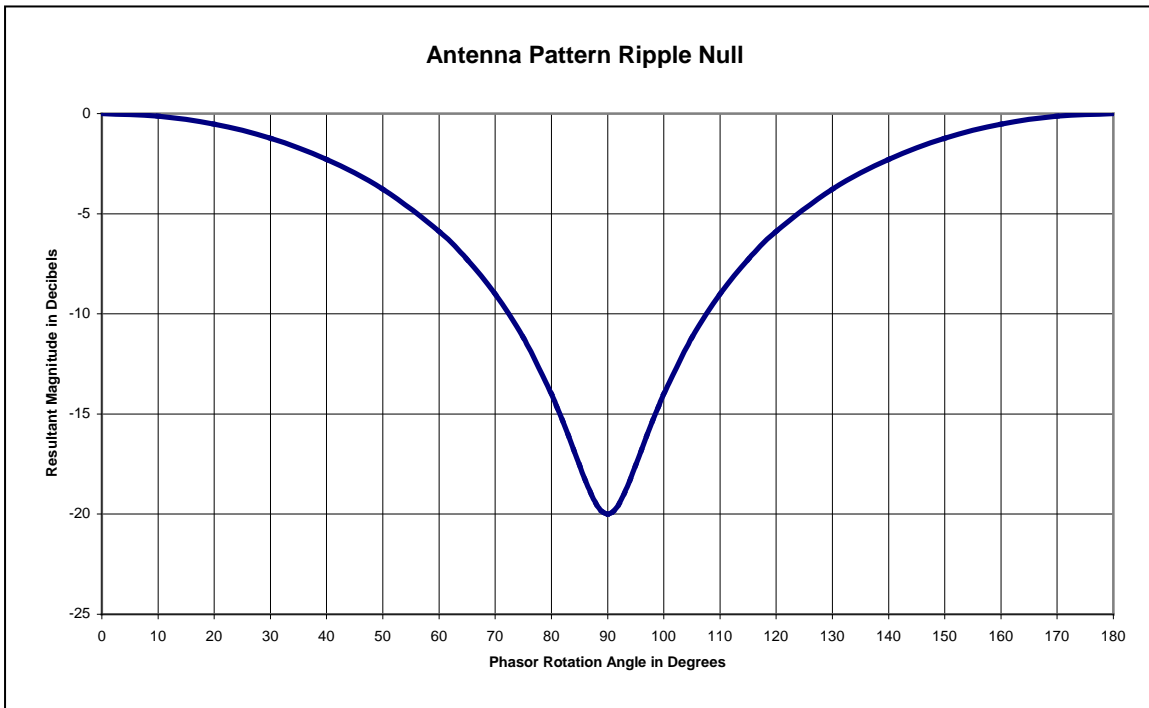


Figure 5-20. Pattern magnitude versus phasor rotation angle.

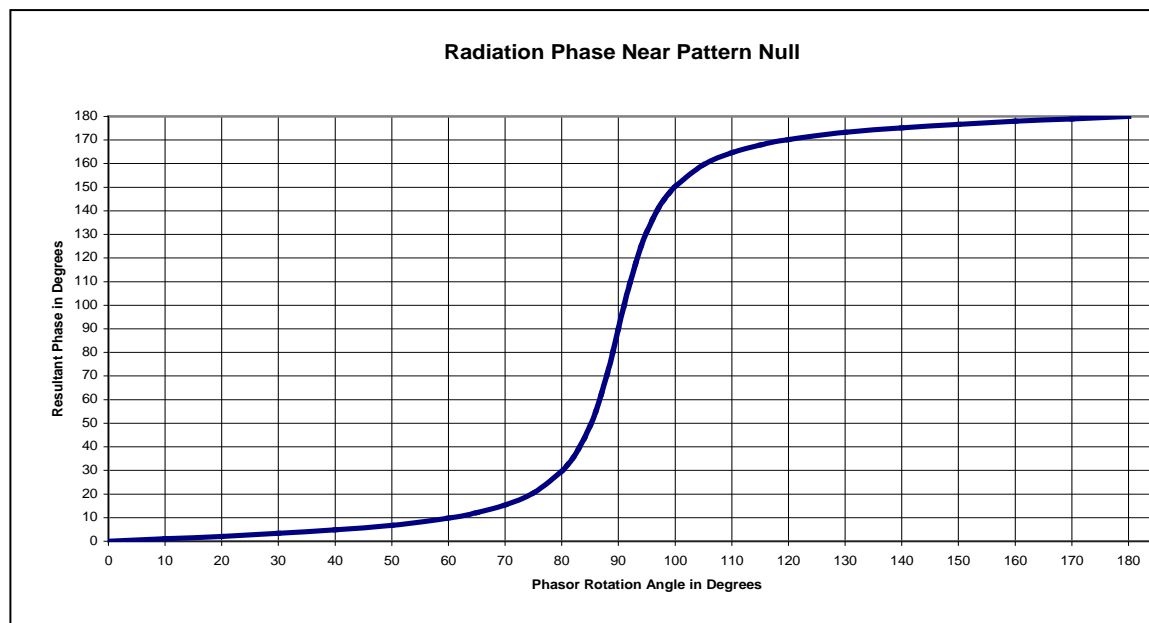


Figure 5-21. Pattern resultant phase versus phasor rotation angle.

5.10.8 Graph of phase gradient at pattern minimum.

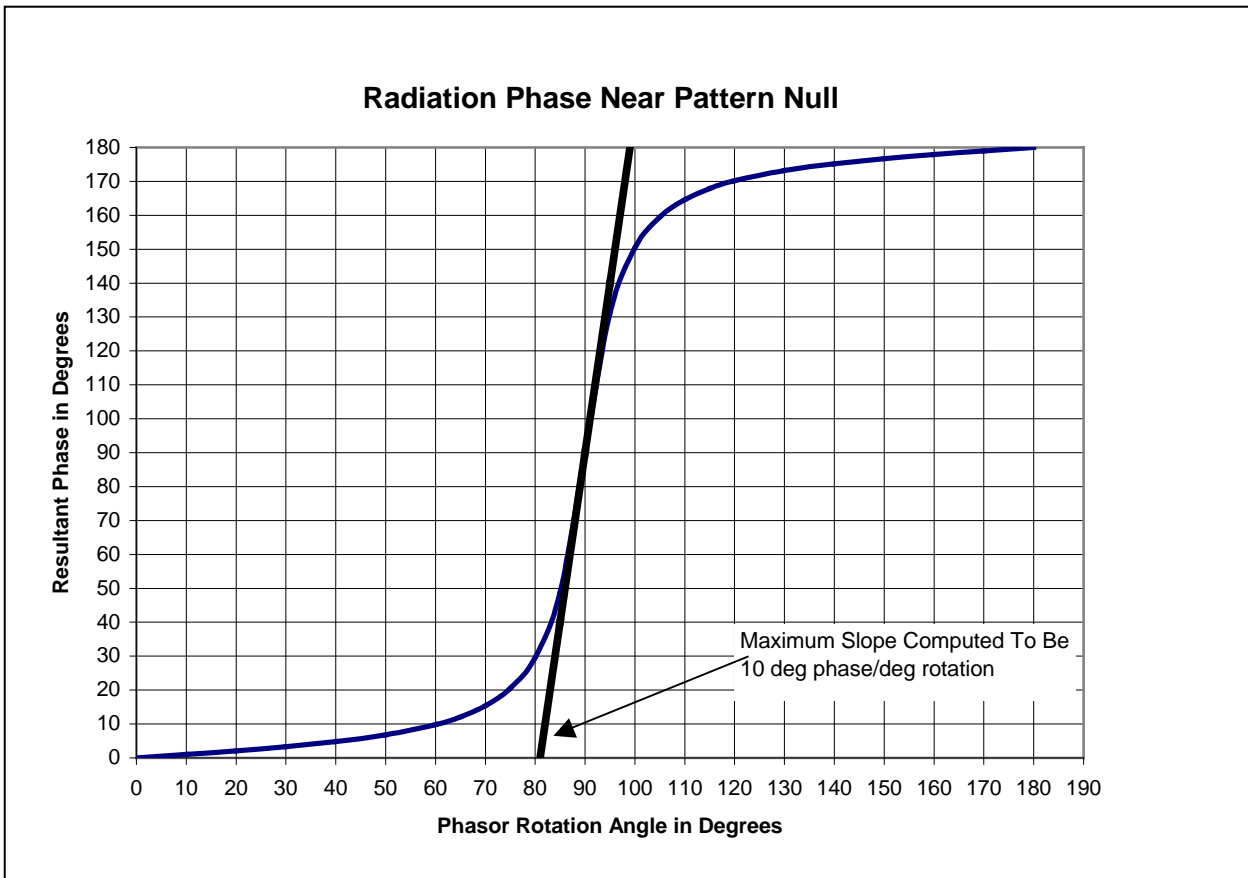


Figure 5-22. Phase slope near a null.

5.11 Transponder Antenna System Phase Patterns

5.11.1 Introduction. Just as the amplitude of the radiation pattern changes with angles from the vehicle, so does the phase of the radiation. A plot of amplitude versus angle(s) is usually assumed to be “the antenna pattern”, but any of the parameters of the radiating wave, when plotted versus angle, can be an antenna pattern. Phase and polarization are sometimes very important and are sometimes required to be plotted as “patterns”.

5.11.2 Tracking. Radar tracking quality can be affected by almost every parameter of the radiation associated with the transponder antenna system. Amplitude variations can cause errors in the range data. Phase variations can cause errors in velocity and acceleration data as well as errors in angle tracking (cross-eye). Polarization (sense, axial ratio, and tilt angle) variations can appear in both amplitude and phase with the associated potential for causing errors.

5.11.3 Measurement of Phase Patterns. Phase pattern measurement is generally considered more difficult than amplitude pattern measurement. Usually, the test antenna system is mounted on a rotation pedestal (positioner) so that a probe (range antenna) will be presented all angles from the antenna under test (AUT). The coordinate system for these measurements is specified in RCC Document 253-93.

For the simplest amplitude patterns, a relatively simple single channel receiver may be used to measure and record the response to a specified polarization component generated by the AUT. The case of phase pattern measurements requires a more complex receiver. A phase sensitive receiver (sometimes a vector network analyzer) is fed both the signal radiated from the AUT and a “steady reference” sample of the transmitter signal. The phase difference is recorded as the “phase pattern” as the AUT is rotated to all spherical angles. In these cases the range antenna (probe) is a single channel device which is configured to respond to the specified polarization component. In order to measure all the components normally required, it is necessary to make several passes over the radiation sphere. Due to several factors, it is normally not possible to get perfect registration from one RDP to another and the samples are not taken at exactly the same places in the subsequent measurements. One of the great advantages of the “polarimetry” technique is that only one pass over the radiation sphere is required to collect all the information necessary to determine the gain and polarization state of the AUT in every specified direction. It is noted that with polarimetry the measurement of phase patterns for “phase center” analysis requires the recording of six parameters at each sample. The two space angles, the two amplitudes, and two phases. When measuring phases, the first phase should be an absolute and the second phase should be a differential phase. Measurement of two absolute phases causes problems in the data analysis because of the “cyclic reset” of each component. The measurement of the differential phase allows the correct calculation of the polarization state, while the absolute phase of one of the components allows the simple computation of the absolute phase of the other.

Another consideration in the measurement of phase patterns is the location of the rotation axes with respect to the radiating elements during pattern measurements. In the case of amplitude patterns, slight changes in range during pattern measurements are considered inconsequential. This is not the case when phase patterns are being measured. The rotation axis offset (from the active element) of only one inch will result in a phase change of nearly a full wavelength over a full RDP. This result implies that additional preparation is necessary for phase patterns; that is, the use of some optical device (theodolite or laser) to establish the rotation axis location on the vehicle.

In recent years, the measurement of amplitude and phase patterns on radar transponder antenna systems has been required and specifications have become more stringent. For example, the document EWR 127-1 (1997) paragraphs 4.11.1.1.1 and 4.11.1.1.2 require measurements over the entire radiation sphere at 1 degree intervals (Refer to the RCC 265-06 Supplement to this document). In the past, the amplitude patterns (and sometimes the phase patterns) were allowed to be sampled at 2 degree intervals in roll and aspect angles. Results are also specified in terms of what are considered acceptable gain and phase variations. Gain variations of +/- 5 dB are allowed in the “roll plane” and “10 dB” in the “pitch plane” between 10 degrees and 170 degrees. The phase must not vary by more than 50 degrees in the “roll plane”. In this case,

the roll plane may mean any “constant theta” or “constant aspect angle” cut. The term pitch plane probably means any “constant roll angle” plane and would be clearer if stated in those terms. Then the limits on variations allowed in roll (phi) would apply to any “theta constant” conical cut instead of the single roll plane cut.

5.11.4 Interpreting Phase Patterns. Since the phase changes with roll and aspect angles from the transponder antenna system, it can be difficult to predict the apparent radial distance change as seen by a coherent radar system. Apparent radial velocity changes (radial acceleration) can be very difficult to track, especially in the presence of deep nulls in the amplitude patterns because of the associated rapid phase shifts. These are also tending to cause pointing errors at the same time which causes additional velocity data errors.

Increasing the range length will result in increasing phase delay. It is important to properly identify on the patterns which direction of phase change is “more lagging” and which is “more leading” phase. A rolling vehicle with two antennas in the array could appear to “wobble” an amount equal to its diameter even when the antennas are fed in equal phase. When one of the antennas has a very large difference in harness lengths between the two antennas, the total phase delay difference can cause a much larger wobble.

5.12 A Problem with Phase Patterns

The lead range sometimes requires phase patterns to be measured on a new target antenna system. Many times these requirements are waived for various reasons. Sometimes the antenna measurement range is not properly instrumented to make meaningful phase pattern measurements on the radiation components of interest, or the cost of making such measurements may be considered too great. In any case, the phase patterns normally measured are made at spot frequencies (i.e., continuous wave (CW)) and can be misleading.

5.12.1 Usually Drop Full Wavelengths in Data. Phase patterns measured at spot frequencies have the problem that they basically lose information involved in multiple wavelength differences in harness leg lengths. This is usually most apparent on large diameter vehicles (launch vehicles) that have a multi-element array of antennas. The power divider/combiner is usually mounted closer to one of the antennas than the others and the coax harness lengths to the elements depend upon the circumferential distance to the radiating element. As many as 10 to 15 wavelengths difference have been measured in actual flight hardware. In the CW case, elements driven with integral number of wavelengths difference appear to be co-phase. The actual time variation in going between two antennas with 15 wavelengths path difference could be seen by a radar as more than 30 inches of “wobble” as the target rolls.

5.12.2 Sampling Interval Too Great. Phase patterns can be used to assess the affect on the radar’s angular errors caused by the target’s antenna pattern. The normal 2 degree by 2 degree sample grid spacing is reduced to 1 degree by 1 degree in some cases. This is an attempt to better measure the pattern nulls which are very “sharp” and to “catch” the phase rate of change near nulls. An example of the obvious “errors” in the 2 by 2 degree sampling may be seen in the roll plane pattern comparisons at Figure 6-4 for a 64 inch diameter vehicle with two unit radiators. A similar comparison is shown at Figure 6-5 of an analog pattern and a sampled pattern for three unit radiators on a 38 inch diameter vehicle.

Data channels that have phase encoding (such as Bi-Phase and quadrature phase shift keying (QPSK)) can be disrupted due to rapidly changing phase patterns. This effect should be taken into account when considering the acceptability of any given vehicle antenna pattern.

5.13 Polarization Basic Concepts

The polarization state of an antenna can be defined as the polarization state of the wave that the antenna radiates. In a sense, the antenna itself doesn't have a polarization; polarization refers only to the wave it transmits. Polarization states vary as a function of the direction around the antenna. In general, every direction around a transmitting antenna may have a different polarization state from the rest. Polarization of a propagating wave is determined by the orientation of its electric field vector. If the electric field vector vibrates in a plane, the polarization state is said to be linear. If the electric field vector describes a circle in the plane perpendicular to its direction of propagation, then it is said to be circularly polarized. The general case is elliptical polarization in which the electric field vector describes an ellipse in the plane normal to the propagation direction. Both linear and circular are special cases of elliptical polarization.

5.13.1 Poincare Sphere. The study of polarization usually leads to a very powerful graphical representation known as the Poincare Sphere. On the surface of the Poincare sphere lie all possible polarization states. The poles represent right and left hand circular polarization (RHCP and LHCP). The equator of the Poincare sphere contains all possible linear polarization states, meaning it represents all possible tilt angles of linear polarization. The polarization ellipse can be described in terms of its axial ratio and tilt angle along with its sense of rotation. Another way of determining an ellipse is to specify its two orthogonal component magnitudes and the phase between them. The Poincare sphere can help in visualizing a polarization state and how coupling between two states varies with the parameters of either wave state.

The radiation sphere (See Figure 5-23) is attached to an antenna and moves with it. The angle theta is the polar angle (supplement of the aspect angle) and phi is the roll angle. The direction of radiation is outward along the radial in the (theta, phi) direction. The polarization components lie in the tangent plane at the tip of the radial. The E-theta component is in the direction of increasing angle theta. The E-phi component is in the direction of increasing angle phi. It is in this tangent plane that the polarization ellipse lies. The reference direction is the E-theta direction with the right hand rule yielding E-theta crossed on E-phi equals the propagation direction.

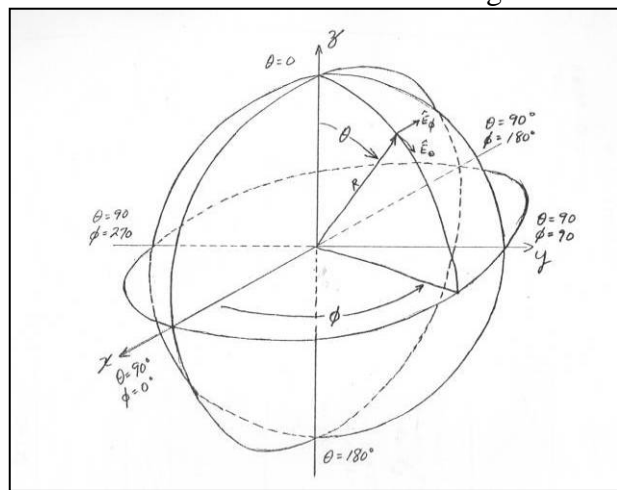


Figure 5-23. Radiation sphere definitions.

5.13.2 Graphics of Radiation and Poincare Spheres. Consider the Poincare Sphere the surface of which contains all possible polarization states. The upper hemisphere represents all left hand elliptical states with the upper pole at LHCP. Conversely, the lower hemisphere represents all right hand elliptical states with RHCP at the lower pole. The equator contains all linear states with the reference for tilt angle at E-theta. Diametrically opposite E-theta is E-phi with E-45 and E-135 at the extremes on the orthogonal axis.

The tilt angle is represented by “double angle” rate around the equator starting at E-theta, thus in going from E-theta to E-45 we progress 90 degrees around the equator. (See Figure 5-24)

It should be apparent that states which are diametrically opposite on the sphere are orthogonal and thus decoupled.

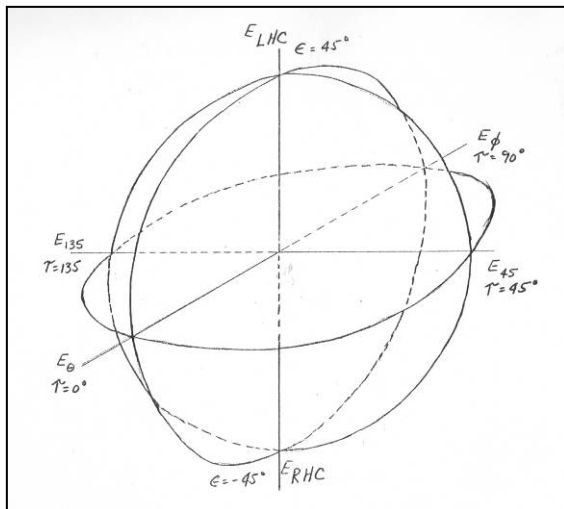
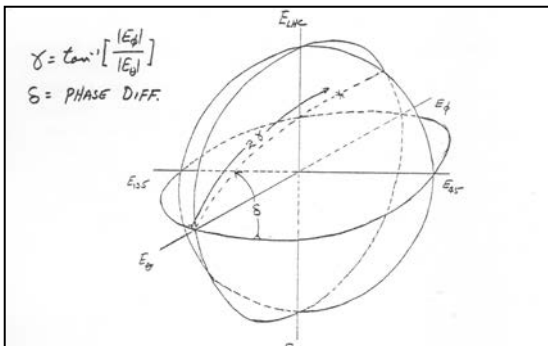
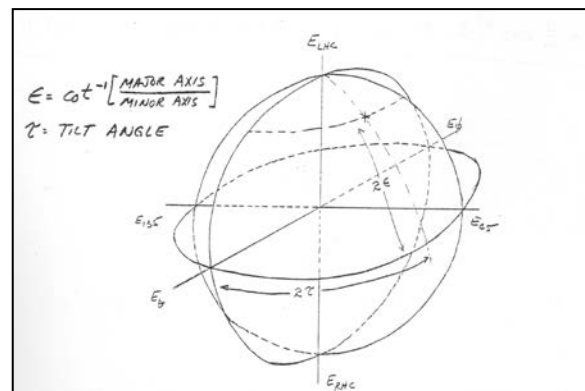


Figure 5-24. Poincare sphere definitions.



Locating a point on the Poincare Sphere (a polarization state) may be done in either of two equivalent ways. Specifying the “component ratio” and “phase difference” is one way while specifying the “axial ratio” and “tilt angle” is the other. The phase difference is measured as the dihedral angle between the equatorial plane and the plane containing the E-theta/E-phi axis and the point in question. This angle is called “delta” (Figure 5-25).

Figure 5-25. State located by polarization ratio and phase.



The axial ratio is measured toward the pole from the equatorial plane on a great circle (longitude) line. This angle is measured at double angle rate as are all angles on the surface of the Poincare Sphere. The tilt angle is measured (double angle) along the equator from E-theta to the longitude of the point in question. (See Figure 5-26).

Figure 5-26. State located by axial ratio and tilt angle.

Contours of constant “axial ratio” and “tilt angle” are shown in Figure 5-27. The equivalent representations of the polarization ellipse in terms of constant “component ratio” and “phase difference” are also shown.

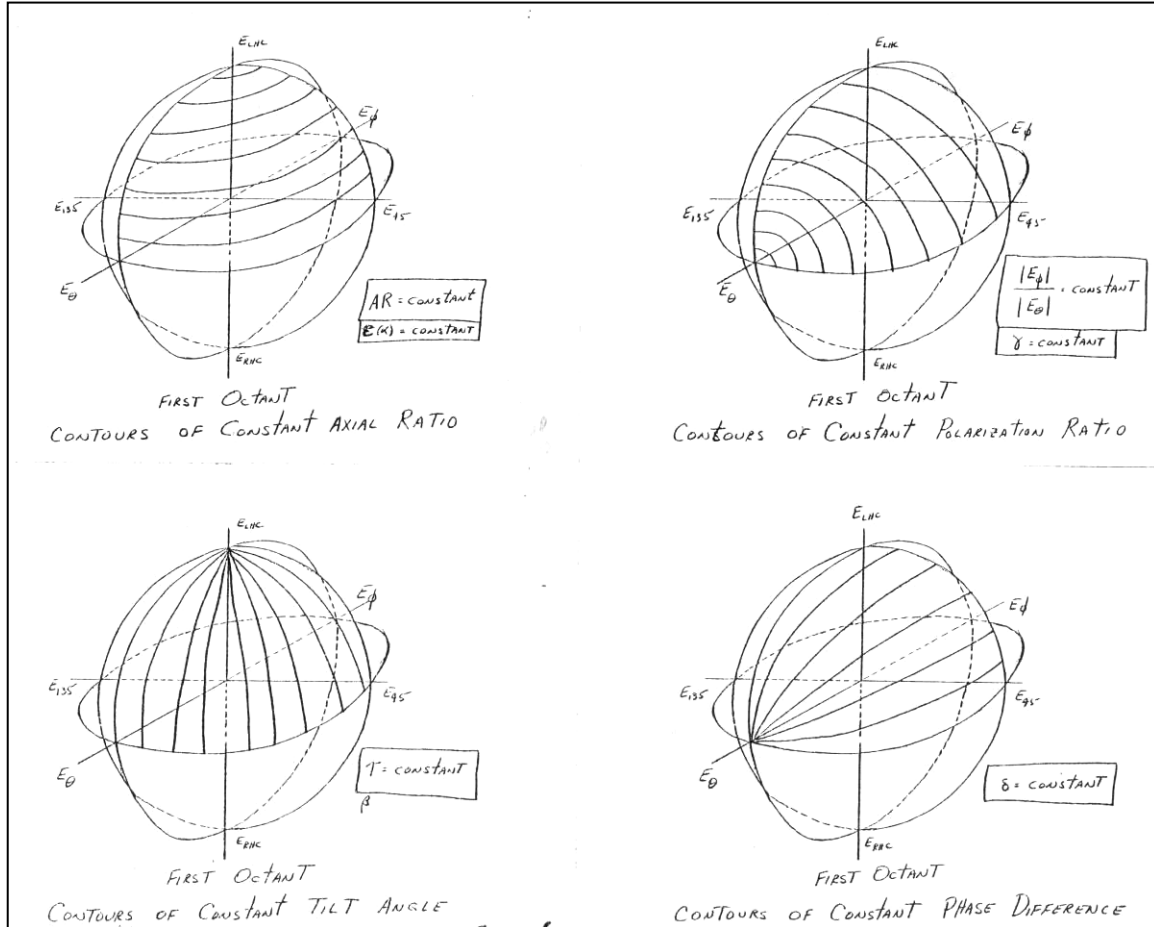
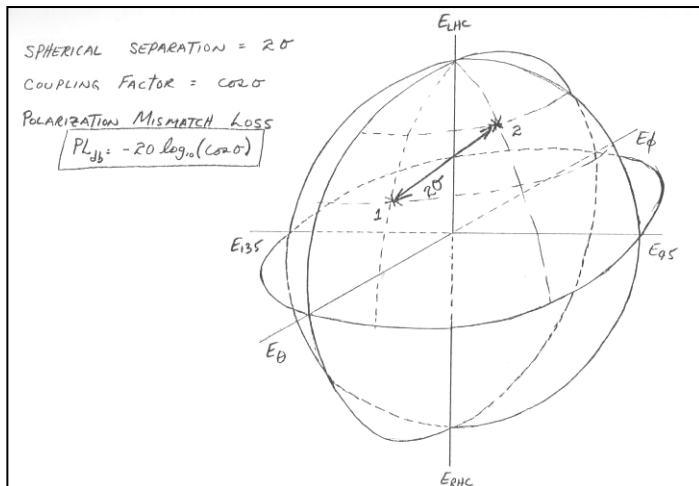


Figure 5-27. Contours of constant axial ratio, tilt angle, component ratio and phase.



The coupling between polarization states is determined by the separation on the surface of the Poincaré Sphere as shown in Figure 5-28. Co-located points couple completely, i.e. no polarization mis-match loss. States that are diametrically opposite are isolated, i.e. infinite polarization mismatch loss. Consider Figure 5-28.

Figure 5-28. Coupling between two states.

5.14 The Poincare Sphere in Polarization Analysis

Radiation Sphere

The standard spherical coordinate system normally used in far field radiation measurements is shown in Figure 5-29. Attention is called to the fact that this system is composed of two essential parts. The first part is the reference system for determination of spatial angles; these are the polar angle (θ , Θ) and the roll angle (ϕ , Φ). The Cartesian system of three axes, x , y , and z , is also shown. The second part is associated with the polarization component reference system.

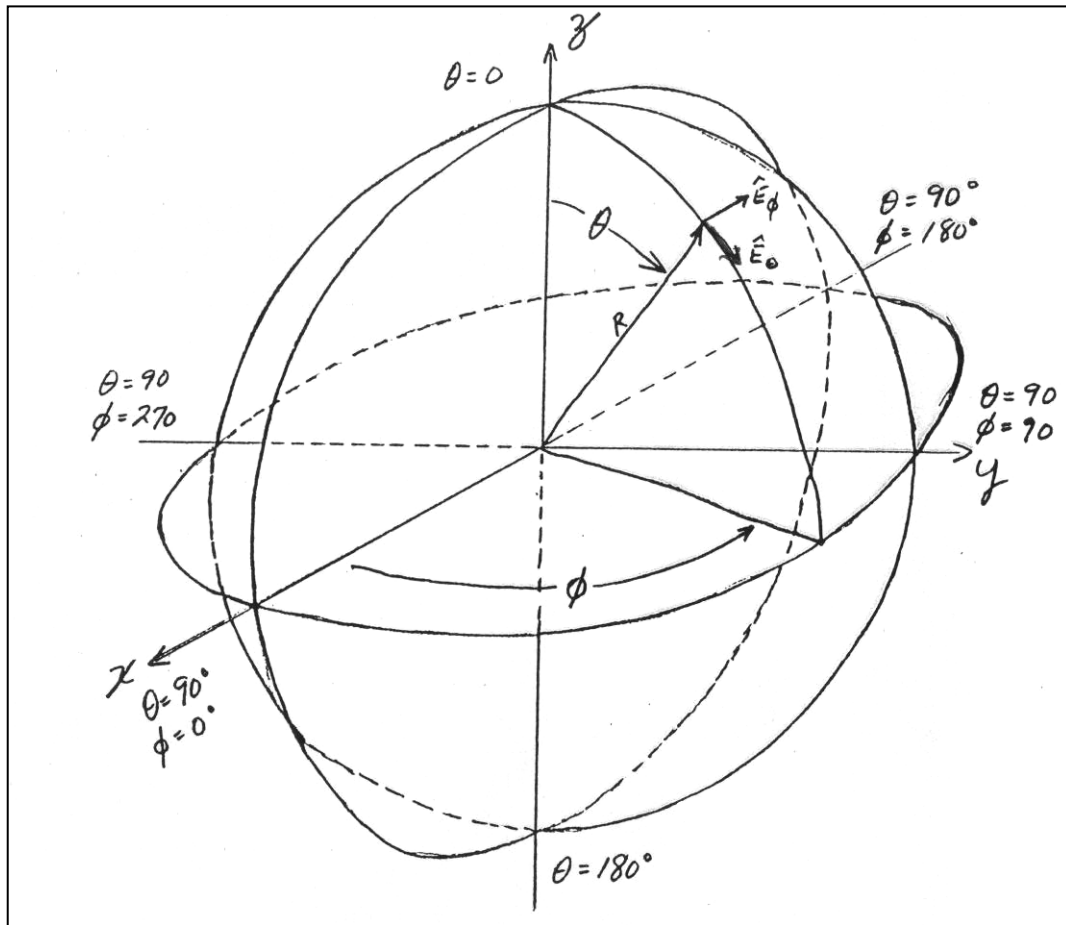


Figure 5-29. Radiation sphere definitions.

In Figure 5-29, a wave propagates outward in the direction of R (radially outward) specified by θ & ϕ and is considered to be a plane wave at the surface of the sphere. Both E_θ and E_ϕ lie in the tangent plane (ie. both are perpendicular to R) and are orthogonal with the propagation direction. Both reference systems thus mentioned are right-handed systems (ie. rotating from x to y advances a right hand screw along positive z . Also rotating from E_θ to E_ϕ advances a right hand screw radially outward).

This tangent plane containing E_θ and E_ϕ is shown detached in Figure 5-30 through Figure 5-33 so that the polarization ellipse can be seen more clearly.

Polarization describes the locus of the tip of the electric field vector. The E vector traces out the polarization ellipse once each cycle of the RF wave. In the following figures, the important features and definitions are sequentially added to complicate the drawing somewhat. Notice that E_θ is used as the reference direction for all polarization analyses that follow. Notice that the ellipse can be described in either of the following two ways:

- Its tilt angle and axial ratio along with sense of rotation describes it geometrically and
- The relative magnitudes of two orthogonal components E_θ and E_ϕ with the phase difference describes it as might be generated. This second method inherently yields the sense of rotation. This distinction will show up later and prove valuable.

Directions For E_θ , E_ϕ , E_{45} , E_{135} RHEP are defined by CCW rotation direction as shown in Figure 5-30.

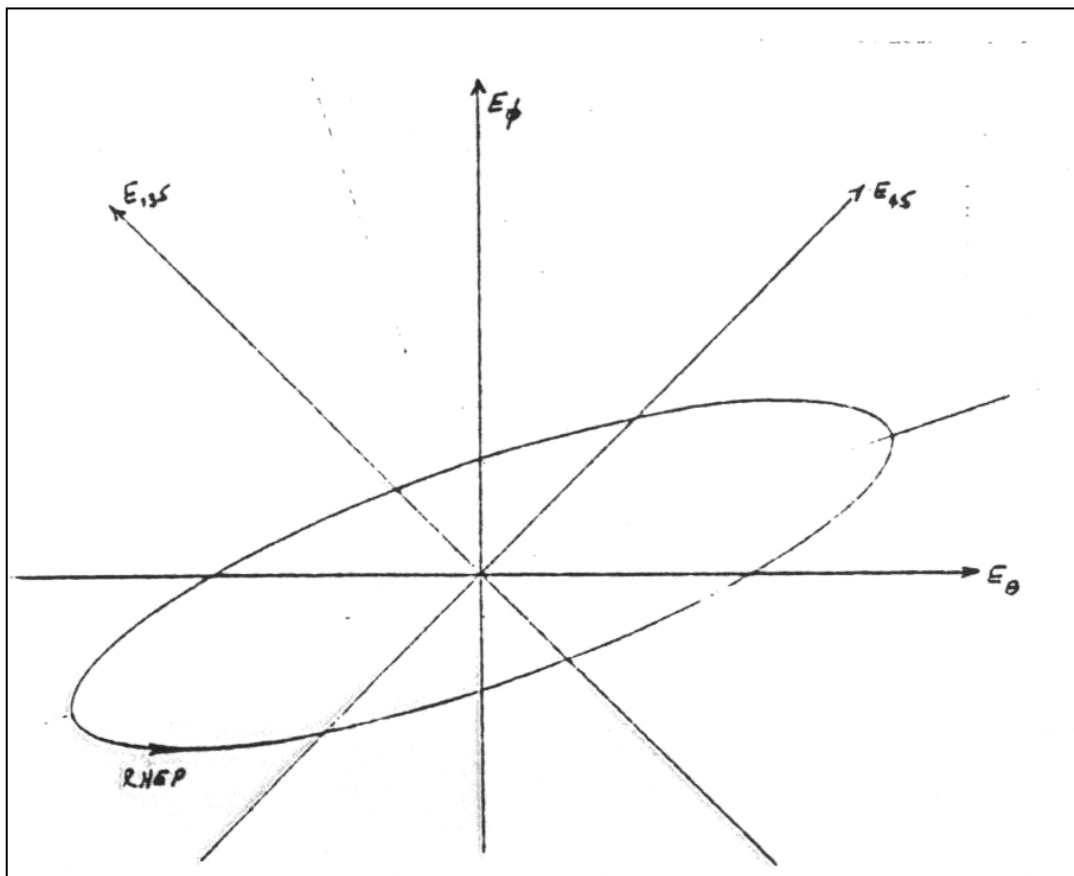


Figure 5-30. Definitions of directions.

Shown in Figure 5-31 are:

- Tilt Angle, τ , is measured from \hat{E}_θ toward \hat{E}_ϕ .
- Magnitudes of E_θ and E_ϕ which are the extremes of the ellipse tangents.
- $0 \leq \tau \leq 180^\circ$

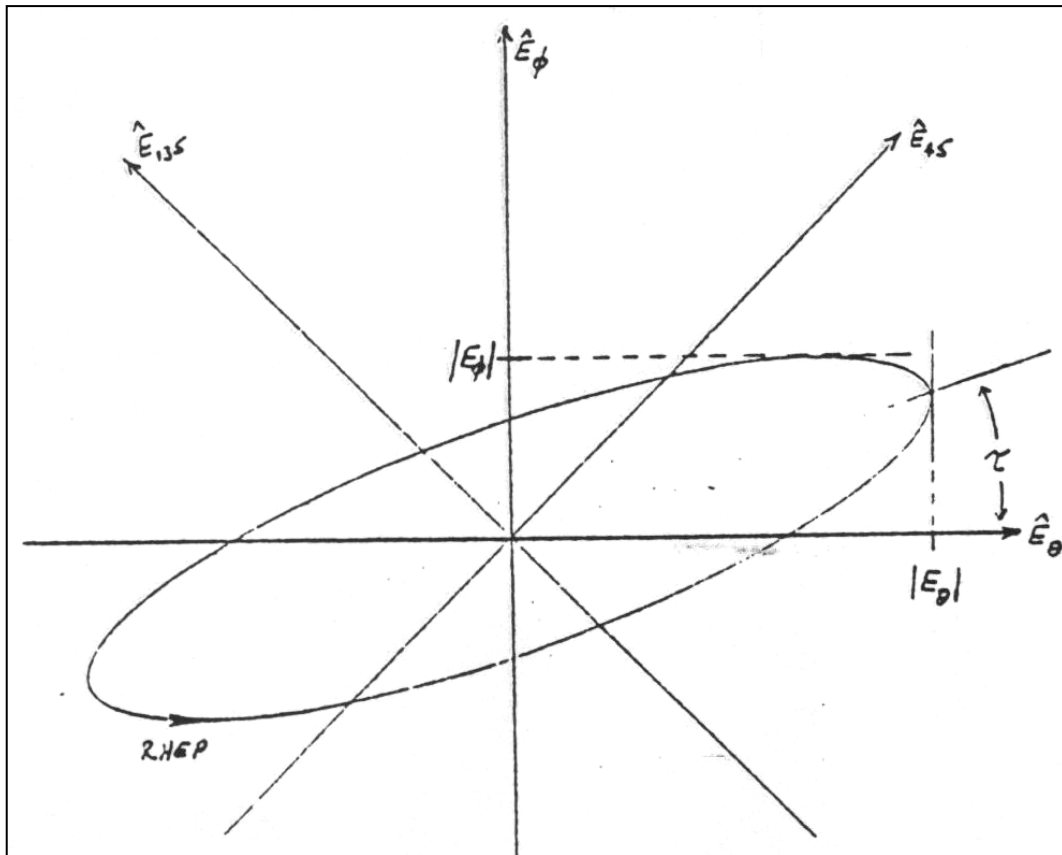


Figure 5-31. Tilt angle and axial ratio definitions.

Definitions of E_{45} and E_{135} are similar to the definitions for E_θ and E_ϕ except that projections are onto the axes rotated 45 degrees to E_θ and E_ϕ (see Figure 5-32).

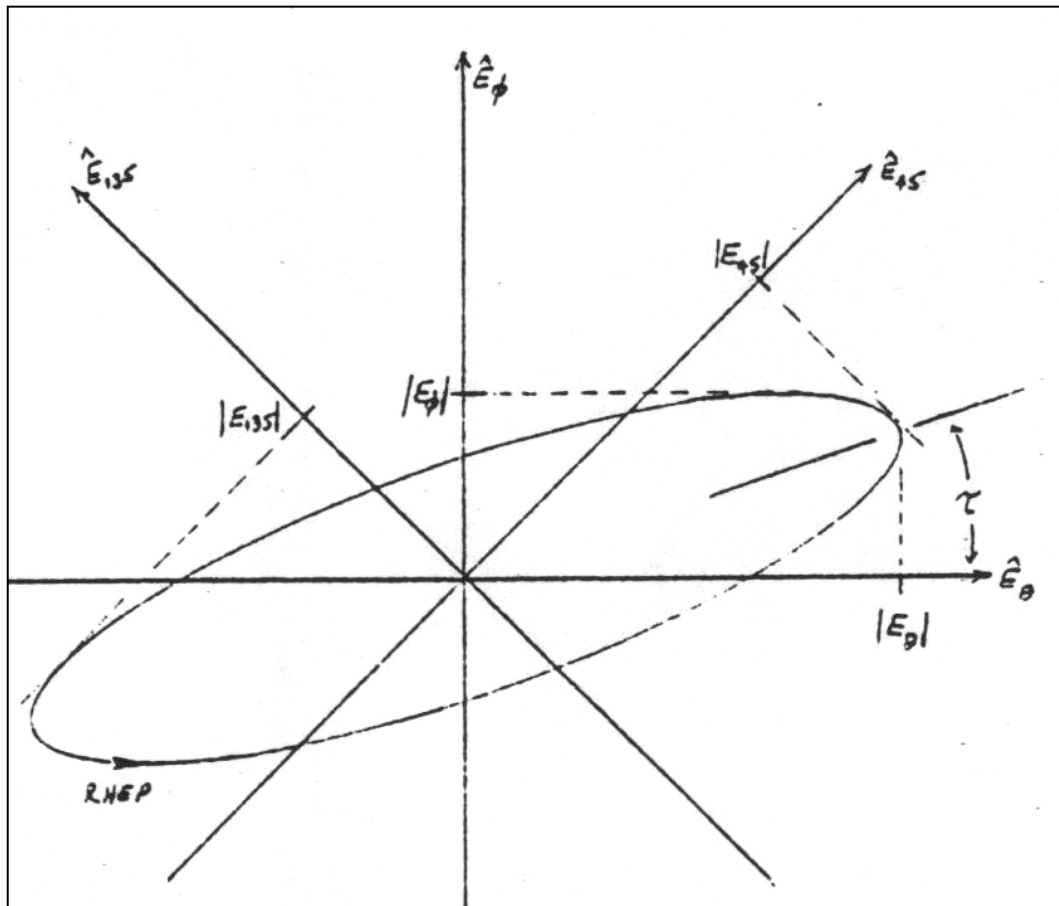


Figure 5-32. Definitions of E_{45} and E_{135} components.

Definition Of Axial Ratio is shown in Figure 5-33:

- a. Axial Ratio = AR = Major Axis/Minor Axis
- b. $AR \geq 1$
- c. $\varepsilon = \cot^{-1}(AR)$

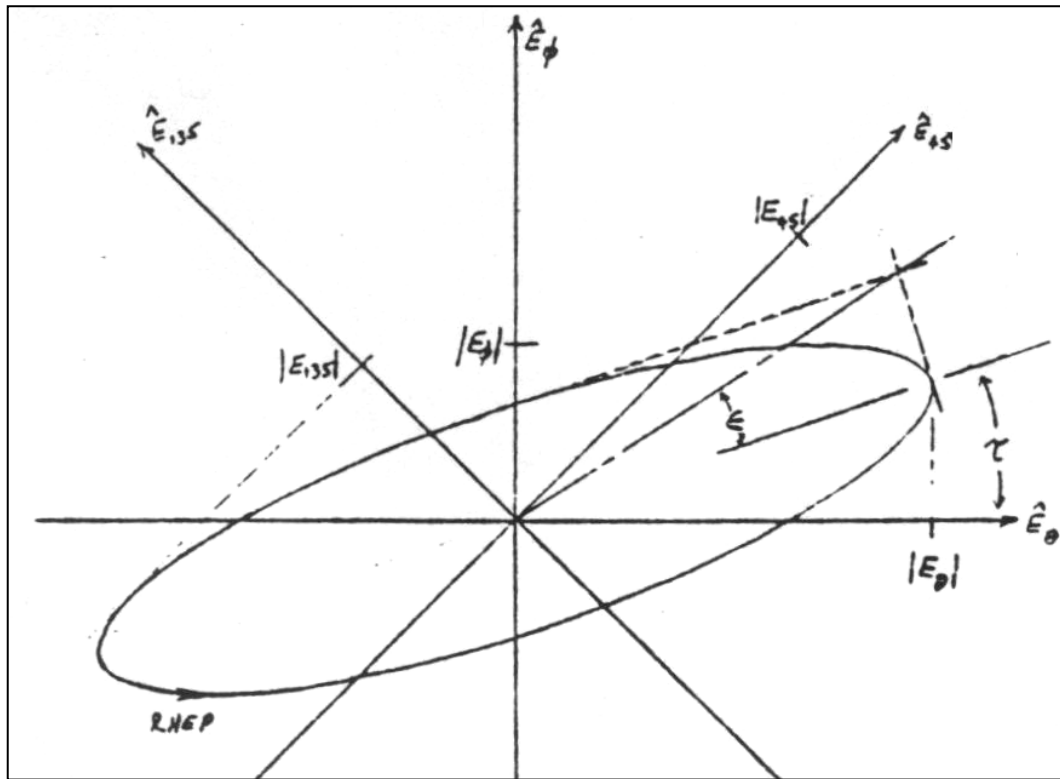


Figure 5-33. Axial ratio definition.

5.14.1 Tutorial on Poincare Sphere Usage. The plane geometry representation of the polarization state of a wave or antenna shown in Figures 5-30 through Figure 5-33 can be used for some limited analysis, usually for one state at a time, but becomes rather cumbersome when a second state is introduced.

There is another graphical aid that allows much more complicated analysis to be performed on polarization states; it is the Poincare Sphere Representation shown in Figure 5-34.

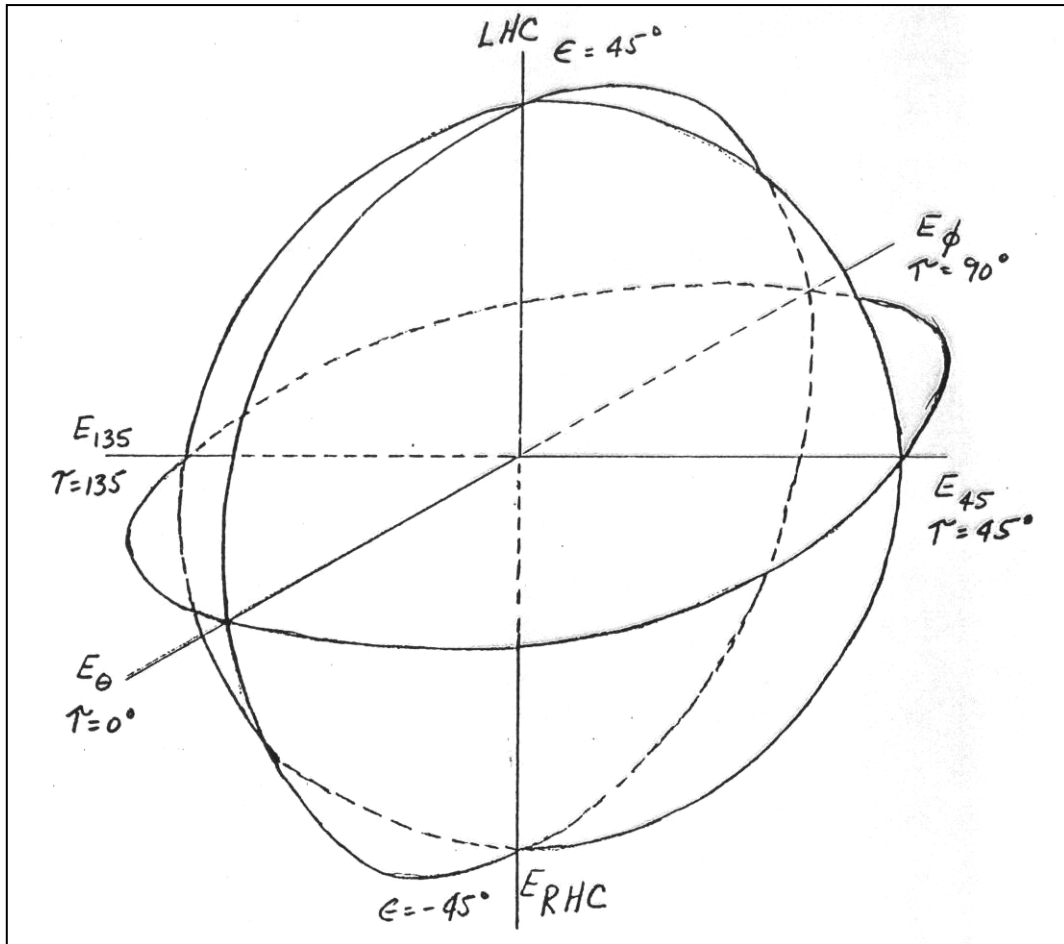
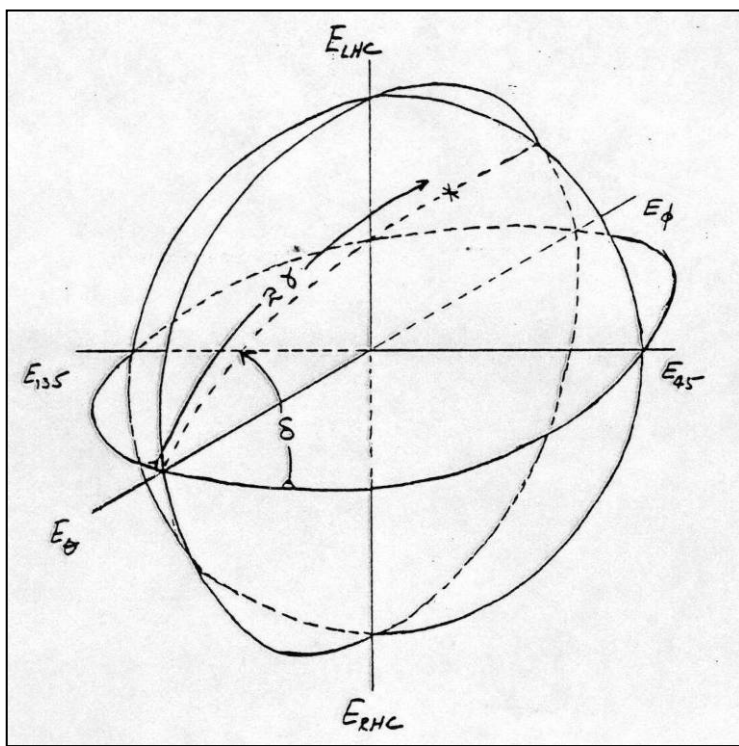


Figure 5-34. Poincare sphere definitions.

The Poincare Sphere is shown with some of the definitions normally used. Prominent features include:

- a. There is a 1:1 correspondence of polarization states and points on the surface of the Poincare Sphere.
- b. All linear polarizations are points on the Equator.
- c. All left hand elliptical states are on the upper hemisphere while all right hand states are on the lower hemisphere.
- d. Left hand circular is located at the upper pole and right hand circular is at the lower pole.
- e. The relative coupling between any two states is determined by their separation on the surface of the sphere. Two points which are diametrically opposite on the sphere have no coupling (ie., infinite loss) while those co-located have perfect coupling (ie. zero loss).
- f. Angles measured on the surface of the Poincare Sphere are twice their counterparts on the polarization ellipse.
- g. Increasing tilt angle corresponds to increasing the angle measured along the equator while axial ratio changes correspond to changes in angle measured between Equator and Pole.
- h. Changes in component ratio (polarization ratio) correspond to changes in the angle measured directly from the E_0 reference axis, while the relative phase between components corresponds to the dihedral angle between the equator and the great circle which contains the E_0 state and the polarization state in question.

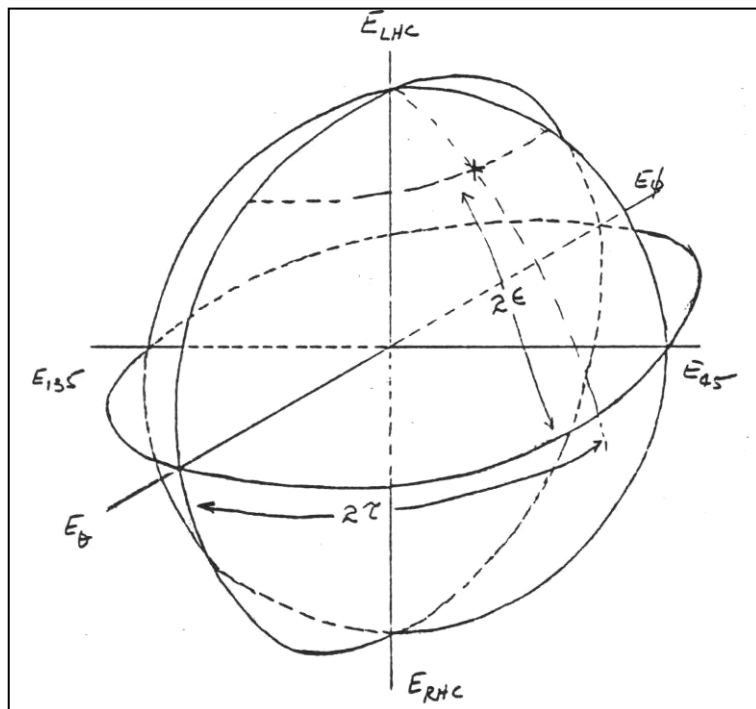
Figure [5-35](#) shows an example of the location of a polarization state by component ratio and phase while in Figure [5-36](#) the same state is located by the geometrically associated quantities axial ratio and tilt angle.



$$\gamma = \tan^{-1} \left[\frac{E_\phi}{E_\theta} \right]$$

δ = Phase Angle

Figure 5-35. Polarization state located by polarization ratio and phase angle.



$$\epsilon = \cot^{-1} \left[\frac{\text{Major Axis}}{\text{Minor Axis}} \right]$$

τ = Tilt Angle

Figure 5-36. Polarization state located by axial ratio and tilt angle.

A quick overview of these angles and the contours generated by holding one constant while varying the other is given in Figure 5-37 and Figure 5-38. Contours of constant axial ratio are shown in Figure 5-37, while contours of constant tilt angle are shown in Figure 5-38. These contours are orthogonal to each other.

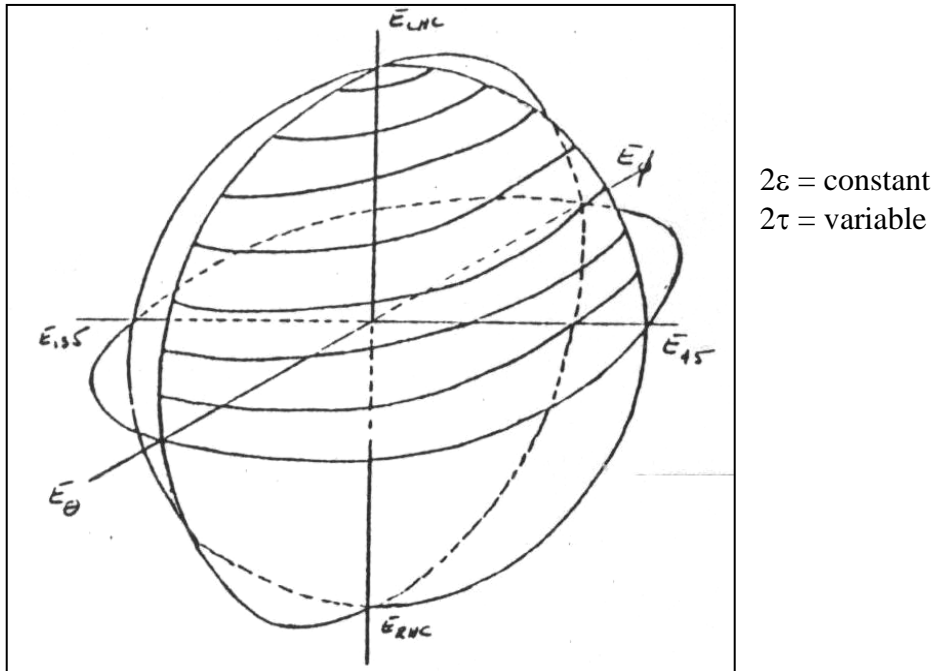


Figure 5-37. Contours of constant axial ratio.

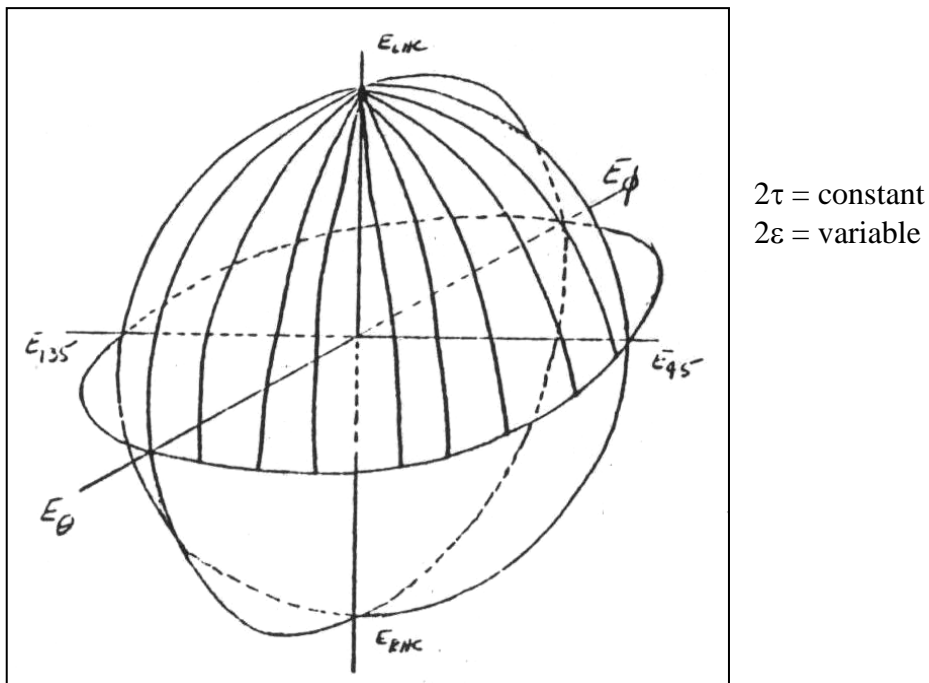


Figure 5-38. Contours of constant tilt angle.

Similarly, Figure 5-39 shows contours of constant component ratio and Figure 5-40 shows contours of constant phase difference. These contour lines are orthogonal to each other.

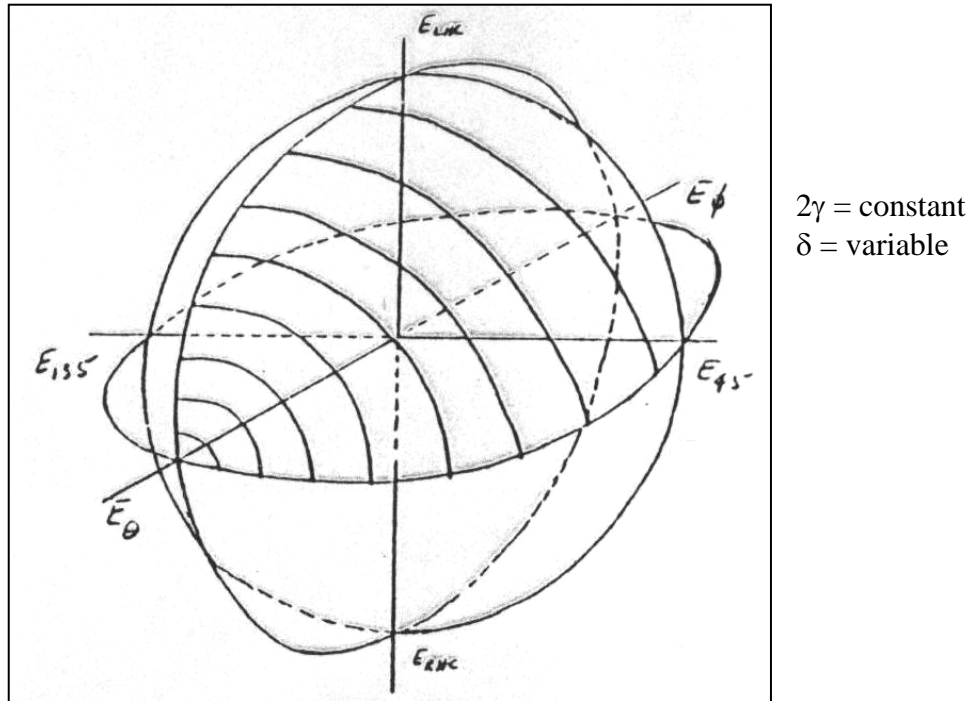


Figure 5-39. Contours of constant polarization ratio.

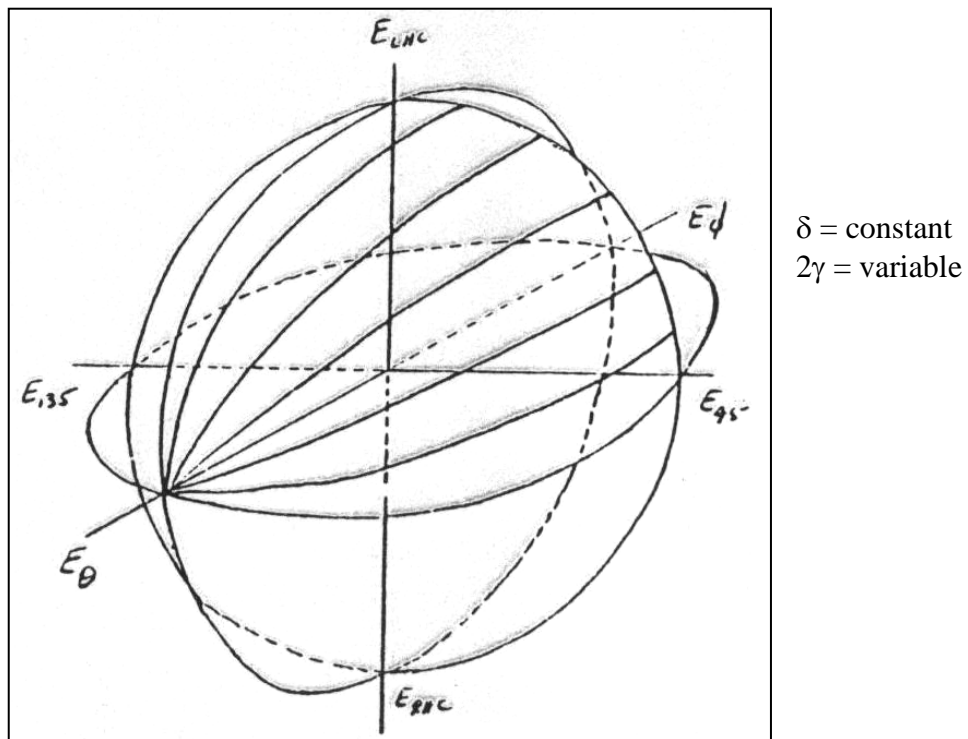


Figure 5-40. Contours of constant phase angle.

5.14.2 Basic Equations For Poincare Sphere. The following are some of the basic relationships among the various angles and parameters on the Poincare Sphere.

Angles

Polarization ratio and phase angle to axial ratio and tilt angle

$$\tan 2\tau = \tan 2\gamma \cos \delta$$

$$\sin 2\varepsilon = \sin 2\gamma \sin \delta$$

Axial ratio and tilt angle to polarization ratio and phase angle

$$\cos 2\gamma = \cos 2\varepsilon \cos 2\tau$$

$$\tan \delta = \tan 2\varepsilon \csc 2\tau$$

Component magnitudes to polarization ratio

$$\tan \gamma = \frac{E_\phi}{E_\theta} \quad \text{or} \quad \gamma = \tan^{-1}\left(\frac{E_\phi}{E_\theta}\right)$$

Coupling

$$Coupling = \cos \sigma$$

$$\sigma = \frac{1}{2} \cos^{-1} [\cos 2\gamma_1 \cos 2\gamma_2 + \sin 2\gamma_1 \sin 2\gamma_2 \cos(\delta_1 - \delta_2)]$$

or

$$\sigma = \frac{1}{2} \cos^{-1} [\sin 2\varepsilon_1 \sin 2\varepsilon_2 + \cos 2\varepsilon_1 \cos 2\varepsilon_2 \cos 2(\tau_2 - \tau_1)]$$

Polarization Mismatch Loss in decibels

Principle Components

$$PL_\theta = -20 \log_{10} (\cos \gamma)$$

$$PL_\phi = -20 \log_{10} (\sin \gamma)$$

Same hand circular and opposite hand circular

$$PL_{SHC} = -20 \log_{10} [\cos(45^\circ - \varepsilon)]$$

$$PL_{OHC} = -20 \log_{10} [\cos(45^\circ + \varepsilon)]$$

Maximum and minimum loss to linear

$$PL_{MAXLinear} = -20 \log_{10} \left\{ \cos \left[\tan^{-1} \left(10^{-\frac{AR}{20}} \right) \right] \right\}$$

$$PL_{MINLinear} = -20 \log_{10} \left\{ \cos \left[\tan^{-1} \left(10^{\frac{AR}{20}} \right) \right] \right\}$$

Total Gain

Principle components

$$G = 10 \log_{10} \left[10^{\frac{E_\theta}{10}} + 10^{\frac{E_\phi}{10}} \right]$$

Polarization & Gain Analysis with Three Linear Components

The following is a brief view of an analysis technique derived by necessity when apparent gain measurement irregularities had to be reconciled with less than the usually required amount of data.

At the outset it should be stated that linear components alone will not determine the polarization sense unless phase information accompanies amplitude information. Except as mentioned below, it is assumed that the sense is known or arbitrary. For many cases of interest this assumption is warranted, but when the sense must be found only one non-linear (preferred circular) component amplitude needs to be added to the measurement scheme.

Begin with the measurement of the amplitudes E_θ and E_ϕ . (It will be assumed that measured values are in dB.) The gain can be found by

$$G_{\text{dB}} = 10 \log_{10} \left[10^{\frac{E_{\theta\text{dB}}}{10}} + 10^{\frac{E_{\phi\text{dB}}}{10}} \right]$$

Also

$$\frac{E_\phi}{E_\theta} \quad \text{in dB} \quad = \quad E_{\phi\text{dB}} - E_{\theta\text{dB}}$$

Then

$$\gamma = \tan^{-1} \left[10^{\frac{E_{\phi\text{dB}} - E_{\theta\text{dB}}}{20}} \right]$$

Polarization mismatch loss between two states is an essential quantity. We can find values for PL_θ (mismatch loss to E_θ) and PL_ϕ (mismatch loss to E_ϕ) by noting that on the Poincare Sphere any coupling factor is numerically equal to the cosine of half the distance between states on the **spherical surface**.

Then in dB

$$PL_{1,2} = -20 \log_{10}(\cos \sigma)$$

This geometry is depicted in Figure 5-41.

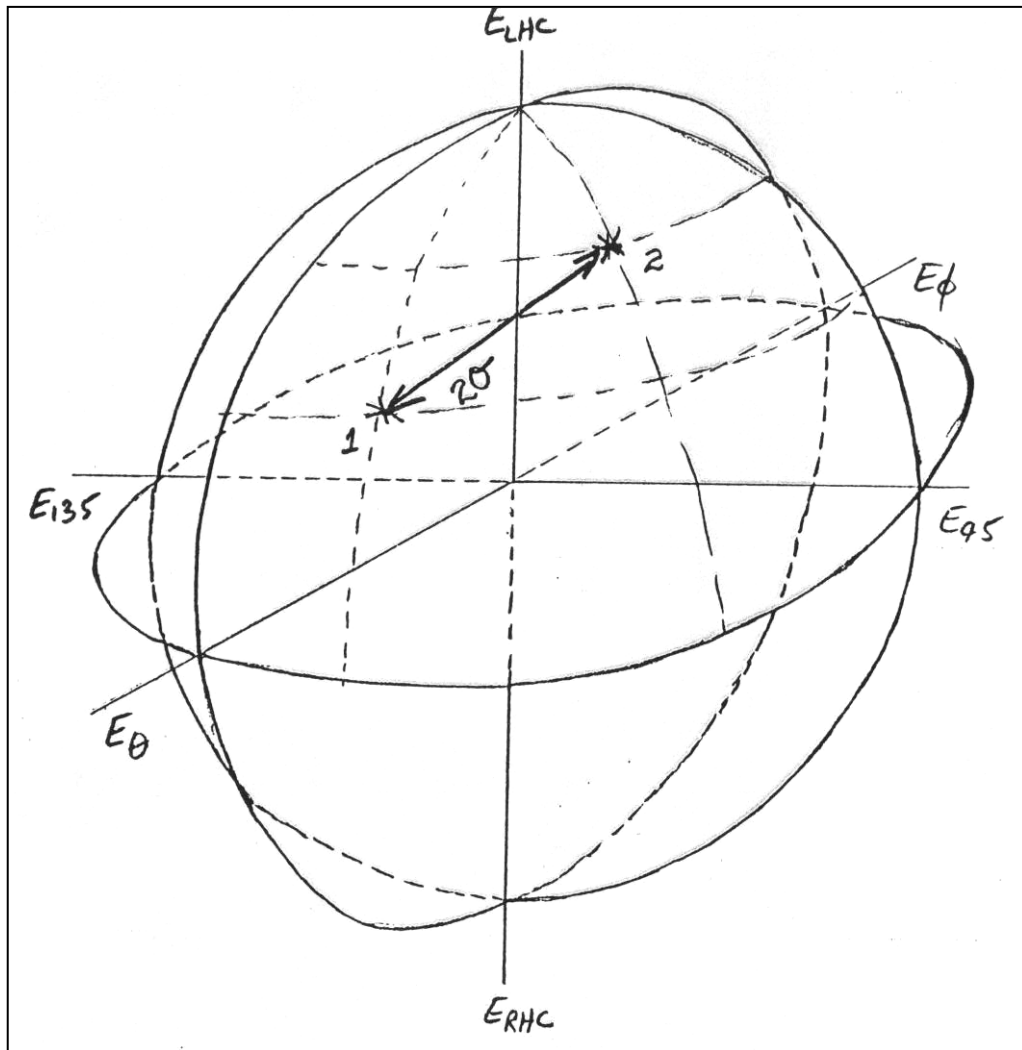


Figure 5-41. Polarization coupling between two states.

Spherical Separation = 2σ

Coupling Factor = $\cos 2\sigma$

Polarization Mismatch Loss in Decibels

$$PL_{dB} = -20 \log_{10}(\cos(\sigma))$$

$$\sigma = \frac{1}{2} \cos^{-1} [\sin 2\varepsilon_1 \sin 2\varepsilon_2 + \cos 2\varepsilon_1 \cos 2\varepsilon_2 \cos 2(\tau_2 - \tau_1)]$$

Note: In some expressions the equivalent angles are substituted as follows:

$$\varepsilon_1 = \alpha_1 \quad \varepsilon_2 = \alpha_2 \quad (\tau_2 - \tau_1) = (\beta_2 - \beta_1)$$

Now it is clear that

$$PL_\theta = -20 \log_{10}(\cos \gamma)$$

and

$$PL_\phi = -20 \log_{10}(\sin \gamma)$$

At this point it is not possible to determine the polarization loss to any other specified state. It is necessary to find the unique location of the state in question (or its image in sense). An additional linear component (E_{45} or E_{135}) can determine the tilt angle and axial ratio, but not the sense. An additional circular component can determine the axial ratio and the sense, but not the tilt angle. Figure 5-42 shows that the unknown state lies somewhere on the 2γ circle. To determine just where it is on the 2γ circle requires at least an intersecting circle.

A circle centered on the equator at $2\tau = 90^\circ$ seems likely to provide the necessary intersection. This is shown in Figure 5-43 as an angle called $2\gamma''$.

Clearly, if two more components could be added we could have E_{45} and E_{135} then γ'' would be solved instantly as was γ . But adding measurements is a luxury and we need to work with the minimum data at the outset, and then expand if it seems justified.

We will work with only E_0 , E_ϕ , and E_{45} to develop a method of analysis **based on three components**.

After some spherical trigonometry, etc. we have

$$\gamma'' = \cos^{-1} \left[(\cos \gamma) \left(10^{\frac{E_{45}-E_\theta}{20}} \right) \right] \quad \text{and} \quad \delta = \cos^{-1} \left[\frac{\cos 2\gamma''}{\sin 2\gamma} \right]$$

then

$$\varepsilon = \frac{1}{2} \sin^{-1} [(\sin 2\gamma)(\sin \delta)]$$

and

$$\tau = \frac{1}{2} \tan^{-1} [(\tan 2\gamma)(\cos \delta)]$$

In order to preserve quadrant information one should use the form:

$$\tau = \frac{1}{2} \left\{ \text{To Polar} \left(\frac{\cos \delta}{[\tan 2\gamma]^{-1}} \right) \right\}$$

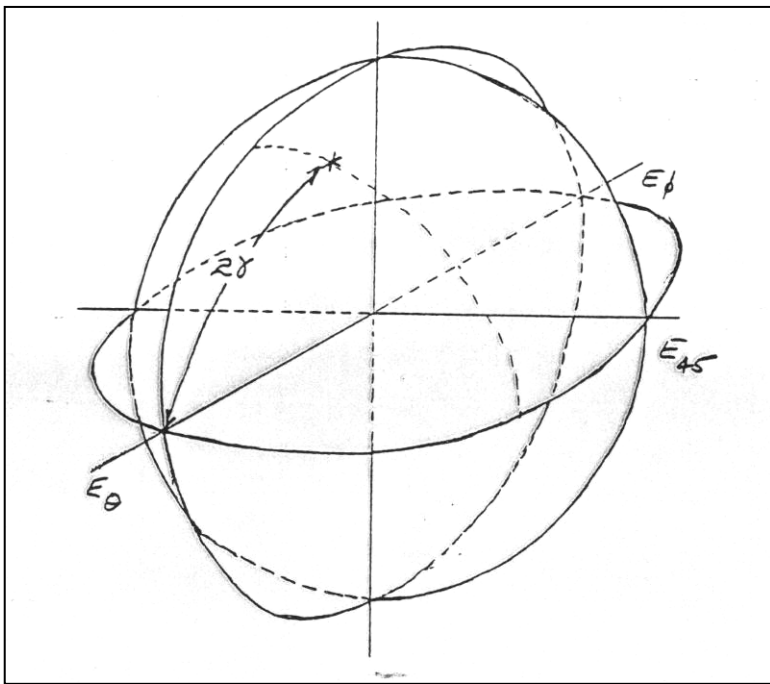


Figure 5-42. Construction of 2-gamma (2γ) circle.

Construction of the 2-gamma circle is shown in Figure 5-42. This information comes from the ratio of the E_{phi} to the E_{θ} components.

Only the first octant construction is shown, but it should be clear that the circle continues into all four octants adjacent to the E_{θ} point.

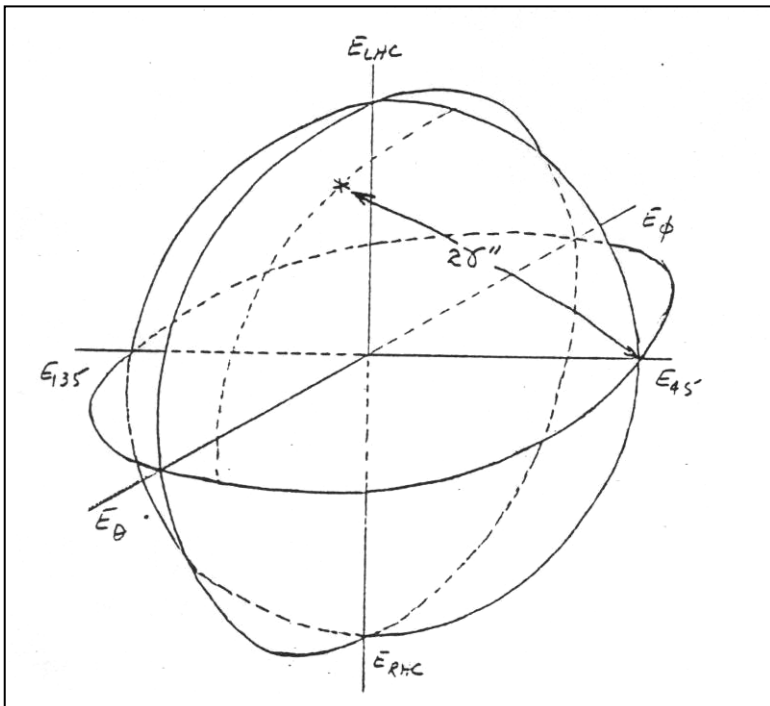


Figure 5-43. Construction of the 2-gamma double-prime ($2\gamma''$) circle.

Construction of the 2 gamma double prime circle is shown in Figure 5-43. This information comes from the magnitude of the E_{45} component.

It should be clear that this circle will intersect the gamma circle in two places, one in the upper hemisphere and one in the lower hemisphere. Without a non-linear component (and no phase) it would be impossible to determine which intersection (sense) is the correct one.

Error Sensitivity

As in any system of analysis, the three linear component system of finding the polarization state and gain of an antenna is subject to errors in output due to errors in measurements.

Probably the best way to see the results of input errors on final results is shown in Figure 5-44 and Figure 5-45. The axial ratio of the resulting ellipse assumes constant values and produces contours with the independent variables being the ratios “Ephi-to-Etheta” and “E45-to-Etheta” in Figure 5-44. For Figure 5-45 tilt angles are held constant with the same variables as in Figure 5-44. These two plots show several interesting features:

From Figure 5-44 & Figure 5-45:

- a. The axial ratio contours crowd together in the upper part of Figure 5-44 so that all values from 0 dB to ∞ dB fall within a 3 dB range of E45/Etheta. In the lower part the contours spread out so that E45/Etheta generally covers a much wider range for any given value of Ephi /Etheta.
- b. The dotted line separating the upper from the lower parts of Figure 5-44 passes through the extremes of the contours as a function of Ephi/Etheta. This is the condition which represents $\delta = 90$ degrees.
- c. In general for a given value of Ephi /Etheta, there are two values of E45/Etheta which yield the same axial ratio. There will be less error in axial ratio for a given change (error) in dB in E45/Etheta for the one with the more negative value ie the lower in Figure 5-44.
- d. On the plot of tilt angles (Figure 5-45) note that for $\tau = 45^\circ$ & 135° the result depends only on Ephi /Etheta not on E45/Etheta. Also here the dotted lines mark the boundaries of all possible values. At the point 0,0 all tilt angles converge because this represents circular polarization.

Improvements - Add E135

From the error analysis above it is clear that for data points measured by only Etheta, Ephi & E45, error sensitivity is very high for states which have tilt angles between zero and 90° . Here the output error (in AR dB) can be many times the dB error in E45/Etheta, while on the other hand data points with tilt angles from 90° to 180° have less error sensitivity. The error in ARdB is approximately equal to the dB error in E45/Etheta. These conditions form on opposite sides of the Poincare Sphere and suggest that when a measurement of E45 would **yield large error** the measurement of E135 would be in a very favorable error position, and vice versa. If one looks into the symmetry involved he finds that for the E135 measurement a set of curves similar to Figure 5-44 and Figure 5-45 result. In fact, only the identification of the vertical variable needs be changed from E45 / Etheta to E135 / Etheta!

This is a great improvement and usually worth the effort (when possible) to add the fourth linear component magnitude. It provides some redundant gain information, provides a

check on γ'' if desired, but most of all it allows an independent solution for polarization which will always put it in the favorable part of the error sensitivity curves.

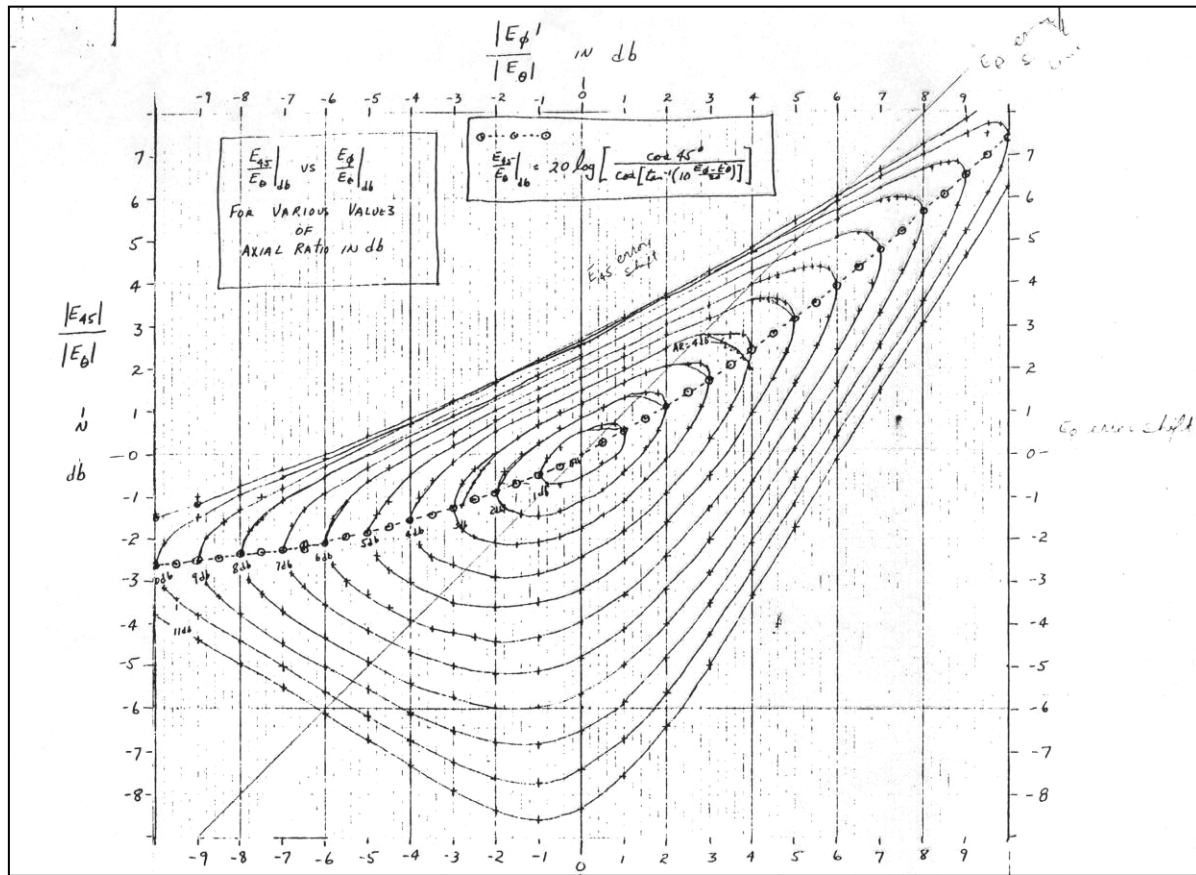


Figure 5-44. Axial Ratio as a function of the ratios E_ϕ -to- E_θ and E_{45} -to- E_θ (in dB).

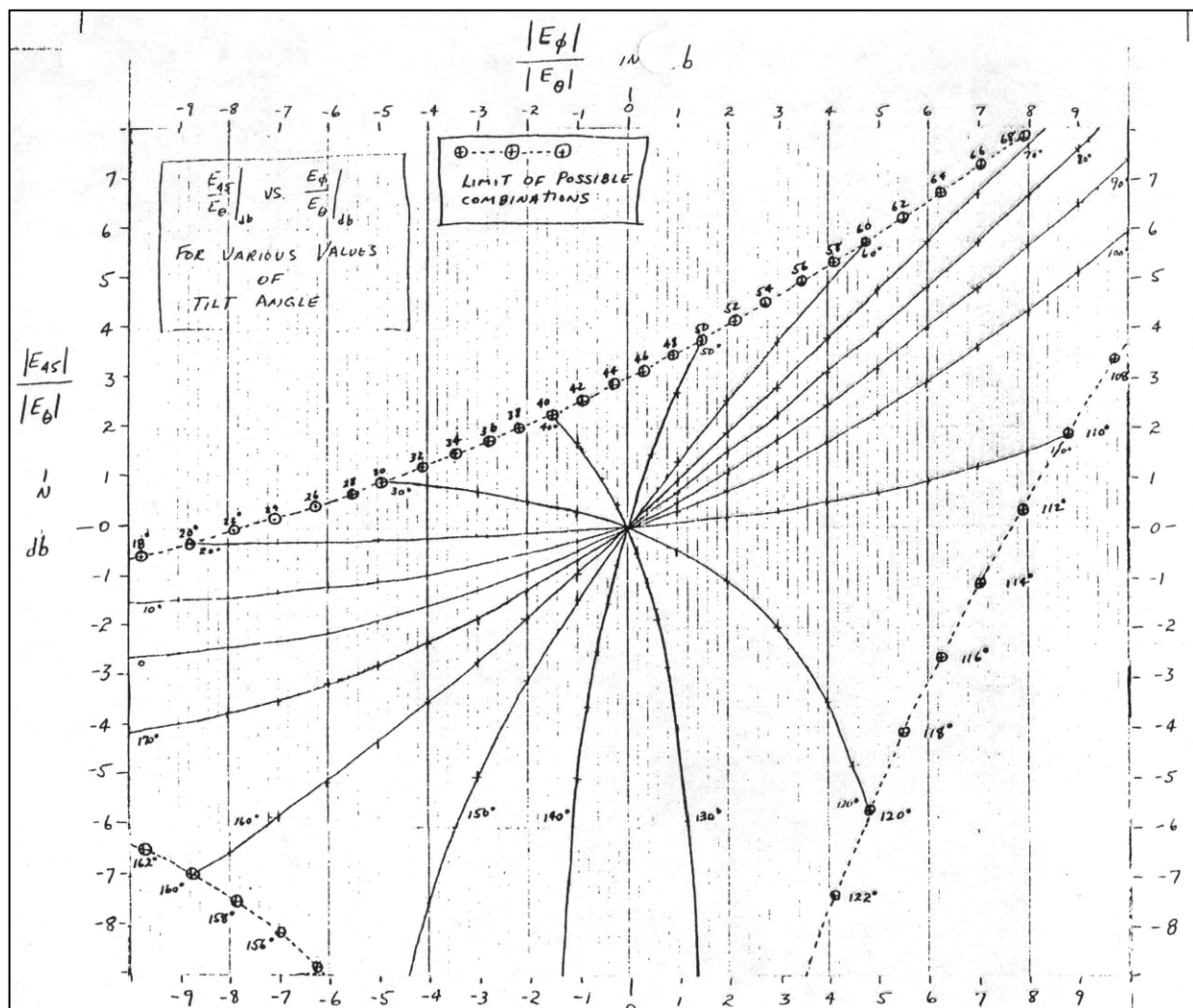


Figure 5-45. Tilt Angle as a function of the ratios Ephi-to-Etheta and E45-to-Etheta.

We can now update the equations to involve the E_{135} component. It is assumed that all components are to be measured in decibels.

Gamma Double Prime

$$\gamma = \tan^{-1} \left[10^{\frac{E_\phi - E_\theta}{20}} \right]$$

or

$$\gamma'' = \cos^{-1} [(\cos 2\varepsilon)(\cos 2\tau)]$$

$$\gamma'' = \tan^{-1} \left[10^{\frac{E_{135} - E_{45}}{20}} \right]$$

or

$$\gamma'' = \cos^{-1} \left[(\cos \gamma) \left(10^{\frac{E_{45} - E_\theta}{20}} \right) \right]$$

or

$$\gamma'' = \sin^{-1} \left[(\cos \gamma) \left(10^{\frac{E_{135} - E_\theta}{20}} \right) \right]$$

or

$$\gamma'' = \cos^{-1} [(\cos 2\varepsilon)(\sin 2\tau)]$$

Gain

$$G = 10 \log_{10} \left[10^{\frac{E_{45}}{10}} + 10^{\frac{E_{135}}{10}} \right]$$

Polarization Loss

We can identify or associate the following:

$$E_\theta \rightarrow \cos \gamma \quad E_\phi \rightarrow \sin \gamma \quad E_{45} \rightarrow \cos \gamma'' \quad E_{135} \rightarrow \sin \gamma''$$

$$\text{Then } PL_\theta = -20 \log_{10} (\cos \gamma)$$

$$PL_\phi = -20 \log_{10} (\sin \gamma)$$

$$PL_{45} = -20 \log_{10} (\cos \gamma'')$$

$$PL_{135} = -20 \log_{10} (\sin \gamma'')$$

And for polarization mismatch losses to “Same Hand Circular”, “Opposite Hand Circular”, “Minimum to Linear”, and “Maximum to Linear”, we have the following:

$$PL_{SHC} = -20 \log_{10} \left\{ \cos \left[45^\circ - \tan^{-1} \left(10 \frac{ARdB}{20} \right) \right] \right\}$$

$$PL_{OHC} = -20 \log_{10} \left\{ \cos \left[45^\circ + \tan^{-1} \left(10 \frac{ARdB}{20} \right) \right] \right\}$$

$$PL_{MinLinear} = -20 \log_{10} \left\{ \cos \left[\tan^{-1} \left(10 \frac{ARdB}{20} \right) \right] \right\}$$

$$PL_{MaxLinear} = -20 \log_{10} \left\{ \sin \left[\tan^{-1} \left(10 \frac{ARdB}{20} \right) \right] \right\}$$

5.14.3 Examples of Polarization Measurement and Analysis.

Worked Practical Example

The following example is meant to simulate actual practical data from an antenna range.

Assume that contour plots of the radiation power response of an antenna were made for Etheta, Ephi, E45°, E135° and for nearly circular ELHEP & ERHEP. (Not all are required for this method). In some direction (Theta, Phi) data samples were picked and are:

Component	Plotted Value (dB)	Correction to Isotropic (dB)	Probe Circularity (dB)
E _θ	-3.117	+10	linear
E _ϕ	-2.636	+ 8	linear
E ₄₅	-3.939	+12	linear
E ₁₃₅	-2.171	+ 5	linear
E _{LHC}	-4.656	+13.5	1.8*
E _{RHC}	-7.108	+ 7.25	2.3*
*Major axis aligned with Etheta during test.			

Problem: Find the following:

- Total gain in dBi.
- Axial ratio in dB
- Tilt angle in degrees
- Polarization ratio amplitude in dB
- Polarization ratio phase in degrees
- Sense of rotation ie handedness

Solution:

First apply contour plot corrections to put all data on same basis (isotropic).

$$\begin{aligned} E_\theta &= -3.117 + 10 \text{ dB} = +6.883 \text{ dBi} \\ E_\phi &= -2.636 + 8 \text{ dB} = +5.364 \text{ dBi} \\ E_{45} &= -3.939 + 12 \text{ dB} = +8.061 \text{ dBi} \\ E_{135} &= -2.171 + 5 \text{ dB} = +2.829 \text{ dBi} \\ ELHC &= -4.656 + 13.5 \text{ dB} = +8.844 \text{ dBi} \\ ERHC &= -7.108 + 7.25 \text{ dB} = +0.142 \text{ dBi} \end{aligned}$$

Some of the important ratios may now be found.

$$\begin{aligned} \frac{E_\phi}{E_\theta} &= -1.519 \text{ dB} & \frac{E_{135}}{E_{45}} &= -5.232 \text{ dB} & \frac{E_{45}}{E_\theta} &= +1.178 \text{ dB} \\ \frac{E_{135}}{E_\theta} &= -4.054 \text{ dB} & \frac{E_\phi}{E_{45}} &= -2.697 \text{ dB} & \frac{E_\theta}{E_{45}} &= -1.178 \text{ dB} \end{aligned}$$

GAIN

Gain can be found from any pair of orthogonal components

$$G = 10 \log_{10} \left[10^{\frac{E_\theta}{10}} + 10^{\frac{E_\phi}{10}} \right] \quad G = 10 \log_{10} \left[10^{0.6883} + 10^{0.5346} \right] = +9.20 \text{ dBi}$$

also

$$G = 10 \log_{10} \left[10^{\frac{E_{45}}{10}} + 10^{\frac{E_{135}}{10}} \right] \quad G = 10 \log_{10} \left[10^{0.8061} + 10^{0.2829} \right] = +9.2 \text{ dBi}$$

and

$$G = 10 \log_{10} \left[10^{\frac{E_{LHCP}}{10}} + 10^{\frac{E_{RHCP}}{10}} \right]$$

But our measurements used not quite orthogonal "circular" probes so we may not use these for gain calculations.

POLARIZATION RATIO MAGNITUDE

The angle gamma depends upon the ratio Ephi to Etheta. We have the ratio in decibels but need to have the numerical value.

$$\frac{E_\phi}{E_\theta} dB = E_\phi - E_\theta = -1.519 dB \quad \frac{E_\phi}{E_\theta} Numerical = 10^{\frac{-1.519}{20}}$$

so that

$$\gamma = \tan^{-1} \left[\frac{E_\phi}{E_\theta} \right] = \tan^{-1}[0.840] = 40.015^\circ$$

Polarization mismatch loss to E_θ & E_φ:

$$PL_\theta = -20 \log \cos \gamma = \underline{2.317 \text{ dB}}$$

$$PL_\phi = -20 \log \sin \gamma = \underline{3.836 \text{ dB}}$$

VALUE OF γ"

Using the E₄₅ component:

$$\gamma'' = \cos^{-1} \left[(\cos \gamma) \left(10^{\frac{E_{45}-E_\theta}{20}} \right) \right] = 28.703^\circ$$

or if E₁₃₅ is used instead of E₄₅

$$\gamma'' = \sin^{-1} \left[(\cos \gamma) \left(10^{\frac{E_{135}-E_\theta}{20}} \right) \right] = 28.701^\circ$$

or using both at once

$$\gamma'' = \tan^{-1} \left[10^{\frac{E_{135}-E_{45}}{20}} \right] = 28.702^\circ$$

These three evaluations could be different due to measurements errors or, as in this case, simply roundoff.

PHASE ANGLE OF THE POLARIZATION RATIO

$$\delta = \cos^{-1} \left[\frac{\cos 2\gamma''}{\sin 2\gamma} \right] = 56.840^\circ$$

THIS IS THE PHASE ANGLE BY WHICH E_ϕ LEADS E_0 .

Now we have γ and δ but wish to find ε and τ . The basic Poincare Sphere transformations are employed.

$$\tau = \frac{1}{2} \tan^{-1} [(\tan 2\gamma)(\cos \delta)] = 36.092^\circ$$

and

$$\varepsilon = \frac{1}{2} \sin^{-1} [(\sin 2\gamma)(\sin \delta)] = 27.769^\circ$$

$$AR_{dB} = 20 \log_{10} (\cot \varepsilon) = 20 \log_{10} \left[\frac{1}{\tan(27.769^\circ)} \right] = 5.571 dB$$

At this point, the state is known except as to the sense or "handedness". We can find the mismatch loss to any linear polarization state and to the circular states if they are identified by "same hand circular" and "opposite hand circular".

$$PL_{45} = -20 \log_{10} \cos \gamma'' = 1.139 dB$$

$$PL_{135} = -20 \log_{10} \sin \gamma'' = 6.371 dB$$

$$PL_{SHC} = -20 \log_{10} \cos(45^\circ - \varepsilon) = 0.399 dB$$

$$PL_{OHC} = -20 \log_{10} \cos(45^\circ + \varepsilon) = 10.568 dB$$

5.14.4 Sense or Handedness. The scheme for determining the sense for the unknown polarization state is simply to calculate the expected value of the response to the nearly circular probe of the known sense for the state in question. Then see which assumption yields a result most nearly equal to the actual measured. That is then the correct sense. The accuracy of this method does not rely on the quality of the circularity -- only that it be known. For unknown states which are very nearly linear-measurement errors could result in selecting the wrong sense.

Only one such measurement is required to find the sense but since this example has two opposite hand measurements, we will do the required trick twice and see how well they agree.

We must use the Poincare Sphere coupling equation

$$\text{Coupling} = \cos(\sigma)$$

but $\sigma = \frac{1}{2} \cos^{-1} [\cos 2\gamma_1 \cos 2\gamma_2 + \sin 2\gamma_1 \sin 2\gamma_2 \cos(\delta_1 - \delta_2)]$

then $\text{Coupling} = \cos \left[\frac{1}{2} \cos^{-1} \{ \cos 2\gamma_1 \cos 2\gamma_2 + \sin 2\gamma_1 \sin 2\gamma_2 \cos(\delta_1 - \delta_2) \} \right]$

Let state #1 be the "nearly circular" LHEP used as the probe. We know that its tilt angle was set to zero for the measurement so $\tau = 0$. We solve for its ε value from its "circularity" (i.e. 1.8 dB).

$$AR = 1.8 \text{ dB} = 20 \log(\cot \varepsilon)$$

$$\varepsilon_1 = 39.105^\circ$$

$$\tau_1 = 0^\circ$$

so that

$$\varepsilon_1 = \gamma_1 = 39.105^\circ \quad \delta_1 = +90^\circ$$

Point #2 is the state of the antenna under test for which we have solved

$$\varepsilon_2 = 27.769^\circ$$

$$\tau_2 = 36.092^\circ$$

and $\gamma_2 = 40.015^\circ$, so that $2\gamma_2 = 80.030^\circ$
 $\delta_2 = \pm 56.840^\circ$ (Note: the + is for LHEP and the - is for RHEP)

Substituting these into the coupling equation we get

PL_{1,2} 0.356 dB (to left hand)
and PL_{1,2} 9.425 dB to right hand

We already know that the gain is +9.20 dBi so we should have measured

G_{meas} if LHEP = +9.2 - 0.356 = +8.844 dBi
or G_{meas} if RHEP = +9.2 - 9.425 = -0.225 dBi

But we actually measured +8.844 dBi so we conclude that the unknown antenna state is Left Hand Elliptically Polarized.

The other independent determination is from the "nearly circular" RHEP data. Proceeding as above knowing AR = 2.3 dB we have

$$\begin{array}{ll} \varepsilon = \gamma = 37.501^\circ & 2\gamma_1 = 75.002^\circ \\ \delta = -90^\circ & \delta_1 = -90^\circ \end{array}$$

The test antenna is the same:

$$\begin{array}{l} 2\gamma_2 = 80.030^\circ \\ \delta_2 = \pm 56.840^\circ \end{array}$$

Then evaluating the coupling equation we find that

$$\begin{array}{l} PL_{1,2} = 9.059 \text{ dB to LHEP} \\ \text{and} \\ PL_{1,2} = 0.359 \text{ dB to RHEP} \end{array}$$

Again, we know gain = +9.20 dBi, so expected values from measurement

$$\begin{array}{l} G \text{ meas if LHEP} = +9.20 - 9.059 \text{ } \underline{+0.141 \text{ dBi}} \\ \text{or} \\ G \text{meas if RHEP} = +9.20 - 0.359 \text{ } \underline{+8.841 \text{ dBi}} \end{array}$$

In fact we measured $G = +0.142 \text{ dBi}$, so again we conclude that the antenna sense is LHEP!!

5.15 Polarization Considerations in Radar Returns

5.15.1 Pre-mission Link Analysis. The importance of considering the target antenna system radiation patterns in a pre-mission link analysis (Paragraph 5.16) can hardly be over emphasized. Situations and scenarios which could occur during a mission must be considered if costly errors are to be avoided. In the analysis of the link budget for a given flight the analyst should be aware of the expectations of the radar operators and the characteristics of the target transponder antenna system. Whether the antenna pattern data is generated by measurements on an actual target (or acceptable mockup) or is simulated by computer analysis, possibilities exist that a relatively simple oversight could jeopardize the tracking mission.

5.15.2 Costly Oversight. An interesting situation illustrating the impact of a simple oversight may have occurred on one of the major RCC ranges. As the story goes, the target vehicle was fitted with a transponder and antenna system to augment the return during a certain tracking mission. The radar normally used "skin track" but for this mission would rely on "beacon track" for better tracking. Presumably, the antenna patterns appeared nominal with adequate coverage. However, during the mission the radar beacon track was practically useless and far worse than skin track would have been. The radar was Right Hand Circular Polarization (RHCP) on transmit and expected left hand circular polarization (LHCP) on receive due to the reflection. It was later "discovered" that the transponder antennas were RHCP. Had the radar used linear polarization, the result probably would have been quite good.

5.15.3 Polarization Sense Reversal. The fact that circular polarization suffers a sense reversal upon reflection (from a conductor) was used in the skin track case. However, the transponder antenna transmits the same polarization state as it receives. Thus the radar which expected to receive LHCP was presented with a healthy RHCP signal and was thus cross polarized.

5.15.4 Typical Reflectors. The sense reversal problem is not restricted to transponder antennas. Radar calibration targets are sometimes “corner reflectors”. For example, reference reflectors come in simple “sphere”, “flat plate”, “dihedral”, and “cube corners”. A sphere or flat plate (i.e., metal disc) produces a single reflection. This would reverse the sense of polarization. The dihedral corner reflector has a broad viewing angle in the plane perpendicular to the “hinge line” or intersection line of the two plane plates. Two reflections are generated in returning the signal to the radar and thus return the same polarization sense. The cube corner has broad viewing angles in both planes but relies on three reflections which again returns a reversed sense on polarization rotation.

The radar operators generally know of these factors. It is important to have the radar operators involved early in the configuration design of a target transponder antenna system to minimize costly system design errors by the vehicle designers who may not be familiar with the radars to be used.

5.16 Notes on Link Analysis

An RF link analysis is required by most national ranges before a test vehicle may be flown on that range. An example of the requirement statement may be found in the document EWR 127-1 (1997) section 4.11.1.1.3. A link analysis is necessary to determine the signal strength available for various mission flight parameters. For range safety purposes it is usually required to demonstrate that command/destruct, telemetry and radar will each have adequate signal strength between the ground station and the flight vehicle to ensure proper control, data and tracking.

The accuracy of the link analysis depends upon the accuracy of the input parameters including the antenna pattern, vehicle trajectory and vehicle orientation and the ground antenna parameters. In the case of the FTS the ground station’s transmit power is a critical ingredient. The FTS receiver sensitivity is a parameter which must be known accurately. Between these two ends the path loss and the antenna gain pattern must be accurately computed in order to obtain a meaningful link analysis. The path loss variable includes the spherical wave “spreading” and in some cases the atmospheric absorption. The path loss is based on the parameter of separation distance which is computed from the known or assumed locations of the end points at any given time. The remaining element in the chain of signal delivery from one end to the other is the antenna pattern. Since the transfer of power depends upon the gains of the antennas and upon the polarization mismatch loss, it is essential to know these parameters of both antennas. The ground antenna portion is relatively simple since (generally) only one part (the main beam) of the pattern is pointed at the flight vehicle. The flight vehicle is another matter altogether. The vehicle may roll and tumble during flight and the portion of the antenna pattern which is directed toward the ground station must be known in order to calculate the link strength.

The coordinate transformations which are required for a proper link analysis must include the transformation from the vehicle antenna pattern data to the direction from the vehicle to the ground station. The line passing from the flight vehicle to the ground station may have a unique direction in the vehicle pattern coordinate system but still may assume any rotational orientation around that line. In so doing, the polarization mismatch loss between that pattern direction and the ground station antenna may take on various values. This is why it is critical to know the orientation of the flight vehicle with respect to the ground station antenna when calculating the link signal strength.

The telemetry antenna system link analysis is very similar to the FTS system with the exception that the signal originates in the vehicle instead of being received by the vehicle. Due to the frequencies involved the vehicle's telemetry antenna pattern might have more "fine detail" but is generally not held to as tight specifications as is the FTS antenna system.

The radar transponder antenna system is more complicated in that it is used a both receive and transmit (at slightly offset frequencies). The frequency band used by the radar transponders generally results in much more fine details in the antenna pattern for most flight vehicles. Several problem areas can appear when considering the link analysis on the vehicle's transponder antenna system. Many antenna pattern sets are still measured and supplied on the old 2 degree by 2 degree grid; however, on the larger flight vehicles with multiple unit radiators, this results in misrepresenting areas which contain many deep, sharp nulls (Paragraph [6.9](#)). These areas are the most important to the tracking accuracy degradation and, unfortunately, are the ones that are most severely misrepresented. A detailed analysis of this problem in antenna pattern measurement is discussed in Paragraph [6.9](#), Paragraph [6.10](#), and Paragraph [6.11](#).

5.17 Polarization Applied to Receiving Antennas

Polarization Upon Receiving

Consider the antenna which generates a wave whose polarization state is plotted on the Poincare Sphere. The location of this state may be specified by polarization ratio (E_ϕ/E_θ) and relative phase or by axial ratio, tilt angle and sense (handedness).

There are at least three interesting situations involving this antenna and others in a transmit and receive configuration.

- a. The image of the antenna in a perfect mirror (Figure [5-46](#))
- b. An identical antenna facing the original antenna (Figure [5-47](#))
- c. An antenna, which will be polarization matched to the original antenna such that it will receive the transmitted wave completely (Figure [5-48](#))
- d. The situation corresponding to the relationship between the transmit and receive polarization states (Figure [5-49](#))
- e. The situation for an antenna and its mirror image (Figure [5-50](#)).

It should be remembered that the polarization state of an antenna is that of the wave it generates. The E_θ direction is the reference for tilt angles and

$$\hat{E}_\theta \times \hat{E}_\phi = \hat{E}_R$$

defines a right handed coordinate system with E_R being the direction of propagation.

The “receiving” polarization is not generally the same as the “transmitting” polarization. Only when the phase between the E_ϕ and E_θ components is 90° will the “receive” and “transmit” polarizations be the same.

Only linear polarizations will be “co-polarized” with their images in a plane mirror.

In the following examples the main antenna is the transmit antenna, the “other” antenna is either a mirror image, an identical antenna as receiver or a polarization matched antenna. The primes refer to the “other” antenna’s parameters. Thus τ' is the tilt angle of the ellipse for the “other” antenna. Similarly, δ' is the phase of the polarization ratio for the “other” antenna and not the phase of the circular component ratio.

(1) Mirror Image of an Antenna

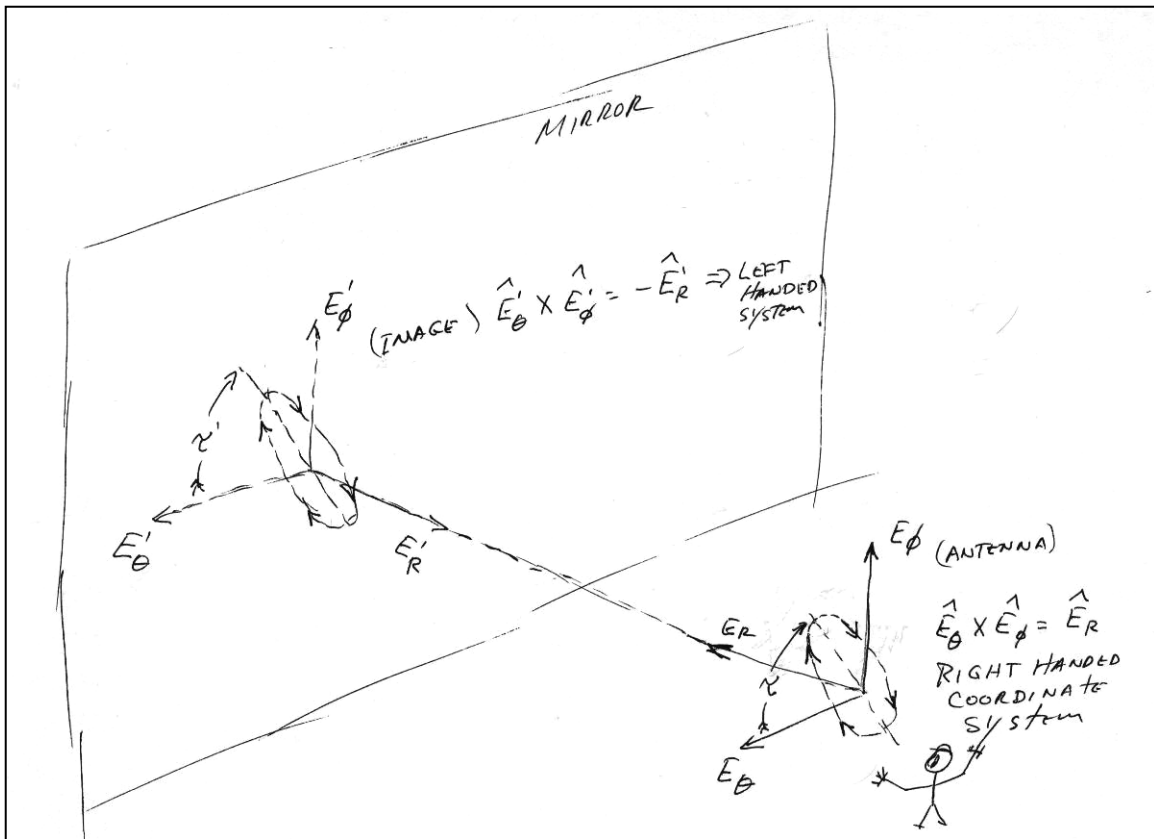


Figure 5-46. Antenna image in plane mirror.

In this example (see Figure 5-46) the antenna generates a right hand elliptical polarization (RHEP) wave with an axial ratio of about 3 and a tilt angle of about 75° . The observer behind the antenna sees the wave progressing toward the mirror with a clockwise rotation of the E-field phasor. The image is seen to have a phasor rotation clockwise (from the observer's point of view) but the direction of propagation is toward the observer not away from him. This represents a Left Hand Elliptical wave (LHEP), which the RHEP antenna cannot fully receive. The mirror image coordinate system is left-handed. The axial ratio is the same, the tilt angle is the same but the "handedness" is opposite. To an observer behind the image the wave propagating away is rotating counterclockwise so it is LHEP.

(2) **Identical Antenna As Receiver**

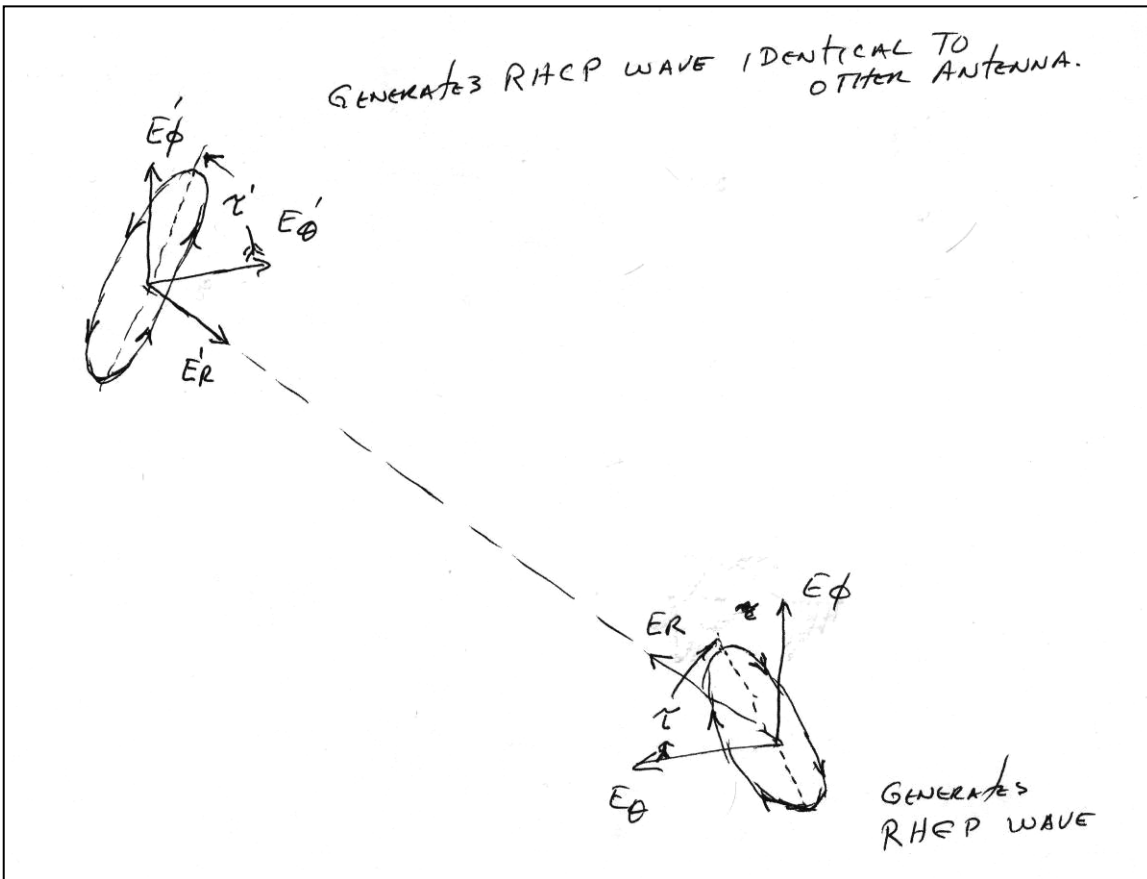


Figure 5-47. An identical antenna receiving.

In Figure 5-47, it can be seen that the receiving antenna is not necessarily co-polarized with the same (identical) antenna transmitting. Circularly polarized antennas are in the small set of antennas which are co-polarized with their identical units in a transmit-receive configuration.

Two polarization states are totally decoupled only when they lie diametrically opposite on the Poincare sphere. This implies that for any non-linear state the “handedness” of the two decoupled states must be opposite, the tilt angles must be at right angles and the axial ratios must be equal. For linear states to be decoupled the tilt angles must be 90° different.

It must be remembered that the polarization is generally different for an antenna used as a receiver, than it is when used as a transmitter.

(3) **Transmitting and Receiving ---- Polarization Matched**

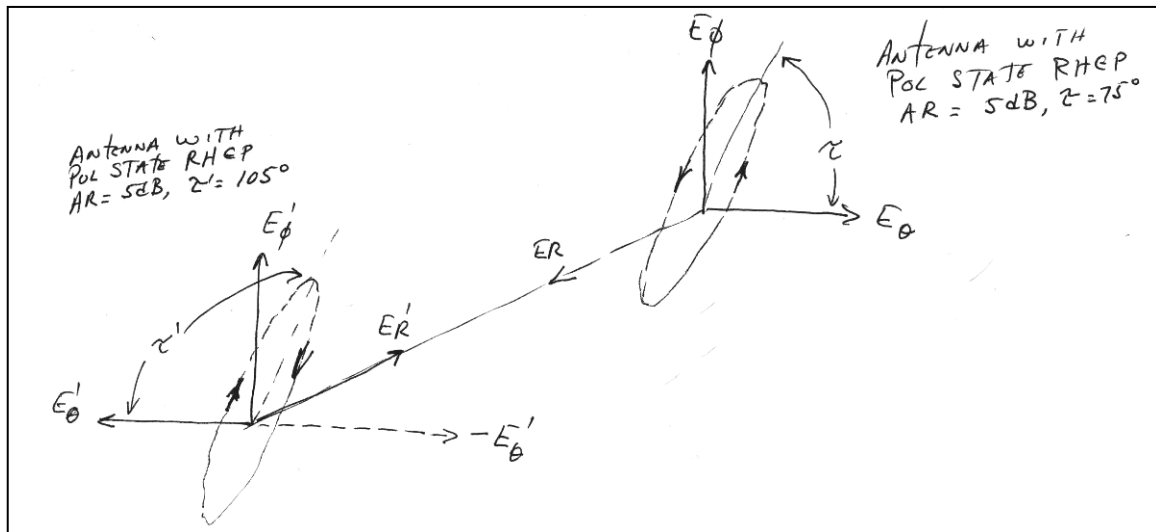


Figure 5-48. Matching polarizations in transmit-receive configuration.

By definition δ = phase by which E_ϕ leads E_θ in the IEEE polarization definition (i.e., upon transmit). Delta is positive for LHEP and negative for RHEP. Thus for a RHCP wave the E_ϕ component lags the E_θ component.

For an E_{45} (linear) result the E_ϕ and E_θ components must be equal and in phase, (i.e., $\delta = 0$). If $\delta = 180^\circ$ then the result would be E_{135} .

Considering the Poincare sphere representation, it is clear that measuring 2τ and $2\tau'$ from the E_θ reference, simply progress equal amounts in opposite directions. For example, if $\tau = 45^\circ$ then $2\tau = 90^\circ$ then $\tau' = 135^\circ$ so that $2\tau' = 270^\circ$. These states are diametrically opposite on the Poincare sphere. In this example the polarization ratio (E_ϕ/E_θ) equals unity and the phase difference is zero for E_{45} and 180° for E_{135} .

Thus

$$\delta' = 180^\circ - \delta$$

which is true in general for a matched transmit and receive pair.

(4) Identical Antennas as Transmit and Receive

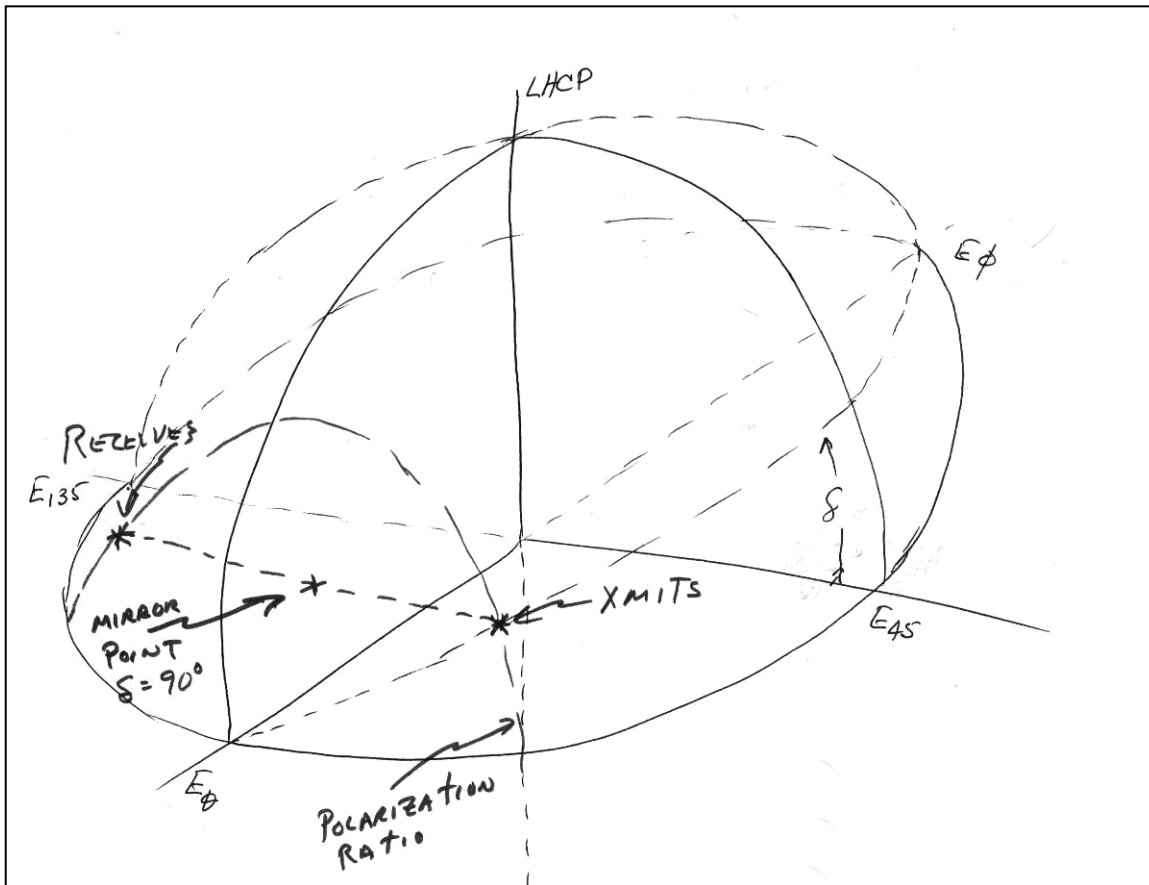


Figure 5-49. Poincare sphere for transmit-receive configuration.

The situation corresponding to the relationship between the transmit and receive polarization states is shown in Figure 5-49.

The $\delta = 90^\circ$ plane is the $E_\theta, E_{\text{LHCP}}, E_\phi$ plane.

The $\delta = -90^\circ$ plane is the $E_0, E_{\text{RHCP}}, E_\phi$ plane.

Mirrored across the $\delta = 90^\circ$ plane:

$$\delta_{RECEIVE} = 180^\circ - \delta_{TRANSMIT}$$

(5) Transmitting Antennas and Mirror Image

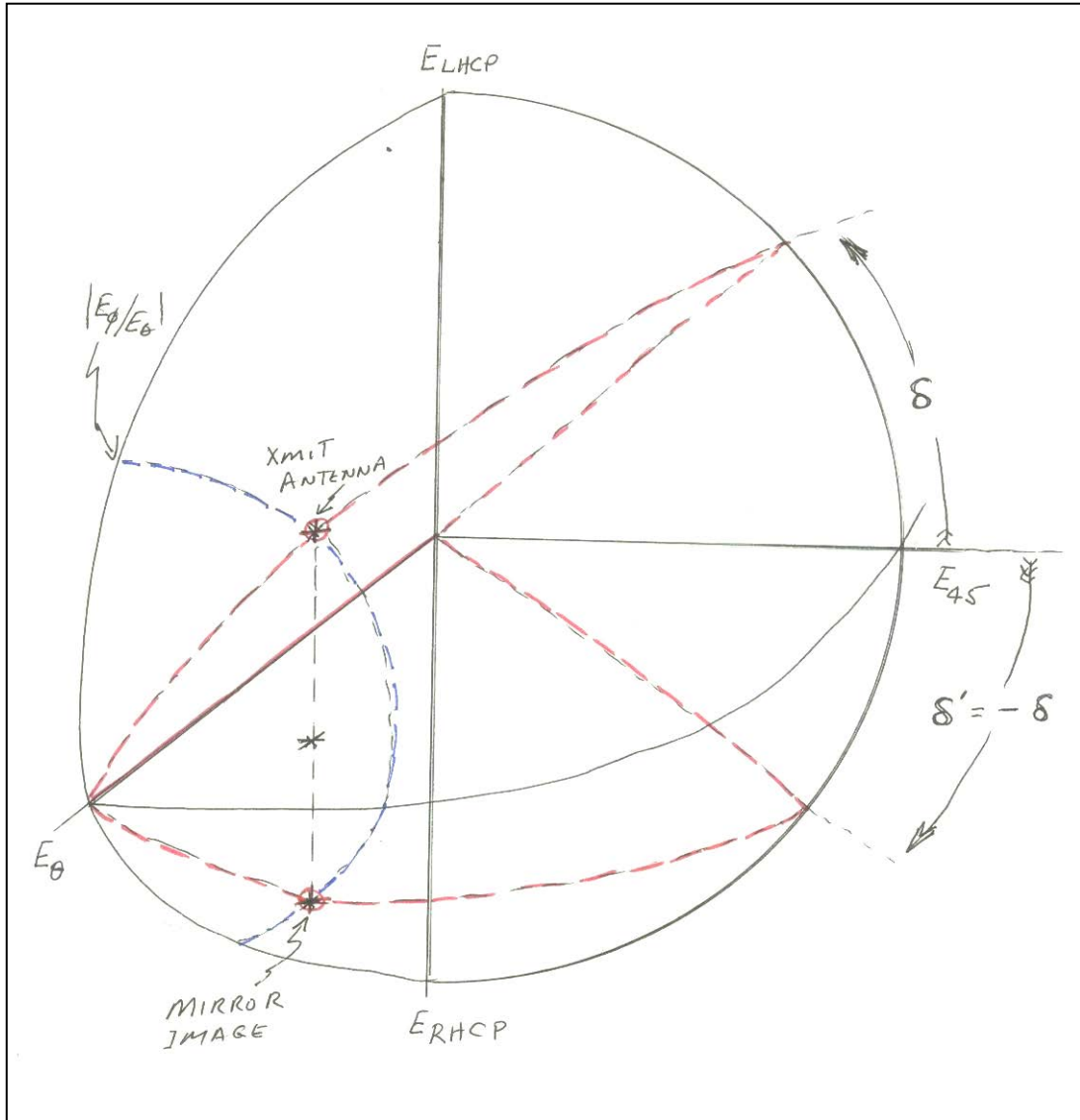


Figure 5-50. Poincare sphere for mirror image transmit-receive configuration.

Figure 5-50 shows the situation for an antenna and its mirror image. The polarization state of a mirror image is the original state mirrored through the $\delta=0, 180^\circ$ plane. The axial ratio and tilt angle are the same but the handedness is opposite to that of the original. All linear states have $\delta = 0$ or 180° and circulars have $\delta = 90^\circ$ or -90° . Thus all linear polarizations are mirrored back to the same original state, but circulars are completely decoupled, i.e., diametrically opposite.

That is,

$$\delta' = -\delta$$

CHAPTER 6

ANTENNA SYSTEM MEASUREMENT AND ANALYSIS

6.1 Generalizations

6.1.1 Component Bench Testing. As the various components of the antenna system become available, they should be measured to determine their radio frequency (RF) characteristics. This testing of individual components (and combinations of components) is generally referred to as “bench testing”. The coax cable, power dividers/combiners, switches, disconnects and sometimes unit radiators are laid out on a bench and subjected to testing. Visual inspection for obvious mechanical problems is part of bench testing. Coax cables that have been kinked or have faulty connector center pins may be found by simple visual inspection. Usually, a calibrated vector network analyzer (and plotter) is employed to make impedance voltage standing wave ratio (VSWR) and insertion loss measurements. Careful identification of the components that have been measured and the association with the correct data plots is a very important aspect of the bench testing. In many cases the insertion loss, and phase are measured and recorded but the measurement of the actual phase length is overlooked. The cable lengths and the power divider/combiner measured lengths in centimeters or nanoseconds should be considered a necessary and valuable part of the bench testing data.

6.1.2 Radiation Pattern Testing. The final configuration of the antenna system complete with flight hardware should be subjected to antenna radiation pattern testing. These measurements should be performed on a properly configured antenna pattern range with the antennas mounted on an appropriate vehicle or mockup. The pattern range should be capable of producing measurements of the full spherical pattern, usually called a radiation distribution pattern (RDP). Certain pattern cuts, such as the roll plane and selected “phi” planes should be made in the analog mode. If the analog mode of measurement is not available and only digitized data is available, then the sampling should be set to produce at least ten samples per smallest interference lobe cycle in any particular scan or “cut”. Care must be taken to properly identify of generate the polarization component specified for the patterns. The measurement technique known as “linear component polarimetry” should be employed in all measurements made in digital form. When analog patterns of circular polarization components are required it is recommended that a properly adjusted “polarization trim network” be utilized. Proper documentation and data conversion techniques are crucial to the accuracy and applicability of the reported pattern data. (Reference RCC Document 253-93, paragraph 1.1)

6.1.3 Data Formats and Conversions. Antenna pattern data formats and coordinate system definitions are given in the document RCC 253-93 and should be considered as essential requirements. Data formats for bench test data are less formalized and allow for considerable innovation on the part of the test engineer. Whatever the format, the data should be complete, accurate, and useable.

6.1.4 Documentation. Any antenna system design, which is to be flown on an RCC range, should be accompanied by a detailed test data “final report”. This report should include all the design details and the performance measurement report produced by the group that made the “qualification” measurements.

6.2 Radar Transponder Antenna Measurements

6.2.1 Introduction. Radar transponder antenna systems are a critical link in the tracking loop. Both the range and angle determined during tracking can be influenced by the performance of the target antenna system. It is therefore important to know certain parameters of these antenna systems in order to obtain the highest quality tracking data. A brief overview of some of the concerns might suggest some revisions in guideline documents.

6.2.2 Antenna As a Transducer. The transponder antenna system is a transducer. It operates both as a circuit element and as a radiation element. The antenna converts transmission line waves into free-space propagating (radiating) waves on transmission and the reverse on receive. Several important parameters, which need to be known and factored into the tracking function, include the propagation delay and the radiation pattern. Each of these has several aspects that must be considered if the highest quality tracking is to be realized.

6.2.3 Propagation Delay. Propagation delay in the antenna and its associated coax harness is of critical importance in the correct measurement of radar ranging. Along with the transponder pulse response delay, the pulse waveform, the radar pulse rise time, and other factors, the antenna system delay must be known accurately. There are several techniques to identify coax harness delays. Sometimes a reasonable estimate can be obtained by using published propagation constants for the particular coax being used. With proper equipment and procedures, it is generally best to measure the actual coax harness. Measurement is preferred to estimating because defects and damage can be found by measurement, whereas published data on coax represent a generic average of good cable and connectors.

6.2.4 Definition of Antenna. Antenna systems for transponder use include the radiating elements (usually several in an attempt to provide full spherical coverage), the phasing harness (which includes a power divider), and sometimes an additional length of coax between the transponder and the power divider. In the classic definition of “the antenna”, all units that determine the relative “aperture distribution” are parts of the “antenna” (See RCC Document 253-93, Paragraph 3.4.1, and Paragraph 3.7.3.8.2). Thus, the coax line from the transponder to the power divider is not strictly part of the “antenna”. However, the coax line does belong to the “antenna system” and must be included separately in the system loss determinations. In this sense “antenna system” means, all circuits placed between the transponder and the radiating elements. The phasing harness determines the “aperture distribution” because if any parts of the harness change the antenna pattern changes directivity. The additional length of coax between the transponder and the “antenna” does not change the directivity but only the link strength.

6.2.5 Bench Testing. Measurements procedures should include tests on each part of the antenna system separately and then as sub-assemblies of various parts. Testing the individual parts helps locate any unacceptable parts at the most basic level. Testing of subassemblies helps find any problems with the interconnections. Testing the complete system helps detect unsuspected interface anomalies. These measurements should include at least the reflection coefficient (impedance) and the insertion loss (amplitude and phase). Calibrated vector network analyzer and reflection/transmission tests set are usually required for these measurements (“bench testing”).

During “bench” measurements of the antenna system, care should be exercised when the antennas are allowed to radiate. Local reflections that can be seen by these antennas could cause errors in the measurements. In addition, the antennas should not be allowed to couple to each other in a way which would be atypical of the way they are to perform when mounted on the flight hardware.

Sometimes “hats” (Paragraph [6.6](#)) are placed over the radiating antennas during impedance testing. This is done so that the antennas will not cause interference to other testing or harm to people Federal Communications Commission (FCC). Care must be taken to ensure that the “hats” themselves do not disturb the natural impedance of the radiating elements. Generally, this is checked by comparison of the impedance seen with no hat to that seen with the hat in place on a single element. These tests are done at very low power levels (typically less than one milliwatt input). If this comparison shows that the hats are not causing an impedance change in the individual radiator, then the high power testing (if any) may be done with the transponder.

6.2.6 Radiation Patterns. The farfield radiation pattern of the transponder antenna system is critical to the quality of radar tracking. It has been shown many times that failure to give adequate attention to the antenna pattern can cause massive amounts of grief to radar operators and flight safety officers alike! The reader is referred to the Pershing II antenna pattern report, *C-Band Antenna System Investigation Final Report*, 4 March 1983, by Mr. Morris Drexler and Mr. Al Waterman, Contract No. DAA07-82-C-0003, Physical Science Laboratory (PSL) Report # PC01019)

It has been found that for radar transponder antenna systems it is best to have the fewest elements possible on a vehicle. The only time that “more is better” is when the elements can be placed within half wavelength of each other. The reason for this observation is that the radiating elements (unit antennas) form a phased array around the vehicle. In any direction around the vehicle that two or more antennas can provide power, there will form a system of interference lobes (peaks and nulls) if the phase difference becomes 180 degrees and the amplitudes are equal. Amplitude ripples are of concern mostly in the effects in range data due to possible changes in transponder trigger time, whereas the nulls are of great concern to angle data. Nulls in the radiation pattern have associated with them rapid phase shifts (Paragraph [5.7](#)). These rapid phase reversals can cause the tracking radar to slew to angles (both azimuth (az) and elevation (el)), which are far from the target. Basically, the radar dish will try to orient so that the aperture is normal to the phase front. With deep nulls, the phase shift across the tracking dish

can be substantial when the dish is actually pointing at the target. The servos will drive the mount to a direction which will minimize the phase across the aperture. This effect is sometimes referred to as “cross eye” or “phase front distortion”. The flight safety officer may get excited and reach for the “red button”!

Antenna patterns may be plots of several different parameters of the radiation from an antenna system. Usually, amplitude is assumed if not otherwise specified; however, the phase pattern can be very important and is often ignored. WSMCR 127-1 paragraph 4.14.5, 4.14.6.3, and 4.14.6.4 specifies some requirements of phase pattern measurement and reporting. Many antenna ranges are not equipped to make the required phase patterns and in most cases, the requirements eventually are waived. As the target rolls, the antenna pattern presents changing phase to the radar. In a coherent system, changing phase might be mistaken for changing range or radial velocity. Of course, the phase difference across the radar receiving aperture can cause pointing errors. With widely spaced antennas on the target, an interference (Paragraph [6.11](#)) forms in angle space near the angle of the plane bisecting the line between the two antennas forming the “phased array”. The broader the beamwidth of the individual antennas, the more extensive will be the interference lobe system.

6.2.7 Antenna Phasing Harness. When connecting the transponder system to the transponder, power divider, and antennas, it is sometimes convenient to use unequal length coax cables from the power divider to the individual radiators. There are cases in which the path lengths should be as nearly equal as possible. From the amplitude pattern standpoint the positions of the peaks and nulls in the interference pattern can shift through only a limited range of angles due to the element spacing and the wavelength. The higher the frequency and the greater the separation of elements, the smaller is the angular range for a null shift due to unequal cable path lengths. However, the actual phase delay (time delay) change in a signal passing from the transponder to a particular antenna can be substantial. So that in the case of a delay measurement on the bench (or on a mockup) using a coupling “hat” on the antenna, substantially different delays could be measured for the different antennas.

6.2.8 Antenna Radiation Pattern Measurements. The antenna pattern measurement systems most commonly used are continuous wave, narrow band. The multiple antenna configurations are the most common applications of transponder antennas on target vehicles; single antenna configurations are rare (except on FAA certified aircraft). A phased array is formed by the power divider and radiating elements. One aspect of allowing different path lengths from the transponder to the antennas is that the continuous wave response (pattern measurement) and the pulse response (transponder tests) can be different. The radar pulse incident upon the antenna system can be distorted by the summing of signals with different delays from different elements. The distortion caused by summing such pulses (in the power divider) could cause a variation in the trigger time of the reply, resulting in a range error.

6.2.9 Recommendations. Possibly, guidelines should be generated which would clarify when antenna harness cables may be of unequal lengths and when they must be kept equal.

Possibly, RCC 253-93 should be revisited (updated) to include guidelines similar to those in WSMCR 127-1 (EWR 127-1) especially sections 4.14 concerning pattern and harness measurements.

6.3 Computer Simulations in Radar Target Tracking

In the pre-mission planning stages of a missile-launch, it is normal to employ computer simulations of the expected trajectory and resulting tracker parameters. In the case of the radar coverage requirements, simulations can be useful in determining the number of radar sets and their placement locations. The dynamics of the trackers and the expected signal levels may be expected to be part of preflight simulations. Several aspects of the flight should be considered when using computer simulations. The accuracy of the results of the simulations depends upon several factors including the assumptions by the computer programmer and the accuracy (and appropriateness) of the data fed into the simulation program.

The coordinates in three-space and the timing of the trajectory on the test range need to be as accurate as possible. These will determine the angular limits and the dynamics of the tracker motions and may indicate the necessity of relocating certain trackers.

Of special interest in the study of transponder antenna systems on targets is the accuracy of the antenna pattern data supplied to the computer simulation program. This pattern data comes from direct measurements on the test vehicle or (sometimes) from another layer of computer simulation. Actually, in some cases, the data apparently comes from neither of the above, but instead from a “similar” vehicle system which has been used in past programs.

Interestingly, the antenna pattern data was originally meant to be derived from measurements of the actual target vehicle (or a mockup) with the same electrical properties as the actual vehicle. It can be argued that even measurements on an example of the flight vehicle are not always reliable and do not always accurately represent the performance of the vehicle in flight. The measurement engineer is responsible for taking into account the various controllable factors which degrade the “free space” assumption when devising the antenna test range configuration. There are standards and guidelines for the calibration and “field probing” of the test range aperture, which are (sometimes) imposed upon the measurement engineer. From the pattern range configuration, calibration, probing, mockup analysis and technique analysis the measurement engineer can estimate the “experimental error bounds” in the final measurement data.

Computer simulations of vehicle antenna patterns can be very good approximations to actual flight conditions if proper attention is given to the data used in the simulation programs. In the case of multiple element arrays on a vehicle, it is necessary to have accurate element pattern data and accurate element interaction data. The geometry of the array configuration must take into account the electrical properties of the surfaces nearby the elements and reflecting surfaces, which may be at some distance from the elements. Polarization and phase of the elements and the combining of waves from individual elements (and reflections) in the far field must be properly handled. Accurate simulations are not generally simple to attain. Some of the best “simulations” of antenna arrays come from measurements of the individual elements and computer analysis of the interactions.

Guidelines and standards which have been written for the measurement and reporting of antenna patterns for qualifications on national ranges delineate many of the requirements which

must be met before a system is approved on certain ranges. It has been suggested that these standards should be reviewed and revised to become more modern and to include significant “simulations” areas. Standards should flexible enough to allow innovation with emphasis on accuracy to the extent warranted by the situation.

There might be a place for a “standard” computer program for the simulation of expected flights. It is well known that certain programs exist for this kind of simulation. However, some programs are so cumbersome that their capabilities are not fully utilized. It might be advisable to standardize on one such program for RCC work and gain a little more in the area of commonality.

6.4 Antenna System Performance

6.4.1 Requirements And Predictions. If the radar transponder antenna system is required to be installed on a vehicle, then it surely has to meet certain minimum performance specifications. These specifications or requirements are imposed by the lead range on which the vehicle is to be flown. Normally, the basic requirements are set forth in published documents and then the specific details and project goals are factored into the overall specifications. The range has certain safety limitations and the user has certain mission goals. When the performance minimums are established the simulations and predictions are used to help decide on the overall design. The trajectory and link analysis accuracy are critical to both parties, the range (radars) and the user (mission).

6.4.2 Documentation Of Requirements And Results. It is very important that the specific requirements, as seen from both range and user, are clearly documented. During the design phase (of the antenna system), the “assessor” engineer is usually involved in many meetings in which details are worked out. Part of the documentation should be a “results” oriented test plan which will be applied to the antenna system design prior to its involvement in range flights. The format for this documentation should not be so rigid and detailed as to stifle innovation but detailed enough to identify the required results.

6.5 Measurement of the Time Delay in Transponder Antenna Systems

6.5.1 Background. The time delay from reception of the radar pulse to the reply transmission is of critical importance to the accuracy of the radar range determination. Technical Memorandum NR-DR 76-1 *Analysis of Transponder Induced Bias Errors* addresses several aspects of the radar and transponder pulse parameters and their effects on the determination of range for any given radar and target. Variation in the apparent time of beginning of the pulse causes corresponding changes in apparent radar range information. The transponder parameters are generally measured without the complete antenna system in place and thus the additional delays due to the antenna system must be considered as modifications to the delays determined by “bench testing”.

Clearly, when a transponder-equipped target is in flight and is interrogated by a radar, the transponder takes the signal from the antenna system as the “radar” signal. Similarly, the reply from the transponder must pass back through the antenna system before it can again radiate back

to the radar. Any delays and variations in delay caused by the antenna system will impact the accuracy of the radar's determination of range. If these delays and variations are known then the radar data can be corrected for those effects. It is not a trivial problem to accurately determine the antenna system's effect on range and direction as seen by various radars, especially when the target may be tumbling.

Static system measurements in the laboratory (bench testing) are routinely done to determine the transponder delay and the antenna system's insertion loss in amplitude and phase. Although there are some standards and guidelines for the measurement of the antenna harness in terms of insertion loss (RCC Document 253-93, Paragraph 3.4.1) for pattern measurement reports, little if any specific guidelines can be found for the measurement of the time delay in the antenna system which effect transponder functioning.

6.5.2 Recommendations. It seems clear that some form of guideline document should be generated for the measurement of the transponder antenna system time delay. The document should address the various methods presently used to measure transponder delays. The document should also incorporate acceptable methods of determining the antenna system's contribution to the possible "error budget" in overall apparent delay of the operational transponder system.

6.6 Antenna "Hat" Couplers

When testing antennas that will radiate substantial power in confined spaces, it is sometimes convenient to use "hoods" or "hats" over the individual radiators. High-powered transponders and some telemetry systems must be tested for overall performance while connected in the final configuration. In order to prevent radiation that might interfere with other equipment (or might harm humans) some form of limiting the strength of the escaping microwave power is needed. Simply placing the system in a "screen room" is not satisfactory because of the reflection of the radiated signal back into the antenna system. Some means of absorbing the radiated signal with the minimum of reflection is the goal. Some forms of "couplers" (or "hats") can be found which restrict the escaping radiation and yet produce little reflection.

There are "hats" which simply cover the antenna with an absorbing device, usually a metal cup filled with radar absorbing material (RAM) but with no attempt to couple a signal out on a coax cable. These are the simplest and can generally be made to produce reasonably small reflections back into the antenna that is covered. Testing of the transmitter into the antenna system may be done quite safely with this type of "hat".

Most testing of antenna systems with transmitters (or transponders) requires that a signal be injected or a sample be extracted by means of the "hat". This would be the case for comparing the relative powers radiated from the antennas in an array on a missile or mockup. Ideally, the array would be measured on a pattern range where very accurate determination could be made (of relative signals from the antennas), but many times such an antenna pattern range is not available in a timely fashion. The case of transponder antenna testing requires injecting a signal into the various antennas in the array (usually one at a time) in order to measure Parameters like overall delay and delay variations.

Coupling “hats” are not as simple as might be imagined. Primarily, a hat should not disturb the antenna under test (AUT) when it is placed over that antenna. This means that the “hat” must appear to be “free space” as nearly as possible, yet it should not let any radiation escape beyond itself. Most antennas mounted on (or in) the skin of a missile or aircraft set up currents on that skin. These currents are important to the forming of the antenna radiation pattern and impedance. When the hat is placed in contact with the skin near the antenna, it has the tendency to disturb the currents. Usually, the solution is to make the “hat” large enough that the essential currents on the skin are all within the confines of the “hat”. This is why coupling “hats” must be designed for the particular type antenna to be covered.

The design must also take into account the polarization of the AUT and the “hat”. Calibration of the coupling coefficient, polarization mismatch, impedance mismatches and time delays are among the parameters of concern to the “hat” designer.

6.7 Choosing a Test Vehicle for Antenna Measurements



Figure 6-1. Firebee drone on positioner during pattern measurements.

The vehicle upon which the antenna system is to be tested should represent the actual flight hardware. The material and geometry should present electrical properties as similar to those of the flight system as practicable. For small vehicles, it is usually possible to use the actual flight vehicle for the antenna pattern tests. Examples of relatively small test articles would be wing-mounted pods used in ECM tests.

When the effort is warranted large test articles can be mounted on the test positioner for critical pattern measurements. An example of a large test article might be the fully flight ready Firebee drone shown in Figure 6-1. The expense of preparing a flight vehicle for mounting on the antenna range involves considerable mechanical engineering to protect both the test article and the testing equipment. A partial mockup is sometimes substituted.

In the case of large full-scale missile assemblies, it is generally accepted that a full sized mockup of the geometry will suffice (See Figure 6-2). The mockups should be made lightweight but rigid. The lightweight feature is to ensure that the test fixtures (positioners and towers) will not be damaged or become marginally safe. Rigidity is important for the quality of electrical and geometrical properties of the mockup while executing antenna tests. Mockups that are allowed to flex under the rotations inflicted by the pattern testing procedures are likely to fatigue and have seams fail. Examples of acceptable mockups construction may be seen in the photos below.



Figure 6-2. Pegasus bulbous fairing mockup prior to antenna testing (PSL).

The choice of the test vehicle involves knowledge of the electrical properties of the flight hardware, including the conductivity of the skin and the proximity of reflecting surfaces, such as fins or other protrusions. Sometimes separate testing must be carried out on the materials involved, especially when the flight hardware utilizes composite materials. In many cases, it has been found that certain types of antennas may be accurately tested on aluminum mockups even when the flight hardware is certain kinds of composite.

The mechanical features of the proposed antenna testing vehicle sometimes drive the design or the compromises which must be made. If the flight hardware might be damaged by the rigors of pattern testing, then a sturdy mockup is probably necessary. Some tests require that the test vehicle be mounted onto the positioner by its aft end. For some programs, this implies modification of vehicle or the design and fabrication of a special mounting fixture. For long cylindrical test vehicles, it is sometimes preferable to use a midsection-mounting cradle. In the case of the ECM pods, this actually allows the direct measurement of the polarization components and pattern "cuts" which are most meaningful.

Figure 6-3. Photo gallery: Firebee Drones and mockups.





Mockups



Mockups (Continued)





Pegasus and PegSat mockups

6.8 Analog Roll Plane Pattern Vs. Sampled Pattern

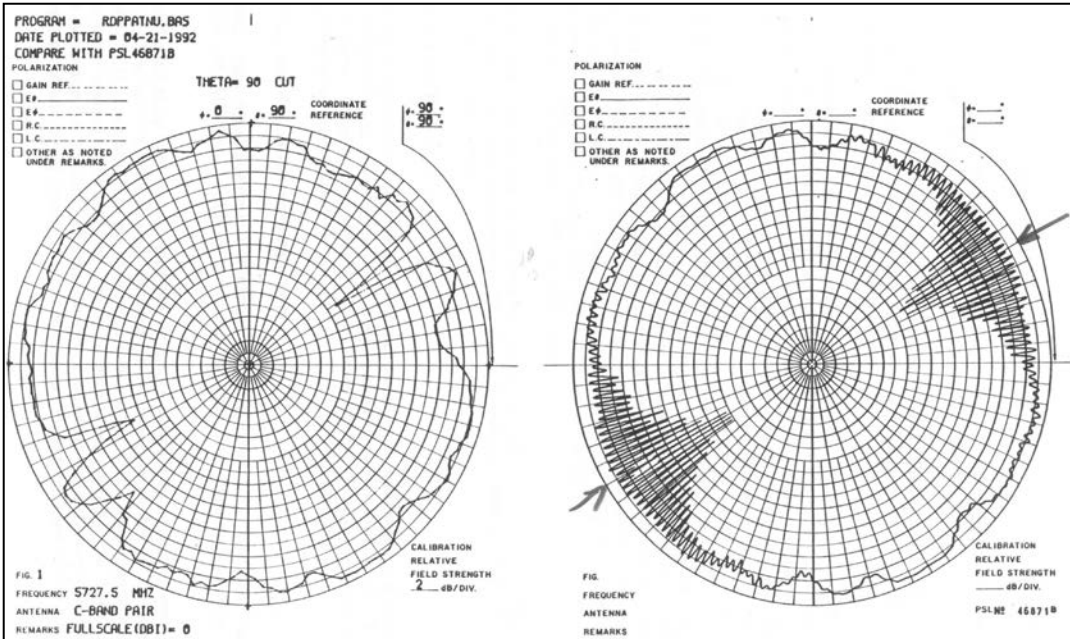


Figure 6-4. Example: Sampling error for two antennas on a 64-inch diameter vehicle.

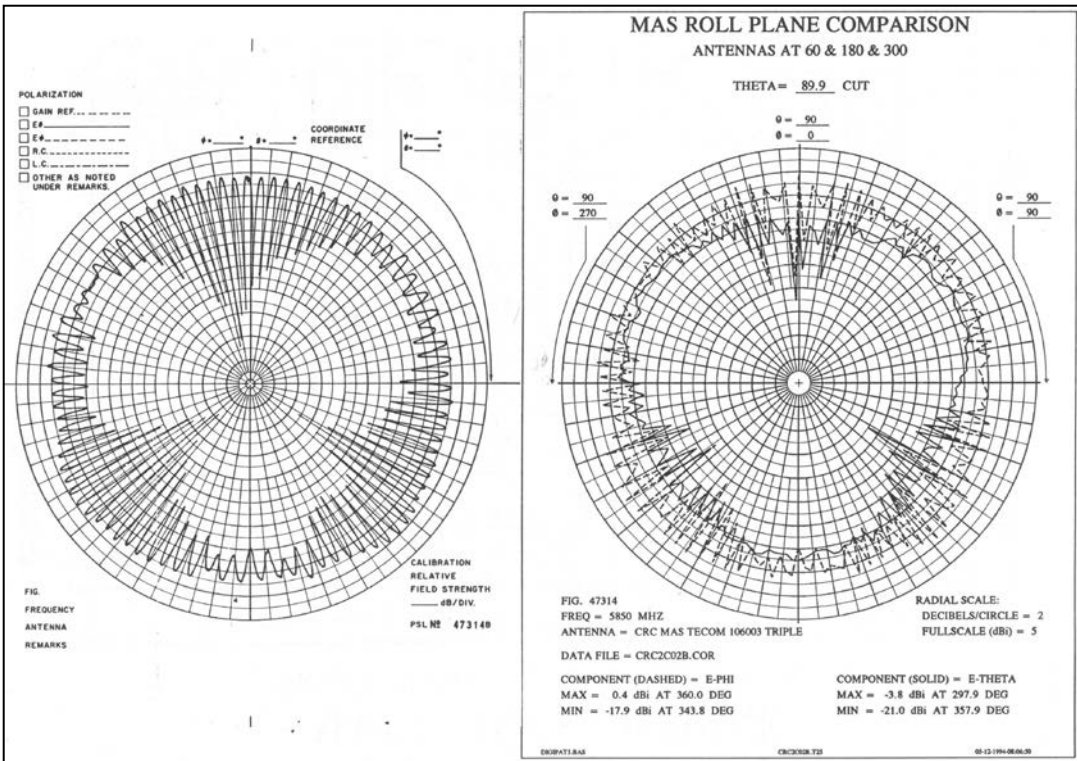


Figure 6-5. Example: Sampling error for three antennas on a 38-inch diameter vehicle.

6.9 Analysis of the Interference Lobe Structure and Sampling

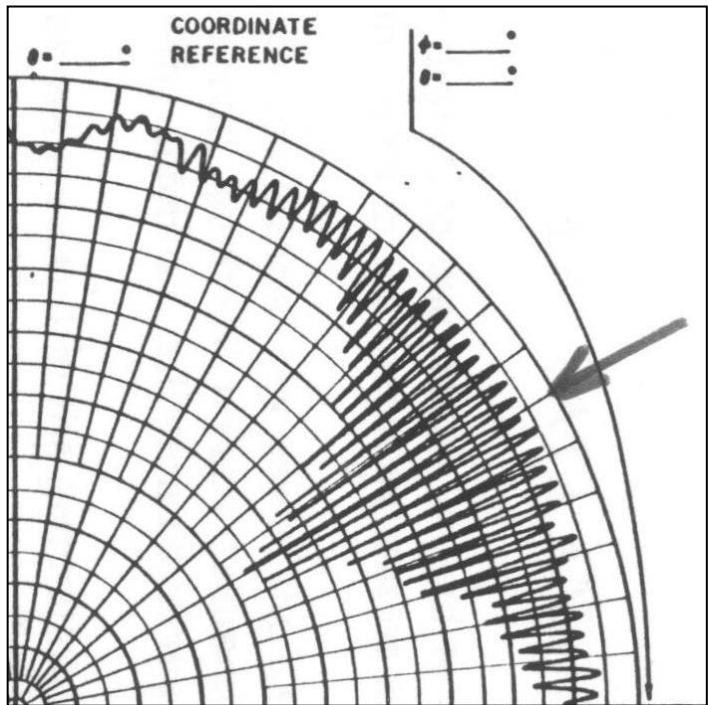


Figure 6-6. Analog measured pattern.

This pattern was measured (analog) with two antennas diametrically opposite on a 64-inch diameter vehicle. Consider the fine detail of the interference lobe structure around the 30 degree angle. The peak-to-null range is 20 dB and the angular separation between peaks (or nulls) is about 1.8 degrees. It can be seen that from 20 to 40 degrees there are approximately 11 full cycles. This indicates that the cycles have a 1.8 degree period, in complete agreement with the 64 inch separation (Paragraph 5.5) between radiators and the 5727.5 MHz frequency. This represents 0.55 cycles per degree. In 10 degrees, 5.5 cycles should be seen. The phase pattern rate of change in the null may be estimated (Paragraph 5.7) knowing the depth-of-null and the peak-to-peak angular range.

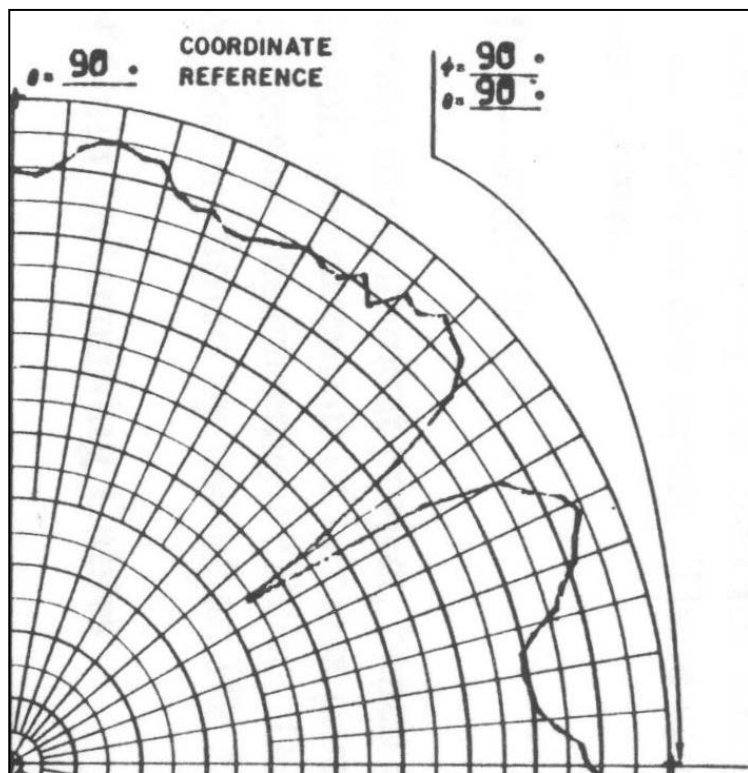


Figure 6-7. Digital measured pattern.

This pattern (digital) of the same antenna pair was sampled at 2 degree intervals and shows peak values at 10 degrees each side of a null. This is exactly what would be expected due to the strobing effect of the sample period (Paragraph 6.10). In each 10 degree interval the actual pattern goes through 5.5 cycles. The half cycle will move the samples from a peak to a null as successive samples are taken.

Pattern integration is done on the digitized pattern so the “coverage” values essentially come from a pattern as seen in the sampled version.

6.10 Strobing or Vernier Effect in Digitized Patterns

When antenna patterns are digitized, the normal angular interval is 2 degrees. Sometimes one degree is specified in an attempt to produce a result that is a more accurate representation of the analog pattern. It is sometimes considered adequate to mention the Nyquist sample rate and require samples be taken close enough together to insure that two samples fall within one cycle of the lobe. Thus if the peak to null angle of the interference pattern is two degrees then sampling at 2 degree intervals should be adequate. This situation is not adequate as will be shown with measured patterns. Consider the case in which two antennas are mounted diametrically opposite on a 28.6 inch diameter cylinder. The frequency of operation is 5860 MHz, which yields a wavelength of 2.014 inches. The antennas are then separated by 14.2 wavelengths and would have a peak-to-null angle of 2.02 degrees (or a full cycle of 4.04 degrees). Measurements on the analog pattern interference lobes show that there are about 5.1 cycles per +/- 10 degrees and about 7.7 cycles per +/- 15 degrees. These compute to 3.9 degrees per cycle in both cases, which agrees well with the computation from separation and wavelength.

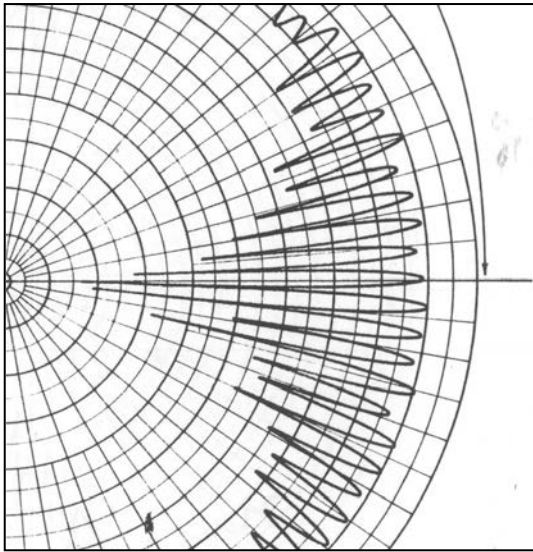


Figure 6-8. Analog pattern.

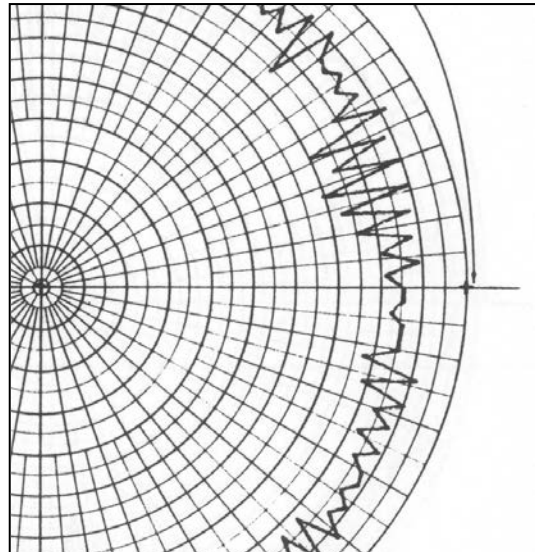


Figure 6-9. Digital pattern

In the zone of deepest nulls in the analog pattern, it can be seen that the sampled or digitized pattern shows relatively high and steady signal. Instead of the samples falling on the peak and then null of the pattern, this demonstrates that it is entirely possible that the samples will fall a few dB down on one lobe, miss the null, and then fall high on the next lobe. The angular extent of the lobe region and the Vernier action of the sampling through this region must be taken into account when analyzing any given digitized pattern. In this case the samples fell in such positions that the pattern looked strong and steady, but with the shift of a degree or so there may have been a very different pattern (possibly more accurate) from the digitizer. When the sample rate is close to the full cycle of the interference pattern the sampled pattern could be produced by samples falling in successive nulls and not seeing the peaks or possibly just the opposite by falling on succeeding peaks and not seeing the nulls. In either case, a misleading digital pattern results. These are the patterns that are integrated and analyzed to produce the values for coverage and directivity and ultimately the efficiency of the antenna under test. Perhaps analog patterns (of at least the roll plane) should be required in all cases. If analog

patterns are not possible, perhaps sampling with four or more samples per cycle of interference lobes should be required.

6.11 Three Antennas on a Cylinder

Consider the case of three antennas on a 38 inch diameter cylinder operating at a frequency of 5850 MHz. The wavelength is 2.018 inches so that the separation between two adjacent antennas is 16.3 wavelengths.

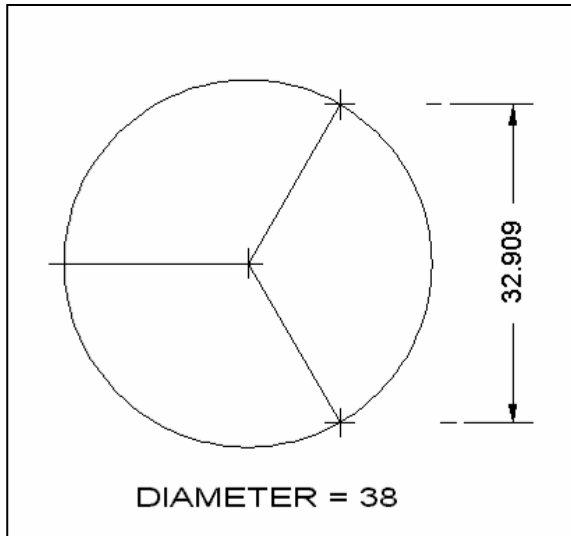


Figure 6-10. Diagram of three elements.

The expected angular distance from a peak in the interference pattern to the adjacent null is computed (Paragraph 5.5) by finding the angle whose sine is the reciprocal of twice the separation in wavelengths. In this case, the peak-to-null is computed to be just 1.757 degrees, which yields a full cycle of interference of 3.514 degrees. In the analog pattern shown below, the antennas are in positions of phi 20, 140 and 260 degrees. Measurements show that there are 11 cycles in +/- 20 degrees (or 11 cycles per 40 degrees) which yields 3.64 degrees per cycle. This essentially agrees with the analysis. This shows that it is not the diameter of the vehicle which determines the lobe structure, but the antenna separation. It indicates that there are 5.5 cycles in 10 degrees, which has implications for 2 degree sample spacing.

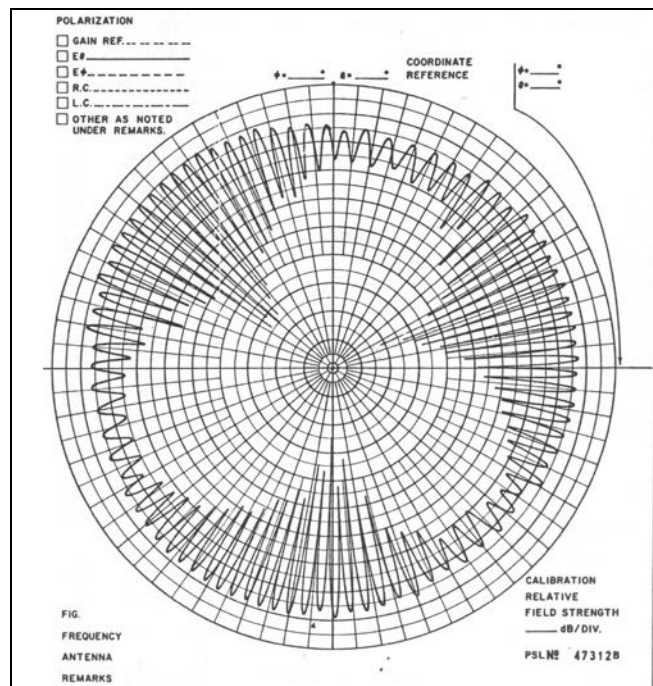


Figure 6-11. Analog pattern of three elements.

6.12 Harness Testing and Documentation

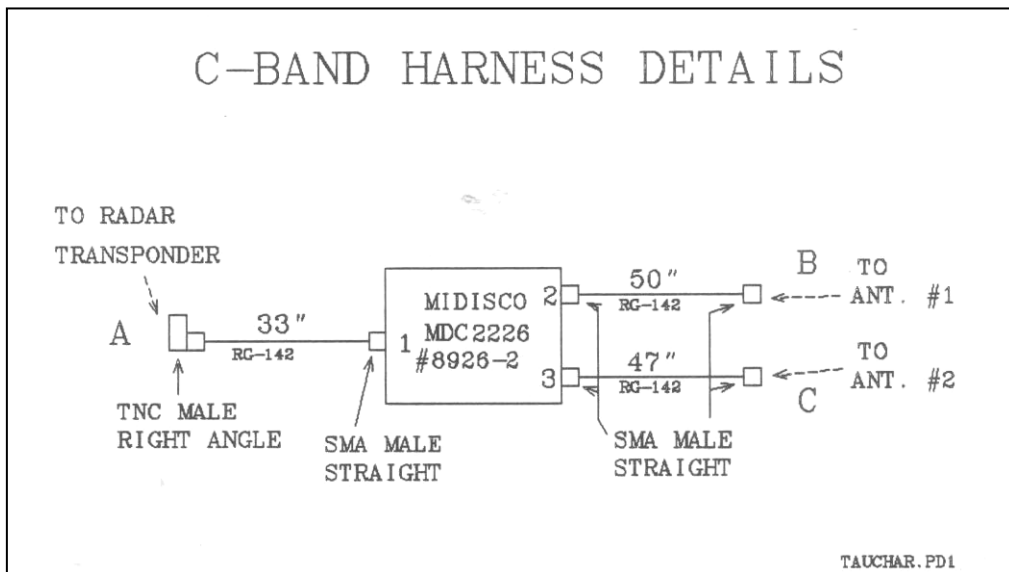
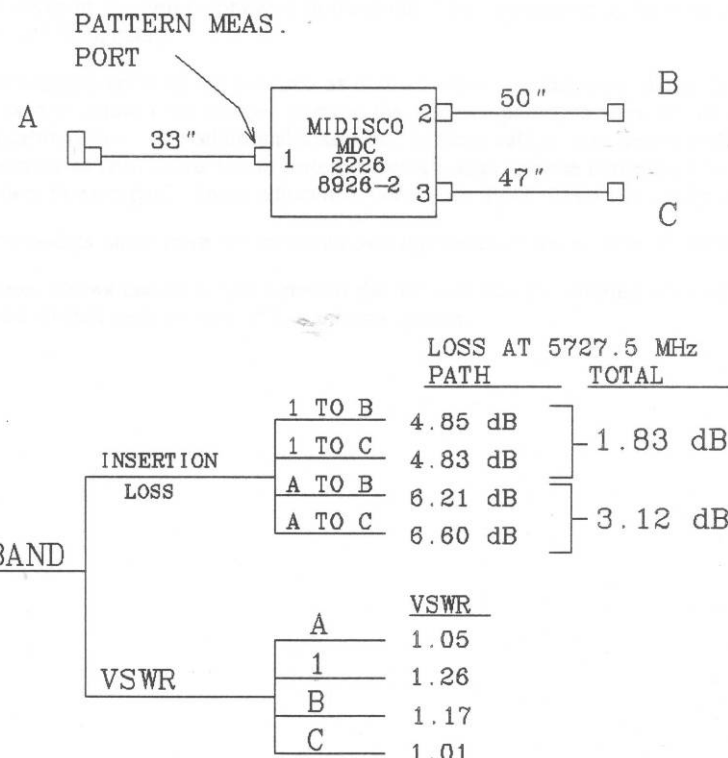


Figure 6-12. Example of harness sketch.

C-BAND BENCH TEST

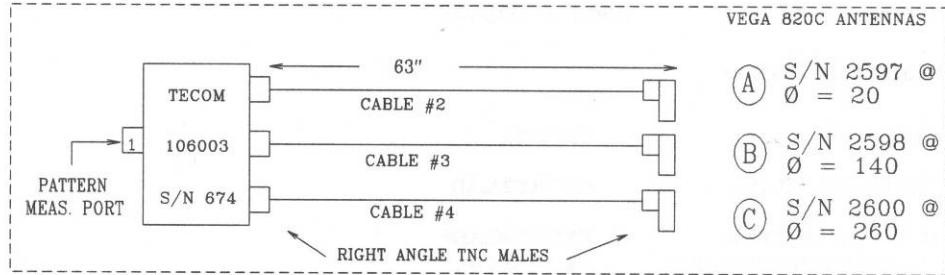


TAUBEN.PD1

Figure 6-13. Example of harness measurement results sketch.

HERA PATTERN TESTING
C-BAND, STAGE 3, CO-PHASE
FREQ = 5850 MHz

HARNESS SUMMARY



PATH	ANT ROLL	LOSS dB	PHASE	REL PHASE	LOSS TOTAL
1-A	20	7.4	78.3	0	2.69 dB
1-B	140	7.7	45.8	-32.5	
1-C	260	7.3	82.1	3.8	

PATTERN SUMMARY

FILE: CRC3C02B.CRC

PEAK GAIN = +2.31 dBi

PEAK DIRECTIVITY = +4.86 dBi

TOTAL EFFICIENCY = -2.55 dB (55.6 %)

ANTENNA EFFICIENCY = +0.14 dB (103.0%)

LHCP -25.4 dBic

RHCP = -13.2 dBic

CRC3CHR1.DC2

Figure 6-14. Example of sketch combining harness and pattern testing results.

6.13 Antenna Test Range Sketch

The method of mounting the test article on the measurement range should be shown clearly in a reasonable sketch.

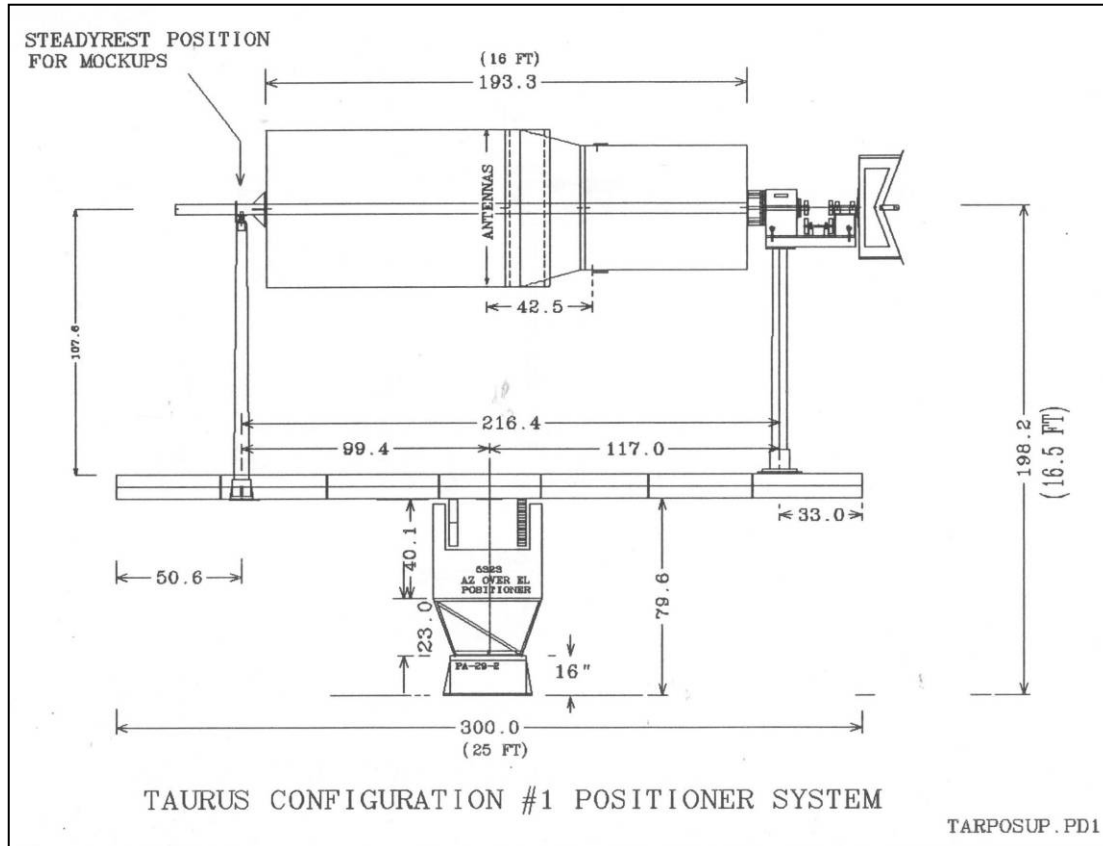


Figure 6-15. Example of measurement configuration sketch.

Antenna locations and critical mechanical details should be shown.

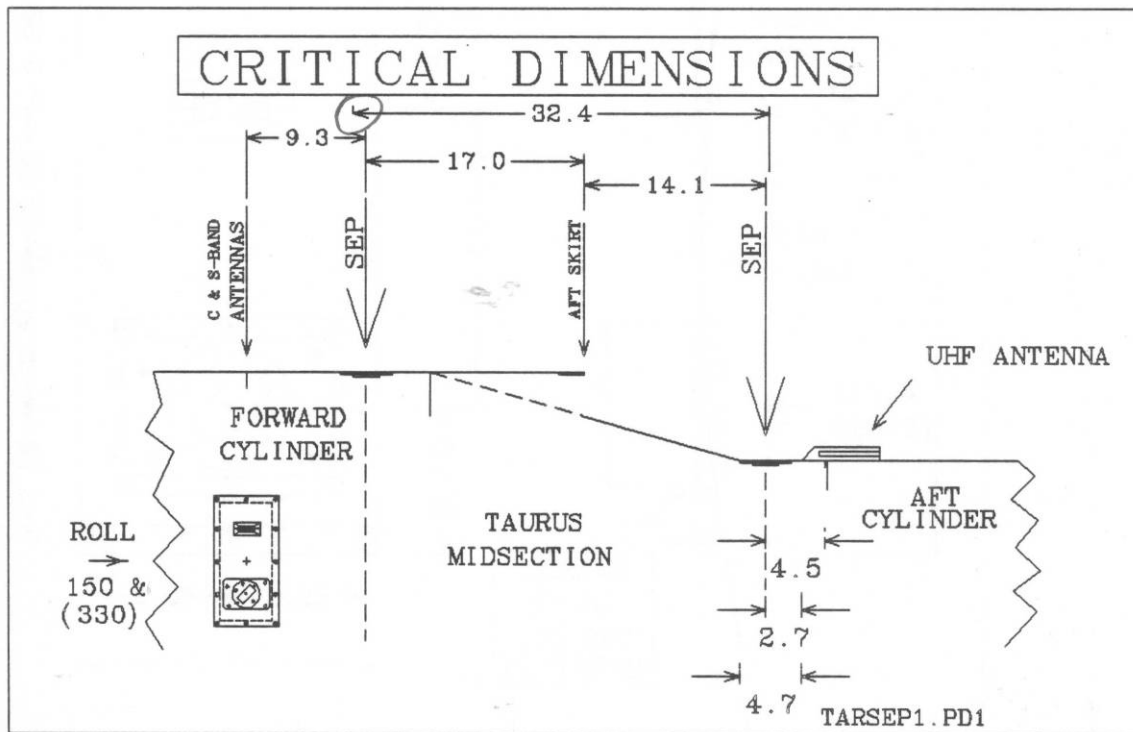


Figure 6-16. Mockup critical dimensions sketch example.

The coordinate system attachment to the vehicle should be clearly specified.

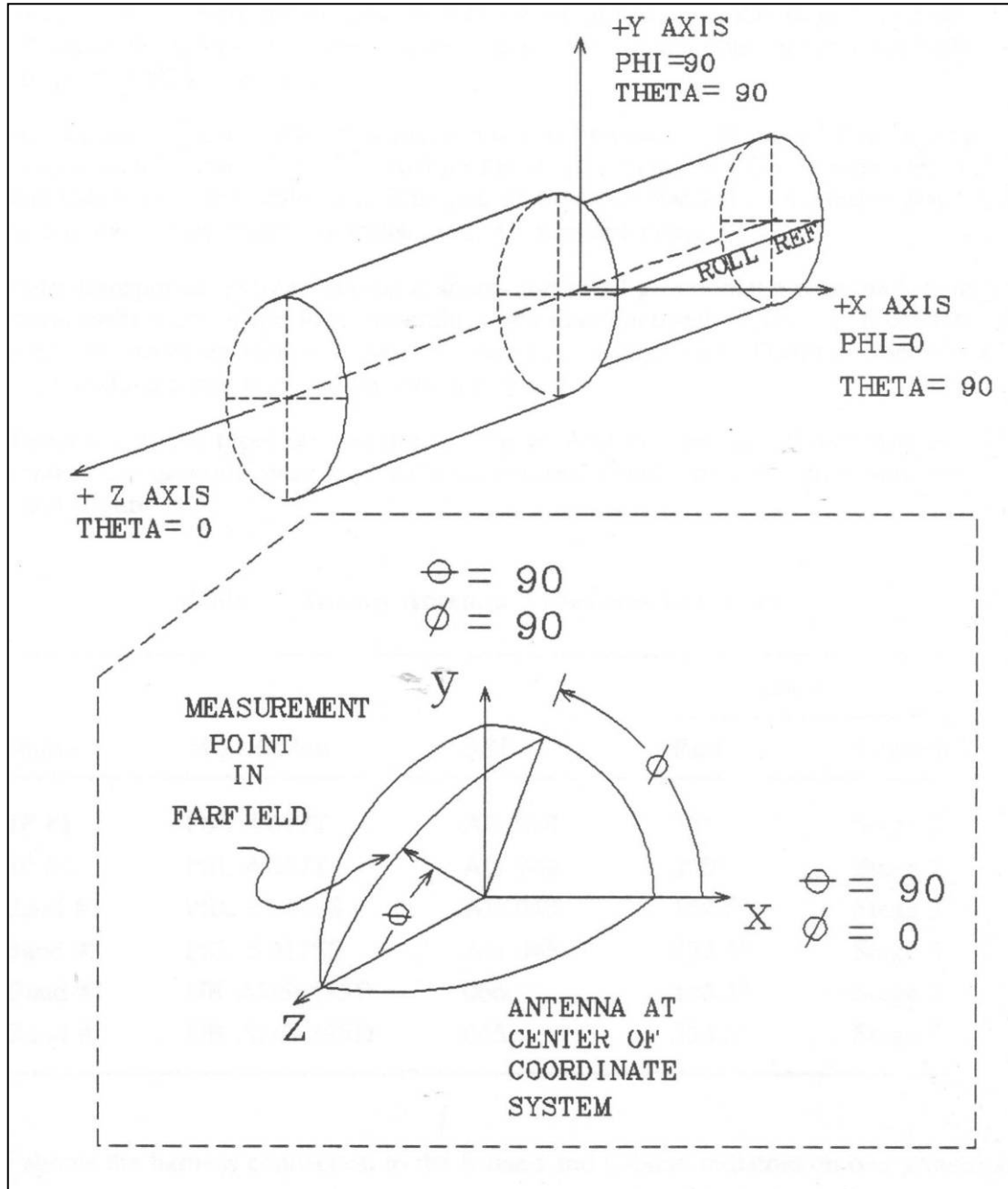


Figure 6-17. Coordinate system attachment to mockup sketch.

The geometry of the measurement range should be depicted in a sketch.

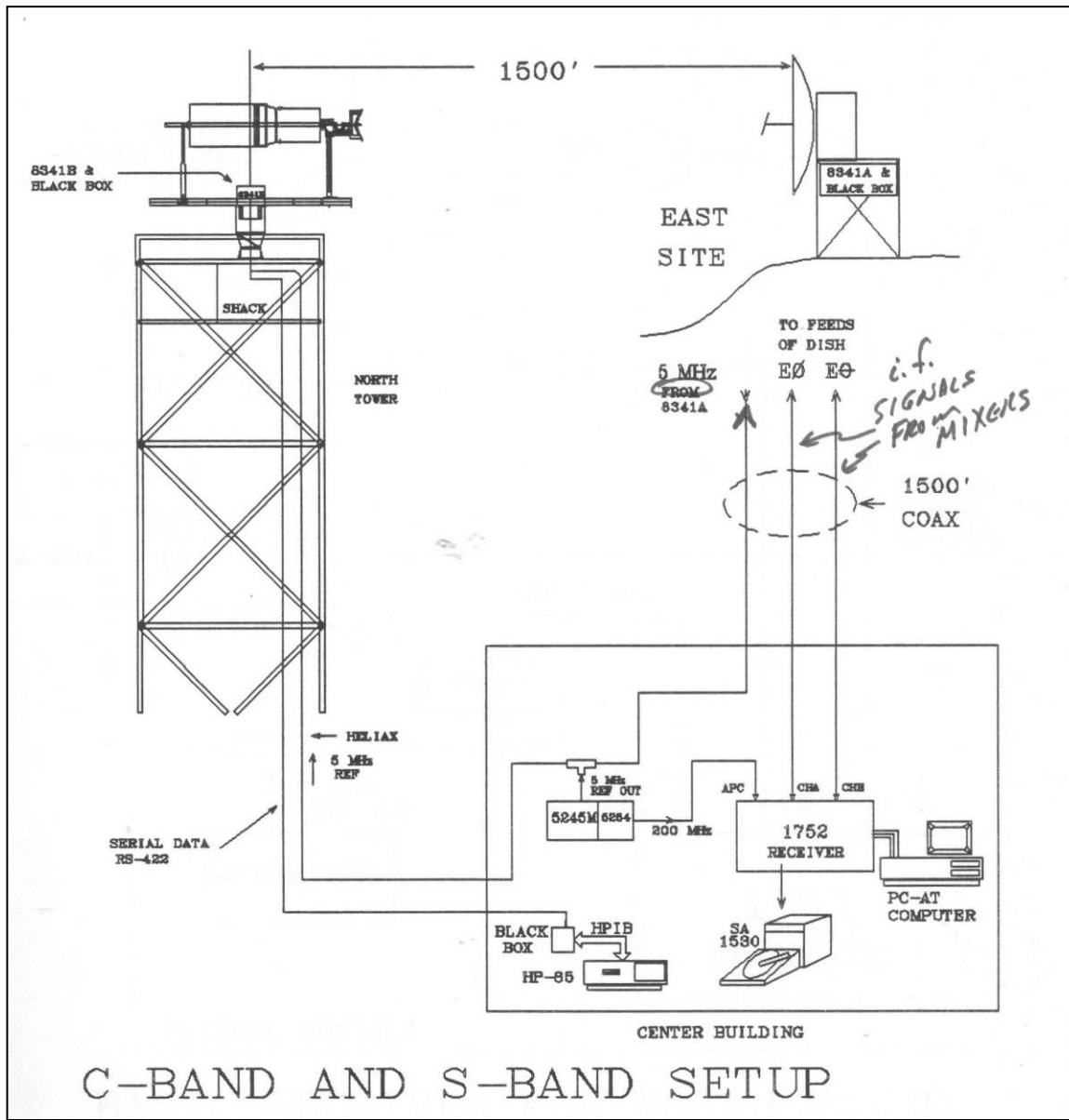


Figure 6-18. Sketch of pattern measurement range equipment configuration.

Basic signal flow diagrams should be considered important documentation.

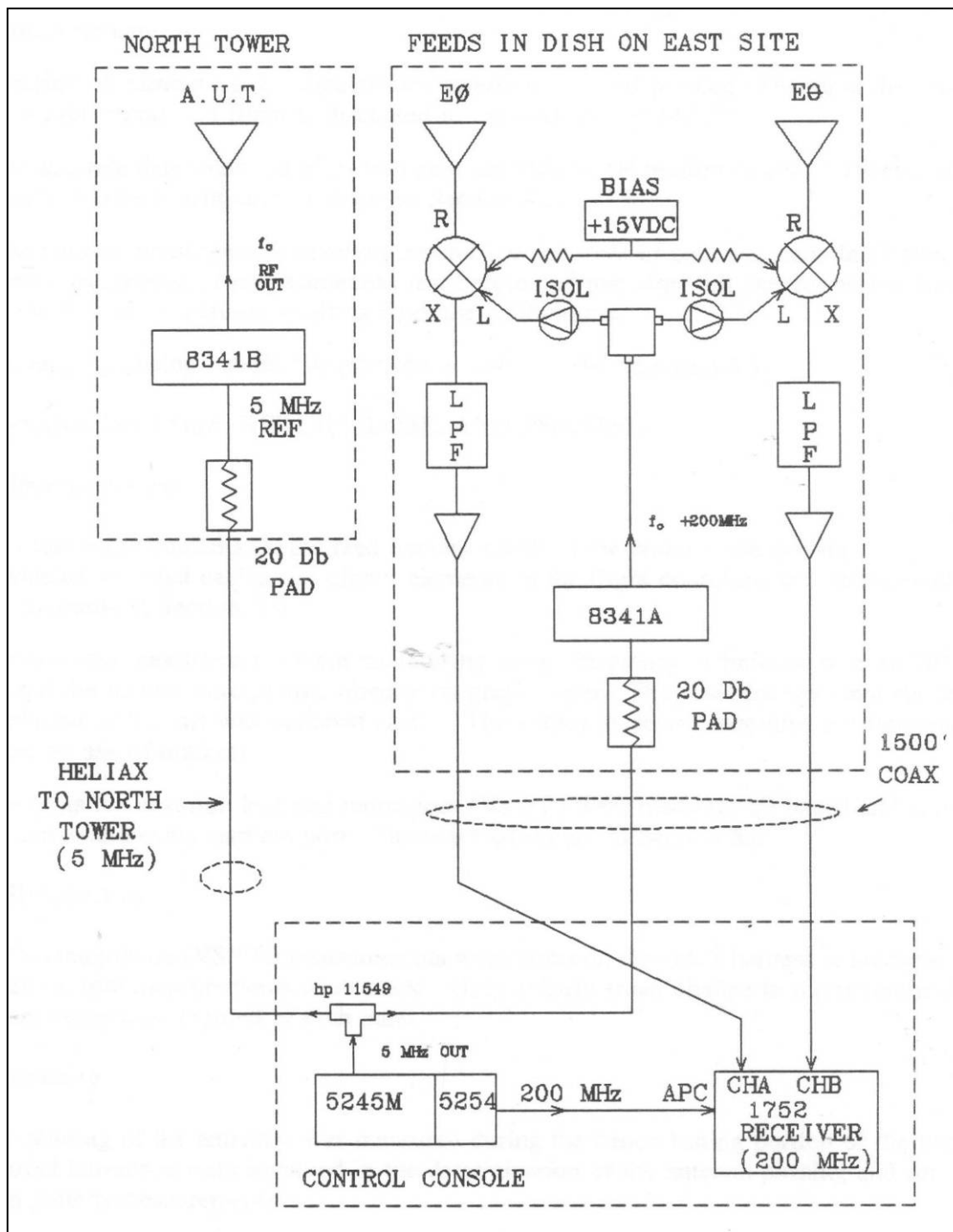


Figure 6-19. Sketch of signal flow configuration.

6.14 Pattern Comparisons

The following sketches are meant to illustrate typical pattern “cuts” and the results for using several antennas in array around a cylinder.

6.14.1 Mockup Sketch. The first sketch is an aft view of the section that contains the radiating elements (Figure [6-20](#)). There are a maximum of four antennas but measurements were made with a single element active, with two diametrically opposite elements active, and with all four elements active.

6.14.2 Coordinate System Sketches. Figure [6-21](#) and Figure [6-22](#) depict the spherical coordinate system and types of cuts used. Constant theta cuts (generally cones) and constant phi cuts (always planes) are shown.

6.14.3 Patterns of One, Two, and Four Elements on a Cylinder. The roll plane (theta equal 90 degrees) is the only constant theta cut which is a plane (Figure [6-23](#)). The measured patterns are analog plots of the specified cuts and are meant to show how the pattern builds as the number of radiators is increased. The single element pattern is needed to analyze the interference lobing structure when multiple element arrays are used. The lower pair of patterns simply compares the results of two different phasing harnesses with all four elements active.

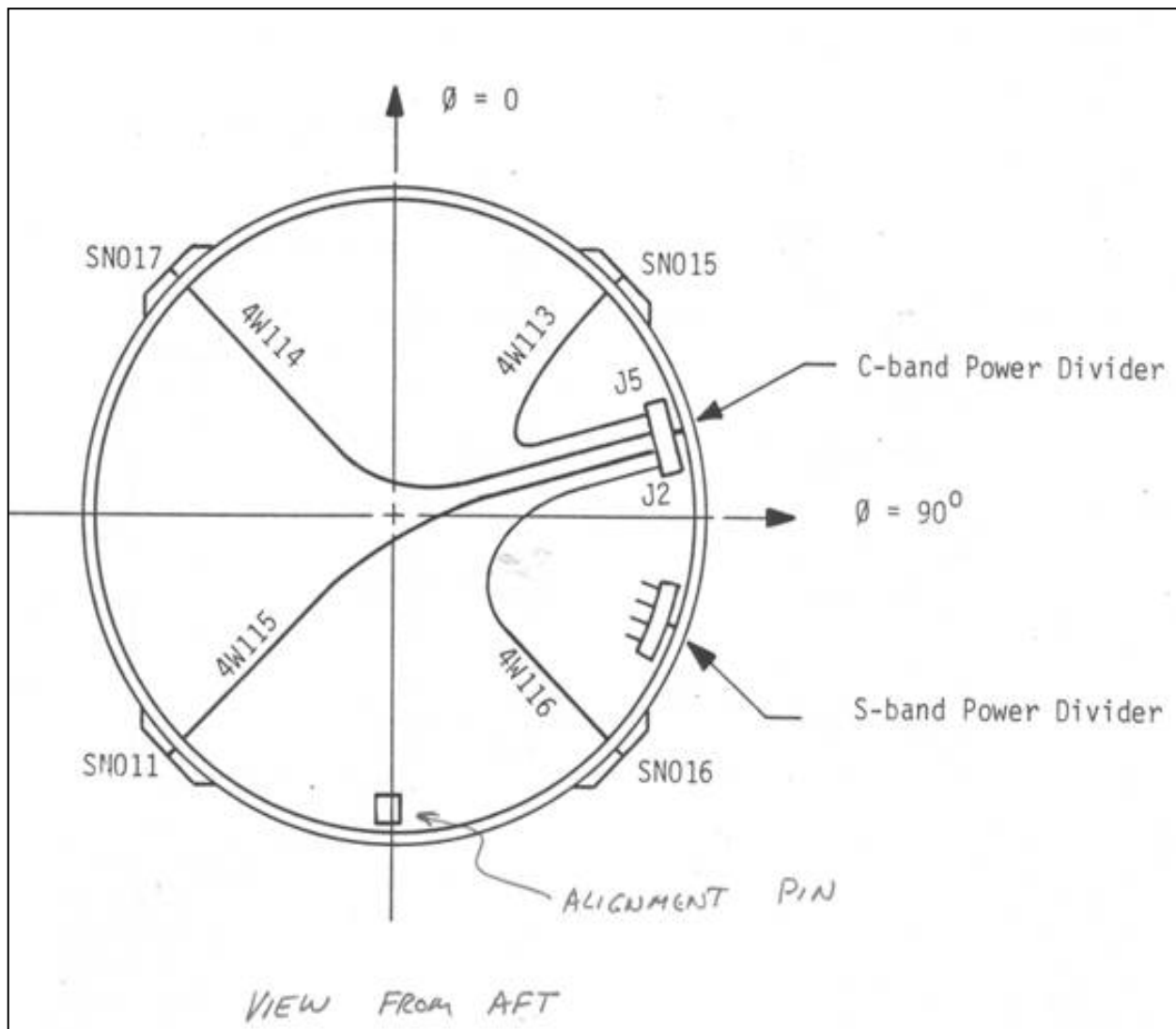


Figure 6-20. Sketch of antenna configuration on mockup.

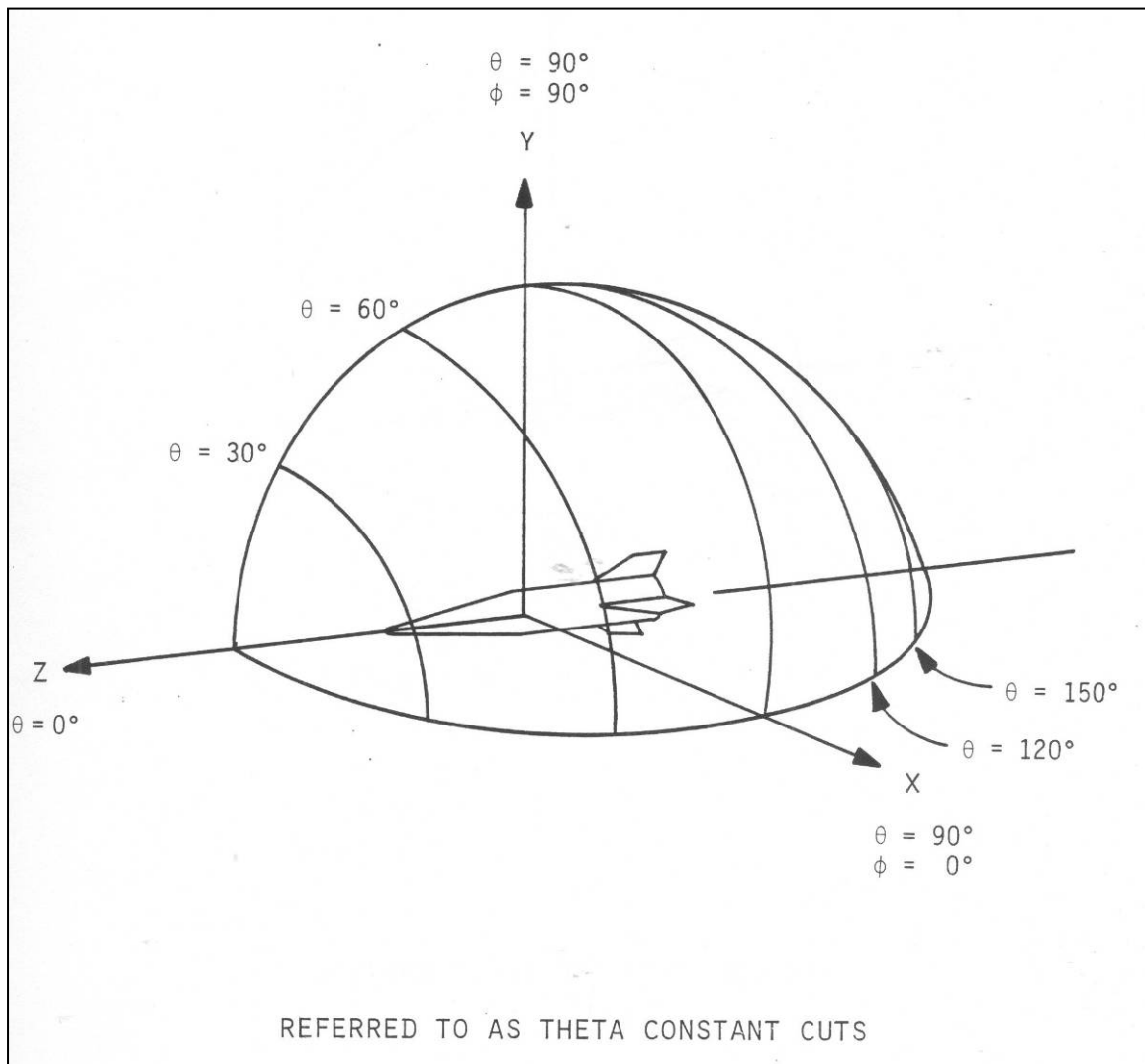
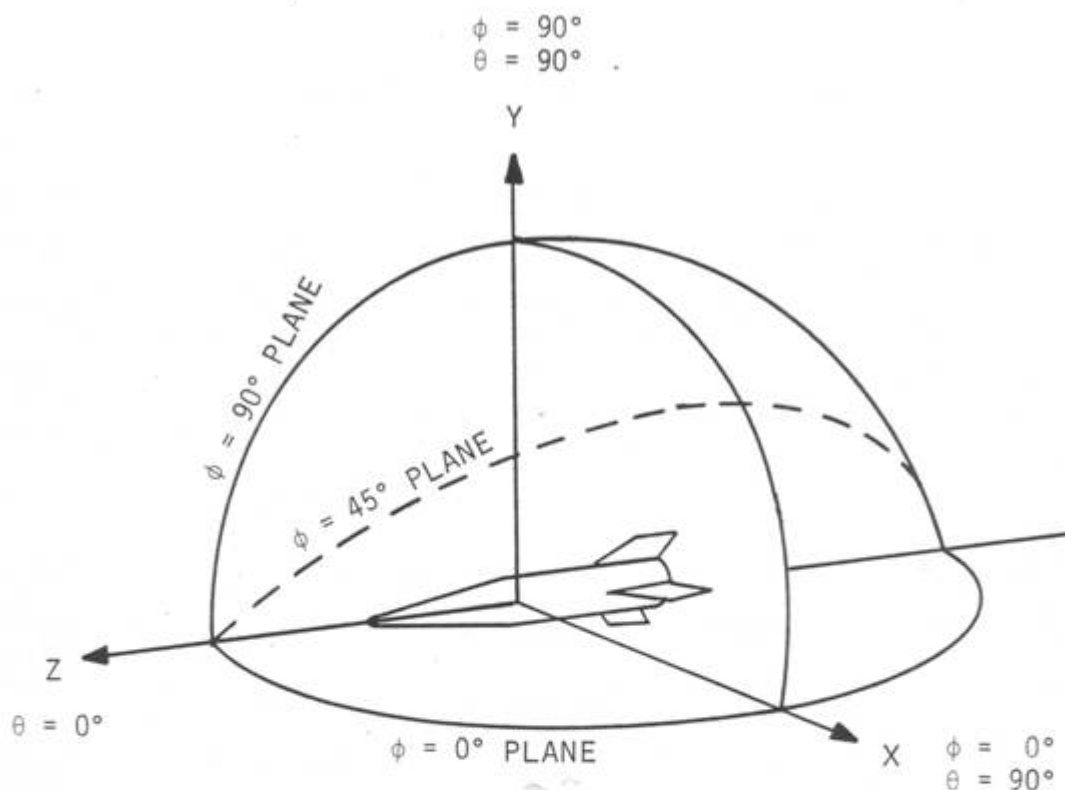


Figure 6-21. Sketch of theta constant / phi variable pattern cuts.



PLANES ACTUALLY CUT

- $\phi = 0^\circ \text{ & } 180^\circ$
- $\phi = 45^\circ \text{ & } 225^\circ$
- $\phi = 90^\circ \text{ & } 270^\circ$
- $\phi = 135^\circ \text{ & } 315^\circ$

REFERRED TO AS PHI CONSTANT CUTS

Figure 6-22. Sketch of phi constant / theta variable pattern cuts.

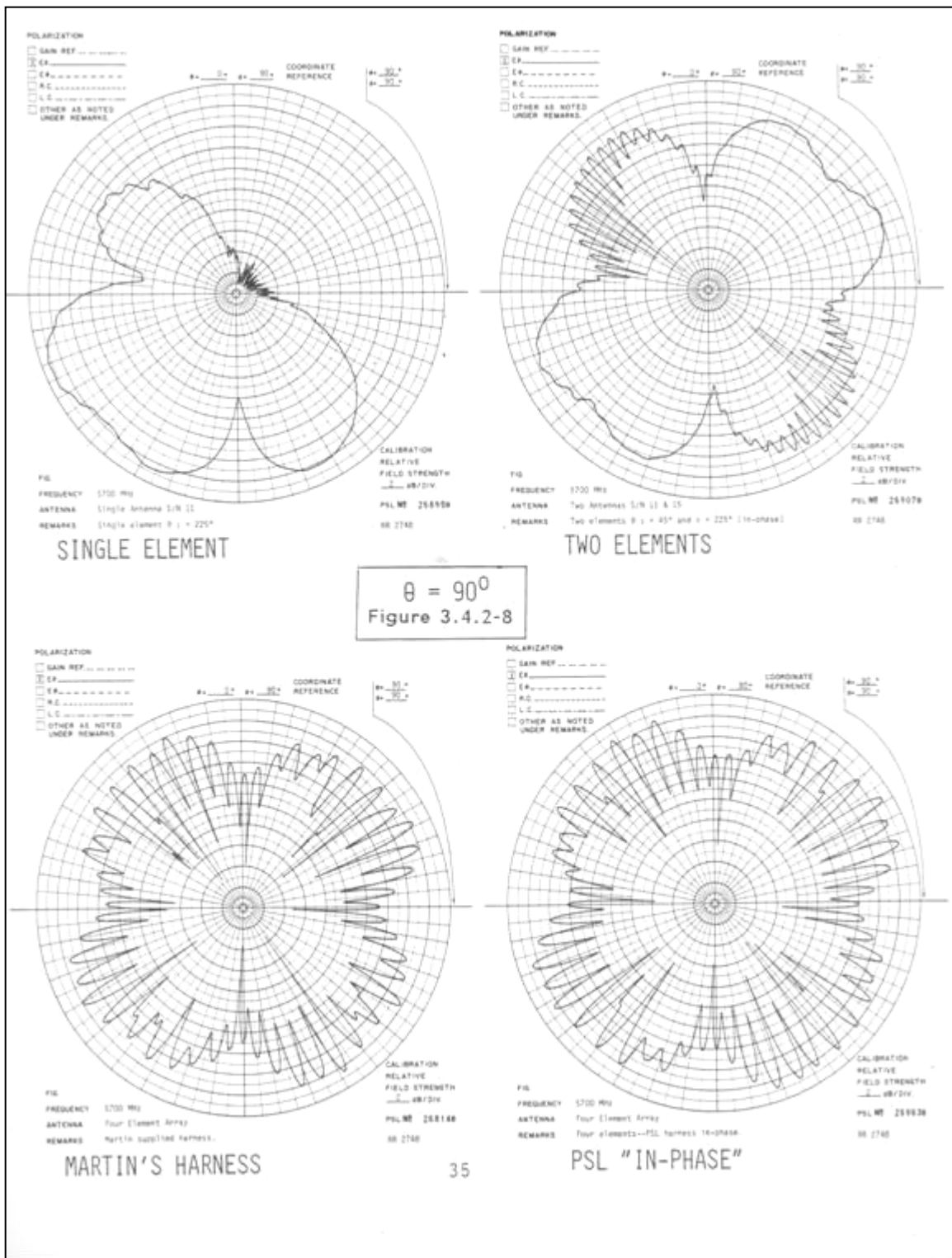


Figure 6-23. Analog roll plane patterns.

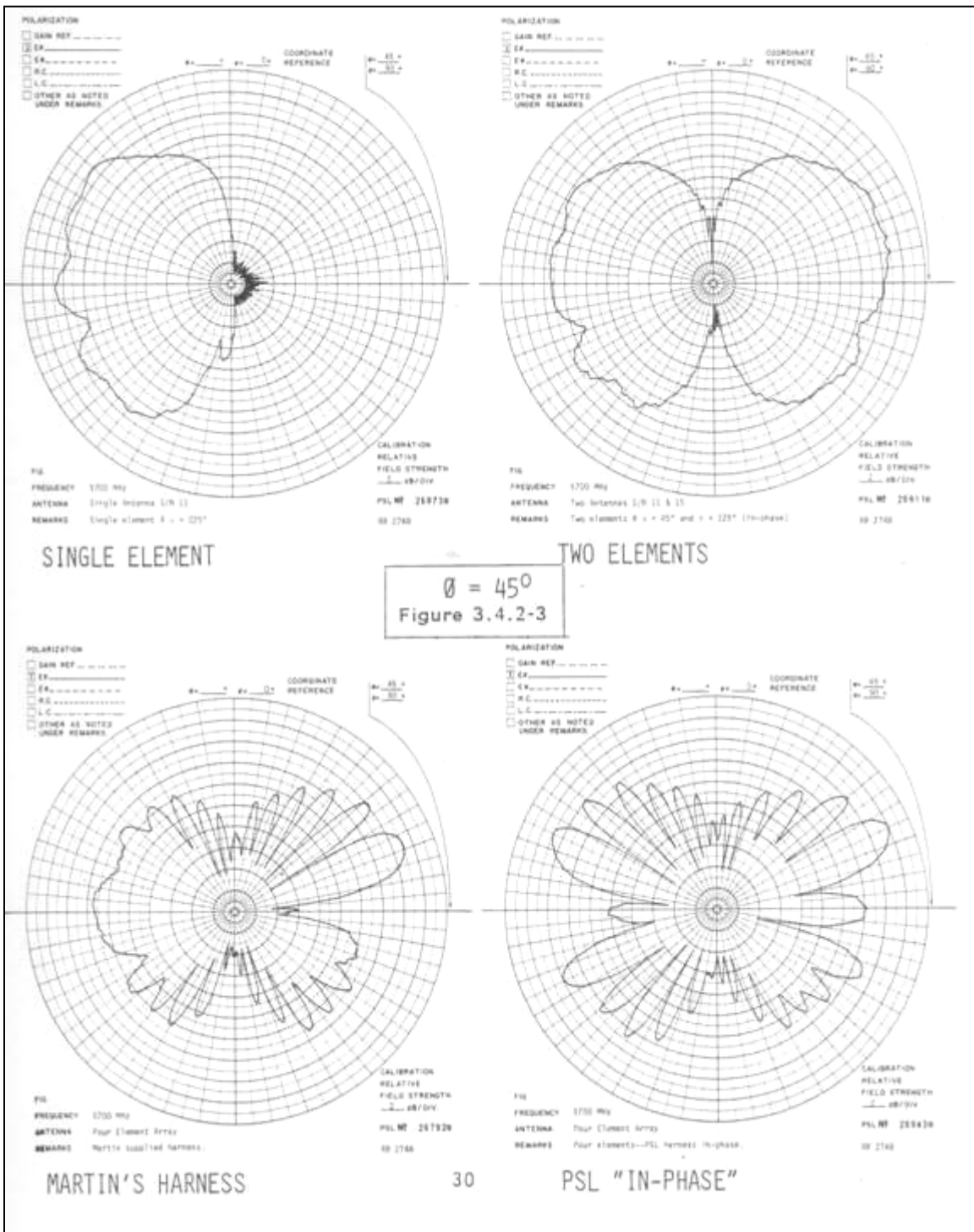


Figure 6-24. Analog phi constant patterns.

6.15 Antenna Pattern Gain Practical Determination

6.15.1 Substitution Method Considerations. The measurement of antenna pattern gain is of such critical importance that it deserves special attention. The antenna system evaluator should be aware of the basic approach to gain determination and some of the practices that introduce errors into the reported value of antenna gain.

Most of the target vehicle antenna systems are measured for pattern and gain on an antenna pattern test range. The general approach is to reference the signal strength of the link with the antenna under test, to the signal strength of the link with a calibrated gain standard. The method most often used is that of “substitution” gain determination. In this technique the transmit-to-receive link level is calibrated with the “standard gain horn” in the circuit and then, **changing nothing else**, exchange the test antenna for the gain standard. This sounds simple enough and should yield a quick and accurate gain for the antenna under test.

The problem is generally in the assumption that “**changing nothing else**” is achieved. In very few cases can this be done. In the practical world, there are various types of connectors on “standard gain horns” and other parts of the antenna system. The process itself (of exchanging the antennas) invites the opportunity for errors. There are cases in which an adapter must be used to change the apparent connector type of the gain standard to that of the antenna under test. Flight vehicles and mockups generally require extra cable lengths to reach the actual antenna under test. Also, the gain standard can sometimes not be placed at the same location as the antenna under test. This is particularly true when large vehicles are held on positioners in such a way that it is very impractical to remove the test antenna each time the gain standard is to be used. In practice the gain standard is sometimes mounted behind the roll positioner and switch selected from a remote location (operator’s console) whenever a “gain check” is desired. This arrangement has several advantages including the convenience and repeatability but it does require careful calibration during bench testing or range setup.

Since the gain standard (usually a linearly polarized horn) is used for polarization determination as well as signal strength comparisons, it is generally fed through a rotary joint system or cable wrap. The careful calibration of the gain determining system on the antenna range must include the basic calibration accuracy of the standard itself and then a careful calibration of all the elements involved in the substitution process.

6.15.2 Gain Determination Worksheet. The rotary joint, switch, cables, and adapters can be calibrated on the bench with a calibrated network analyzer. The “environment” in which the substitution is made must be done with calculations. Any range (distance) change between the gain standard and the test antenna must be taken into account. The following is a “worksheet” that has been found helpful in keeping track of some of the elements in the “gain calibration” of antenna patterns.

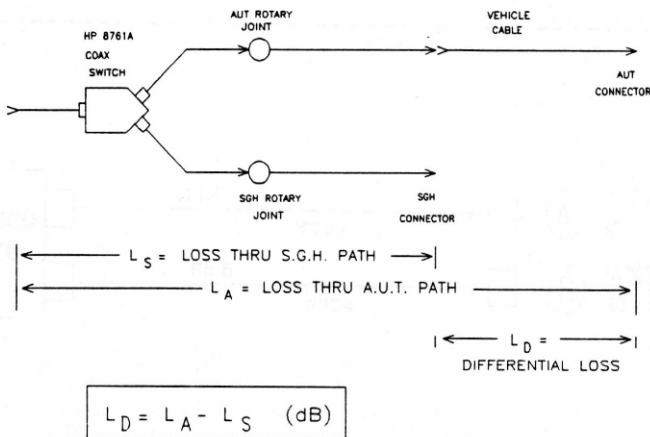
GAIN DETERMINATION WORKSHEET

FREQUENCY = 5765 MHz

GAIN STANDARD = SGH-3.9

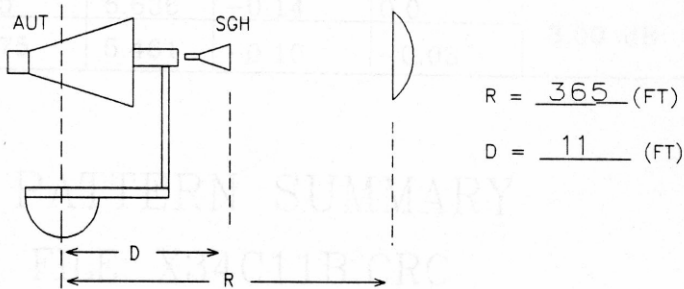
(1) BOOK VALUE OF GAIN = GB = +19.4 dBil

(2) CABLE SWITCHING CONSIDERATIONS:



L_D (MEASURED) = 3.13 dB

(3) RANGE LENGTH CHANGE



$$\text{PEAK GAIN DELTA GAIN} = 20 * \log\left(\frac{R+D}{R}\right) = \underline{0.27} \text{ dB}$$

(4) EFFECTIVE GAIN OF STANDARD

$$G_E = G_B + L_D + \text{DELTA GAIN} = \underline{+22.8} \text{ dB}$$

Figure 6-25. Example of gain determination worksheet.

6.16 Antenna Pattern Test Range Siting

6.16.1 Antenna Range Geometry. The most important considerations in determining the geometry of any radiation pattern range are the size of the test article and the wavelength of operation.

When the test vehicle is required to take on two different configurations there may be a considerable change in the largest dimension. In this example, the longest dimension is about 16 feet and the highest frequency (shortest wavelength) is 5727.5 MHz. A widely accepted rule-of-thumb is that the range length should be at least twice the square of the longest dimension, divided by the wavelength, or

$$Range \geq \frac{2D^2}{\lambda}$$

Other considerations enter the decision process and sometimes have less definite specifications. The far-field criterion stated above gives an idea of how long the range should be but, as the range gets longer without compensating increases in the tower heights, problems of ground reflection begin to outweigh the advantages of length.

The test vehicle should be illuminated with a beam that holds the energy tightly on the vehicle and away from the ground between towers. As the wavelength gets longer (lower frequencies), the required illuminator size gets larger than the available illuminator antennas. Compromise must be struck between greater range length for phase front uniformity and the ability to control the ground reflections that would disturb the illuminating wave in phase and amplitude. Figure [6-26](#) shows the mockup section that meets the criterion.

Another consideration involves the measurement technique to be employed in generating and collecting pattern data. The most desirable technique involves the use of polarimetry. In polarimetry, the test antenna generates a wave and the illuminator receives and decomposes the wave into orthogonal polarization components in amplitude and phase. With this technique, only one pass over the radiation sphere is needed to collect all the data needed to determine the complete gain and polarization information for the measured frequency and configuration. Without this polarimetry technique, a set of individual passes over the radiation sphere is required to collect data on separate polarization components (amplitude only). The absolute minimum number of amplitude-only components is four, but due to many considerations, the full set of six components is usually measured.

To use polarimetry, the pattern test range must be configured to allow remote control and signal sampling between both towers (ends of the range) and the control console (usually located at one end of the range). The shorter ranges generally have this capability or can configure for it with little cost; however, long ranges require low-loss coax between towers and other electronic capabilities, which can be expensive.

6.16.2 Illumination Taper-General. Normally, the test antenna on a far-field range should be “illuminated” by a uniform plane wave. For reciprocal antennas, the direction (transmit or receive) of the “arrows” on the link diagram is reversible without changing the antenna's gain or pattern. At an antenna test range using polarimetry, the antenna at the end of the range, opposite the test antenna, is used to receive rather than to transmit. Regardless, this antenna is sometimes termed the “illuminator”. Referring to it as the “range” antenna is perhaps more appropriate for this setup.

The beamwidth and the beamshape of the “range” antenna should be such that, when it is aimed at the coordinate origin, the greatest extent swept out by the rotating test antenna (vehicle) should not fall outside of the 0.25 dB points of the beam. The 0.25 dB may be more restrictive than necessary, but is certainly is adequate for missile-type antenna systems. By studying the beamshape of typical illuminator antennas, it can be seen that a half-power beamwidth (HPBW) of about 3.5 times the subtended angle should be used. Greater beamwidths will have less direct taper at the test aperture but will also tend to produce higher standing waves and thus disturb the measurement.

6.16.3 Test Aperture Taper-Illuminator Beamshape. The pattern of the illuminator dish contributes to the equation for quality of test aperture illumination uniformity. Any systematic taper across the test aperture due to dish beamwidth can be determined from the geometry of the range. Knowing the range length and the dish's beamwidth (or pattern), we can easily determine the test aperture taper. The mockup geometry shows that the mockup occupies only 16 feet. Viewed broadside from 1500 feet, the mockup subtends about 0.6 degrees. Usually, the half-power beamwidth of the illuminator should be 3.5 times the subtended angle to reduce taper to 0.25 dB. Thus, dishes should produce a beamwidth of 3.0 degrees for this example.

In Figure [6-26](#), the 16 feet long mockup is shown broadside as seen from the location of the range antenna. For the given range length of 1500 feet and the frequency of 5727.5 MHz, the portion of the mockup which meets the farfield criteria is within the circle centered on the active antenna.

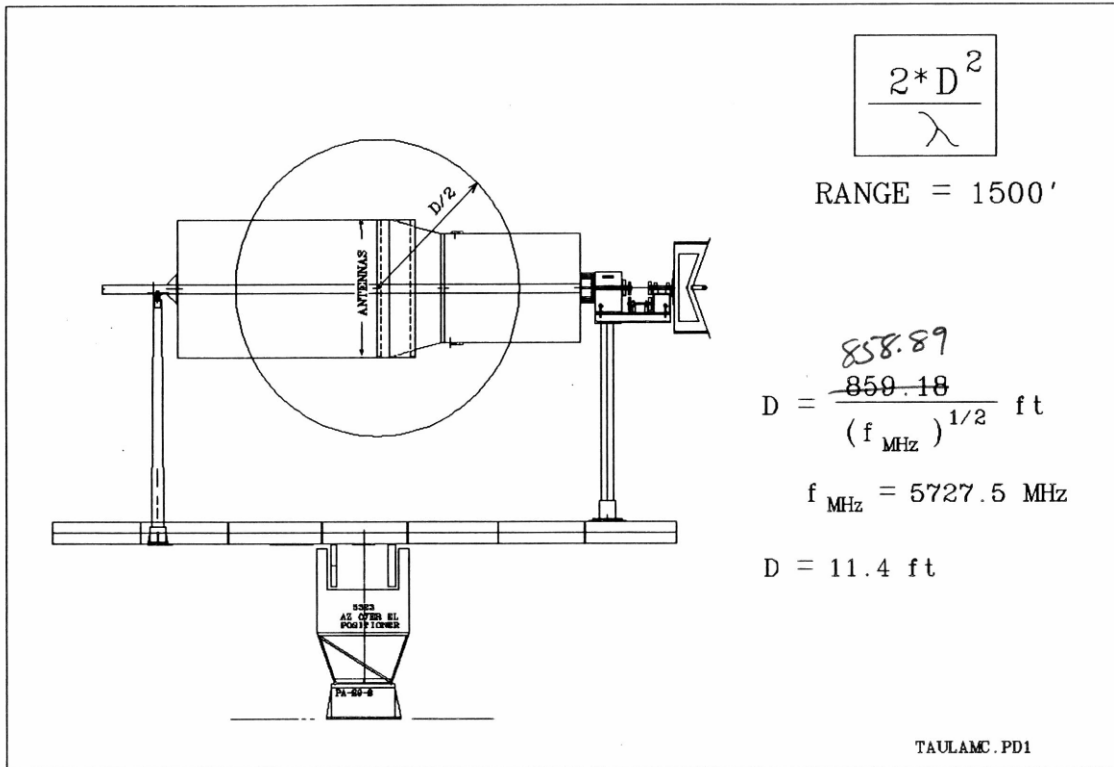


Figure 6-26. Sketch showing section meeting far field criterion.

6.17 Standing Wave Fields and Probing

6.17.1 Two Interfering Waves Generate a Standing Wave. Reflections on the antenna pattern test range result in the formation of standing waves. The existence of a standing wave field in the measurement aperture causes errors in the radiation pattern measurements on elevated farfield test ranges.

As in treating reflections on transmission lines, there are two ways of measuring and specifying the effects of reflections. The “standing wave” approach measures the combined reference and reflected waves. The result is specified in terms of a “standing wave ratio” (SWR) or “voltage standing wave ratio” (VSWR). Another way of dealing with reflections is the “reflectometer”, which separates the waves according to direction. On the transmission line, there are two directions, reference or outbound wave and the returning or reflected wave. The result is specified in terms of a “reflection coefficient”. When properly done these two methods can be equivalent in determining the severity of the reflections. On the pattern measurement range, there are many directions for traveling waves and reflections may come from almost any direction. On an outdoor elevated far field range, it is unusual for reflections to come from above, but almost any other direction must be suspect.

Range reflections are of critical importance because the measured patterns will be responses to the entire group of “sources”, both the (intended) direct wave and the (unwanted) reflected waves. Gain values and pattern features are distorted by reflections on elevated far field ranges. Determination and documentation of the reflections may be done by moving

(translating) a wide field-of-view probe in the measurement aperture (standing wave approach) or by rotating a narrow field-of-view (beam) probe to look in all directions from the measurement aperture (reflectometer approach). When properly done the methods can be equivalent; however, at low frequencies, it is difficult to get narrow beam probes and at high frequencies it is difficult to get wide beam probes. Therefore, it is most common to employ the translating probe method at low frequencies. Analyzing the traces (recordings) of the “field probing” can be complex and demanding, especially if the specification of reflection level for the range is unusually low. Some relationships and graphs are included to assist in analyzing the field probing standing wave plots.

The sketch below illustrates the presence of two plane waves passing through the test aperture from different directions. In practice, there could be several significant reflections, which would produce waves passing through the aperture, but the principle can be seen clearly by considering two waves.

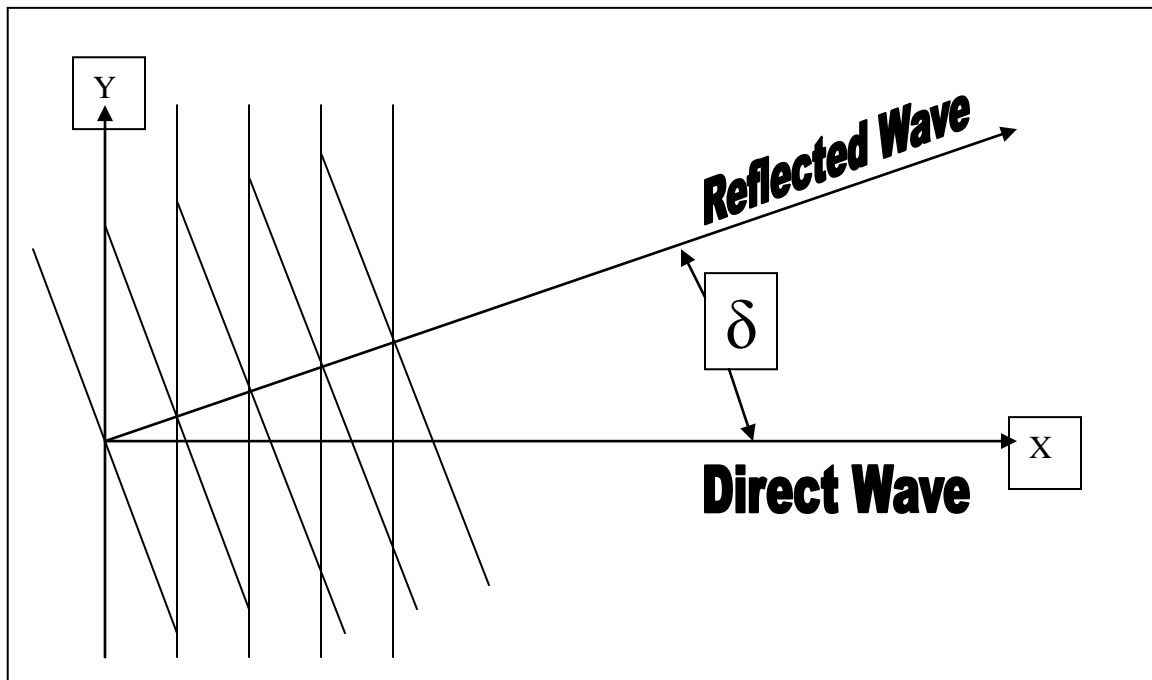


Figure 6-27. Sketch of two interfering wavefronts.

Because these wavefronts are coherent, they will form a standing wave pattern in the area. The magnitude of the standing wave and the locations of the maxima and minima may be determined by moving a (non invasive) probe in the field and recording the signal strength received. The probe must be able to “see” in all the directions from which important reflections might come. If the probe has directivity which may prefer some directions over others, then it is important to know the probe pattern and correct the measured results for the pattern. Probe movement should be established along lines (in planes) which are essentially parallel to the main (direct) wavefront (vertical probing) or parallel to the propagation direction of the direct wave (horizontal probing). The spacing of the maxima and minima may be analyzed to determine the direction of arrival of the reflection.

In the graphs that follow, it may be noticed that the curve for standing wavelength for vertical probing is symmetrical about 90 degrees, whereas for horizontal probing the value of standing wavelength is unity for arrival angle of 90 degrees but continues to diminish to a value of one half for the 180 degree arrival angle. For horizontal probing, the probe is progressing in the direction of the direct wave and thus “cutting” through phase of the direct wave. In the case of vertical probing, the probe moves along a line of constant phase (i.e., not cutting phase) of the direct wave and cutting (at an angle) through the phase of the reflected wave. The phase difference between the direct and reflected waves at each point determines the position on the standing wave.

6.17.2 Derivation Of Probing Equations

The phase of the direct wave in the X-direction is:

$$\Psi_{DH} = \left(\frac{360^\circ}{\lambda_0} \right) x$$

The phase of the direct wave in the Y-direction is:

$$\Psi_{DV} = 0$$

The phase of the reflected wave in the X-direction is:

$$\Psi_{RH} = \left(\frac{360^\circ}{\lambda_0} \right) \{x \cos(\delta)\}$$

The phase of the reflected wave in the Y-direction is:

$$\Psi_{RV} = \left(\frac{360^\circ}{\lambda_0} \right) \{y \sin(\delta)\}$$

Forming the phase difference:

$$\Delta\Psi = \Psi_D - \Psi_R$$

For horizontal probing, we have:

$$\Delta\Psi_H = x \left(\frac{360^\circ}{\lambda_0} \right) \{1 - \cos(\delta)\}$$

For horizontal probing when $\Delta\Psi_H$ becomes 360° then we have x equal to the standing wavelength for horizontal probing.

$$x = \lambda_{SH}$$

Then

$$\Delta\Psi_H = x \left(\frac{360^\circ}{\lambda_0} \right) \{1 - \cos(\delta)\} \text{ becomes } 360^\circ = \lambda_{SH} \left(\frac{360^\circ}{\lambda_0} \right) \{1 - \cos(\delta)\}$$

or

$$1 = \frac{\lambda_{SH} [1 - \cos(\delta)]}{\lambda_0}$$

then for horizontal probing we have

$$\frac{\lambda_{SH}}{\lambda_0} = \frac{1}{[1 - \cos(\delta)]}$$

Similarly, for vertical probing,

$$\Delta\Psi_V = \Psi_D - \Psi_R$$

but

$$\Psi_{DV} = 0$$

$$\Psi_{RV} = y \left(\frac{360^\circ}{\lambda_0} \right) \sin(\delta)$$

then

$$\Delta\Psi_V = y \left(\frac{360^\circ}{\lambda_0} \right) \sin(\delta)$$

When $\Delta\Psi_V$ equals 360° , then y equals the standing wavelength for vertical probing.

$$360^\circ = \lambda_{SV} \left(\frac{360^\circ}{\lambda_0} \right) [-\sin(\delta)]$$

which is

$$1 = [-\sin(\delta)] \left(\frac{\lambda_{SV}}{\lambda_0} \right)$$

so that for vertical probing we get the relative standing wavelength of

$$\frac{\lambda_{SV}}{\lambda_0} = \frac{-1}{\sin(\delta)}$$

6.17.3 Graphs of horizontal and vertical probing wavelengths

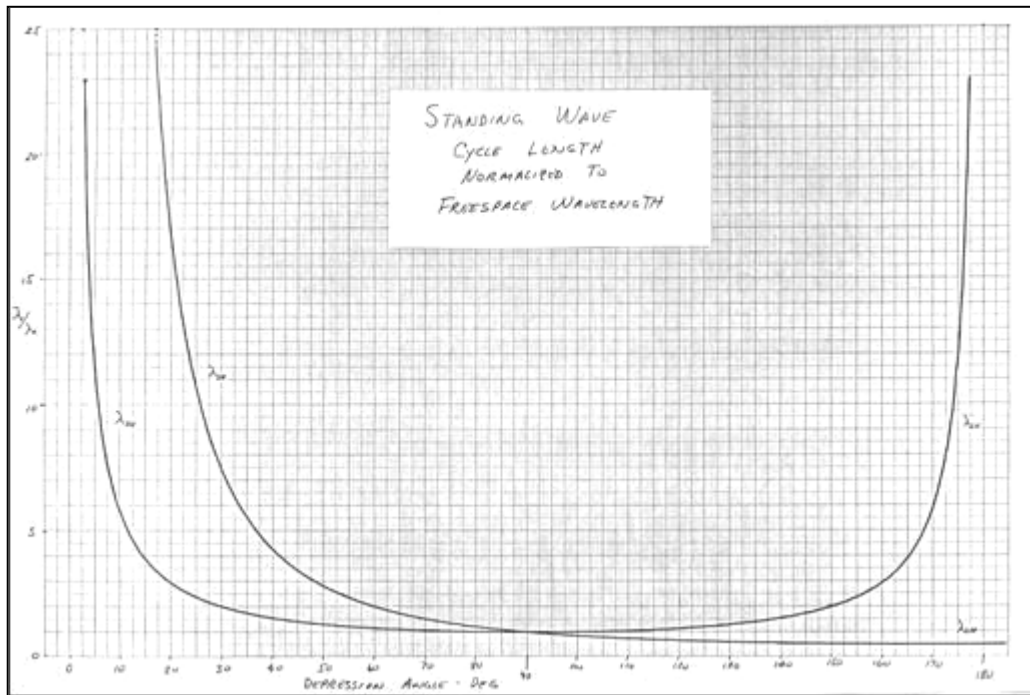


Figure 6-28. Standing wavelength for both horizontal and vertical probing.

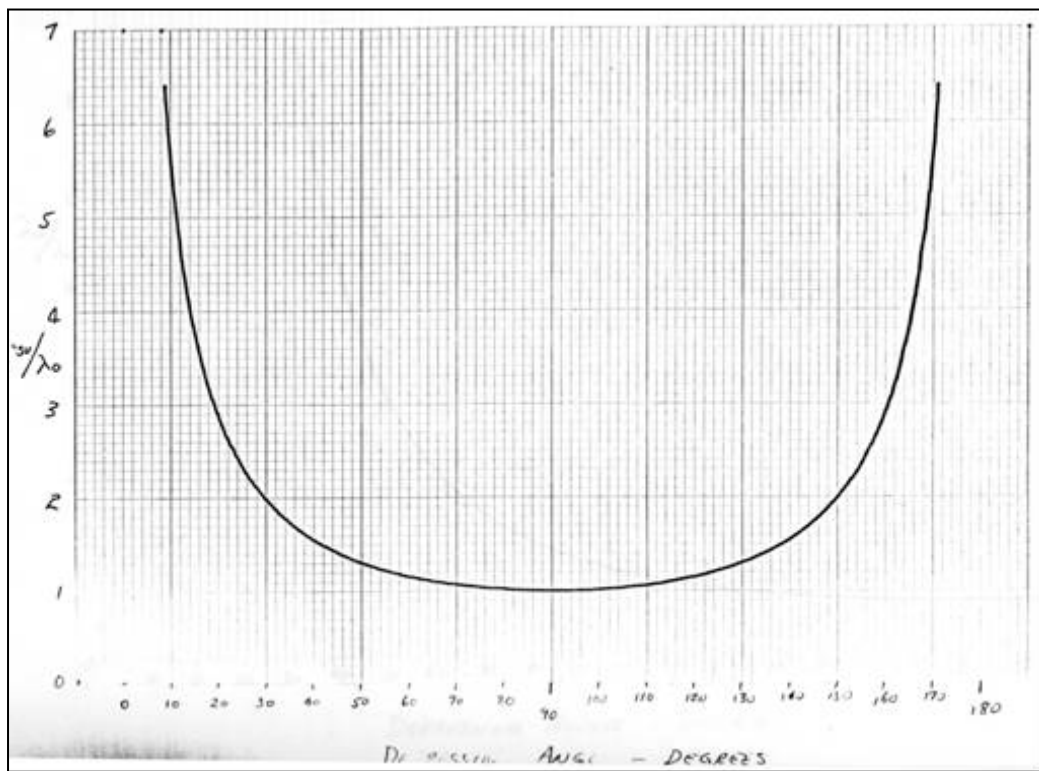


Figure 6-29. Standing wavelength for vertical probing.

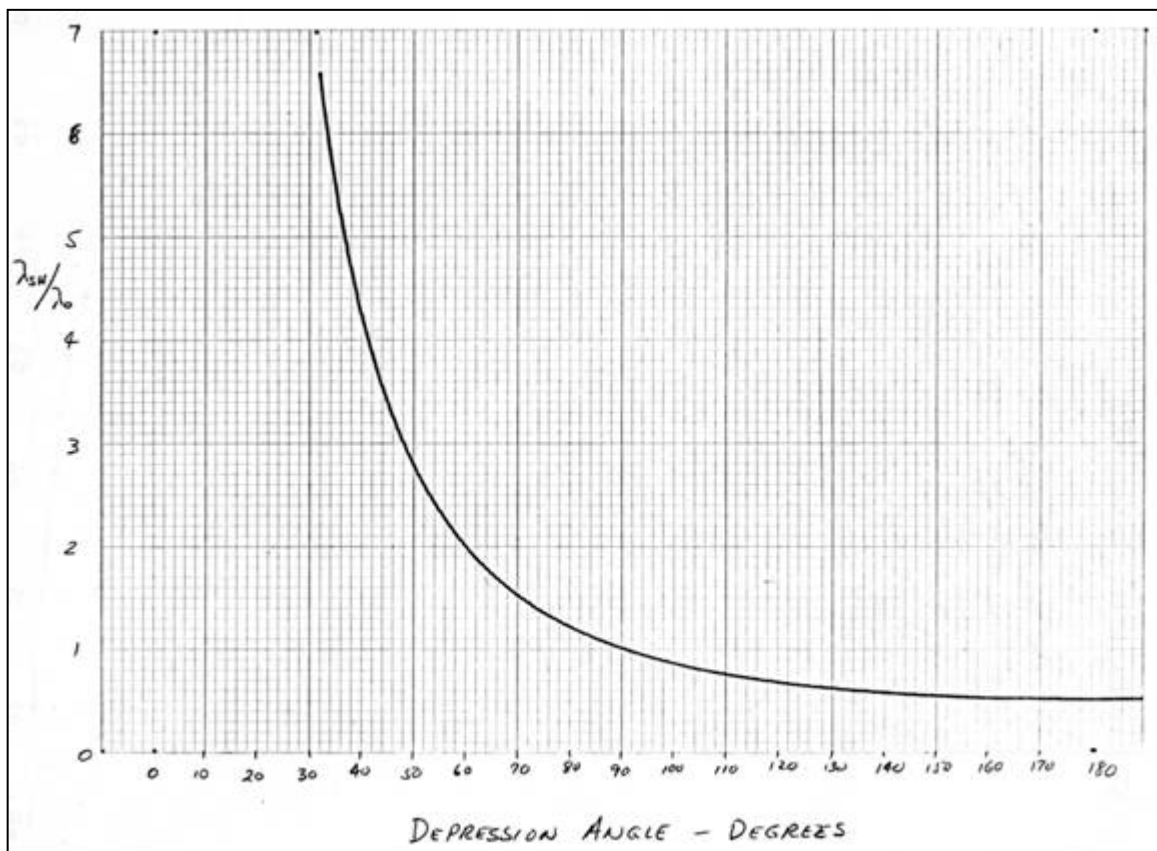


Figure 6-30. Standing wavelength for horizontal probing.

6.17.4 Probing by Movement in an Arc. The movement of the elevation control sometimes accomplishes probing. In the diagram below the translation for horizontal probing is actually an arc “probing” path. Over small angles near the center of the measurement aperture, the arc approximates (to an adequate degree) the linear motion required for horizontal probing. For reflections arriving from very low angles, such as from the table and deck below the antenna under test, the translation need be only a few wavelengths to yield several cycles of interference pattern. In practice, several settings of the roll angle are used so that the antenna under test may help discriminate against the direct wave and emphasize the reflection. In this way, the comparison of several probing arcs may better yield the magnitude of the reflection. With reasonable care, this technique can be used to make a very good estimate of the reflections present. In order to analyze the resulting probing information, it is necessary to know the length of the arc radius, the wavelength of operation, and a reasonable estimate of the antenna pattern. Usually, the roll plane pattern is plotted prior to the probing so that it can be used to set the approximate level of discrimination against the stronger (direct) wave so that the weaker (reflection) wave can produce a greater magnitude of ripple pattern. This technique may be used to obtain accurate estimates of relatively weak reflected waves.

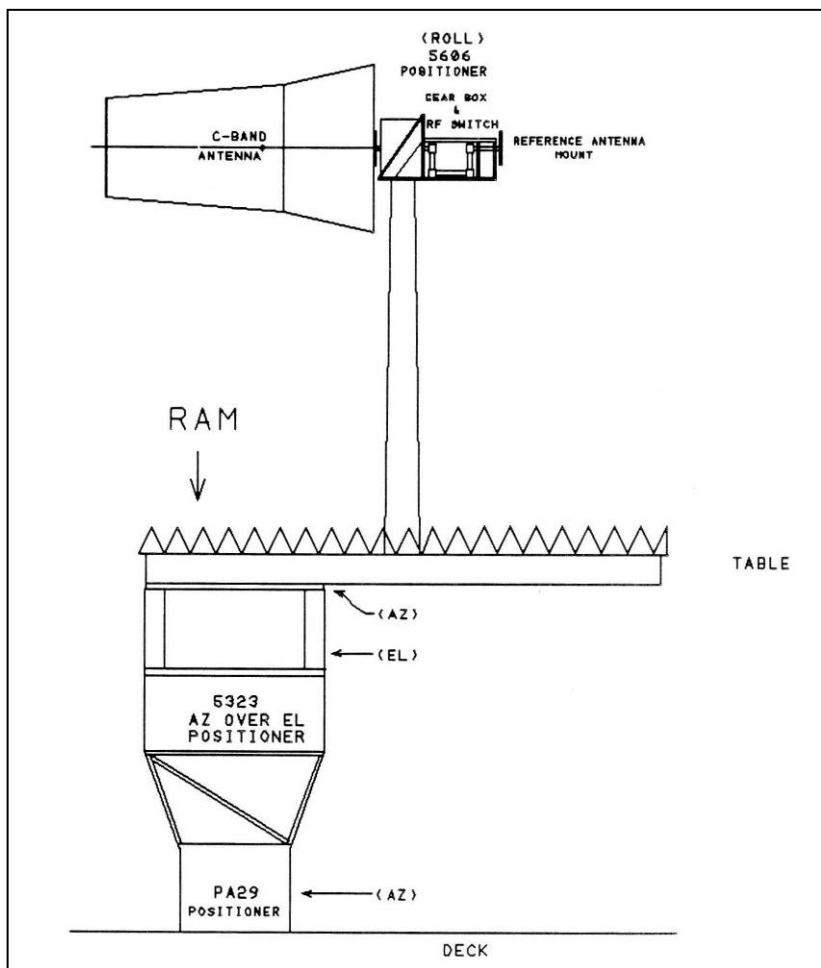


Figure 6-31. Mockup sketch used in arc probing (side view).

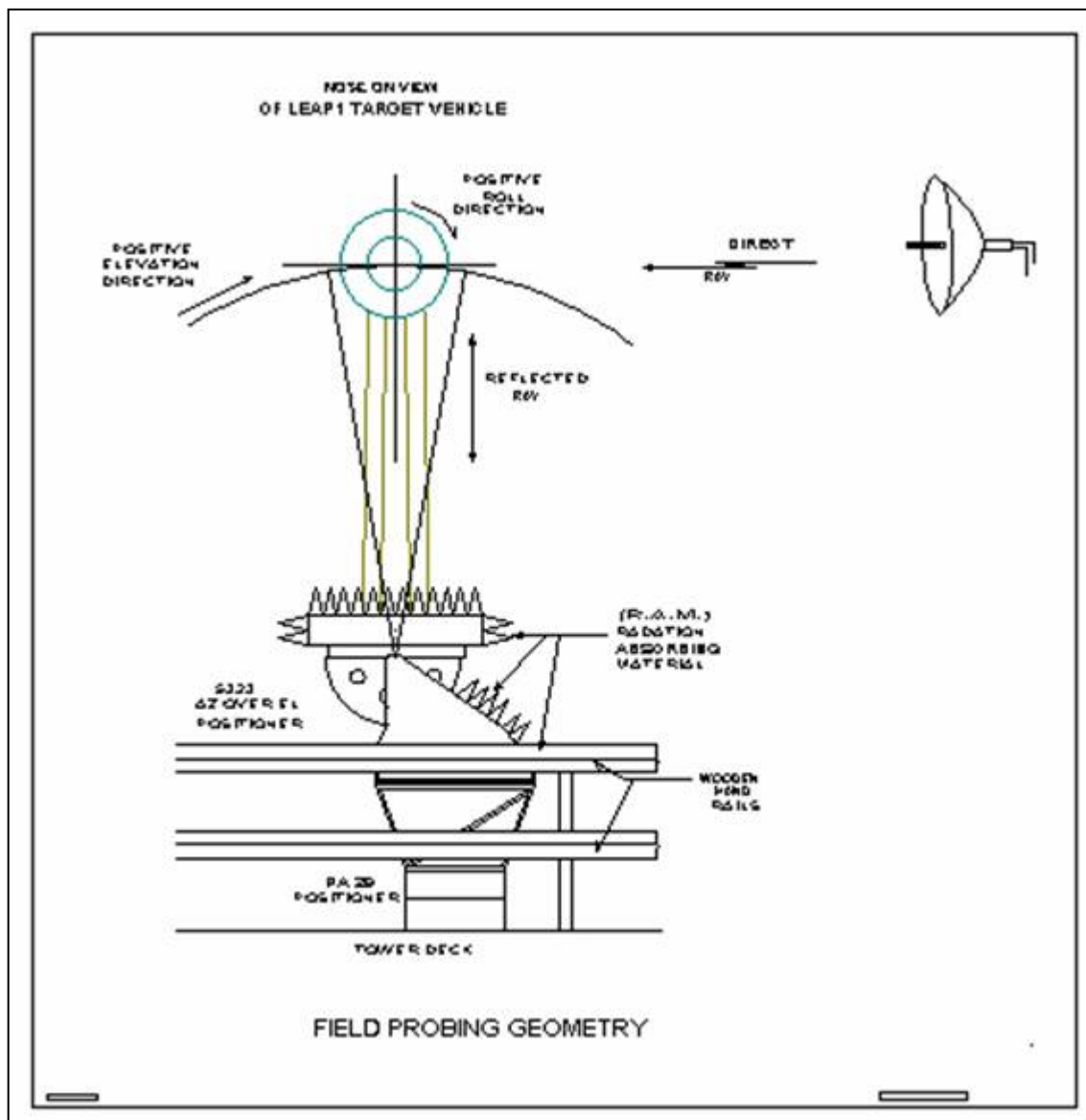


Figure 6-32. Sketch of motion for arc probing.

The sketch shown above is a “nose-on” view of the geometry used in “arc” probing. It shows a mockup mounted on a “roll-over-az-over-el-over-az” positioner. The typical absorbing material panels used to cover the metal positioner parts are shown. The wooden tower safety rails were also covered with RAM in most cases.

6.17.5 Separation Of Phasors By Ripple Analysis. For any two unequal numbers (magnitudes) the sum and difference may be analyzed to determine the magnitude of each.

$$\begin{aligned}\text{Maximum} &= \text{Large} + \text{Small} \\ \text{Minimum} &= \text{Large} - \text{Small}\end{aligned}$$

In the case of “ripple” on an antenna pattern, we know only the maximum and minimum values and desire to find the magnitudes of the two phasors that produce the ripple.

It is clear that if we know the values of the max and min then we can form the following relationships.

$$\mathbf{Max + Min} = (\text{Large} + \text{Small}) + (\text{Large} - \text{Small}) = \mathbf{2 \times Large}$$

And

$$\mathbf{Max - Min} = (\text{Large} + \text{Small}) - (\text{Large} - \text{Small}) = \mathbf{2 \times Small}$$

Then we have the results:

$$\text{Large} = \frac{(\text{Max} + \text{Min})}{2}$$

$$\text{Small} = \frac{(\text{Max} - \text{Min})}{2}$$

6.17.6 Magnitude of Each Phasor Vs Ripple Magnitude. Many times the only measurable quantity in the antenna pattern ripple is the difference in magnitudes, maximum and minimum. These are usually known in decibel. The quantities desired are the magnitudes (in dB) of these two voltage phasors that produce the observed ripple. From the relative magnitudes of the max and min, we want to solve for the relative magnitudes of the two individual phasors. We identify this ripple magnitude as a “delta in dB”.

$$\Delta_{\text{dB}} = \text{max-to-min in decibels}$$

For Unity Maximum

If the maximum of the ripple (sum of two voltage phasors) is unity (0 dB) then the minimum equals $-\Delta_{\text{dB}}$ and the minimum in linear voltage terms is:

$$V_{\text{min}} = 10^{-\frac{\Delta_{\text{dB}}}{20}}$$

and of course

$$V_{\text{max}} = 1$$

Then the larger of the two voltages is the average of the max and min,

$$V_{Large} = \frac{1 + 10^{-\frac{\Delta_{dB}}{20}}}{2},$$

and the smaller of the two voltages is half the difference between max and min,

$$V_{Small} = \frac{1 - 10^{-\frac{\Delta_{dB}}{20}}}{2}$$

From this analysis the desired phasor magnitudes in decibels are

$$V_{LargeDB} = 20 \log_{10} \left[\frac{1 + 10^{-\frac{\Delta_{dB}}{20}}}{2} \right]$$

and

$$V_{SmallDB} = 20 \log_{10} \left[\frac{1 - 10^{-\frac{\Delta_{dB}}{20}}}{2} \right]$$

For Unity Larger Phasor

The above derivation is for the maximum of the ripple set to unity. There are times and situations in which it is desirable to set the larger of the two voltage phasors to unity. Thus, the max will be larger than unity and the min will be less than unity.

In this case the ripple magnitude varies between $1 + \rho$ and $1 - \rho$, where rho is the smaller phasor and unity is the larger phasor. Then the max-to-min ratio is:

$$\Delta = \frac{(1 + \rho)}{(1 - \rho)}$$

Then we have:

$$\Delta_{dB} = \left[\frac{(R_{max})}{(R_{min})} \right] \text{ in decibels}$$

and then

$$\Delta_{dB} = 20 \log_{10}(\Delta) = 20 \log_{10} \left[\frac{(1 + \rho)}{(1 - \rho)} \right]$$

Realize that the linear form of rho relates to the decibel form as:

$$\rho = 10^{\frac{\rho_{dB}}{20}} \quad \text{or} \quad \rho_{dB} = 20 \log_{10}(\rho)$$

Consider the equation above for Δ_{dB} . Then dividing by 20 and raising 10 to the power of both sides we obtain

$$10^{\frac{\Delta_{dB}}{20}} = \frac{1+10^{\frac{\rho_{dB}}{20}}}{1-10^{\frac{\rho_{dB}}{20}}}$$

This can get a little messy so simplify by substituting some simpler terms for the exponential terms. Let

$$X = 10^{\frac{\Delta_{dB}}{20}} \quad \text{and} \quad Y = 10^{\frac{\rho_{dB}}{20}}$$

Then we can write

$$X = \frac{(1+Y)}{(1-Y)}$$

So that we get

$$X(1-Y) = (1+Y)$$

Which may be rearranged to yield

$$Y = \frac{(X-1)}{(X+1)}$$

Then finally we have rho as

$$\rho = \frac{10^{\frac{\Delta_{dB}}{20}} - 1}{10^{\frac{\Delta_{dB}}{20}} + 1}$$

and rho in decibels is

$$\rho_{dB} = 20 \log_{10}(\rho) = 20 \log_{10} \left[\frac{10^{\frac{\Delta_{dB}}{20}} - 1}{10^{\frac{\Delta_{dB}}{20}} + 1} \right]$$

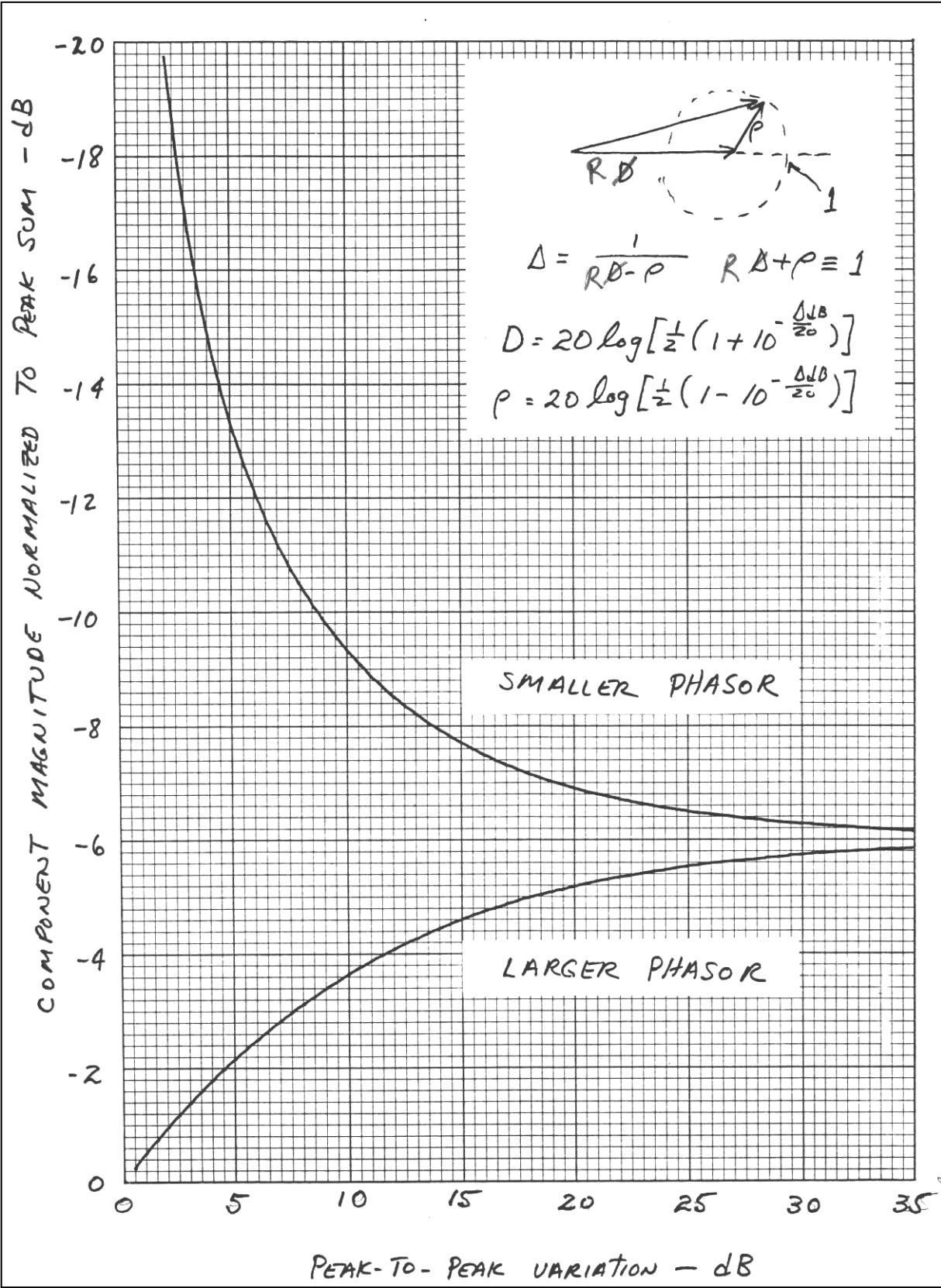


Figure 6-33. Phasor separation graph.

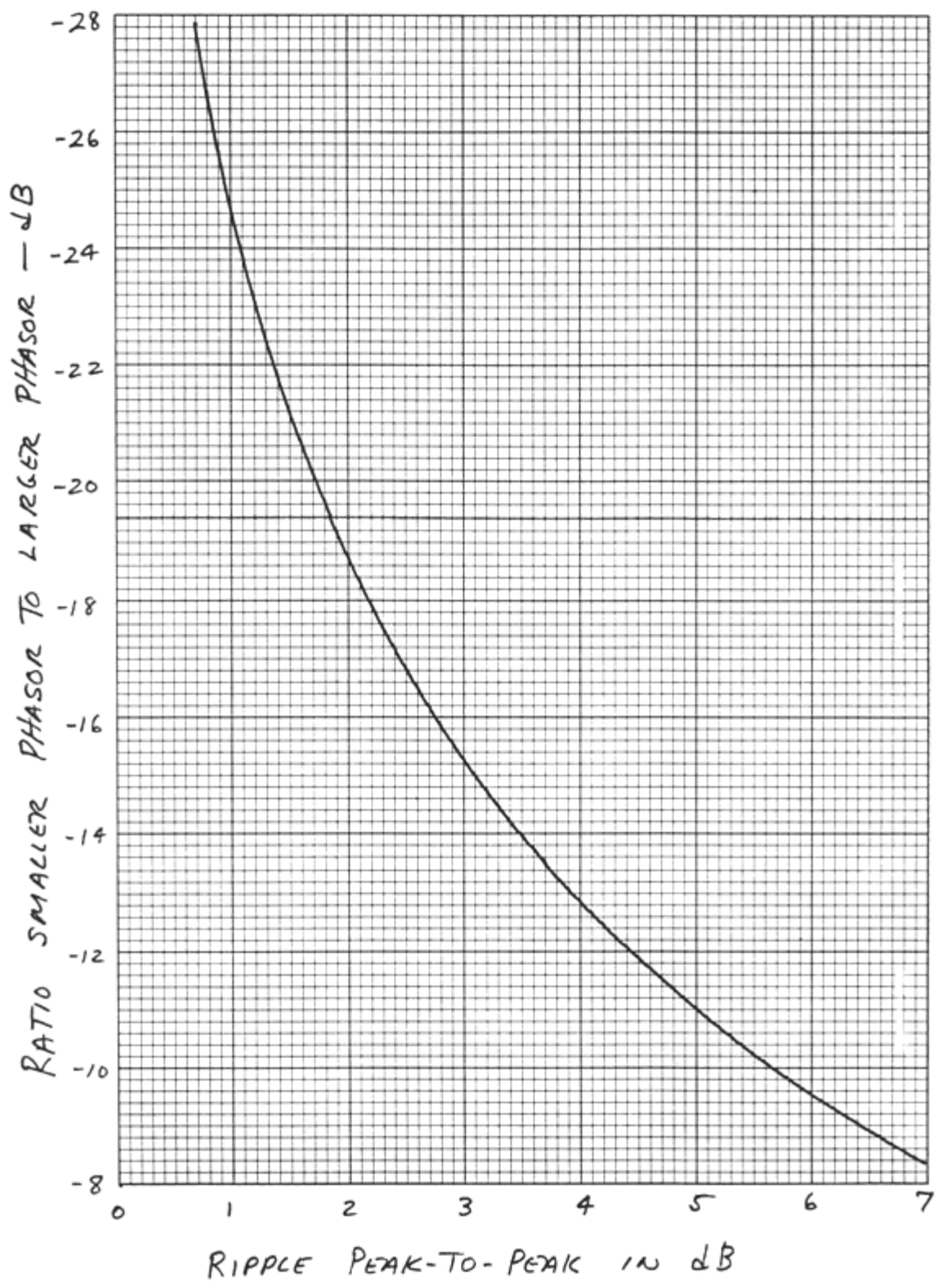


Figure 6-34. Graph for smaller phasor for ripple zero dB to 7 Db.

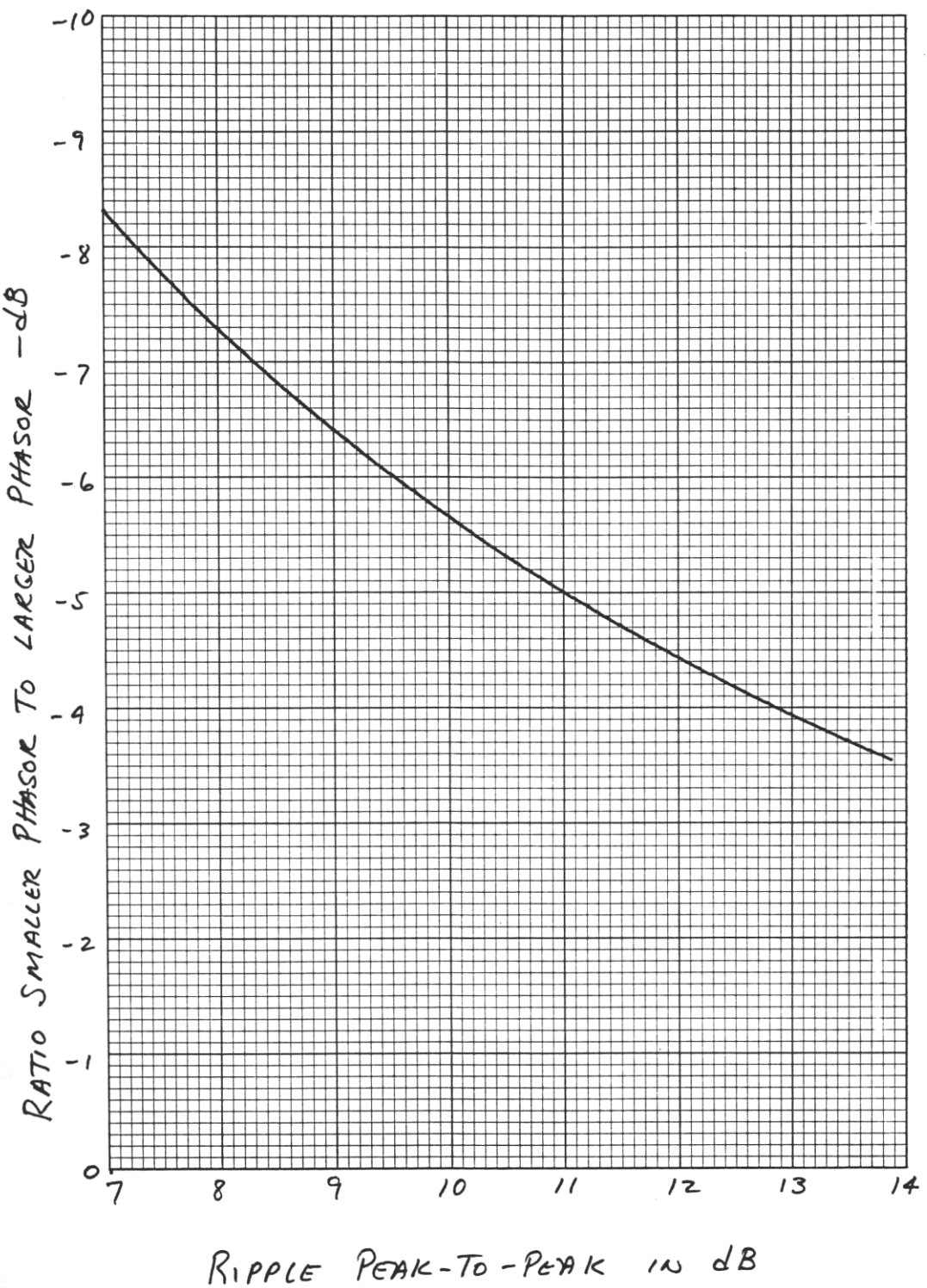


Figure 6-35. Graph for smaller phasor for ripple 7 dB to 14 dB.

6.18 Probing by Sweeping Frequency

6.18.1 Introduction. During gain measurements of many antennas, especially high gain dishes, the range geometry invites reflection problems. This is the case when the range is long and the towers on which the test antenna and the range antenna (“illuminator”) are short. The reflection will come from an angle not far removed from the direct wave.

Probing by translation of a wide beam probe is usually not practical because of the low angle of arrival (small difference in directions) requires too great a translation distance.

High directivity “angular” probing is sometimes acceptable, but not always. This is especially true when the angle of arrival is very close to the direct ray.

Another method is sometimes available if the antenna system is sufficiently wide band. By changing the frequency over a band equal to (or greater than) the frequency whose wavelength equals the path length difference, one (or more) complete cycles of phasor interference pattern will be generated (for stationary antennas). The peak-to-peak variation can be used to compute the magnitude of the reflection. The frequency difference required to produce a cycle of interference pattern can yield the information necessary to determine the locus of possible points of the reflection.

6.18.2 Derivation of Ellipse Parameters from Frequency Scans. A geometric property of the ellipse suggests the method for reflection analysis by sweeping frequency. The ellipse is the locus of all points, the sum of whose distances from two fixed points (foci) remains constant. Thus, any point on the ellipse may be chosen and the sum of the distances from that point to the two foci will equal to the length of the major axis of the ellipse. In the three-space environment of antenna measurements, this ellipse will become an ellipsoid whose axis of revolution coincides with the range axis (direct ray). In principle any given reflection could be coming from any point on the surface of that ellipsoid, but in practice it is possible to readily dismiss the possibility of reflections arriving from certain directions, the upper hemisphere for example on an outdoor elevated range. Other directions may suggest a high probability of containing reflections and would be investigated first.

In the analysis of reflections, it is reasonably obvious that the antennas at each end of the link should be chosen as the foci of the ellipse to be computed. The fact that the reflection must begin at one of these antennas and terminate at the other makes this choice obvious. The path of the reflected ray (ray tracing will be employed in this analysis) begins at one antenna, goes to a point on the ellipse, then proceeds directly to the other antenna. The length of this path is just the length of the major axis of the ellipse.

The difference between the reflected ray path length and the direct ray path length may be determined by the frequency difference required to generate one cycle of interference pattern. The frequency for one null is noted and the frequency shifted through the interference maximum then on to the next null at which time the frequency is again recorded. The difference between these two frequencies is the frequency whose wavelength is the path length difference between the direct and reflected rays. Since the direct ray path length is (presumably) known, (since it is the range length), and the reflected ray travels the greater distance, then the actual length of the reflected path is known.

With these quantities known, the essential parameters of the ellipse are determined. The distance to each focus is just half the range length, assuming a coordinate origin midway between the antennas (foci). From each focus out to the ellipse (on the major axis), the distance is half the path length difference. With this on each “end” of the ellipse, it is clear that the reflected ray length equals the major axis of the ellipse. In the sketch below the reflected ray path length is equal to $2*c$ (or $d + e$). The major axis extends from E1 to E2 and the focal length is half the distance from F1 to F2. The semi-major axis is “a” and the semi-minor axis is “b” so that (consider the origin at the center of the ellipse) the value of “b” can be computed from the right triangle that has “c” as the hypotenuse. The classic equation for the ellipse is given as

$$(X / A)^2 + (Y / B)^2 = 1$$

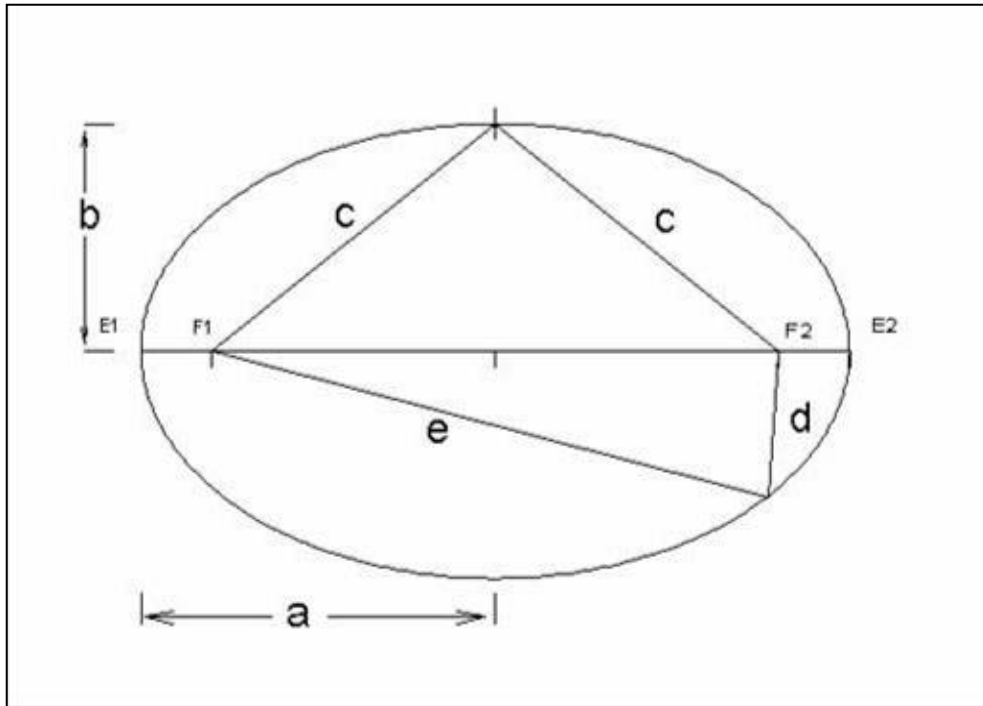


Figure 6-36. Sketch of ellipse associated with path length difference.

In practice, the test antenna has some directivity that may be utilized to discriminate against the direct wave and in favor of the reflected wave in order to obtain a greater “ripple pattern” during probing. This technique, when applied repeatedly with the “beam” pointed at suspected reflecting objects, can result in reasonably accurate estimates of the reflection levels

and directions on the range. Sometimes the identification of the reflecting object or area can result in modifications (screens, absorbing materials, etc) which lower the overall reflections on the range. As in all probing with a directive probe the approximate pattern of the probe should be determined prior to the probing exercise.

Example of frequency sweep probing:

Consider the case on a 3000 feet long test range in which the frequency was changed 245.9 MHz in order to produce one full cycle of the interference pattern. The ripple amplitude (max to min) was 1.0 dB with a wide angle of view probe. In order to find the reflection ellipse parameters the path length difference must be found. The path length difference is equal to the wavelength of the 245.9 MHz wave.

$$\text{Wavelength} = \lambda = c/f = 983.571 / 245.9 = 4 \text{ feet}$$

The focal length, f , is equal to half the range length or 1500 feet.

The semi-major axis is the focal length plus half the path length difference or 1502 feet.

From geometry, the semi-minor axis is equal to the square root of the difference between the square of the semi-major axis and the square of the focal length.

$$b = (a^2 - f^2)^{0.5}$$

$$b = 77.5 \text{ feet}$$

$$a = 1502 \text{ feet}$$

With these parameters of the ellipsoid, it would be possible to compute the likely sources of reflection. In this case, if the test antenna towers were about 80 feet tall and the base of the tower were visible from the test antenna location, the tower base would be a suspect. However, if the “source tower” were on a short tower but on a small hill, it would be likely that something near the source tower, or possibly the tower itself, is the source of the reflection.

The one dB of ripple may be converted into the reflection level by entering the [graphs](#) for separating the two phasors causing a ripple. The smaller phasor (normalized to the larger phasor) is seen to be -24.7 dB. In the practical world of probing, the pattern of the probe and the angle of arrival of the reflection must be factored into the calculations for the reflection level.

It might be noted that sometimes the “reflection” is really another coherent source of signal. The analysis suggested here can become confusing when the interfering wave comes from a “secret” source rather than an actual reflection. There have been occasions in which a “leaky” coax cable feeding the source antenna was found to be the elusive “reflection”.

6.19 Antenna Analysis Quick References

When working with antennas and the link analysis between two antennas, it becomes apparent that some basic equations are used repeatedly. In this section, some of the most often needed relationships are presented.

6.19.1 Path Loss (Range Loss). This is the link loss caused by the separation distance between the two antennas. It is sometimes known as “spreading loss”. The assumption is that each antenna is in the farfield of the other.

$$\text{RangeLoss}_{\text{dB}} = 20 * \log_{10}(4 * \pi * \text{Range} / \text{wavelength})$$

For compactness we will refer to $\text{RangeLoss}_{\text{dB}}$ as RL_{dB} .

Then, collecting terms we have

$$\text{RL}_{\text{dB}} = 20 * \log_{10}(4 * \pi) + 20 * \log_{10}(\text{Range}) - 20 * \log_{10}(\text{Wavelength})$$

Usually we have frequency instead of wavelength. And the first term is a constant:

$$\text{RL}_{\text{dB}} = 21.98 + 20 * \log_{10}(\text{Range}) - 20 * \log_{10}(c) + 20 * \log_{10}(\text{freq})$$

For metric, range in kilometers and frequency in gigahertz:

for: $c = 2.997925 \times 10^5$ km/sec,

$$\text{RL}_{\text{dB}} = 92.45 + 20 * \log_{10}(R_{\text{km}}) + 20 * \log_{10}(f_{\text{GHz}})$$

For English, range in feet and frequency in gigahertz:

for: $c = 9.8335 \times 10^8$ ft/sec,

$$\text{RL}_{\text{dB}} = 22.13 + 20 * \log_{10}\{(R_{\text{ft}})(f_{\text{GHz}})\}$$

For English, range in yards and frequency in gigahertz:

for: $c = 3.2778 \times 10^8$ yd/sec,

$$\text{RL}_{\text{dB}} = 31.67 + 20 * \log_{10}\{(R_{\text{yd}})(f_{\text{GHz}})\}$$

6.19.2 Antenna Gain and Beamwidth. Estimates of an antenna's gain and beamwidth are routinely required during signal strength and link margin calculations. The gain is directly proportional to its effective area and inversely proportional to the square of the wavelength.

$$\text{Gain} = [4\pi / \lambda^2] * A_{\text{eff}}$$

For aperture type antennas such as parabolic reflectors and horns the effective area is approximately half the mechanical area. So for reasonable estimates we use

$$\text{Gain} = [2\pi / \lambda^2] * A_{\text{mech}}$$

When the beamwidth is desired and the diameter, D, (of the dish) is known, then a good estimate is that the half power beamwidth is 70 wavelengths divided by the diameter.

$$\text{HPBW}_{\text{deg}} = 70 * \lambda / D$$

When the beamwidths (HPBW_{deg}) are known (in two orthogonal planes, BW_e and BW_h) then the gain in decibels with respect to isotropic can be estimated by:

$$\text{Gain}_{\text{dBi}} = 44 - 10 * \log_{10}[(\text{BW}_e)(\text{BW}_h)]$$

By substituting the expression for the beamwidth from diameter and wavelength with the expression for gain in terms of beamwidths we can get the gain in terms of diameter and wavelength.

$$\text{Gain}_{\text{dBi}} = 44 - 20 * \log_{10}[\text{HPBW}_{\text{deg}}]$$

$$\text{Gain}_{\text{dBi}} = 44 - 20 * \log_{10}(70) - 20 * \log_{10}(\lambda/D)$$

Which becomes:

$$\text{Gain}_{\text{dBi}} = 7.098 + 20 * \log_{10}(D/\lambda)$$

Converting the D/λ to D in feet and frequency in gigahertz we get:

$$\text{Gain}_{\text{dBi}} = 6.95 + 20 * \log_{10}[(D_{\text{ft}}) * (f_{\text{GHz}})]$$

Dish Beam Shape

There are times when the shape of the beam and the “close in” sidelobes are desired for estimates in certain analyzes. A useful equation for the calculation of beamshapes of prime focus dishes is given below. This is the normalized gain (pattern) as a function of the angle off boresight. One simply selects a desired beamwidth and computes the gain pattern.

$$G(\phi)_{\text{db}} = 27 * \log_{10}\{\sin[138.4(\phi/\text{HPBW})]/[2.42(\phi/\text{HPBW})]\}$$

CHAPTER 7

EXISTING STANDARDS AND GUIDELINES

7.1 Introduction

This chapter contains some standards and guidelines that could be helpful to many readers. Included is a partial list of RCC documents and other useful standards and guidelines.

7.1.1 RCC Documents (On Line). Included also (for those with Internet connection) is a link to the RCC online documents. The RCC documents contain a wealth of useful information for individuals who review antenna systems for national range use.

These references contain statements which quantify some of the more important considerations involved in antenna systems qualifications for use on RCC test ranges. A review of some of the current and earlier versions of standards documents makes some suggestions for the modification of some sections of these standards.

Some of the standards and guidelines referred to herein are shown in the on-line supplement to this document. The reader can access the [RCC web site](#) and download RCC Document 265-06, Radar Transponder Antenna Systems Evaluation Handbook (Supplement). Some notes and comments may be found in Paragraph [7.2](#). Specific suggestions concerning RCC-253-93 are at Paragraph [7.3](#).

7.1.2 Range Commanders Council (RCC) Documents. Many documents related to this handbook are available on the [RCC web site](#). Some key documents are shown below.

RCC-250-91	Frequency Standards for Radar Transponders
RCC-251-80	IRIG Standard for Pulse Repetition Frequencies and Reference Oscillator Frequency for C-band radars
RCC-253-93	Missile Antenna Pattern Coordinate System and Data Formats
RCC-255-80	Error Sources Applicable To Precision Trajectory Radar Calibration
RCC-256-93	IRIG Radar Calibration Catalog
RCC-257-86	Coherent C-Band Transponder Standard
RCC-260-98	The Radar Roadmap
RCC-262-02	C(G) – Band & X(I) – Band Noncoherent Radar Transponder Performance Specification Standard
RCC-322-98	Guidelines Document: Global Positioning System (GPS) as a Real-Time Flight Safety Data Source
RCC-323-99	Range Safety Criteria for Unmanned Air Vehicles (UAVs)
RCC-324-01	Global Positioning and Inertial Measurements Range Safety Tracking Systems' Commonality Standard

7.1.3 Other Reference Documents (See RCC 265-06 Supplement)

MIL-STD-461	Control of EMI
MIL-STD-810e	Environmental Test Methods
MIL-STD-810f	Environmental Engineering Considerations
TSPI	Time, Space and Position Information Data Formats
Western	Western Space and Missile Center (WSMC)
4A Radar	WSMR Range Test Capabilities (Radar Instrumentation)
NR-DR 76-1	Analysis of Transponder Induced Bias Errors
STD 149-1979	IEEE Standard Test Procedures for Antennas

7.2 Considerations of Existing Guideline Documents

The first part of the Radar Transponder Antenna Study was to consider whether a guidelines document should be generated. If such a guidelines document is attempted in the future, then some of the following documents might be included in that resulting document.

Various parts (or the whole) of the RCC 253-93 should be included. However, the parts used should be updated and modified to reflect general current computer usage and capabilities.

The Eastern and Western Range Safety document EWR-127-1 would provide a very good basis upon which to form a "guidelines" document. Two ranges (Vandenberg 30th Space Wing and Cape Canaveral 45th Space Wing) use this as their primary requirements statement. Paragraphs dealing with radar transponder antennas and range interfacing should be included.

Earlier document versions should be considered, such as:

SAMTOR 80-4 (June 1981)

Department of the Air Force
Space and Missile Test Organization (SAMTO), (later version is below)

WSMCR 127-1 (April 1983)

Chapter 4, specifically 4.1; 4.2; 4.8.3.4; 4.8.4.1.2; 4.8.4.2.2; 4.8.6;
4.8.6.1.3.2

SAMTOR 80-4 (June 1983)

Department Of The Air Force
Headquarters Space and Missile Test Organization (AFSC)
Vandenberg Air Force Base, California, 93437
(To be used in conjunction with UDS document RCC 501-79)
Chapter 2, specifically 2-1b; 2-2; Chapter 3 (all)

WSMCR 127-1 (December 1989)

(Supersedes WSMCR 127-1 15 May 1985)
Western Space and Missile Center
Chapter 4 specifically 4.14

ERR 127-1 (30 June 1993)

Published by Eastern Range (45th Space Wing)

WRR 127-1 (30 June 1993) Chapter 4 is identical to ERR 127-1 (June 1993).

Headquarters 30th Space Wing (AFSPACEROM)

Vandenberg Air Force Base, California, 93437-5000

Updates WSMCR 127-1 (15 Dec 89) paragraph numbering changed

Updates 1 STRADR 127-200

Chapter 4 specifically 4.8; 4.8.2 (4.8.2.1.5 & 4.8.2.2.5); 4.11.4.1;
4.11.4.2.5.2; 4.11.4.2.5.3.3; 4.12.7

RCC 253-93 (August 1993)

Electronic Trajectory Measurement Group (ETMG)

Range Commanders Council (RCC)

White Sands Missile Range

Chapter 3 (all) Missile Antenna Pattern Requirements

EWR 127-1 (31 October 1997)

Published jointly by the 30th and 45th Space Wings

Presents users of Eastern and Western Ranges common requirements

Chapter 4 specifically 4.11 and 4.11.1.1 (4.11.1.1.1 & 4.11.1.1.2;
4.11.1.1.3 and 4.11.1.1.4)

Summary: Each document should be studied and the paragraphs mentioned given special attention. Consideration should be given as to include each (unmodified or modified) or to eliminate it. Additional material should be considered as a matter of information concerning techniques, which have been found commendable.

7.3 Suggested References To EWR 127-1 Document

At least two national ranges, 30th Space Wing at Vandenberg Air Force Base and 45th Space Wing at Cape Canaveral Air Station, use a standards document known as EWR 127-1 for range safety requirements. Other ranges may use its guidelines when determining specifications of antenna systems and their testing. EWR 127-1 has some excellent statements concerning antenna performance requirements.

RCC 253-93 is referenced in EWR 127-1 (paragraph 4.11.1.1.3) concerning the reporting of antenna pattern measurement results.

Even though RCC 253-93 is basically a standards document concerned with “Missile Antenna Pattern Coordinate System and Data Formats”, in chapter 1 it makes some assertions that should be reconsidered.

- a. Paragraph 2 of section 1.1 states that when the tracking antenna is circularly polarized only one component pattern is needed. This would be the “co-polarized” component pattern, of course.
- b. Paragraph 3 of section 1.1 seems to slightly contradict a statement in the preceding paragraph. It states that when the “supporting system” (presumably the tracking system) is “linear or circular polarized” then an “absolute minimum” of four measurement patterns are required. It asserts that six measurements are preferred.
- c. Paragraph 4 of section 1.1 is a slight refinement of the preceding paragraph without any hint as to why the particular components are chosen.

These statements seem out of place in a “Coordinate System and Data Format” document. However, if they are to be included then some explanation should be added. It should be stated that an assumption is made that measurements can be made with an “amplitude only” pattern measurement system. With amplitude (gain) only patterns, it is necessary to generate a known “non-linear” component in order to determine the sense (handedness) of the elliptical polarization state. Therefore, the linear gain components (actually only three required) could determine the axial ratio and tilt angle but not the sense of the ellipse.

The introduction, section 1.1, could be rewritten to include a brief statement of the general practice of antenna pattern measurements. In that case, it should be mentioned that the technique of “linear component polarimetry” is the preferred technique to use in measurements of antenna radiation patterns. This technique utilizes two orthogonal (linear) polarization components and the phase between them. Linear components are preferred because in practice it is easier to maintain pure polarization over a wide frequency range with linear than it is to maintain circular polarization over a wide frequency range. Since the link analysis can be done with any known polarization states at both ends of the link (as long as the gains and path loss are known), any measurement that yields the gain and polarization state of the antenna under test is adequate. There is no good reason for a standards document to restrict the technique of measurement to “amplitude only” when much better techniques are widely in use at most reputable antenna ranges.

Also, if the RCC 253-93 is to be more than simply a “coordinate system and data format” document it might well incorporate the provisions of EWR 127-1 section 4.11.1.1 on the required performance of the antenna systems being measured.

Of course, the sections dealing with the data formats and magnetic medium need to be updated in light of the changes in techniques and computer hardware since 1993

CHAPTER 8

FREQUENTLY ASKED QUESTIONS (FAQ)

- a. If I have a choice, what are the considerations for placing antennas on the vehicle? (i.e. nose, tail, wing, upper/lower, etc.)

The type of vehicle being tracked, the type of antenna, and the directions from the vehicle which must be covered, will dictate the antenna placement. For high flying aircraft, which will do only mild rolling, the belly mounted or vertical stabilizer mounted stub antenna might be adequate. The simple approach of “if I can see the antenna, I have coverage” probably works for single element antenna systems. When two or more antennas are driven in an array, tracking may be highly compromised by the interference lobes in the overall pattern. The broader the pattern of each individual element, generally the broader will be the zones of significant interference lobing. This handbook (Paragraph [4.4](#) and Paragraph [4.5](#)) contain some discussions about design considerations.

- b. How do I handle or mitigate potential Multipath problems?

Multipath problems are generally thought to be those stemming from the reflections of the target vehicle by the earth or other structures. As such, they are not so much a matter of vehicle antenna performance as they are the range environment. By careful consideration of the polarization changes upon reflection, it might be possible to select polarizations of the vehicle antenna and the tracker to attempt mitigation of the multipath effects. Of course, on a more intimate scale the reflections from missile fins or aircraft control surfaces could be considered multipath that affects the overall effective vehicle antenna pattern (Paragraph [4.4](#)).

- c. How can a circularly polarized beacon antenna be the “same hand” in both receive and transmit?

The polarization of an antenna is defined by the polarization state of the wave it generates in transmission. An antenna receives a polarization state which is the transmit state mirrored across the principal plane ($E_\theta, E_\phi, E_{rhep}, E_{lhep}$) on the Poincare sphere (Paragraph [5.14.1](#)). As such, any antenna whose polarization lies on this plane receives the same polarization as it transmits. However, if the antenna is polarized off this principal plane it will receive (be polarization matched to) a different polarization than it transmits. As an example, an antenna polarized at 45° (E_{45}) will be cross-polarized to another identical antenna and will be polarization matched to an antenna with polarization E_{135} . The example of two “moon walking” astronauts with antenna wires running diagonally from left shoulder to right hip in their space suits would be crossed polarized when facing each other trying to communicate. In the case of a Right Hand Circularly Polarized (RHCP) antenna facing another identical antenna, the condition leads to polarization matched antennas. However, if the RHCP antenna “faces” itself in a mirror then it is cross polarized and would not receive a return signal. It has been suggested that these situations are essentially the same, with the real identical antenna being replaced with the true mirror image of the original. That they are not the same may

be seen by considering the rotation of the electric field phasor and the direction of propagation. The definition of RHCP has the electric field phasor rotating clockwise as it progresses forward. In the case of the “mirror image” antenna, the electric field rotates clockwise when viewed from the original transmit antenna, but it would appear to rotate counter-clockwise to an observer behind the image and thus would become a LHCP wave upon reflection because of the reversed direction of propagation without a reversal in rotation sense. (See Polarization Upon Receiving (Paragraph [5.17](#)).

This is very much like a “right hand” thread on a screw that progresses in the direction away from observer who sees a clockwise rotation of the slot in the screw. Whether it is progressing “into” or “out of” the material, the observer who sees the clockwise rotation sees it progressing away from him. It remains a right hand screw regardless of the direction of progress.

- d. The project is offering to measure antenna patterns, but they want to know exactly what kind and what level of detail I need. What do I tell them?

The answer to this will depend upon what you plan to do with the patterns. If a mission profile link analysis is to be performed, the antenna patterns should probably adhere to the requirements stated in RCC 253-93 and EWR 127-1. The kind of patterns should include full spherical measurement of radiation distribution patterns (RDP’s). In order to solve the link it is necessary to know the gain and polarization state of the target antenna and the tracker antenna (Paragraph [5.14.2](#) and Figure [5-41](#)). Probably the best approach is to require RDP’s by linear component polarimetry techniques for each frequency of interest. The detail required will depend upon the vehicle diameter-to-wavelength ratio for multi-element array antenna systems. The sample spacing in the RDP should yield more than two samples per interference pattern cycle (Paragraph [5.5](#), and Paragraph [6.9](#)).

- e. Okay, I have the antenna patterns, now what do I do with them?

Any time measured patterns are supplied it is prudent to investigate how they were measured and determine the likelihood of their being accurate. It is possible to measure antenna patterns with techniques and in environments which render them almost useless. (Discussions of some factors are found in Paragraph [6.7](#), Paragraph [6.13](#), Paragraph [6.14](#), Paragraph [6.15](#), Paragraph [6.16](#), and Paragraph [6.17](#)).

Probably the next thing is to determine how complete the pattern data is. Check to see if the sample spacing is adequate to “find” sharp nulls in the pattern (Paragraph [5.5](#), and Paragraph [6.9](#)). Use the diameter of the vehicle and the radiating element configuration to determine the separation between two adjacent antennas. Use that information to estimate the angular parameters of possible interference lobes. If the sample spacing is more than half the lobe spacing then the pattern fine details could be lost. If the mission profile can be determined as to the angles from the target, which are directed to the tracker, then that profile may be plotted on the RDP’s. The distance, gains of each antenna (target and tracker) and the polarization mismatch loss must be determined in order to do a link analysis. By applying the known transmit power and receiver

sensitivity a link margin may be computed. This is usually done on a second-by-second basis for relatively short duration flights. The mission requirements will dictate how the link analysis should be done.

- f. How should I estimate coverage if I do not have access to a link analysis program (Rules, Statistical procedures, charts, etc.)?

Antenna pattern coverage is usually determined from the measured (or simulated) patterns. Normally, a specific target antenna gain level is determined by some form of link analysis prior to the mission. The path loss for the longest distance required might be used along with the known transmitter power of the tracker and the sensitivity of the receiver in the target. This might establish a “worst case” for signal strength. From this, the minimum target antenna gain would be determined. This minimum gain would then be specified as the level at which 95 percent or more of the antenna pattern spherical surface must exhibit. Polarization mismatch loss to the specified tracker antenna polarization state must be taken into account (Paragraph [5.2](#) and Paragraph [5.3](#)).

- g. Is there a RCC certified PC based Link Analysis package that I can access?

To my knowledge there is no such RCC certified PC based program. A good link analysis program should consider important factors such as plume attenuation, polarization mismatch loss, spherical spreading loss with distance, transmit power and receiver sensitivity. It should allow the input of vehicle trajectory with vehicle orientation at each sample point as well as vehicle antenna pattern data from a full spherical pattern (RDP). There are other factors to consider for a complete link analysis (Paragraph [5.16](#)).

- h. How can I estimate if I can track or if the data quality will be degraded if I have the placement of antennas on the vehicle but I do not have any measured antenna patterns?

By knowing the type and placement of the antennas, it should be possible to make some reasonable approximations to the antenna pattern. It is necessary to know the spacing between the radiating elements if multiple element arrays are used. In the areas where two or more antennas can provide coverage there will be interference patterns or ripples in the overall pattern. Paragraph [5.5](#) and Paragraph [6.9](#) in the handbook have discussions of determining the spacing of the peaks and nulls in the ripple pattern. The actual gain of the pattern will be determined by the efficiency of the radiating elements and the feed harness. Pattern simulations may be of some help if the geometry is known and the radiating element manufacturer’s specifications are used.

- i. How would I compute polarization mismatch loss between my radar and the target?

The measured pattern (RDP) will contain the gain and polarization state of the target antenna. By standard definition, this is the transmit polarization. The receive polarization is (in general) or may be, different (Paragraph [5.16](#) and Paragraph [5.17](#)). The radar polarization must be known in the target antenna pattern coordinate system (or

visa versa) in order to make meaningful polarization mismatch loss determination. This is an important part of the link analysis when full use is to be made of measured patterns.

j. Will a dihedral corner reflector always return a “co-polarized” signal?

No, not always. Even though the dihedral corner reflector utilizes two reflections and will return the same handedness circular polarization, tilted linear polarizations will exhibit rotation of the polarization tilt angle (Paragraph [5.15.4](#)).

k. Does knowing the direction of the radar from the target and the gain in that direction (from pattern data) allow computation of link margin?

Not entirely. These are necessary ingredients in the calculation of the link loss but must be accompanied by knowledge of the polarization states at both ends of the link and the powers required (or supplied) at both ends (Paragraph [5.16](#)).

l. I have patterns but how do I compute the coverage level?

To properly compute the coverage, it is necessary to have a pattern over the entire radiation sphere (RDP). See Paragraph [5.2](#) for details.

m. The antenna pattern coordinate system angles seem confusing, where can I find the correct definitions of the coordinate system?

Sometimes the confusion comes from the fact that not all those who measure or compute antenna patterns adhere to the approved definition of the coordinate system. The recipient (or evaluator) should insist on having the antenna pattern data supplied in the RCC standard terminology and format. Refer to RCC Document 253-93, Missile Antenna Pattern Coordinate System and Data Formats.

n. Phase Patterns.... how would I use them?

Phase patterns are sometimes required by the lead range but the usefulness of the patterns depends upon several factors including the sample spacing. Phase patterns can be useful in predicting the tracking angle error and data link error rates (See Paragraph [5.11](#) and Paragraph [5.12](#)).

o. How can I estimate the tracker angle error from the target antenna pattern?

Tracking angle errors can be associated with the rapid phase changes in the vicinity of pattern nulls. The magnitude of the angle errors may be estimated by knowing the relative depth of the pattern nulls and the spatial frequency of the “ripple” pattern (Paragraph [5.10](#)).

- p. If I have the opportunity to specify the antenna pattern sample spacing, what value should I request?

The maximum spacing of the pattern samples should be determined by the antenna spacing in the array on the target vehicle in terms of wavelength. When the spacing is greater than one third or one fourth of the angle from maximum to minimum in the ripple pattern, it is possible to miss important details in the pattern. This is covered in detail in the Handbook. (See Paragraph [6.8](#), Paragraph [6.9](#), and Paragraph [6.10](#)).

- q. From the RDP for the RHCP component response I find that the target vehicle antenna has a gain value of -10 dBic . Since my radar antenna is “vertical linear”, is it safe for me to assume that I will have a mismatch loss of another 3 dB and thus see a -13 dBi response?

It is not safe to make that assumption. The polarization state, which produced the -10 dBic in the RDP, may have been almost anything, not purely RHCP. It might be a linear which could be cross-polarized to your radar. It could be a left hand elliptical state with much higher gain that could couple to your linear state to yield a link much higher than a -13 dBi . It is necessary to determine the polarization state by looking at two orthogonal components and the phase between them. Only then can a proper determination of the polarization mismatch loss be made to any other specified state. See “Poincare Sphere” (Paragraph [5.14](#)) and “Polarization Upon Receiving” (Paragraph [5.17](#)).